EFFECTS OF GROWING PROGRAMS AND β-ADRENERGIC AGONISTS ON GENE EXPRESSION IN ADIPOSE TISSUE DEPOTS IN FINISHING BEEF STEERS

By

DANIEL RAY STEIN

Bachelor of Science in Agriculture Ecology
Northwestern Oklahoma State University
Alva, Oklahoma
1978

Master of Science in Animal Science
Oklahoma State University
Stillwater, Oklahoma
2004

Submitted to the Faculty of the
Graduate College of the
Oklahoma State University
in partial fulfillment of
the requirements for
the Degree of
DOCTOR OF PHILOSOPHY
July, 2009

EFFECTS OF GROWING PROGRAMS AND β-ADRENERGIC AGONISTS ON GENE EXPRESSION IN ADIPOSE TISSUE DEPOTS IN FINISHING BEEF STEERS

Dissertation Approved:

Dr. Clint R. Krehbiel

Dissertation Adviser

Dr. Udaya E. DeSilva

Dr. Patricia J. Ayoubi

Dr. J. Brad Morgan

Dr. Rodney D. Geisert

Dr. A. Gordon Emslie

Dean of the Graduate College

Many doors had to be opened at the right time for this achievement to occur at this stage in my life. At times when I thought all doors were closed, one would open and a new direction taken. I thank the Lord, Jesus Christ for his unconditional love and for watching over me, opening (and closing) those doors, and directing my life in a path to better serve him. In all your ways acknowledge him and he shall direct your paths (Proverbs 3:6).

ACKNOWLEDGMENTS

I would first like to express my sincere appreciation to Dr. Rodney Geisert for giving me the opportunity to pursue my Ph.D. in Animal Science at Oklahoma State University. Not often does a person have the opportunity and good fortune to attain a dream or goal they have set in life, let alone the opportunity and possibility to attain a second. My first goal, to be successful in the registered seedstock business – made my resolve for my second goal, to attain a Ph.D. degree, teach at the university level, and make a difference in the lives of young people, permissible. Dr. Geisert, your understanding, support, guidance, and mentorship are truly appreciated. The teaching opportunity given me after you accepted the position of Department Head at the University of Missouri awarded me a great number of opportunities and recognitions never imagined.

I would also like to express my deepest gratitude to Dr. Clint Krehbiel and Dr. Udaya DeSilva for not only serving on my Ph.D. graduate committee, but also for agreeing to serve as my Ph.D. committee co-advisors. Your insight and guidance in the research and teaching arena and your support through my Ph.D. program were very much appreciated.

I would also like to thank Dr. Patricia Ayoubi and Dr. Brad Morgan for serving on my Ph.D. graduate committee. Dr. Ayoubi, I truly appreciate the time you took to answer the many questions that came up while performing the microarrays and

completing the data analysis; your expertise, support and friendship through this endeavor was greatly appreciated. Dr. Morgan, a big "Thanks" for your support, encouragement, and perspective of things along the way.

I would like to acknowledge and truly thank my mother, Rosevelyn, for her encouragement, support, and prayers through these past seven years. It has been a struggle at times, but a sincere "Thank You" for believing in my goals and my ability to attain them. To the rest of my family and in-laws, I truly appreciated your prayers, support, and encouragement.

I would also like to acknowledge my many friends, the entire OSU Animal Science Family including; all faculty (past and present), fellow graduate students, all support personel, and my undergraduate students who have assisted, encouraged, and supported not only me, but Jana, through our time at OSU. I also need to express my gratitude and appreciation to Morgan Ashworth for his friendship and encouragement over the years.

Above all, I would like to thank my wife, Jana, for her never-ending love and support. It has been a long seven years since we began this journey; I could have never accomplished this undertaking without your love, patience, friendship and understanding. I truly appreciate the sacrifices that you have made for our future. You have constantly helped me keep a perspective on what is important in life and for that I am truly indebted. All my love.

Dedications

I would like to dedicate this manuscript to my father, Leroy, who did not live long enough to see me finish my Ph.D. degree. It is not often a son has the opportunity and privilege to work side by side with his father for nearly thirty years – for that I am truly blessed.

Dad, your wisdom, character and spirit gave me strength when needed.

I'm Just a Farmer, Plain and Simple

I'm just a farmer, plain and simple.
Not of royal birth, but rather a worker of the earth.
I know not of riches, but rather of patches on my britches

I'm just a farmer, plain and simple.
I know of drought and rain, of pleasure and pain.
I know the good, the bad, the happy and the sad.

I'm a man of emotions.
A man who loves this land and the beauty of its sand.
I'm just a farmer, plain and simple.

I know the spring's fresh flow and autumn's golden glow.
Of a new born calf's hesitation and an eagle's destination.
I'm just a farmer, plain and simple.

I know of tall pines and long waiting lines.
I know the warmth of campfires and the agony of flat tires.
I'm just a farmer, plain and simple.

I'm a man who loves his job
And the life that I live.
I'm just a farmer, plain and simple

I'm a reaper of harvest.
I'm the sower of seeds and I'm the tender of stock.
I'm just a farmer, plain and simple.

I know of planting wheat and baling hay and animals going astray.
I live in a complex world, but my faith guides me.
I'm just a farmer, plain and simple.

I am a man who works with God. I cannot succeed without his help.
For you see, I'm just a farmer, plain and simple.

TABLE OF CONTENTS

Chapter Page

LIST OF TABLES

Table Page

LIST OF FIGURES

Figure Page

CHAPTER I

INTRODUCTION

In 2007, over 33.7 million head of cattle were harvested in the United States with steers and heifers accounting for 51.2% and 30.2% of that number, respectively (USDA, 2007). According to the 2005 National Beef Quality Audit (Garcia et al., 2008), the number one contributor to lost economic opportunities per slaughter steer/heifer to the industry was quality grade which accounted for almost one-half, or $26.81 of the total loss of $55.68 per head. The remainder of the loss was attributed to yield grade and carcass weight. This calculated to nearly a two billion dollar loss to the beef industry for 2007. This figure does not include losses incurred from the remaining 18.6% of animals harvested consisting mainly of dairy/beef cows and bulls. One also needs to consider the waste of resources and resulting inefficiencies in production incurred by over-fattening cattle to improve the palatability and acceptability of meat for the consumer (Smith et al., 2000). Producing quality beef is at the forefront of concerns facing the U.S. fed-beef industry as evidenced by the top ten challenges put forth by participants in the 2005 National Beef Quality Audit (Garcia et al., 2008). Six of the top ten challenges can be related to either “inadequate” or “excessive” adipose tissue deposition. Over the past several years, the beef industry has moved from a live- or carcass-weight pricing structure towards a “grid” based pricing structure in the marketing of fed cattle

.

(Schroeder et al., 2003), with the main components of most grid pricing frameworks consisting of quality grade and yield grade. The majority of the "waste" and "taste" inefficiencies in the beef industry are due to either excess or insufficient fat deposition (Dolezal, 2000); thus, it is important to characterize the differences between "waste" fat and "taste" fat deposition sites relative to the value of the carcass.

Numerous factors have been shown to affect the rate of intramuscular adipose tissue deposition (marbling) in beef cattle including regulation of lipogenesis, genetics, age, nutrition, vitamins, management, and environment (Smith, 1995; Pyatt and Berger, 2005; Ross et al., 2005). The genetic relationships between body composition and adipose tissue (fat) accretion are of particular interest as they are directly related to final carcass composition and consequently the ultimate value of the carcass. A moderate to strong genetic antagonism exists between carcass fatness traits and carcass yield percentage, across and within breeds of cattle (Gwartney et al., 1996; Vieselmeyer et al., 1996; Burrow et al., 2001), which creates difficulty in resolving the problem of "waste" vs. "taste" adipose tissue deposition.

The ability to utilize exogenous compounds to manipulate different aspects of muscle and adipose tissue to increase feedlot efficiency has had a great economic impact on the beef industry in recent years. One such class of exogenous compounds is phenethanolamines or β-adrenergic agonists. β-adrenergic agonists seem to act by increasing the efficiency of growth by preferentially stimulating skeletal muscle growth as compared to adipose tissue (Baxa, 2008). Zilpaterol hydrochloride, commercially available as Zilmax® (Intervet/Schering-Plough Animal Health, Millsboro, DE), is a synthetic β_2-adrenergic agonist used for increased rate of weight gain, improved feed

efficiency and increased carcass leanness in cattle fed in confinement for slaughter (Dikeman, 2007; Kern et al., 2009). In 2006, Zilmax was approved by the U.S. Food and Drug Administration (FDA) as a feed ingredient for cattle during the last phase of the feeding period. Zilpaterol hydrochloride (Zilmax®) has been shown to have an affect on growth performance, dressing percent, hot carcass weight, and carcass muscling in several studies.

As adipose tissue accretion in the bovine is controlled by a balance of adipocyte proliferation and differentiation. It is essential to evaluate how diet or the administration of exogenous compounds affects and/or regulates adipocyte proliferation in order to improve the quality of beef produced. Knowledge and understanding of the relationships between mechanisms regulating metabolic and signaling pathways and other contributing factors which orchestrate adipose tissue deposition within and between adipose tissue depots could possibly be integrated into management practices in a value-based marketing system to produce a consistent and desirable product that would ultimately enhance consumer beef consumption, increase efficiency of production, and increase profitability for the beef industry.

Research Objectives

1. Determine the gene expression profiles of bovine intramuscular and subcutaneous adipose tissue depots at the end of the growing and finishing production phases using microarray and RT-PCR analysis. The array used consisted of a 1,089 cDNA non-redundant clone library constructed from subcutaneous and visceral adipose tissue.
2. Determine the gene expression profiles of bovine intramuscular, subcutaneous, and visceral adipose tissue depots and *Longissimus* muscle tissue in cattle fed Zilpaterol hydrochloride the last 20 days of the feeding phase plus a 3-day withdrawal period using microarray and RT-PCR analysis. A bovine array containing a total of 24,000 oligonucleotide probes was used in this research which includes 16,846 probes designed from ESTs that were aligned to homologous vertebrate proteins and to the 6X bovine genome assembly (BGA). The probe set was supplemented with oligos designed from 703 predicted RefSeq genes, 5,943 reproductive tissue ESTs with a BGA but no protein alignment, and 504 positive and negative controls.

CHAPTER II

REVIEW OF LITERATURE

Introduction

Value based marketing seems to be steadily driving the beef industry. An increasingly larger percentage of cattle seem to be moving from a live- or carcass-weight pricing structure through a grid pricing structure and/or a production alliance program (Schroeder et al., 2003; Johnson and Ward, 2005). Grid pricing allows for adjustment with premiums, as well as discounts, to a base price according to the merits of the individual beef carcass (Feuz et al., 1993). Grid premiums and discounts send a signal to the producer regarding those traits processors are looking for based on consumer preference (Johnson, 2006a). In comparing different marketing methods of slaughter cattle including sales on a live-weight basis, sales on a dressed carcass weight, sales on a dressed weight/grade and yield basis, and following a value based marketing approach, it was determined that feedlot production variables best explained the profit/loss differences under live-weight marketing better than did the carcass characteristics. However, carcass characteristics appeared to become as important, or more important, to profit/loss differences as the feedlot production variables when cattle were marketed on a grade and yield basis or through a value-based marketing program (Feuz et al., 1993). Feuz et al. (1993) also pointed out in his analysis of marketing strategies that the amount of

subcutaneous (s.c.) fat, unwanted by the consumer, was negatively related to profit, regardless of the marketing method. The components involved in most grid pricing or value based pricing structures are quality grade and yield grade. Quality grade is an indication of eating satisfaction or palatability while yield grade is an estimate of the percentage of closely trimmed retail cuts to be derived from the carcass. Marbling, or intramuscular (i.m.) fat, is a component of quality grade and is evaluated in a cross section of the *Longissimus* muscle (LM). Yield grade is determined by the amount of external fat on the carcass at the 12^{th} rib (s.c.) and is factored by the percentage of kidney, pelvic and heart (KPH) fat determined in the carcass (USDA, 2001). The single most important factor for determining carcass quality in the United States and abroad continues to be marbling score; however, during the last three decades, there has been a noticeable decrease in USDA beef carcass quality grades with no change in the average USDA yield grade (Chung and Johnson, 2008). Marbling is considered to be a moderately to highly heritable trait, with approximately 37% of the observed differences attributed to heredity (Utrera and Van Vleck, 2004). This means that approximately 63% of marbling in an animal depends on environment, management and nutrition.

What affects the industry as a whole actually begins at the cow/calf sector, as that sector's end product is dealt with downstream in the industry. The route a calf takes to get to the feedyard can track in many different directions. In 2007, over 33.7 million head of cattle were harvested in the United States with steers and heifers accounting for 51.2% and 30.2% of that number, respectively (USDA, 2007). According to the 2005 National Beef Quality Audit (Garcia et al., 2008), the number one contributor to lost economic opportunities per slaughter steer/heifer to the industry was quality grade, which

accounted for almost one-half, or $26.81 of the total loss of $55.68 per head. The remainder of the loss was attributed to yield grade and carcass weight. As divergent as the beef industry may seem at times, there are still shared concerns between the different production sectors. The "Top Ten Quality Challenges" put forth in the 2005 National Beef Quality Audit by those engaged in the four production sectors; consisting of the seed stock, cow/calf, stocker/backgrounding and feedlot/finishing sectors included: 1) insufficient marbling and low quality grades, 2) lack of uniformity in cattle, 3) inadequate tenderness of beef, 4) yield grades too high, 5-tie) low cutability, 5-tie) carcass weights to heavy, 7) injection site lesions, 8) inadequate flavor, 9) inadequate muscling, and 10) excess fat cover (Smith et al., 2006a). Six of these ten "quality challenges" or concerns can be tied to and/or trace back to "inadequate" or "excess" adipose tissue deposition. The majority of the "waste" and "taste" inefficiencies in the beef industry are due to either excess or insufficient fat deposition (Dolezal, 2000) and calculates to an annual loss of nearly 2 billion dollars to the beef industry. This does not include the inefficiencies of production that are incurred due to over-fattening cattle, trying to create that "higher quality carcass" that will fit the consumer's wants and expectations (Smith et al., 2000). Thus, it is important to characterize the differences between "waste" fat and "taste" fat deposition sites relative to the value of the carcass.

Due to geographical regions in the United States, there is diversity in management skills and systems within and between the different sectors of the beef industry (Bennett and Williams, 1994). The diversity in geographic regions also extends between the extremes as it pertains to feedstuff availability during the growing or stocker phase of production. Backgrounding, a term used predominately in the northern regions of the

United States (Peel, 2000), has been described as the production phase between the time a calf is weaned until it's placement into a feedyard for finishing (Thomson and White, 2006). Stockers, a term used predominately in the southern regions of the United States (Peel, 2000), describes young lightweight calves which are raised primarily on available forage or pasture diets until they reach a desired weight and placed in the feedlot (Bock et al., 1991). The importance of these backgrounding or stocker programs are evident as it is estimated that on January 1 of a given year, 76% of the previous year's calf crop is still available for feedlot placement (Peel, 2000). Animals in stocker/backgrounder programs may be raised to 1/2 to 2/3 harvest weight (Sainz and Vernazza Paganini, 2004) and can serve to combine smaller groups of cattle into larger groups and distribute cattle numbers from a seasonal production cycle to a year-round production cycle (Bennett and Williams, 1994).

Due to geographical regions in the U. S., backgrounding/stocker programs involve a wide range of production environments and management skills, such that, not all programs and systems are feasible for producers in the various locations in the U.S. (Peel, 2006). Though stocker cattle are most often grazed on forages; resources, environment and/or market conditions might warrant the confinement of the animal to a drylot system with those animals fed a grain-based ration (Thomson and White, 2006). Two alternatives to roughage or pasture based programs are: 1) program fed, defined by Galyean, (1999) as the use of net energy equations to calculate the quantities of feed required to meet the needs of maintenance plus a specific average daily gain (ADG), and 2) calf-fed programs, a system where cattle are placed on an *ad libitum* finishing diet immediately following weaning (Lardy, 1998). Advantages of program fed cattle using a

high concentrate diet vs. grazing include; reduced feed costs when pasture costs are high or in short supply and easier adaptation of cattle to an *ad libitum* finishing diet (Galyean, 1999). Advantages of a calf-fed program may be realized when large framed cattle are placed on a high concentrate diet offered *ad libitum* after weaning in order to insure an adequate level of body fat is achieved (Lardy, 1998). Implementing a calf-fed program for smaller framed cattle may be detrimental to the quality of the carcass due to a shift in the animal's physiological maturity to a point where those cattle do not have time to develop i.m. fat (Schoonmaker et al., 2004; McCurdy, 2006)

Nutrition during the growing phase has been shown to affect the performance of cattle during their finishing phase as hot carcass weight, *Longissimus* muscle area, and marbling score were greater for steers grazing winter wheat compared to steers grazing native range prior to feedlot placement (Choat et al., 2003). Cattle fed grain-based diets have been shown to have increased i.m. fat compared to those fed forage-based diets as marbling scores were significantly lower for steers grazed on summer pasture and then fed for either 45 or 75 d in the feedlot compared to steers taken to the feedlot immediately after weaning (Schaake et al., 1993). Furthermore, steers fed a diet consisting of 68% high-moisture corn and 25% alfalfa silage had increased i.m. fat compared to cattle fed a 95% alfalfa silage diet for the same number of days on feed (Mandell et al., 1998). In addition, grazing-based growing programs prior to feedlot entry resulted in cattle with lower marbling scores compared to calves placed directly in a drylot and fed a silage-based diet followed by a corn diet (Hedrick et al., 1983). More so, using suppressive subtractive hybridization, Ross et al., (2005) reported different nutritional background in beef steers (i.e., steers on supplemented native range or steers

on high-gain wheat pasture) altered gene expression in s.c. and i.m. adipose tissue depots during the feedlot phase. Thus, it is important to determine the effects of background, previous nutrition and management systems throughout the production phases on marbling and subsequent quality of the carcass.

Adipose Tissue

Adipose tissue can be described as a loose association of lipid filled adipocytes held in a framework of connective tissue containing not only adipocytes, but also preadipocytes, stromal vascular cells, multipotent mesenchymal stem cells, endothelial progenitor cells, fibroblastic connective tissue cells, leukocytes, and macrophages (Albright and Stern, 1998; Cinti, 2005; Tchkonia et al., 2007). Most adipose tissues form at sites of loose connective tissue (Rosen and Spiegelman, 2000); more so, i.m. adipose tissue has been shown to develop within perimysium connective tissue alongside myofibers (Moody and Cassens, 1968). Each individual adipocyte is supported by a basement membrane composed of collagens and other extracellular matrix (ECM) components (Pierleoni et al., 1998), with adipocyte size varying dramatically depending on varying physiological conditions (Farnier et al., 2003). The onset of adipogenesis is usually defined by ECM remodeling with the ECM adhesion molecules and other signaling components changing with adipose differentiation (Liu et al., 2005). Each adipocyte is in contact with at least one capillary providing support for metabolism (Albright and Stern, 1998; Harper and Pethick, 2004; Vázquez-Vela et al., 2008) with each adipocyte being highly innervated (Fliers et al., 2003; Cinti, 2005). Arteriolar development precedes adipose development in internal fat depots as the earliest event

associated with adipogenesis is the increase in the abundance of the capillary networks in regions of s.c. loose connective tissue (Hausman and Richardson, 2004). A key characteristic of angiogenesis is the breakdown of connective tissue and basement membrane proteins (Yancopoulos et al., 2000), which include several angiogenic factors including vascular endothelial growth factor (VEGF), VEGF receptors, matrix metalloproteinases and the plasminogen enzymatic system (Hausman and Richardson, 2004). Hausman and Thomas (1984) reported that in pigs, capillary beds in dense connective tissue are immature and contain few adipocytes, whereas capillary beds in loose connective tissue are mature and contain more adipocytes. Although angiogenesis is unmistakably linked to adipogenesis, it is not apparent whether adipogenesis can induce angiogenesis or vice-versa or both (Rosen, 2002).

Bovine adipocytes have been shown to vary in size according to depot site (Moody and Cassens, 1968). According to work by Smith and Crouse, (1984), i.m. adipose tissue had smaller mean cell diameter and smaller mean cell volume than s.c. adipose tissue with the i.m. adipose tissue tending to have a greater number of cells per gram of tissue than s.c. adipose tissue. More so, i.m. adipose tissue cell diameter has been reported to differ within the same deposition site between different breeds of cattle (Hood and Allen, 1973; Miller et al., 1991); between different deposition sites between different breeds of cattle (Cianzio et al., 1985; May et al., 1994); and between different deposition sites within the same breed of cattle, with i.m. adipose cell diameter smaller than s.c. cell diameter (Lin et al., 1992). Adipocyte diameter was reported to be larger in the intermuscular adipose tissue than in the s.c. and i.m. adipose tissues in Japanese Black x Holstein crossbred steers (Yang et al, 2003). The contribution of hypertrophy

(increased cell size) and hyperplasia (increased cell number) to i.m. fat deposition is controversial; however, Yang et al. (2006) reported that hyperplasia plays a greater role in i.m. fat deposition than hypertrophy. It is unclear whether cell size reflects features of the muscle environment or a genetically determined potential for cell growth (Harper and Pethick, 2004), as marbling adipocytes from Wagyu steers exhibited twice the rate of DNA synthesis at the same physiological maturity as marbling adipocytes from Angus steers suggesting that the adipose tissues from Wagyu steers possessed a greater capacity for cell proliferation than adipose tissues from Angus steers (May et al., 1994). Cianzio (1985) reported the adipose cell number/gram of intramuscular adipose tissue a better indicator of marbling score than adipose cell diameter.

Mature adipocytes function in lipid storage and energy flow but also can act as an endocrine organ in the production of hormones or regulatory compounds termed "adipokines" (Otto and Lane, 2005; Wang et al., 2008; Dodson and Fernyhough, 2008). The adipocyte is essentially a lipid storage container whose morphology is supported by components of the extracellular matrix (Pierleoni et al., 1998; Wang et al., 2008) and can be controlled by, not only the level of metabolites in the blood, but by paracrine, autocrine and/or endocrine factors as well as neural regulation (Fliers et al., 2003; Cinti, 2005; Otto and Lane, 2005).

A mature white adipocyte cell can range in size from 25 to 200 microns and usually contains only one large fat droplet, or is termed unilocular; however, multiocular cells can occur. The adipocyte cell contains mitochondria and a nucleus, which are usually located, due to the size of lipid droplet, near the outer rim of the cytoplasm (Harper and Pethick, 2004; Cinti, 2005; Vázquez-Vela et al., 2008). This unilocular lobe

contains no intracellular organelles and is composed mainly of triglycerides; however, some free fatty acids, diglycerides, cholesterol, and phospholipids, proteins, and water are present. Over twenty different fatty acids have been profiled in bovine i.m. fat; however, over 92% of the total fatty acid content was composed of six main fatty acids; oleic (C18:1; 41%), palmitic (C16:0; 27%), stearic (C18:0;15%), linoleic (C18:2; 3.9%), palmitoleic (C16:1; 3.7%) and myristic (C14:0; 3.6%) (Albright and Stern, 1998; Duckett, 2001). In ruminants, *de novo* fat synthesis, consisting mainly of C18:0 and C16:0 in an approximate 2:1 ratio (Jenkins, 1992), occurs in adipose tissue rather than the liver and has been shown to occur three to five times greater in adipocytes from s.c. deposition than from adipocytes from i.m. deposition (Hood and Allen, 1973). Precursors include acetate, glucose, propionate, valerate, isobutyrate, isovalerate, and 2-methyl butyrate. Acetyl Co-A is at the center of synthesis and can be produced from fatty acids, glucose (through pyruvate), amino acids, and ketone bodies. In addition, i.m. and s.c. adipose tissues exhibit characteristic patterns in the uptake of lipogenic precursors used for fatty acid synthesis as indicated by *in vitro* studies.

In s.c. adipose tissue, acetate has been shown to provide 70 to 80% of the acetyl units used in lipogenesis compared to i.m. adipose tissue, where acetate has been shown to provide only 10 to 25% of the acetyl units for lipogenesis. On the other hand, in s.c. adipose tissue, glucose provides only 1 to 10% of the acetyl units for lipogenesis while providing 50 to 75% of the acetyl units in i.m. adipose tissue (Smith and Crouse, 1984).

Adipose tissue can be divided into four distinct depots (Rouse and Wilson, 2001); fat surrounding the internal organs or internal fat/mesenteric fat; fat between the muscles or seam/intermuscular fat, which is higher in the forequarter than hindquarter area in

bovine (Swatland, 2009); fat on the surface of the animal under the hide or s.c., which is similar in both the forequarter and hindquarter area in bovine (Swatland, 2009); and fat within the muscle or i.m./marbling. The order of deposition occurs at different times in the animal's life with the order of deposition in cattle being mesenteric, intermuscular, s.c. and finally, i.m. (Pethick et al., 2004). Seam fat, s.c. fat, and internal fat can be regarded as "waste fat", while i.m. fat can be considered "taste fat" (Rouse and Wilson, 2001; Pethick et al., 2004). As mentioned earlier, the majority of the "waste" and "taste" inefficiencies in the beef industry are due to either excess or insufficient fat deposition (Dolezal, 2000).

The literature indicates that i.m. and s.c. adipocytes represent cell populations that differ from each other, both morphologically and metabolically, as fatty acid biosynthesis in marbling adipocytes is 5 to 10% of the rates seen in s.c. adipose tissue with rate of incorporation of palmitic acid in i.m. adipose tissue exceeding the rate of incorporation in s.c. adipose tissue (Hood and Allen, 1973; Lin et al., 1992; Smith et al., 2000). Hood and Allen (1973) reported adipocyte growth in young beef cattle was due to both hyperplasia (proliferation of cell number) and hypertrophy (enlargement of cell size) up to a juncture in the animal's growth phase (reported at 8 mo of age), after which s.c. adipose tissue hyperplasia ceased and growth was due exclusively to hypertrophy; however, i.m. adipose tissue hyperplasia continued throughout 14 mo of age.

As previously mentioned, adipose tissue can be distinguished from other lipid depots by its location within the perimysium connective tissue alongside myofibers (Moody and Cassens, 1968). However, in some cases subjective judgment is necessary to discriminate i.m. adipose tissue (marbling) from connective tissue. Marbling, or i.m.

fat, does not include fat that connects with any s.c. or intermuscualr fat depot. When connections do occur, this seam fat is considered an invasion and is not included in the marbling score. From a developmental point of view, this exclusion may or may not be appropriate as the fore mentioned depots can be described as adipose tissue *per se*, in that it is made up of adipose cells imbedded in connective tissue in close proximity to a blood capillary network (Harper and Pethick, 2004). More so, myocytes have the ability to store some fat as droplets termed intramyocellular lipid that are not visible with the naked eye and thus are not regarded as a major contributor to the total intramuscular (marbling) fat pool of the beef carcass (Harper and Pethick, 2004).

Adipose Development

Numerous genes are expressed exclusively in adipose tissue during adipogenesis, the process by which mature fat cells develop from preadipocytes (Rosen and Spiegelman, 2000; Rosen et al., 2002). The fate of the adipocyte precursor cell depends on the orchestration of various factors including the adhesion of the cell to the surrounding ECM or to neighboring cells, the combination of growth factors, the endocrine environment, neural inputs and the availability of macro- and micronutrients (Hausman et al., 2009). Preadipocytes are an intermediate cell type which develop prior to obtaining the expression characteristics of differentiated adipocytes (Harper and Pethick, 2004), but can be induced to terminally differentiate into mature adipocytes when treated with “adipogenic” factors. The timing of adipose tissue development, which tends to occur in multiple locations in the body (Rosen and Spiegelman, 2000), depends not only on the species studied, but also on the specific adipose location, or

depot, being studied (Corino et al., 2005). For a specific depot to acquire and maintain the adipocyte phenotype, the timing of expression of these genes is critical (Tanaka et al., 1997). The adipocyte cell lineage develops from multipotent stem cells of mesenchymal (mesodermal) origin that can also give rise to muscle, bone, and cartilage (Rosen, 2002; Otto and Lane, 2005; Singh et al., 2007). Even though these multipotent cells can undergo commitment to several different and distinct lineages, all are within a particular physiological system. Although several factors have been identified that lead to the transformation of the multipotent mesenchymal cell to the adipocyte cell lineage *in vitro*; the signal(s), factor(s), or gene(s) responsible for this molecular transformation *in vivo* is still yet to be identified (Boone et al., 2000; Otto and Lane, 2005). The potential for cellular development of adipocytes is thought to be fixed relatively early in life after which, changes in either the size of the cells or in the numbers of cells occurs in proportion to the initial number of cells and the lipogenic enzymes expressed (Pethick et al., 2004; Cartwright et al., 2007; Wang et al., 2009).

Our present-day understanding of adipocyte development has been acquired from the study of adipogenesis employing cell culture models. These models have mainly utilized two types of cell lines, each representing cells arrested at different stages of adipocyte development (MacDougald and Lane, 1995; Novakofski, 2004; Otto and Lane, 2005). The pattern of adipose differentiation observed *in vitro* appears to follow that of *in vivo* differentiation in that the adipocyte cells express markers of terminal differentiation; that is, the ability to accumulate lipid, and express signaling and metabolic pathways associated with mature adipocytes with the cells becoming hormone, or insulin sensitive (Gaillard et al., 1991; MacDougald and Lane, 1995; Gregoire et al., 1998; Novakofski,

2004; Rosen, 2005). The first example consists of a model system utilizing multipotent stem cells that have not yet undergone commitment to the adipose lineage, i.e. C3H10T1/2, NIH-3T3, or BALB/3T3cell lines (MacDougald and Lane, 1995; Otto and Lane, 2005). Commitment, as defined by Otto and Lane (2005), is the process by which a stem cell from the vascular stroma responds to signal(s) and undergoes restriction to the adipocyte lineage, but does not express markers of terminal differentiation. The second model system utilizes preadipocytes, or cell lines, which have already been committed to the adipocyte lineage, i.e. 3T3-L1, 3T3-F442A, or Ob17. The *in vivo* adipogenic factors used to stimulate differentiation usually consists of a combination of 3-isobutylmethylxanthine, insulin, and dexamethasone (Rubin et al., 1978; Gaillard et al., 1991; MacDougald and Lane, 1995; Otto and Lane, 2005). Individual exposure to any of the three differentiation factors stimulates only a low degree of differentiation (Tang et al., 2003a). Committed preadipocytes maintain the propensity for growth but withdraw from the cell cycle before adipose conversion or differentiation (Gregoire et al., 1998). Prior to differentiation the morphological characteristics of the preadipocyte cell line is similar to that of a fibroblastic preadipose cell found in the stroma of adipose tissue. However, upon the initiation of differentiation, the fibroblastic appearance is abandoned and a rounded “unilocular” appearance is assumed and the cell acquires the morphological and biochemical characteristics of an adipocyte (Ailhaud et al., 1992; MacDougald and Lane, 1995; Otto and Lane, 2005).

The differentiation process involves the interaction of both positive and negative factors, of both a cis-acting and trans-acting nature, regulating an intricate cascade of signaling pathways (MacDougald and Lane, 1995; Gregoire et al., 1998; Boone et al.,

2000; Rosen, 2005). Some pathways involve the suppression of negative effectors that act to maintain the undifferentiated state (Boone et al., 2000; Moldes et al., 2003), some pathways act to regulate transcription factors which orchestrate differentiation (Boone et al., 2000; Prusty et al., 2002), and yet other pathways regulate the adipocyte in response to certain physiological condition(s) of the individual. The first stage of differentiation of the preadipocyte is growth arrest at the G_0/G_1 (G_1/S_1) checkpoint of the cell cycle (Gregoire et al., 1998). Preadipocytes grown under cell culture conditions begin to differentiate shortly after confluency or cell to cell contact. Preadipocyte differentiation requires this period of growth arrest, not cell confluency or cell to cell contact. Although confluency leads to growth arrest, cell to cell contact is not a prerequisite (Ailhaud et al., 1992; Gregoire et al., 1998). Following growth arrest, an appropriate combination of mitogenic and adipogenic signals are needed for the preadipocytes to re-enter the cell cycle, in what is termed a period of mitotic clonal expansion, a period where cells carry out at least one round of DNA replication and cell doubling (Gregoire et al., 1998; Tang et al., 2003a; Otto and Lane, 2005). Numerous studies have established that mitotic clonal expansion inhibition clearly blocks adipogenesis and is a prerequisite for *in vitro* terminal differentiation (Gregoire et al., 1998; Tang et al., 2003a; Otto and Lane, 2005). Rosen et al. (2000) pointed out that even though mitotic clonal expansion is required for *in vitro* preadipocytes, a debate over the *in vivo* requirement still exists. Upon completion of mitotic clonal expansion, the cells enter a distinct arrest stage of the cell cycle termed G_D; cells must arrest and be maintained at this stage for differentiation to occur. Cells arrested at this stage can either re-differentiate or reinstate cell proliferation (cell mitosis) (Scott et al., 1982a; Otto and Lane, 2005). However, once the cells exit the

G_D stage, they become committed to terminal differentiation and growth is directed towards deposition of intracellular fat globules. Mitotic clonal expansion comes to an end with the expression of the transcription factors, peroxisome proliferator-activated receptor-gamma (PPARγ) and CCAAT/enhancer binding protein alpha (C/EBP/α), that act synergistically to coordinate the regulation of gene expression and whose actions characterize the differentiated adipocyte (Tanaka et al., 1997).

Three types of PPAR identified are α, δ, and γ; with four isoforms of PPARγ arising from differential promoter action and alternate gene splicing PPARγ(1-4) (Metzger et al., 2005; Fernyhough et al., 2007). PPARγ1 and 2 differ by 30 amino acids with PPARγ2 expressed selectively in adipocytes, while PPARγ1 is expressed in several different tissues and PPARγ 3 has been shown to be expressed in macrophages, adipocytes, and the large intestine (Spiegelman, 1998; Tsai and Maeda, 2005; Fernyhough et al., 2007). PPARγ3 and 4 produce translated proteins identical to PPARγ1; thus, only two receptors result in the biological system, PPARγ1and 2 (Fernyhough et al., 2007). PPARγ expression in adipocytes is 10 to 30 times higher than in other tissues (Spiegelman, 1998) with the roles of PPARγ1 and 2 still remaining an open question, as no clear consensus has been drawn from the literature thus far (Rosen and MacDougald, 2006). However, several genes involved in adipocyte differentiation have been found to be regulated by PPARγ2, including CD36 and phosphoenolpyruvate carboxykinase (Fernyhough et al., 2007).

PPARγ and C/EBP/α are elevated throughout the differentiation process as well as the rest of the life of the adipose tissue (Tontonoz et al., 1994, 1995; Rosen, 2002). The increase of PPARγ and C/EBP/α is preceded by the activation of two other members

of the C/EBP family expressed within two to four hours after induction of differentiation, C/EBPβ and C/EBPδ (Lane et al., 1999; Wu et al., 1999a; Tang et al., 2003b). A slight reduction in adipose development has been observed in cells under *in vitro* conditions which lack either C/EBPβ or C/EBPδ; however, if both C/EBPβ and C/EBPδ are lacking the cells are severely restricted in their development (Rosen and Spiegelman, 2000). Despite C/EBPβ and C/EBPδ having been shown to be required for differentiation *in vitro*, Tanaka et al. (1997), in studies using C/EBPβ(-/-) and C/EBPδ(-/-) null mice, reported C/EBPβ and C/EBPδ were not required for differentiation *in vivo*, although it was shown that adipogenesis was drastically impaired. Likewise, even though PPARγ and C/EBP/α can be induced in the absence of C/EBPβ and C/EBPδ, co-expression of PPARγ and C/EBP/α alone is not adequate for complete adipocyte differentiation *in vivo* (Tanaka et al., 1997). As previously mentioned, PPARγ and C/EBP/α act synergistically to coordinate the regulation of gene expression and are required for adipogenesis both *in vitro* and *in vivo*; however, C/EBP/α is not capable of supporting adipogenesis in the absence of PPARγ. Rosen et al. (2002) reported that ectopic C/EBP/α, using a retroviral delivery system, failed to induce lipid accumulation in PPARγ (-/-) cells; suggesting C/EBP/α is limited to the induction and maintenance of PPARγ levels and the establishment of insulin sensitivity in the cell, as adipocytes lacking C/EBP/α are not insulin sensitive (Wu et al., 1999a; Wu et al., 1999b). On the other hand, Wu et al. (1999b), using C/EBPα (+/+) and C/EBPα (-/-) cell lines, demonstrated that PPARγ was capable of supporting adipogenesis in the absence of C/EBP/α, but only when PPARγ is ectopically expressed and observed the number of C/EBPα (-/-) cells were comparable to

the C/EBPα (+/+); however, the C/EBPα (-/-) cells accumulated less lipid in smaller droplets than the C/EBPα (+/+). Also, ectopically delivered PPARγ, via a retroviral delivery system, was shown to rescue the adipogenic potential in PPARγ (-/-) cells demonstrating that PPARγ is required for adipogenesis (Rosen et al., 2002). The preceding indicates both PPARγ and C/EBP/α contribute to a single pathway of adipose development, maintaining each other's expression and acting to synergistically initiate adipogenesis gene expression.

Adipose Related Genes

Fatty Acid Binding Protein 4

Fatty acid binding protein 4 (FABP4) is one of nine members in the superfamily of lipid-binding proteins. Expression of fatty acid binding proteins (FABP) are tissue-specific and are regulated at the transcriptional level with most exhibiting patterns of expression related to cellular development and differentiation (Glatz and van der Vusse, 1996; Storch and Thumser, 2000; Zimmerman and Veerkamp, 2002; Chmurzynska, 2006). FABP's have been shown to modulate intracellular lipid homeostasis, as they bind with high affinity to both long chain ($C \geq 14$) saturated and unsaturated fatty acids and regulate the transport of fatty acids between cellular compartments, enzymes, and/or the metabolism of fatty acids in the cell (Zimmerman and Veerkamp, 2002; Jenkins-Kruchten et al., 2003; Chmurzynska, 2006; Storch and McDermott, 2008). Two different transfer mechanisms are utilized by FABP's in the transfer of fatty acids to membranes; an aqueous phase diffusion transfer and a transfer involving a direct interaction with the membrane (Weisiger, 2002). FABP4, shown to be expressed in both adipose tissue and

macrophages, is expressed in fully differentiated cells exhibiting high rates of fatty acid metabolism and constitutes approximately 1 to 6% of the cytosolic protein in a mature adipocyte (Smith and Storch, 1999; Storch and Thumser, 2000; Storch and McDermott, 2008). FABP4 is thought to transfer lipids to membranes through a direct, or collisional mechanism, involving ionic interactions with the lysine residues within the helix-turn-helix domain (Smith and Storch, 1999). FABP4 also has been shown to interact with hormone-sensitive lipase (HSL), the rate limiting enzyme of lipolysis or the break down (or hydrolysis) of stored fat in the cell. Substrates for HSL include triglycerides, cholesterol esters and retinyl esters (Shen et al., 1999; Kraemer and Shen, 2002; Jenkins-Kruchten et al., 2003). FABP4 has been shown to enhance the transcriptional activities of PPARγ and PPARβ (Tan et al., 2002; Storch and McDermott, 2008), and the activity of keratinocyte fatty acid binding protein (KFBP), also found in adipocytes and macrophages (Storch and McDermott, 2008). The association between FABP's and PPAR's seems to be highly selective for different FABP/PPAR pairings and dependent on the presence of specific ligands. For example, FABP4 specifically enhances PPARγ while KFBP activates PPARβ (Tan et al., 2002). Work by Deng et al. (2006) demonstrated that PPARγ positively up-regulated HSL in the presence of the transcription factor, specificity-1 (SP1), as the use of mithramycin A, a specific inhibitor of SP1, abolished the up-regulation of HSL. Previous work by Moore et al. (1991) showed the activity of FABP4 in the *Longissimus* muscle not to be a good index for the determination of i.m. fat accretion in bovine. However, FABP4 polymorphisms from high- and low-marbling animals revealed two single nucleotide polymorphisms (SNPs): AAFC01136716.1:g.7516G>C and g.7713G>C and were shown to be associated with

both marbling (i.m.) and s.c. fat depth in cattle (Michal et al., 2006). Also, FABP4 polymorphisms were shown to be associated with fatness traits and i.m. fat accretion in pigs (Chmurzynska, 2006; Damon et al., 2006). When adipose cells were compared at the same size and same age in porcine, the FABP4 transcript and protein content was lower in i.m. adipocytes compared to s.c. adipocytes (Gardan et al., 2007).

More recently, Jurie et al. (2007) reported on the possibility of the FABP4 mRNA levels and protein content, indicators of i.m. adipocyte number and oxidative enzyme activities, as indicators of the ability of steers to deposit intramuscular fat according to muscle type and breed. In looking at two different breeds of cattle, Japanese Black (JB) and Holstein (HOL), FABP4 expression level was higher in all stages of cells from preadipocytes to differentiation in JB than HOL suggesting a higher potential for the JB to accumulate lipids (Ohsaki et al., 2007). In JB and HOL animals (approximately 11 months of age) after a fattening period of 60 d, Wang et al. (2005b) reported FABP4 mRNA levels to be elevated in JB cattle vs. HOL, indicating that JB animals had accumulated more mature adipocytes per unit of muscle than HOL. More so, in a study conducted to identify marbling-related genes in high and low marbled Hanwoo steers, the gene expression of FABP4 was approximately two times higher in high marbled relative to low marbled steers (Lee et al., 2008b). Similar results between animals with marbling potential were reported by Wang et al. (2009), where FABP4 mRNA levels were shown to be elevated at the time of weaning in Wagyu x Hereford crossbred animals vs. Piedmontese x Hereford crossbred animals suggesting evidence of early cellular development of adipocytes in animals with marbling potential. In animals of the fore-mentioned crosses, fetal *Longissimus* muscle was sampled at four stages of myogenesis

and muscle maturation; primary myogenesis (d 60), secondary myogenesis (d 135), beginning (d 195) and final stages (birth). FABP4 expression was greater in the *Longissimus* muscle of Wagyu-sired fetuses at d195 and birth than Piedmontese sired fetuses (Lehnert et al., 2007). In a later study by Lee et al. (2007) looking at FABP4 gene expression in the *Longissimus* muscle between high and low marbling Hanwoo cattle, FABP4 gene expression was greater in the high marbling group of cattle relative to the low marbling group.

Stearoyl-CoA Desaturase

Two main transformations occur when dietary lipids enter the rumen. The first is the hydrolysis of the ester bond present in the triacylglylcerides, phospholipids and glycolipids by bacterial lipases with the glycerol that is released being readily utilized by the rumen microorganisms. The second arises due to the fact that polyunsaturated fats are toxic to rumen microorganisms, so a process termed biohydrogenation transforms the unsaturated fatty acids to saturated fatty acids (Church, 1988; Bauman et al., 2003; Nam and Garnsworthy, 2007). Biohydrogenation involves the isomerization of the fatty acid chain to a monoenoic acid and then ultimately to stearic acid (C18:0) (McDonald et al., 2002; Bauman et al., 2003), which is one of the main fatty acids that dictates fat hardness (Smith et al., 1998). Stearoyl-CoA desaturase (SCD) is an integral membrane protein of the endoplasmic reticulum that catalyzes the Δ^9 desaturation of saturated fatty acids that are synthesized *de novo* or derived from the diet. The main fatty acids involved in desaturation by SCD are myristate, palmitate, and stearate into the Δ^9 monounsaturated fatty acids (MUFA), myristoleate, palmitoleate and oleate, respectively (Cameron et al.,

1994; Miyazaki and Ntambi, 2003; Dobrzyn and Ntambi, 2005; Ohsaki et al., 2007). MUFA's are key substrates used in the synthesis of complex lipids such as triglycerides, diacylglycerol, cholesterol esters and wax esters (Miyazaki and Ntambi, 2003; Dobrzyn et al., 2008). However, long chain polyunsaturated fatty acids (PUFA's) such as eicosapentanoic acid (20:5) and docosahexaenoic acid (20:6) are not incorporated into triglycerides to any extent in ruminants, but are mainly restricted to membrane phospholipids, and thus, are found primarily in muscle rather than fat tissue (Wood et al., 1999). Oleic acid (18:1) is the most abundant fatty acid in US beef and is the active precursor for acyl-CoA cholesterol acyltransferase (ACAT) in cholesterol ester synthesis and diacylglycerol acyltransferase (DGAT) in triacylglycerol synthesis; thus, SCD activity can affect both the fatty acid composition in the plasma membrane and lipid metabolism in adipose tissue (Chung and Johnson, 2007).

SCD activity and gene expression has been shown to be higher in bovine adipose tissue than in muscle, liver, or intestinal mucosa (Smith et al., 2006b). SCD activity appears to be essential for subsequent development of lipogenic activity of s.c. adipose tissue in growing steers (Smith et al., 2006b; Hausman et al., 2009) as s.c. adipose tissue was shown to have approximately twice the SCD catalytic activity as i.m. adipose tissue, and also a greater concentration of MUFA than i.m. adipose tissue (Archibeque et al., 2005). However, in many breed types of cattle, there has been shown to be an almost linear increase in i.m. adipose tissue deposition over time on a finishing diet with this increase in i.m. adipose tissue deposition being consistent with an increase in i.m. adipose tissue MUFA and SCD activity (Hausman et al., 2009). Depot differences in SCD

mRNA expression have also been reported in sheep where SCD expression was higher in s.c. adipose tissue compared to omental or perirenal adipose tissue (Daniel et al., 2004).

Grain-based diets provide carbon for i.m. adipose tissue development and promote fat softness by stimulating the expression of SCD (Smith and Lunt, 2007). More so, in cattle fed a grain based diet, the fatty acids in adipose tissue typically become less saturated between weaning and slaughter (Smith et al., 2006b). In looking at SCD gene expression in the *Longissimus* muscle between high and low marbling Hanwoo cattle, Lee et al. (2007) observed SCD gene expression to be greater in the low marbling group of cattle relative to the high marbling group, and suggested the SCD gene may be related to fatty acid composition rather than the amount of fat accumulation. In a recent study by Smith et al. (2009), where 8 mo old steers were adapted to a corn-based diet (calf-fed) or allowed to graze native pasture until 12 mo of age (yearling-fed), SCD gene expression was only barely detectable in s.c adipose tissue of the 8 mo old weaned calves. The SCD gene expression was almost eight times greater in both the s.c. and i.m. adipose depots in steers on the corn-based diet than those allowed to graze native pasture. It was suggested the difference to be from the higher concentrate intake of the corn-fed steers relative to those on native pasture. Additionally, SCD gene expression declined in the corn-fed diet steers between 12 and 16 mo of age in both the s.c. and i.m. adipose depots.

However, in comparing s.c. adipose tissue from the mid-loin region of pasture-fed cattle or cattle placed in the feedlot fed a diet consisting of sorghum, roughage, and 5% whole cottonseed for 100, 200, or 300 d, SCD activity was observed to be 60 to 85% greater in cattle from the pasture-fed diet than cattle on the feedlot diet suggesting that feeding whole cottonseed reduced the activity of SCD (Yang et al., 1999). Cattle from

the pasture-fed diet had lower total saturated fatty acids and higher total unsaturated fatty acids in adipose tissue than cattle in the feedlot. However, no differences were observed in the fatty acid composition or in SCD activity in the s.c. adipose tissue between cattle fed in the feedlot for 100, 200 or 300 d (Yang et al., 1999).

Multiple SCD isoforms have been identified in several animal species including rat, hamster, humans and most recently bovine, with the discovery of the SCD5 isoform (Lengi and Corl, 2007). The isoforms seem to follow a pattern of tissue-specific expression with evidence of specific-substrate preferences, giving rise to the concept that the isoforms play distinct physiological roles in the body (Lengi and Corl, 2007; Lengi and Corl, 2008). For example in the mouse, SCD1, SCD2, and SCD4 desaturate both palmitoyl-CoA and stearoyl-CoA, while SCD3 desaturates palmitoyl-CoA but not stearoyl-CoA (Miyazaki et al., 2006). SCD mRNA levels were shown to be affected by breed as SCD mRNA was higher in both *Longissimus* muscle and s.c. adipose tissue in JB cattle than in HOL cattle. Subsequently, JB cattle had a higher MUFA percentage in the s.c. adipose tissue than HOL cattle (Taniguchi et al., 2004).

More recently, three polymorphisms in SCD1 were found to be associated with six fat deposition and fatty acid composition traits in skeletal muscle in a Wagyu x Limousin reference population. Positive correlations were shown for beef marbling score, amount of MUFA, and conjugated linoleic acid (CLA) content but a negative correlation was shown for saturated fatty acid content. However, these three SNPs were observed not to be associated with s.c. fat depth or percent KPH fat in the same reference population (Jiang et al., 2008).

CD36

CD36, originally referred to as fatty acid translocase (Su and Abumrad, 2009), is a membrane bound glycoprotein, expressed at the cell surface and in lysosomes and belongs to the class B scavenger receptor family with the primary role varying with cell type (Hajri and Abumrad, 2002). CD36 can facilitate the translocation of long chain fatty acids in adipocytes as well as in heart and muscle cells (Nicholson et al., 2000; Febbraio et al., 2001; Su and Abumrad, 2009). CD36 can also function as a cell adhesion molecule and as a class B scavenger receptor (Hajri and Abumrad, 2002). There are eight different subclasses to the scavenger receptor family (A-H) (Murphy et al., 2005). Class B receptors recognize a wide range of ligands including collagen, fatty acids, anionic phospholipids, thrombospondin, apoptotic cells, native LDL, Ox LDL, HDL and VLDL (Murphy et al., 2005). CD36 has been shown to be expressed by macrophages, dendritic cells, platelets, endothelium, adipocytes, smooth muscle and certain epithelia such as the breast, retina, and intestine (Nicholson et al., 2000; Febbraio et al., 2001; Murphy et al., 2005).

CD36 within cellular membranes seem to be associated with lipid rafts which can be described as detergent-resistant membranes with a microdomain size of 50 nm containing high levels of sphingolipids and cholesterol (Ehehalt et al., 2006; Ehehalt et al., 2008; Su and Abumrad, 2009). Long chain fatty acid (LCFA) uptake was shown to be dependent on the integrity of these lipid rafts. Decreasing the level of cholesterol decreased the level of long chain fatty acid uptake by as much as 50%. Also, decreasing ceramide synthesis was shown to lower long chain fatty acid uptake (Ehehalt et al., 2008). Caveolae are formed from lipid rafts that contain the proteins caveolin-1, -2 and

-3, and can be described as small invaginations (50 to 100 nm) of the plasma membrane of many cell types, especially adipocytes, which have been shown to interact functionally with CD36 (Shu et al., 2008). Caveolin-1 deficient mice have reduced levels of CD36 (Ring et al., 2006; Frank et al., 2008) or the CD36 is mistargeted away from the membrane reducing fatty acid uptake (Shu et al., 2008) and exhibit phenotypic features similar to CD36 null mice (Razani et al., 2002).

In vitro studies using 3T3-L1 cells showed no CD36 protein detected in preadipocytes; however, CD36 was detected in cells 3 days post-differentiation (Qiao et al., 2008). CD36 has been identified as an important marker of preadipocyte differentiation into adipocytes as CD36 mRNA expression was induced during the differentiation process and fatty acid uptake coincided with the up-regulated expression of CD36 (Abumrad et al., 1993; Sfeir et al., 1997). CD36 gene expression in weaning piglets was shown to be higher in visceral adipose tissue as compared to s.c. and i.m. However, an *in vitro* preadipocyte culture showed CD36 mRNA expression to be greater in adipocytes from i.m. adipose tissue than from s.c. adipose tissue (Shu et al., 2008). CD36 has been shown to be regulated by all three peroxisome proliferator receptors (PPAR) α, γ, and δ in a tissue specific manner (Hajri and Abumrad, 2002). More so, CD36 contains a C/EBP response element and C/EBP α and β were shown to increase CD36 expression with C/EBPα being a more potent inducer of CD36 than C/EBPβ, indicating C/EBPα involvement in regulating CD36 expression at the transcriptional level (Qiao et al., 2008).

The *in vivo* uptake and metabolism of two iodinated fatty acid analogs, beta-methyl-iodo-phenyl pentadecanoic acid (BMIPP) and 15-(p-iodophenyl) pentadecanoic

acid (IPPA), was investigated in different tissues of CD36 null mice along with the *in vitro* lipid incorporation of palmitate by adipocytes. Uptake of BMIPP and IPPA was reduced in tissue such as heart (50-80%), skeletal muscle (40-75%), and adipose tissue (60-70%) of CD36 null mice compared to that of the wild type. These tissues normally have high expression levels of CD36. However, in tissues where there is normally a low expression level or an undetectable level of CD36, no alteration of intakes was detected (Coburn et al., 2000). Triglyceride synthesis was inhibited at the level of diacylglycerol acyltransferase as a 50-68% decrease in labeled incorporation into triglyceride along with a 2 to3 fold increase in labeled incorporation into diglycerides was observed (Coburn et al., 2000). Similarly, the rate of long chain fatty acid transport across the cell membrane was increased with increased CD36 expression at the membrane level with long chain fatty acid transport decreased with decreased CD36 expression at the membrane level (Coburn et al., 2001). The transport of fatty acids was shown to be increased in contracting muscle as a result of CD36 being translocated from an intracellular depot to the plasma membrane (Bonen et al., 2004; Holloway, 2008). Also, fatty acid oxidation has been shown to be regulated in part by both carnitine palmitoyltransferase I (CPT1) and CD36 in the mitochondria (Holloway, 2008). More so, insulin has been shown to induce the translocation of FAT/CD36 from an intracellular depot to the plasma membrane via a phosphatidylinositol signaling step revealing a level of regulation that may further help our understanding of the relation between fatty acid metabolism and insulin resistance (Luiken et al., 2002).

Fatty Acid Synthase

Fatty acid synthase (FAS) is a multienzyme complex containing seven distinct domains which catalyzes the last step in the fatty acid biosynthetic pathway (Zhang et al., 2008). Changes in FAS mRNA content are tissue specific and are affected by altered rates of gene transcription, mRNA processing, and/or mRNA stability (Clarke, 1993). The thioesterase domain (discussed below) is responsible for termination of fatty acid synthesis and thus plays an essential role in the determination of the chain length of the FAS final product (Clarke, 1993). Recently, single nucleotide polymorphisms have been reported in the bovine FAS gene (Roy et al., 2006; Morris et al., 2007; Zhang et al., 2007; Zhang et al., 2008). FAS polymorphisms were reported to be associated with milk-fat percentage in HOL cows (Roy et al., 2006), and the five polymorphisms reported by (Morris et al., 2007) were associated with variations in the fatty acid composition in milk and s.c. adipose tissue, as increased percentages of C14:0 were shown in milk fat with an opposite effect occurring in s.c. adipose tissue. Furthermore, two of the three polymorphisms identified in the thioesterase domain, g.17924A>G and g.18663 T>C were significantly associated with fatty acid composition of several fatty acids, phospholipids, triacylglycerides, and the overall total lipids in Angus cattle (Zhang et al., 2007; Zhang et al., 2008). Cattle with the g.17924GG genotype had a greater percentage of oleic acid (C18:1), docosapentaenoic acid (C22:5), and total monounsaturated fatty acids (MUFA) compared to the g.17924AA genotype. In contrast, the eicosatrienoate (C20:3) content was greater and the polyunsaturated fatty acids tended to be greater in cattle with the g.17924AA genotype vs. the g.17924GG genotype, indicating that contributions in the variation of MUFA content in cattle is not only from variation in the

SCD genotype (mentioned earlier), but also from the FAS genotype (Zhang et al., 2007; Zhang et al., 2008).

The FAS complex consists of seven subunits; β-ketoacyl synthase (KS), malonyl/acetyl transferase (MAT), β-hydroxyl dehydratase (HD), enoyl reductase (ER), β-ketoacyl reductase (KR), acyl carrier protein (ACP), and palmitoyl thioesterase (TE) (Asturias et al., 2005; Carlisle-Moore et al., 2005; Cronan, 2004; Maier et al., 2006; Witkowski et al., 2004). The first committed step in the synthesis of palmitate is the formation of malonyl-CoA from HCO_3 and acetyl-CoA catalyzed by acetyl-CoA carboxylase. One "primer" molecule of acetyl-CoA and six molecules of malonyl-CoA interact, one-after-the-other, with the FAS complex to yield palmitate. Entry into fatty acid synthesis cycle, involves the transfer of a "primer" acetyl-CoA to the ACP involving MAT to produce a "transient" acetyl-ACP; as there is a subsequent transfer of the acetyl group of acetyl-ACP to a cysteine residue of ß-KS. Malonyl-ACP is formed from the transfer of malonyl-CoA to ACP again involving MAT. For both the preceding reactions, the attacking group of MAT is the oxygen of a serine hydroxyl group. The next reaction is a condensation reaction and involves the transfer of the acetyl group of the β-KS to the methyl group of malonyl-ACP to form aceto-acetyl-ACP. This involves the decarboxylation of malonyl, followed by the attack of the resultant carbon ion on the carbonyl carbon of the acetyl group. Aceto-acetyl-ACP is reduced to D-β-hydroxybutyryl-ACP by β-KR which is converted, in a hydration reaction, to α–β-trans-butenoyl-ACP by β-HD. The α–β-trans-butenoyl-ACP is then hydrogenated to form butyryl-ACP by ER. NADPH is used in the two preceding reduction reactions. The butyryl-ACP then cycles back through the FAS complex, entering in the place of acetyl-

ACP; another malonyl-ACP is formed via MAT. This elongation cycle repeats six times to form palmitate, as each cycle elongates the fatty acid chain by two carbons. At the end of the last cycle, TE terminates the chain elongation and releases palmitate from the ACP by hydrolyzing the acyl-S-phosphopantetheine thioester bond (Chakravarty et al., 2004). Palmitoyl thioesterase is very crucial, as it is the monitor to ensure that palmitate is the major end product of the FAS complex (Chakravarty et al., 2004). Only the last two carbons of the fatty acid chain of palmitate originate from acetyl-CoA, the remaining carbons are from malonyl-CoA (Murray et al., 2003; Voet and Voet, 2004b; Asturias et al., 2005; Maier et al., 2006). The following reaction (Figure 1, Maier et al., 2006) illustrates the interaction of the subunits involved in FAS beginning with the initial transfer of the acyl group of acetyl Co-A to the ACP (1); the six repeating cycles (2-6); and the termination cycle involving the release of palmitate from the ACP (7).

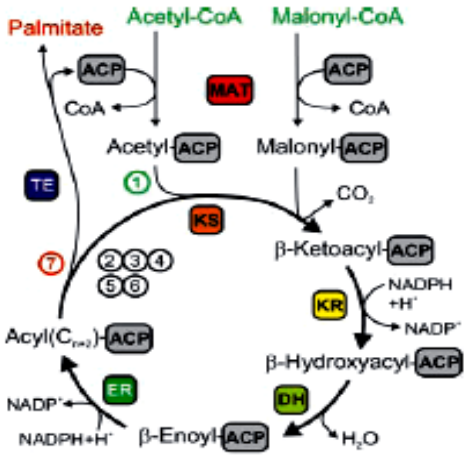

Figure 1. FAS catalytic cycle and domain organization. Adapted from Maier et al. (2006).

The following equation sums the fatty acid synthesis reaction; keep in mind that malonyl-CoA is originally derived from acetyl-CoA (Murray et al., 2003; Voet and Voet, 2004b).

8 acetyl-CoA + 14 NADPH + 7 ATP →

Palmitate + 14 $NADP^+$ + 8CoA + 6 H_2O + 7 ADP + 7 P_i

The ACP is bound to the growing fatty acid chain throughout fatty acid synthesis and is released at the end of the last cycle through FAS. The intermediate products during fatty acid synthesis are attached as thioesters to the ACP (Majerus, 1967). The acyl binding site of both the ACP and CoA is 4'-phosphopantetheine which is linked to the ACP subunit via a serine residue and acts like a long flexible arm to orientate the intermediates to the active sites of the other subunits within the FAS complex (Majerus et al., 1965; Majerus, 1967).

Palmitoyl Thioesterase

The TE subunit of FAS is made of two subdomains made up of nine α-helices and eight β-strands. Domain A, the larger of the two subdomains, consists of α–helices and β-strands while subdomain B consists of α-helices. In human FAS, subdomain A contains the catalytic triad (Figure 2) consisting of serine-2308, aspartic acid-2338, and histdine-2481. The palmitoyl chain-binding site consists of a long groove at the interface between subdomains A and B leading into a small "pocket", in close proximity to the catalytic site. The orientation and hydrophobic nature of the residues along the groove and the TE subunit's orientation to the ACP, more or less, cause the groove to act as a "ruler" to ensure that palmitate (C16) is the correct end-product. Approximately the last four carbons of the elongating fatty acid chain extend into the "pocket", allowing room for two carbons to be added, before chain termination commences. The TE subunit exhibits a high specificity for C16 compounds with a marked decline in enzyme activity

for fatty acid chains shorter than C16 and chains longer than C18. The residues lining the chain-binding groove arise from the α8 (Phe-2418, Ala-2419, Ser-2422, Lys-246) and α5 (Phe-2370 & 2371) helix of subdomain B, α1 (Leu-2223 & 2223, Val-2224) and the loop between β2 and α2 (ILe-250, Glu-2251) of subdomain A, (Chakravarty et al., 2004).

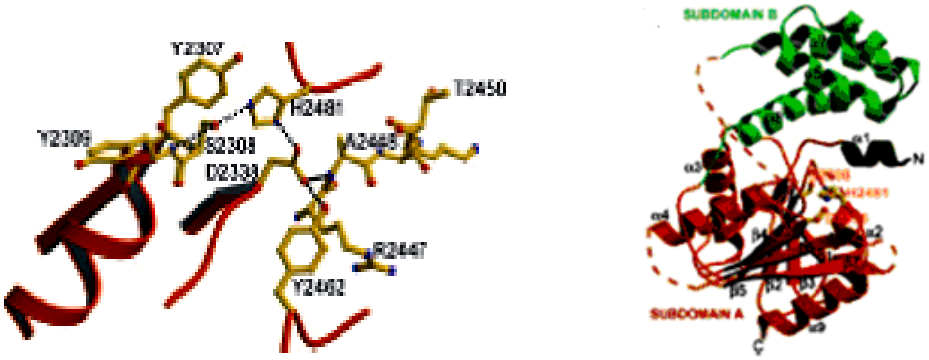

Figure 2. Structure and Molecular Organization of Mammalian Fatty Acid Synthase. Adapted from Chakravarty et al. (2004).

Conventional Dogma of FAS Organization

From the early 1980's to as late as 2004, models in the literature depict the two monomers of FAS in a "head to tail" organization; that is, the monomers are laying side-by-side in an extended anti-parallel orientation allowing for two centers of fatty acid synthesis (Jayakumar et al., 1997; Voet and Voet, 2004b). Biochemical, electron microscopic and small-angle neutron-scattering studies revealed FAS to take on the appearance of side-to-side chains with a dimension of 160 x 146 x 73 Å. By using various proteases, the sequence of the FAS catalytic subunits from the amino to carboxyl end was postulated (Figure 3; Jayakumar et al., 1997). The conventional dogma of FAS organization is based on studies where 1,3,dibromo-2-propanone formed a cross-link between the active site of the ß-KS subunit on one monomer of FAS and to the 4'-phosphopantetheine group of the ACP subunit on the other monomer of FAS (Chirala

and Wakil, 2004; Cronan, 2004; Witkowski et al., 2004; Asturias et al., 2005). Residues 1-406 are assigned to ß-KS, 428-815 to MAT, 829-969 to ß-HD, 1630-1850 to ER, 1870-2100 to ß-KR, 2114-2190 to the ACP, and 2200-2505 to TE. There is a non-catalytic region extending from 970 to1630 (Joshi et al., 1997, 1998). Keep in mind that in the hypothesized sequence of the subunits, the ß-ketoacyl synthase subunit is the first subunit of the sequence and the ACP subunit is next to the last subunit of the sequence. During fatty acid synthesis, the interaction between the ß-KS subunit and the ACP subunit, due to the "loading" of the acetyl group from the ACP to the cysteine of the active site of ß-KS, is more critical than the interaction between the ACP and the active sites of the other subunits where the ACP orientates the substrate at the active site to facilitate enzymatic action (Cronan, 2004). So, the postulated "head to tail" FAS model (Figure 3), which allows the –SH group of the 4'-phosphopantetheine group of the ACP of one monomer to be in close proximity to the –SH of the cysteine at the active site of the ß-KS on the other monomer, was deemed acceptable (Cronan, 2004; Voet and Voet, 2004b; Witkowski et al., 2004).

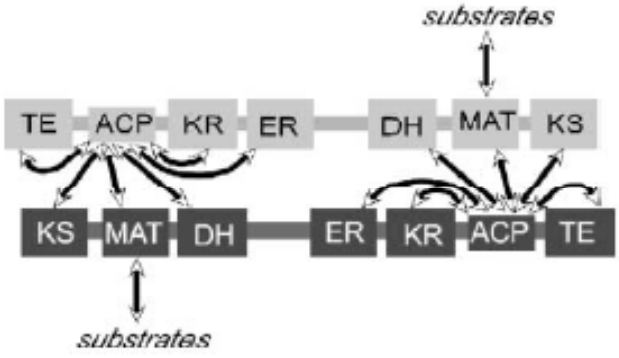

Figure 3. Postulated "head to tail" FAS model. Adapted from Voet and Voet (2004b).

Alteration of Conventional Dogma Model

Stuart Smith's lab in 1997 (Joshi et al., 1997) and 1998 (Joshi et al., 1998) suggested the conventional model for FAS be revised to reflect the discovery that the two monomers of FAS are not simply positioned side-by-side in a fully extended conformation, but are coiled in a manner that allows the ACP to access the ß-HD domain on the same monomer. This was accomplished by using monomers where the active sites in the subunits were altered by mutations, but still produced fatty acids. Further work using monomers with altered mutations led to yet another proposed alternative model of FAS organization.

Proposed Alternative Model of FAS Organization

In 2004, Stuart Smith's lab (Witkowski et al., 2004) noted several more discrepancies in this altered conventional model and proposed an alternative model; this time describing the FAS complex as an intertwined head to head dimer (Figure 4). This model was proposed based on findings where altered FAS dimers, constructed from a wild type (functional) monomer and a nonfunctional monomer, due to altered subunit active sites by mutation, were still able to synthesize fatty acids. In this model, there is a still a separation of the ß-KS of the two monomers; however, it was observed that for FAS to form dimers the ß-KS subunits had to be present and the function of the ß-KS active site be maintained.

The transition of the ß-KS subunits from a monomer to dimer paralleled the successful "loading" of the acetyl group from the ACP to the ß-KS cysteine residue at the active site. The conditions that interrupted the monomer to dimer transition of the ß-KS

subunits also interrupted the monomer to dimer formation of the entire FAS complex (Cronan, 2004; Witkowski et al., 2004; Asturias et al., 2005). FAS dimers constructed with subunits consisting of different mutations and studied under conditions that limit the conformation variability in the monomers using Cyro-Electron Microscopy and gold labeling of the N-terminal lended support to this proposed alternative model, as the ß-KS and MAT domains were shown to be able to access the ACP subunits of either monomer, which is not possible in the "head to tail" model (Asturias et al., 2005). In addition, the symmetry shown within the FAS complexes constructed with different mutations implied that monomers in a functional FAS complex could exhibit different conformations suggesting the possibility of a different rate or stage of fatty acid synthesis occurring between the two monomers; possibly elongation occurring in one monomer and β-carbon processing occurring in the other (Smith, 2006).

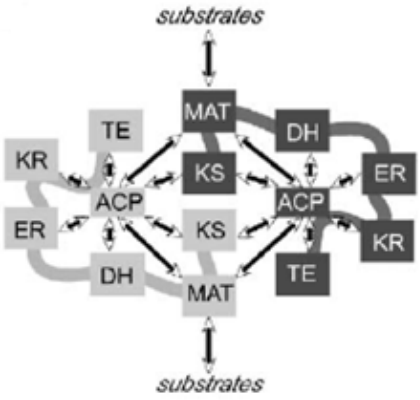

Figure 4. Proposed Alternative Model of FAS Organization. Adapted from Witkowski et al. (2004).

Alteration of the Proposed Alternative Model of FAS Organization

Maier et al. (2006), using x-ray crystallography, revealed a 4.5 Å partial structure of porcine FAS. For the most part, this structure agreed with the alternative model proposed by Smith, (2006) that is the FAS complex is indeed an intertwined head to head

dimer. However, the subunit positioning is altered to some degree. Maier's group described FAS as an X-shaped unit consisting of a central body region with arms and legs (Figure 5-a). The x-ray crystallography was able to offer the positioning of the catalytic subunits of the FAS dimer involved in elongation of the fatty acid chain. The ACP and TE subunits could not be mapped with any degree of certainty due to their high degree of flexibility; the white stars in the figure below indicate possible regions of attachment. The ACP of each monomer is able to interact with the ß-KS and MAT subunits of its own monomer or the adjacent FAS monomer. In Figure 5-b, the active sites of each subunit are depicted by the white and blue balls, while the hollow spheres around each of the active sites depicts the length of the 4'-phosphopantetheine arm, giving an estimate of how close the ACP has to be for interaction with the active site of the subunit. Maier et al. (2006) speculated that the 4'-phosphopantetheine arm may not serve as the lone "swinging arm" to facilitate substrate presentation per se, but may combine with the modest movement of the "arms", "legs", and "waist" regions of the monomer allowed by the interconnecting regions, with movement caused by the binding and releasing of substrate. Although 65 to 80% of fatty acid chain elongation occurs from inter-monomer ACP/ ß-KS interaction and 20 to 35% occurs through intra-monomer interaction (Asturias, 2006), Maier et al. (2006) put forth that there may be difficulty in the ACP reaching the active centers of the opposite monomer based on this x-ray crystallography model and the predicted sites of the ACP location. The intersubunit and interdomain connections are shown in figure 5-b. The importance of the ß-KS dimerization for FAS activity was previously mentioned (Witkowski et al., 2004), however, there seems to be a dimerization interface which extends through the body of FAS into the ER monomers.

The pseudo-dimer of ß-HD is not between the different monomers, but is within the chain of one monomer (Maier et al., 2006). Therefore, there may be more significance to the FAS dimerization than the ß-KS subunit itself. The evidence for the new structural model for FAS is evident; however, detailed understanding of the FAS complex is warranted. Cronan sums up these new findings very well;…"despite the wrong turn, it seems unlikely that the incorrect head to tail model seriously impeded progress with FAS. The difficulties have been technical, rather than conceptual, and working with such a large enzyme remains a formidable challenge" (Cronan, 2004).

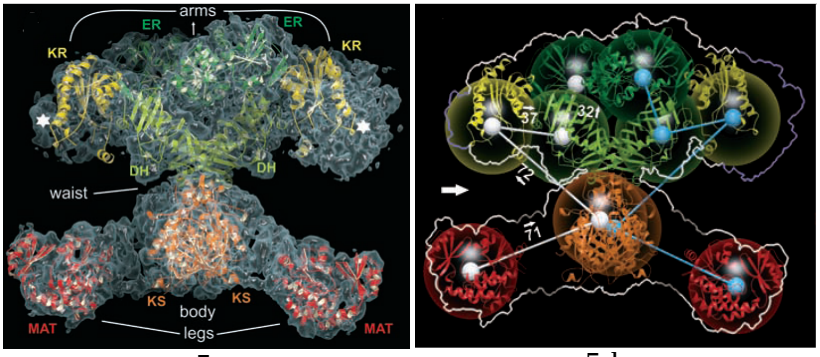

5-a 5-b

Figure 5. Alteration of the Proposed Alternative Model of FAS Organization. Adapted fromMaier et al.(2006).

Zilpaterol Hydrochloride

Zilmax® (Intervet/Schering-Plough Animal Health, Millsboro, DE) is a synthetic β_2-adrenergic agonist used for increased rate of weight gain, improved feed efficiency and increased carcass leanness in cattle fed in confinement for slaughter (Dikeman, 2007; Kern et al., 2009), and contains the active ingredient zilpaterol hydrochloride (ZH), (±)-trans-4,5,6,7-tetrahydro-7-hydroxy-6-(isopropylamino) imidazo [4,5,1-jk]-[1]benzazepin-2(1H)-one, hydrochloride (Intervet, Inc. 2007). Synthetic β-adrenergic agonists (β-AA) are similar pharmacologically and chemically to the naturally occurring catecholamines

dopamine, norepinephrine, and epinephrine (Vasconcelos et al., 2008), with epinephrine being the methylation product of norepinephrine. Norepinephrine and epinephrine are inactivated by the enzymes catechol-o-methyltransferase (COMT), which introduces a methyl group to the catecholamine 3-hydroxyl group of the aromatic ring, and monoamine oxidase, which uses oxygen to remove the amine group (Smith, 1998). Some aromatic hydroxylations are not deactivated by COMT as some substitutions are deactivated in the liver and intestine by conjugative biotransformation enzymes, mainly through glucuronidation and sulfation. As β-agonists exist as racemates, they have been shown to be susceptible to stereospecific biotransformations, with those β-agonists containing halogen ion substitutions for hydroxyl groups on the aromatic ring being resistant to rapid degradation by conjugative biotransformation enzymes (Smith, 1998).

In 2006, ZH was approved by the U.S. Food and Drug Administration (FDA) as a feed ingredient for cattle during the last phase of the feeding period to improve production efficiency, but has been used since the 1990's in Mexico and South Africa (Avendano-Reyes et al., 2006). Zilpaterol hydrochloride is administered through the feed the last 20 to 40 days of the feeding period at levels of 60 to 90 mg/animal/d and is required to be withdrawn three days prior to harvest. In 2008, the FDA approved ZH for use in cattle feeds in five different combinations with MGA® (melengestrol acetate), Rumensin® (monensin, USP), and Tylan® (tylosin phosphate) [Zilpaterol, Rumensin, and Tylan; Zilmax and Rumensin; Zilmax and MGA; Zilmax, MGA, and Rumensin; Zilmax, MGA, Rumensin, and Tylan].

Repartitioning agents developed in meat animals require safety and residue testing, and there is limited data on zilpaterol residues for Zilmax-treated food animals.

In humans, plasma levels of other β-AA generally occur within 1to3 hr after administration with excretion of radioactivity nearly completed by 48 to 72 hr following administration in most animals studied (Smith, 1998). A rise in plasma levels of the β-AA, clenbuterol, was detected within 20 min to 1 hr after administration in veal calves where peak plasma levels plateaued between 2 and 7 hr (Meyer and Rinke, 1991). In lactating dairy cows, clenbuterol was present in plasma within 2 hr after initiation of treatment and shortly thereafter in the mammary gland with a plateau being reached in plasma by 3 to 4 d and in milk by 5 to 7 d (Stoffel and Meyer, 1993). Similar findings were reported by Dave et al. (1998), where steady state clenbuterol concentrations were achieved at 5 d in 18 wk old calves.

Zilpaterol hydrochloride residue levels in cattle have been below the threshold that poses any human health risk (Moody et al., 2000; Anderson et al., 2004) which are 0.02, 0.05, 0.10, and 0.10 ppm for muscle, liver, kidney, and fat, respectively (Intervet, Inc. 2006). The Freedom of Information Summary for Zilmax (Intervet, Inc. 2006) indicates that when cattle were fed 0.15 mg/kg BW (or 6.8 g/ton in the diet) of ^{14}C-zilpaterol, concentrations in edible tissues reached a steady state after 12 days of feeding (approximately 300 ng/g in liver and 25 ng/g in muscle) and levels of total residues (unchanged ZH and the major metabolite, deisopropyl-zilpaterol) in liver, kidney, muscle and fat after a 12-hr withdrawal to be 256±49.1, 161±27.0, 19±2.1, and 9.2 ppb, respectively. Levels at the 24 hr withdrawal were 180±12.1, 88±4.3, 11±2.3 ppb, and non-detectable (ND), respectively. Levels at the 48 hr withdrawal were 138±19.8, 32±21.9 ppb, ND, and ND, respectively, while levels at the 96 hr withdrawal were 99±14.9, 8±3.1 ppb, ND, and ND, respectively. The data for total residue indicates the

residues deplete more slowly from the liver than the other tissues tested. Zilpaterol hydrochloride concentrations in liver, kidney and muscle tissue in cattle fed 0.15 mg of ZH per kg body weight for 14 days after a one day withdrawal was 27.1, 44.3, and 6.93 ug/kg (ppb), respectively, and after a ten day withdrawal were 0.03, 0.03, and 0.01 ug/kg (ppb), respectively (Stachel et al., 2003). In sheep fed 0.15 mg of ZH per kg body weight for 10 days, liver ZH residues after a 0, 2, 5, and 9-d withdrawal were 29.3, 1.5, 0.13, and 0.10 ng/g (ppb). Kidney residues were 29.6, 1.10, 0.09, and ND ng/g (ppb), respectively, after a 0, 2, 5, and 9-d withdrawal and muscle residues were 13.3, 0.86, 0.12, and 0.08 ng/g (ppb), respectively (Shelver and Smith, 2006). Also, during the first three days of withdrawal, urinary ZH half-life in sheep was estimated to be approximately 15.3±1.87 h (Shelver and Smith, 2006).

The current generation βAA's possess structural configurations which have resulted in shorter half-lives and lower potencies allowing for their continued safe use in the livestock industry (Smith, 1998). As the minimum concentration of Zilpaterol, or its metabolic products, in liver and muscle tissues to elicit a positive growth response is unclear, the continued action of Zilpaterol after withdrawal periods greater than 3 d is doubtful.

Adrenergic Receptors

The concept of α- and β-adrenergic receptors in the late 1940's came about through work by Ahlquist (Bylund, 2007) investigating the physiological functions stimulated or inhibited by norepinephrine and epinephrine and a few other compounds (Mersmann, 1998; Bylund, 2007). Adrenergic receptors (AR) are categorized into two

main groups, α-adrenergic and β-adrenergic. Original classification of the AR was based on their response in involuntary muscle to an adrenergic drug; α-AR causing contraction in involuntary muscle and β-AR causing relaxation of involuntary muscle (Peters, 1989). In general, alpha receptors mediate excitation or increased activity of the effector cells and beta receptors mediate relaxation or decreased activity of the effector cells. The subtypes of the α-AR, α_1 and α_2, were further classified as either post-synaptic or pre-synaptic, respectively, with classification of the β-AR; β_1, β_2, and β_3 based on the specific response of the tissue to the β-adrenergic drug (Peters, 1989). Currently, the α_1-AR, α_2-AR and β-AR are considered subfamilies with further subtype classification consisting of α_{1A}-AR, α_{1B}-AR, α_{1D}-AR, for the α_1-AR subfamily; α_{2A}-AR, α_{2B}-AR, α_{2C}-AR for the α_2-AR subfamily; and β_1, β_2, and β_3, with some speculation of a β_4 in mouse, for the β-AR subfamily (Granneman, 2001; Mersmann, 2002; Badino et al., 2005). However, some have classified the β_4 as a β_3 isoform (β_{3a} and β_{3b}, respectively) (Evans et al., 1999). The subtypes of the β-AR subfamily, β_1, β_2, and β_3, share an approximate 45 to 60% homology within any given species (Mersmann, 2002), while an approximate 70% homology is shared for any given subtype across species (Pietri-Rouxel and Strosberg, 1995; Mersmann, 2002). The β_1, β_2, and β_3-AR subtypes range in size from approximately 460 to 420 to 410 amino acids, respectively, with the species-specific amino acid sequence able to cause functional modification to any given β-AR subtype (Mersmann, 2002; Cherezov et al., 2007). The distribution of the receptor subtypes depends on tissue type with the β_1-AR subtype and β_2-AR subtype co-expressed in most tissues with the ratio of these subtypes varying according to tissue type, while the β_3-AR

subtype has a more limited pattern of expression and is found in both white and brown adipose tissue (Mills, 2002a).

Phenothalamines developed for use in the livestock industry target the β_1- and β_2-subtype receptor (Moody et al., 2000). The adrenergic receptors are anchored to the plasma membrane and consist of seven transmembrane helices connected by extracellular and intracellular loops (Lefkowitz et al., 1988; Lefkowitz et al., 2008) and are present in essentially all mammalian tissues (Mersmann, 1995). Ligand/receptor binding involves numerous amino acids from several of the domains and occurs at the center of the seven transmembrane domains (Mersmann, 1998), with the β-AR being deactivated by several different mechanisms. Messenger RNA of all three β-AR subtypes has been shown to be expressed in bovine adipose tissue and have been shown to be involved in the multifaceted regulation of lipolysis in dairy cattle (Sumner and McNamara, 2007). β_2-AR is the primary receptor (75%) found in bovine adipose tissue as compared to β_1-AR (25%) (Van Liefde et al., 1994). β_2-AR was also reported as the primary receptor in perirenal adipose tissue and the *Longissimus* muscle (Sillence and Matthews, 1994). β_3-AR mRNA expression was very low or undetectable in animals after three months of age (Casteilla et al., 1994; Van Liefde et al., 1994); however, adipocytes in rodents exhibit a strong response to β_3–AR while human adipocytes are poorly responsive (Langin et al., 1995). More so, the most abundant β-AR mRNA in semimembranous muscle of finishing steers was for β_2-AR as ractopamine supplementation for the last 28 d on feed had no effect on the abundance of ß$_1$-AR or ß$_3$-AR mRNA, but tended ($P = 0.09$) to increase ß$_2$-AR mRNA (Winterholler et al., 2007). Similar findings were reported by (Sissom et al., 2007) for heifers supplemented with ractopamine the last 28 d on feed as

there was no effect of ractopamine supplementation on ß$_1$-AR mRNA expression; however, there was a tendency for ractopamine supplementation to increase expression of ß$_2$-AR mRNA. In *Longissimus* muscle of beef steers, Winterholler et al. (2008) reported ractopamine tended to increase the abundance of β1-AR mRNA, but did not affect β_2-AR or β_3-AR. Contradictory results were reported by (Walker et al., 2007) as β_1-AR, β_2-AR, and β_3-AR mRNA levels were present in LM of steers, but mRNA expression of β_1-AR and β_2-AR mRNA was decreased by ractopamine supplementation for 28 d. Transcript mRNA for β_1-AR, β_2-AR, and β_3-AR were present in adipocytes of porcine (McNeel and Mersmann, 1995) and in the adipocytes in humans (Seydoux et al., 1996). In swine, β_1-AR and β_2-AR were reported to comprise nearly 95% of the β-AR in adipocytes with β_1-AR representing 80% of the total β-AR (McNeel and Mersmann, 1999), and the primary subtype mediating lipolysis (Mills et al., 2003). However, β_2-AR was reported to be the predominately expressed receptor in muscle while in the adipocyte β_1-AR and β_2-AR were reported to be expressed in almost an equal percentage (Spurlock et al., 1994; Sillence et al., 2005).

The β_2-adrenergic agonist zilpaterol has a greater affinity for the β_2-AR subtype receptor compared to the β_1-AR subtype but is capable of binding both the β_1-AR subtype (Ki = 1.0 x 10-5) and β_2-AR subtype (Ki = 1.1 x 10-6) receptor (Verhoeckx et al., 2005). Zilpaterol [(rac)-1] is a 1:1 mixture of (+)-1 and (-)-1 as hydrochlorides. Competitive binding assays using recombinant human β_2-AR subtype receptors to determine the affinities of (rac)-1 and its enantiomers revealed that the β_2-AR subtype

receptor activity stems from the (-)-1enantiomer alone, as the (+)-1 displaced only 3% of the ligand at the β_2-AR subtype receptor (Kern et al., 2009).

β-Adrenergic Agonists

β-adrenergic agonists (β-AA) can be defined as "organic molecules" which bind the β-AR such that the agonist-receptor complex activates the stimulatory G-protein (G_s protein) (Mersmann, 1998). To confer biological activity the β-AA must embrace distinct conformational configurations which include; a substituted six-member aromatic ring, a hydroxyl group bonded to the β-C in the R configuration, a positively charged N in the ethylamine side chain and a bulky substituent on the aliphatic N (Smith, 1998). As mentioned earlier, ligand/receptor binding occurs at the center of the seven transmembrane domains and involves numerous amino acids from several of the domains. More specifically, ligand/receptor binding occurs at three points on the β-AA; the β-C hydroxyl group, the aliphatic N and the aromatic ring with alterations or substitutions at any of these points having a profound effect on receptor binding (Spurlock et al., 1993; Patil et al., 2008). Physiological activity depends on not only the "organic molecule"/receptor affinity, but also the rate of absorption, rate of metabolism, rate of elimination, and rate of distribution to target tissues (Smith, 1998). These "organic molecules" are a class of phenothalamines similar in structure to endogenous epinephrines and catecholamine with pharmacological similarities (Barnes, 1995). However, not all phenothalamines are classified as β-AA. Some phenothalamines bind the α-AR, while others are classified as β-antagonists. Even more, some are specific for a specific subtype within the α_1-AR, α_2-AR and β-AR subfamilies (Smith, 1998).

The β-AA cannot pass through the cell membrane, thus ligand binding occurs on the plasma membrane of the cell. Plasma membrane receptors mediate two main functions: 1) binding of ligands outside of the cell, and 2) the activation of an effector system leading to the generation of a second messenger system capable of activating various downstream processes (Lefkowitz et al., 1988). The binding of a β-AA promotes the interaction between the intracellular domains of the β-AR and the heterotrimeric G-protein, G_s (Strosberg, 1993). The G_s protein is a member of the superfamily of regulatory GTP-ases that are collectively known as G-proteins (Voet and Voet, 2004d). The AR is one of the most extensively studied groups of G-protein-coupled receptors (Strosberg, 1993). The G-protein-coupled receptors are not a simple on/off switch; instead, they behave more like a rheostat that can dial in any level of activity from inactive to active (Kobilka and Deupi, 2007). The heterotrimeric G-protein is comprised of three different subunits, α, β, and γ. On the basis of sequence similarity, the α subunits have been divided into four families, G_s, Gq_{11}, $G_{12/13}$ and $G_{i/o}$ (Neves et al., 2002). The $G_s\alpha$ subunit activates adenylate cyclase; the enzyme that converts ATP to cAMP, the second messenger in the system, which binds to the "regulatory units" of the inactive protein kinase A (PKA) holoenzyme, which in turn is "activated", causing the release of the "catalytic subunits", which in turn phosphorylates various downstream intracellular proteins (Mersmann, 1998; Voet and Voet, 2004d). The catalytic subunits are able to diffuse into the nucleus where they phosphorylate cAMP response element binding (CREB) which binds to certain DNA sequences or cAMP response elements (CRE) which can increase or decreases the transcription of certain genes (Voet and Voet, 2004d; Lynch and Ryall, 2008). Proteins that can be activated by PKA phosphorylation

are Hormone-sensitive lipase (HSL), which is the rate limiting step in lypolysis, and perilipin A, which is a key regulator of triacylglycerol storage and assists the docking of HSL onto lipid droplets to facilitate maximal lipolysis (Mersmann, 1998; Marcinkiewicz et al., 2006; Granneman and Moore, 2008). On the other hand, acetyl-CoA carboxylase, which is the rate limiting step in lipogenesis, is deactivated by PKA phosphorylation (Tong, 2005). Down-regulation of PKA occurs by a negative feedback mechanism as PKA also activates a cyclic nucleotide phosphodiesterase enzyme, which converts cAMP back to 5'AMP, thus reducing the amount of cAMP that can activate PKA in the cell (Mehats et al., 2002). Cyclic AMP is short lived in the system. The cAMP/PKA signaling pathway is a versatile pathway involved in the regulation of cardiovascular function, reproductive function, metabolism in adipocytes, and immune function (Tasken and Aandahl, 2004).

The β-AA is effective for a limited period of time as the efficacy of β-AA can be altered by desensitization caused by the continuous exposure of the β-AR to the β-AA (Hausdorff et al., 1990b; Lynch and Ryall, 2008). Desensitization can be defined as *the attenuation of response despite continued presence of the stimulus* (Mills, 2002b). There are three mechanisms of desensitization. The first is the functional uncoupling of the β-AR from G_s, which involves the phosphorylation of the β-AR which occurs very rapidly (usually within seconds or minutes) when agonist exposure occurs and reduces the β-AR affinity for the agonist and is considered a completely reversible process (Mills, 2002b; Badino et al., 2005). Upon agonist binding to the βAR, a conformational change to the βAR occurs that allows phosphorylation to take place (Kohout and Lefkowitz, 2003). This β-AR phosphorylation involves two kinases; protein kinase A (PKA) and the G-

coupled receptor kinases (GRK), which consists of seven known isoforms (Kohout and Lefkowitz, 2003), including a specific enzyme which phosphorylates Ser and Thr residues in the βAR carboxy tail, GRK-2 or β-adrenergic receptor kinase1 (βARK1) (Mills, 2002b; Kohout and Lefkowitz, 2003). The β-AR exhibits an increased affinity of G_i over G_s when phosphorylated, essentially switching the signaling pathway from G_s to G_i, can inhibit the production of cAMP from ATP. The β_3-AR is usually less responsive to desensitization than β_1-AR or β_2-AR; with β_2-AR more readily desensitized than β_1-AR, as there are subtype differences to phosphorylation. In human β-AR, the β_1-AR contains one PKA site and ten βARK sites, the β_2-AR contains two PKA sites and eleven βARK sites, and the β_3-AR contains no PKA sites and three βARK sites (Hausdorff et al., 1990a) and is resistant to short-term uncoupling responses (Granneman, 1992). GRK phosphorylation also promotes the βAR to bind arrestin. The arrestin family consists of four proteins that regulate the signaling and trafficking of numerous G-protein-coupled receptors. Arrestin can further block G-protein-mediated signaling, in some cases as much as 80% (Kohout and Lefkowitz, 2003), or lead into the second mechanism of desensitization which is physical sequestration of the receptor away from the cell surface by targeting the receptor for internalization where the receptor can be either targeted for degradation or recycled back to the plasma membrane (Gurevich and Gurevich, 2006; Moore et al., 2007). β-AR sequestration is a reversible process which is not a significant mechanism underlying rapid desensitization (Hausdorff et al., 1990a; Yu et al., 1993). The third mechanism is down-regulation of the total number of receptors (Yu et al., 1993; Mills, 2002b; Badino et al., 2005). Down-regulation was defined by Mills (2002b), as the decline in the total β-AR and contributes to desensitization from chronic exposure to

an agonist. Down-regulation, shown to occur in both *in vitro* and *in vivo* models, develops more slowly, taking hours or days to occur, with the decline in binding sites related to potency and efficacy of the agonist. Down-regulation of the β-AR is not rapidly overcome and is slower to overcome than the event of uncoupling (Mills, 2002b). Antagonists do not cause down-regulation in the β-AR, but have been shown to increase the number of β-AR in number and responsiveness (Glaubiger and Lefkowitz, 1977). Interestingly, work by Lanzara (2005) demonstrated that with the combination of an agonist and a competitive antagonist in an optimal and specific ratio maintains the active state and supports the concept that desensitization can be controlled *in vivo* at the level of the initial receptor response. Intracellular homeostasis is maintained due to the ability of the β-AR to down-regulate following chronic activation (Lynch and Ryall, 2008). However, following down-regulation, transcription and translational processes are required to restore membrane receptor numbers (Johnson, 2006b). Though an abundance of information regarding β-AR desensitization and down-regulation exists in the literature, the body of information about the regulation of β-AR synthesis is somewhat lacking (Lynch and Ryall, 2008).

Phenothalamines are often referred to as repartitioning agents because of their ability to redirect nutrients away from adipose tissue and toward muscle (Ricks et al., 1984; Moody et al., 2000). Enhanced muscle hypertrophy observed due to β-AA feeding occurs by direct, receptor-mediated changes in protein synthesis and degradation rates of skeletal muscle tissue. β-AA seem to act by increasing the efficiency of growth by preferentially stimulating skeletal muscle growth as compared to adipose tissue. This repartitioning affect is thought to be brought about by an increase in protein synthesis, a

decrease in muscle protein degradation or a combination of both, or by the release of free fatty acids from adipose tissue, which then could be used as a source of energy for amino acids (muscle mass) (Baxa, 2008; Chung and Johnson, 2008). One of the major proteins involved in protein synthesis is myosin, the most abundant protein present in striated muscle cells, constituting approximately 25% of the total protein pool (Baldwin and Haddad, 2001). Muscle is composed of various ratios of Type I (slow contracting, oxidative) and Type II (fast contracting, mixed glycolytic/oxidative) fibers (Yang and McElligott, 1989). The four major myosin heavy chain (MHC) isoforms found in adult mammalian skeletal muscles are, MHC type I, slow fiber type, and MHC type II, fast fiber type, IIA (MYH2), IIX/D (MYH1), and IIB (MHY4) (Schiaffino and Reggiani, 1994; Pette and Staron, 2000) with the contractile characteristics of the muscle determined by the overall contribution of each fiber type (Depreux et al., 2002). In pigs when ractopamine was fed for 42 d, MHCIIA (MYH2) and IIX (MYH1) fiber types were decreased while MHCIIB (MHY4) fiber type, the fastest and most glycolytic fiber type, was increased. In contrast, MHCIIA (MYH2) and IIX (MYH1) fiber types were increased in the control pigs (Depreux et al., 2002). Chikuni (2004) was not able to detect MHCIIB (MHY4) in bovine skeletal muscle. Baxa (2008) reported no differences in MHC-I mRNA expression in Zilpaterol supplemented cattle; however, MHC-IIX (MYH1) mRNA expression was increased while MHC-IIa (MYH2) mRNA expression had a tendency to be decreased due to Zilpaterol supplementation.

In studies where lambs (Pringle et al., 1993) and steers (Wheeler and Koohmaraie, 1992) were fed the β-AA $L_{644,969}$, the rapid alteration of muscle growth was closely related to the activity of the calpain-calpastatin system. In lambs fed a finishing

diet and supplemented with or without 4 ppm of the β-AA, $L_{644,969}$, and slaughtered after 0, 2, 4, and 6 wk, Pringle et al. (1993) reported cathepsin-B activity was higher and cystatin-like activity was lower after 2 wk in supplemented lambs than in control lambs, but returned to control levels thereafter. In steers weighing approximately 350 kg supplemented with 0 or 3 ppm of the β-AA, $L_{644,969}$, for 6 wk in a high-concentrate diet; Wheeler and Koohmaraie (1992), reported higher calpastatin activity in muscle from the β-AA-fed steers at 0 and 7 d postmortem than control steers. There were no differences in μ- or m-calpain or in cathepsins-B or -B+L or cystatin between steers supplemented with β-AA and control steers. Furthermore, in steers supplemented with the β-AA cimaterol, calpastatin mRNA and calpain II large subunit mRNA was increased 96% and 30%, respectively, vs. nonsupplemented steers (Parr et al., 1992).

Page et al. (2004) reported a significant increase in apoptosis in epididymal and parametrial adipose tissue in rats treated with the β-AA clenbuterol and ractopamine, suggesting the activation of β-AR's can trigger the apoptotic process in adipocytes. β-AR signaling has also been implicated in the apoptotic process in other tissues such as heart and skeletal muscle; however, there is deliberation over whether apoptosis is promoted or inhibited in these tissues (Lynch and Ryall, 2008).

The following figure (Figure 6) is a schematic of the mode of action for β-AA proposed by Ricks et al. (1984).

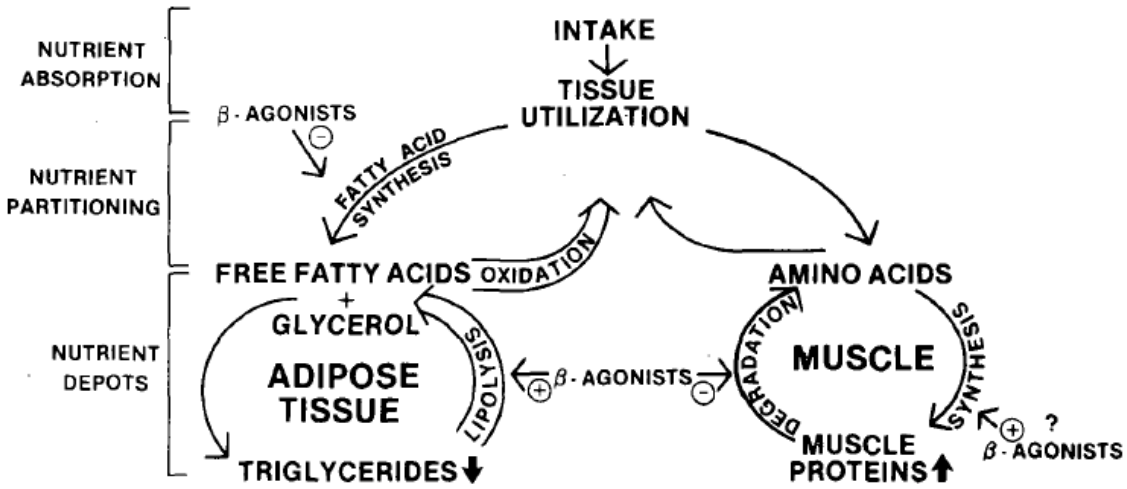

Figure 6. Mode of action for β-AA proposed by Ricks et al., (1984).

The β-AA clenbuterol has been shown to increase blood flow when administered via close arterial infusion into the iliac artery in the hind limb in cattle, suggesting that β-AA may have an indirect effect on muscle hypertrophy by increasing the nutrient availability to specific tissues. Also reported was a progressive net uptake of amino acids, as amino acid uptake was increased by 50% and 80% at d 7 and 14, respectively, after infusion (Byrem et al., 1998). The increased blood flow may also allow for non-esterified fatty acids to be carried away from adipose tissue to increase lipid degradation (Mersmann, 1998). In general, when β-AA were fed to cattle, pigs, poultry, and sheep, an increase in muscle mass and decrease in fat mass has been reported (Mersmann, 2001; Sillence, 2004). However, cattle and sheep seem to have a greater response to β-AA compared to swine, while poultry appear to be the least responsive (Moody et al., 2000). The level of responsiveness seen in poultry may be attributed to the current level of genetic selection in the industry, as poultry may be approaching the maximum biological growth rate that can be achieved (Mersmann, 1998).

Different species of animals seem to have different responses to β-AA (Mersmann, 1995, 1998) as a particular β-AA may not activate the target β-AR or the target tissue as well in one species as another. This may involve differences in the number of receptors in the tissue, the agonist affinity towards the receptor, the coupling of the agonist-receptor complex to the signal transduction system, the differences in delivery of the agonist to the receptor site, the differences in agonist or receptor deactivation, or the β-AR subtype may change with the phase of differentiation or the hormone environment of the cell (Mersmann, 1998). For example, the β-AA ractopamine was shown to be a full agonist at the β_1-AR and a partial agonist at the β_2-AR in the guinea pig (Colbert et al., 1991). More so, the β-AA ractopamine had a higher affinity for middle s.c. adipose tissue than for *Longissimus* muscle and *Semitendinosus* (ST) muscle in porcine; while the β-AA clenbuterol had an overall greater binding affinity than ractopamine for i.m. and s.c. adipose tissue as well as *Longissimus* muscle and *Semitendinosus* muscle (Spurlock et al., 1993). Interestingly, several antagonists for β_1-AR and β_2-AR have been shown to be partial or full agonists for β_3-AR (Mersmann, 1998); whereas, several antagonists for β_1-AR had little selectivity for β_1-AR over β_2-AR in humans (Baker, 2005).

Effect of Zilpaterol Hydrochloride on Feedlot and Carcass Performance

Zilpaterol has been shown to have an affect not only growth performance, but also on carcass characteristics in several studies, including hot carcass weight (HCW), dressing percentage, and *Longissimus* muscle area. Plascencia et al. (1999) reported zilpaterol to increase ADG by 29%, carcass weight by 4.5%, dressing percentage by

3.6% and *Longissimus* muscle area 2.7% with no affect on KPH, fat thickness or marbling score vs. control steers when zilpaterol was fed the last 42 d of the finishing period. When carcasses were adjusted to a constant weight, gross primal cuts, boneless closely trimmed primal cuts, and boneless closely trimmed retail cuts were increased 1.7%, 2.9%, and 3.2%, respectively. More recently, Hilton et al. (2009) reported zilpaterol supplemented cattle to have a greater subprimal yield of several cuts vs. control. Furthermore, zilpaterol supplementation decreased trimable fat. Zilpaterol supplementation also increased Warner-Bratzler shear force values for *Longissimus* muscle at 7, 14, and 21 d postmortem and decreased sensory-panel juiciness, tenderness, and flavor intensity of *Longissimus* muscle steaks aged for 14 d. In a recent study where zilpaterol was fed to steers the last 33 d of the finishing period, ADG was increased 26% with significant increases reported in HCW, carcass yield, and *Longissimus* muscle area in zilpaterol supplemented steers vs. control. Meat from the zilpaterol supplemented cattle had greater Warner-Bratzler shear force values than control steers (Plascencia et al., 1999). When zilpaterol was fed the last 20 d of the feeding period and paired with a withdrawal period of 3, 10, 17, and 24 d, steers supplemented with zilpaterol had carcasses with greater individual side weights and an increase in the overall percentage of lean than control steers. Zilpaterol supplementation did not affect carcass fat determinations (Shook et al., 2009). Furthermore, increased withdrawal time increased carcass weights with improvement in percent lean for some carcass cuts seen for up to 10-d withdrawal time. Warner-Bratzler shear force values were higher at each of three aging times, 7, 14, and 21 d, in steaks from steers supplemented with zilpaterol (Shook et al., 2009). Vasconcelos et al. (2008) investigated the affects of supplementing zilpaterol

for 0, 20, 30, or 40 d before slaughter with a three day withdrawal and days on feed of 136, 157, 177, and 198 d and showed, regardless the length of time of zilpaterol supplementation, steers supplemented with zilpaterol had greater HCW, greater dressing percent, less 12th rib fat, larger *Longissimus* muscle, less KPH, and lower yield grade than 0-d control. However, marbling scores were greater for 0-d steers and a greater percentage of steers graded USDA Choice or greater than zilpaterol supplemented steers. The percentage of USDA Select carcasses was greater in zilpaterol supplemented cattle than 0-d control. These results suggest that supplementation of zilpaterol for 30 or 40 days as compared to 20 had no substantial effects on performance and carcass measurements. In looking at zilpaterol supplementation for 20 or 40 d in both steers and heifers, Montgomery et al. (2009a), observed final body weight (BW), ADG, and feed to gain (F:G) increased with zilpaterol supplementation. Also, HCW, dressing percentage, and *Longissimus* muscle area were increased in both steers and heifers while 12th rib fat and KPH were not affected. In steers and heifers quality grade was significantly decreased with the decrease in steers tending to be greater with 40-d zilpaterol supplementation vs. 20 d. Marbling score in steers was significantly decreased with the decrease tending to be greater in 40-d zilpaterol supplementation vs. 20 d. Marbling score in heifers had a tendency to be decreased with zilpaterol supplementation. In cattle from the same study, Leheska et al. (2009) reported increases in *Longissimus* muscle and Warner-Bratzler shear force values in both steers and heifers supplemented with zilpaterol. Also, sensory panel scores of juiciness, tenderness, and flavor intensity ended to be decreased in steers and heifers supplemented with zilpaterol.

CHAPTER III

Effects of winter growing programs on gene expression in different adipose tissue depots in beef steers at the end of the growing phase

D.R. Stein[1], A. Pillai[1], C.R. Krehbiel[1], G.W. Horn[1], M. McCurdy[2], J.J. Wagner[3], J.B. Morgan[1], R.D. Geisert[5] P.J. Ayoubi[4] and U.E. DeSilva[1]

[1]OSU Dept. of Animal Science, [2]Nutrition Service Associates, Kenmore, QLD, Australia, [3]Southeast Colorado Research Center, Colorado State University, Lamar, CO, [4] OSU Dept. of Biochemistry & Mol. Biology, and [5]Dept. of Animal Science, University of Missouri, Columbia

Abstract

Previous research in our laboratory demonstrated that nutrition during the growing phase affects performance of beef cattle during the finishing phase. More so, the nutritional background of beef steers (i.e., steers on supplemented native range or steers on high-gain wheat pasture) altered gene expression in s.c. and i.m. adipose tissue depots during the finishing phase in the feedlot. Microarray analyses, validated by RT-PCR, was utilized to investigate the effects of different winter growing programs on gene expression in s.c. and i.m. adipose tissue depots in beef steers at the end of the growing phase. Steers of similar breed, type, and age were assigned to initial harvest or one of three treatment diets; steers grazed on wheat pasture (WP); steers fed a sorghum silage-based growing diet (SF); or steers program fed a high-concentrate diet (PF). SF and PF were fed to gain BW similar to WP. At the end of a 112-d growing phase (GP), 6 steers

from WP, SF, and PF were harvested, with the remaining steers from each diet placed in the feedlot. A 7.6 cm^3 section was dissected from the *Longissimus* muscle at the 12^{th} rib and s.c. and i.m. adipose tissue were collected. Total RNA was extracted and cDNA microarray hybridizations performed. Preprocessing and normalization of data was accomplished utilizing GenePix AutoProcessor (GPAP 3.2). Ontology analysis was carried out using GFINDer. Ingenuity Pathways Analysis (IPA) was also utilized to identify the most relevant biological mechanisms, pathways and functions of the annotated genes. A total of 376 genes were differentially expressed (DE) between s.c. and i.m. adipose depots. Almost twice the number of DE genes was observed in WP and PF diets as SF diets. The data presented indicates the metabolic machinery for adipose tissue accretion was down-regulated in i.m. adipose tissue compared to s.c. adipose tissue as genes relevant to β-oxidation and the synthesis and transport of triacylglycerides and fatty acids were down-regulated in i.m. adipose tissue, while genes involved in glycolysis and oxidative phosphorylation were up-regulated in i.m. adipose tissue compared to s.c. adipose tissue. The main effect of diet could possibly influence adipose tissue deposition at the end of the GP as fatty acid binding protein 4 (FABP4) exhibited a tendency to be influenced by diet. IPA metabolic and signaling pathway analysis provided insight into possible differences in the molecular mechanisms affecting gene expression in i.m. and s.c. adipose tissue in beef steers at the end of the growing phase managed under different growing diets.
Key words: beef cattle, microarray, adipose tissue, gene expression

Introduction

The terms backgrounding and stockers are synonymous (Peel, 2000) and describe the production phase between the time a calf is weaned until placement into a feedlot for

finishing (Bock et al., 1991; Thomson and White, 2006). Stockers are raised primarily on forage or pasture diets in the south central and southern U.S., while silage is the primary diet fed in backgrounding lots in the north central and northern U.S. (McCurdy, 2006). Lack of available forage or pasture due to inclement weather or market conditions may warrant the confinement of animals to a drylot and fed a grain-based ration (Thomson and White, 2006). Two alternatives to roughage or pasture based programs are; 1) program feeding, defined by Galyean (1999) as the use of net energy equations to calculate the quantities of feed required to meet the needs of maintenance plus a specific ADG and 2) calf-fed programs, a system where cattle are placed on an *ad libitum* finishing diet immediately following weaning (Lardy, 1998). Due to geographical regions in the U. S., backgrounding/stocker programs involve a wide range of production environments and management skills, such that not all programs and systems are feasible for producers in the various locations in the U.S. (Peel, 2006). Previous work in our laboratory demonstrated that nutrition during the growing phase affects the performance of beef cattle during the finishing phase (Choat et al., 2003; McCurdy, 2006). More so, using suppressive subtractive hybridization, we have reported different nutritional background in beef steers (i.e., steers on supplemented native range or steers on high-gain wheat pasture) altered gene expression in s.c. and i.m. adipose tissue depots during the feedlot phase (Ross et al., 2005). Therefore, the objective in the present study was to determine the effects of different winter growing programs on gene expression in s.c. and i.m. adipose tissue depots in beef steers at the end of the growing phase.

Materials and Methods

Animals and Treatment Groups (Diet)

Adipose tissue samples utilized in the present study were collected from a previous study published by McCurdy, (2006). A total of 260 British crossbred steers were utilized for this study which included fifty steers from the Oklahoma State University cow herd and 210 steers purchased by Colorado Beef (Lamar, CO) of similar breed, type, and age (average initial BW: 236 ± 22.0 kg). Four steers were randomly selected for initial serial slaughter (INT) and were transported to the Robert M. Kerr Food & Agricultural Products Center abattoir (FAPC), located on the campus of Oklahoma State University, Stillwater, OK. The remaining steers were blocked by initial weight and randomly allotted to one of three treatment groups for winter-feeding for the growing phase (GP). The three treatment groups were managed under three different growing systems. One treatment group (WP; n = 64) was grazed as a single group on wheat pasture with unrestricted forage availability; the second treatment group (SF; n = 8 pens; 8 steers/pen) was fed a sorghum silage-based growing diet; and the third treatment group (PF; n = 8 pens; 8 steers/pen) was program fed a high-concentrate diet. Steers in the SF and PF groups were fed to gain BW at a similar rate as WP steers. All steers were implanted with progesterone (USP 200 mg) and estradiol benzoate (20 mg) (Component E-S, VetLife, West Des Moines, IA) at the start of the GP. Steers from all treatment groups were weighed at 28 d intervals. Wheat pasture grazing took place at the Oklahoma State University Wheat Pasture Research Unit in Logan County, OK, while all pen feeding was conducted at the Southeastern Colorado Research Center, Lamar, CO. Steers at OSU allocated to the SF, PF, and CF groups were transported from Stillwater, OK to Lamar, CO (688 km), while purchased steers allocated to the WP

group were transported from Lamar to Stillwater prior to the beginning of the trial. At the end of the growing phase (112 d), six steers were randomly selected from each of the WP, SF, and PF treatment groups and transported to the Robert M. Kerr Food & Agricultural Products Center **(**FAPC) abattoir in Stillwater, OK for slaughter.

Sample Collection and RNA Extraction

At slaughter, steers steers harvwested at FAPC were stunned with captive bolt and exsanguinated. Following exsanguination, a 7.6 cm^3 section was dissected from the *Longissimus* muscle between the 12^{th} and 13^{th} rib, from which s.c. and i.m. adipose tissue was collected and frozen at -80º C. Total RNA was extracted using TRIzol reagent (Invitrogen, Carlsbad, CA) (4 ml TRIzol per 1 g of adipose tissue). The adipose tissue, in TRIzol, was homogenized and centrifuged at 3,500 x g at 4º C for 15 min to separate insoluble material and excess fat. The lower aqueous (TRIzol) phase was transferred to a fresh tube and 0.2 ml chloroform/ml of TRIzol was added. Samples were centrifuged at 3,500 x g at 4º C for 30 min and the upper aqueous phase was transferred to a fresh tube. Isopropyl alcohol (0.5 ml/ml of TRIzol) was added and samples were maintained at -20º C overnight followed by centrifugation at 3,500 x g at 4º C for 10 min. The supernatant was removed and the RNA pellet washed with 75% chilled ethanol and suspended in DNase/RNase free water. A subsequent phenol:chloroform:isoamyl alcohol (25:24:1; pH 5.2) extraction of the RNA (1:1 ratio, respectively) was carried out. The RNA/phenol:chloroform:isoamyl alcohol mixture was centrifuged at 10,600 x g at 4º C for 5 min and the upper aqueous phase was transferred to a fresh tube and precipitated with 0.01 volumes of sodium acetate (3M; pH 5.2) and 2.5 volumes of chilled 98% ethanol. The

samples were then maintained at -20º C overnight and centrifuged at 10,600 x g at 4º C for 30 min. The supernatant was removed and the RNA pellet was washed with 70% chilled ethanol and suspended in DNase/RNase free water and stored at -80º C. The integrity of the RNA was analyzed utilizing gel electrophoresis (1.5%) and the RNA was quantified using a NanoDrop® ND-100 Spectrophotometer (NanaDrop Technologies, Willington, DE). The low amount of s.c. and i.m. adipose deposition in steers from INT and the i.m. adipose deposition of WP steers warranted pooling of the RNA samples to assure the abundance of RNA for the planned microarray comparisons. Three steers from each diet were selected for microarray comparison with the pooled s.c. and i.m. from INT repeated three times and individual s.c. samples from WP hybridized against the pooled i.m. sample.

Microarray Experiment

A bovine specific adipose tissue cDNA array prepared by Dr. Udaya DeSilva, Animal Molecular Genetics, Oklahoma State University, was used in this study. The printed array consisted of a 1,089 cDNA non-redundant clone library constructed from s.c. and visceral adipose tissue spotted onto Corning® UltraGAPS™ Coated Slides (Corning, NY). Array printing procedures were adapted from published literature (Hegde et al., 2000). The library was sequenced, with the EST sequences submitted to GenBank. GenBank accession numbers and dbEST IDs are presented in a supplementary table available at http://www.ansi.okstate.edu/faculty/desilva/papers/table.html. Library annotation was accomplished, with EST sequences queried against the Peptide, Unigene, and nonredundant (nr) GenBank database (Bos Taurus) with unknown EST sequences queried against the nr GenBank database (mammalian).

The OmniGrid 100 microarrayer (Genomic Solutions Ann Arbor, MI) used to print the microarray slide was equipped with a print head containing 16 print tips in a 4 by 4 fashion, with subarrays printed by the print head representing a block. The array consisted of 16 blocks in a 4 by 4 design with each probe (sequence) being printed once per array. The array was printed in triplicate on each slide to give a final 4 by 12 block slide design; accordingly each probe was represented three times on the microarray slide. The adipose microarray contained a positive control consisting of a pooled sample of cDNA used to create the library and a negative control consisting of the printing buffer. The slides were left in a humidified atmosphere after printing for 6 to 8 h to facilitate probe attachment to the slide. The slides were then baked at 80º C overnight and then stored in a vacuum desiccator at room temperature until the implementation of the hybridization protocol. The microarray slides were rinsed in 0.1% SDS for 5 min and then rinsed in sterile ddH_2O for 15 s and immediately dried for 2 min using a slide centrifuge. The microarray slides were then placed into a screw-top 50 ml conical vial containing a pre-warmed (48º C) commercial pre-hybridization buffer (BlockIt Microarray Blocking Solution, TeleChem Int., Sunnyvale, CA) and incubated at 48º C for 4 h. Slides were removed and rinsed in sterile ddH_2O for 15 s and immediately dried for 2 min using a slide centrifuge.

To compare i.m. adipose tissue expression relative to s.c. adipose tissue expression, total RNA (2.5 μg) from s.c.(reference sample) and i.m. (test sample) adipose tissue was reverse transcribed into cDNA in separate tubes using both random and dT primers and reverse transcriptase (Superscript II RT, Invitrogen, Carlsbad, CA). The reaction was carried out at 42º C for 6 h and the cDNA was subsequently labeled using the 3DNA Array 900MPX Expression Array Detection Kit (Genisphere, Hatfield, PA). The cDNA was then purified

using the Qiagen MinElute PCR Purification Kit (Qiagen Inc., Valencia, CA). Following a poly-T tailing reaction, the "tagged" cDNA was ligated to the 3DNA Capture Sequence, a 31-mer sequence specific for each the Alexa Fluor™ 546 and Alexa Fluor™ 647 and subsequently purified as previously described. For the primary hybridization (hybridizing the tagged cDNA to the array), the hybridization solution (75 ul) consisting of: 10.0 μl of cDNA/3DNA Capture Sequence of each the Alexa Fluor™ 546 and Alexa Fluor™ 647; 40.0 μl of the supplied 2X formamide-based hybridization buffer; 2.0 μl LNA dT blocker and 13μl nuclease-free water was denatured at 80º C for 10 min and deposited to a pre-hybridized array slide under a 24 x 60 mm lifterslip (Erie Scientific, Portsmouth, NH). The array was then incubated at 48º C for 18 h in a humidified hybridization cassette. Following incubation the lifterslip was allowed to wash off in a 2X sodium chloride/sodium citrate (SSC) /0.2% sodium dodecyl sulfate (SDS) solution prewarmed to 48 º C. The array slides were then washed in 2X SSC/0.2% SDS, 60º C,15 min; 2X SSC, RT,15 min; and 0.2X SSC, RT, 15 min. Following the final wash, the array slide was immediately dried for 2 min using a slide centrifuge. For the secondary hybridization, the hybridization solution (75 ul) consisting of: 2.5 μl of the fluorescent 3DNA Capture Reagent (capture reagent is complement to the capture sequence of the primary hybridization) of each the Alexis Fluor™ 546 (reference sample) and Alexa Fluor™ 647 (test sample); 40.0 μl of the supplied 2X formamide-based hybridization buffer and 30 μl nuclease-free water was deposited to the array under a 24 x 60 mm LifterSlip (Erie Scientific, Portsmouth, NH). The array was then incubated at 48º C for 4 h in a hybridization cassette. The array slide was washed and dried as previously described and stored in a light-proof container until image acquisition.

Microarray Data Analysis

To compare i.m. adipose tissue expression (Alexa 647) relative to s.c. adipose tissue (Alexa 546), hybridization signals were captured by scanning the microarray slides with lasers at two wavelengths, Alexa 546 (s.c.) and Alexa 647 (i.m.), using a ScanArray™ Express confocal laser scanner (PerkinsElmer Life Sciences Inc., Boston, MA) at a pixel size resolution of 10 microns with the resulting images saved as 16 bit TIFF images. For each slide, the laser power and photomultiplier tube (PMT) gain were adjusted to minimize variation between channels. Using a local background subtraction method (spots with foreground intensity minus background intensity), the commercial software package GenePix™ Pro 4.0 (Axon Instruments Inc., Union City, CA) was used to analyze the signal intensity values of each feature (spot) in the Alexa Fluor™ 546 and Alexa Fluor™ 647 channels. The GenePix Pro Result (GPR) files generated from the results of the image analysis from each biological and technical replication were used for further downstream analysis and ratio calculations. Preprocessing and normalization of data was accomplished utilizing the R-project statistical environment (http://www.r-project.org) with the Bioconductor and LIMMA packages (http://www.bioconductor.org) through the GenePix AutoProcessor (GPAP 3.2) website (http://darwin.biochem.okstate.edu/gpap32/) (Weng and Ayoubi, 2004). Background correction was performed using Robust Multi-array Average (RMA) algorithm (Allison et al., 2006) available in the Bioconductor/LIMMA package. Following background correction, poor quality features were removed by filtering. Such poor quality features were defined as features displaying an intensity value of 200 Relative Fluorescence Units (RFU) or less in both the Alexa Fluor™ 546 and Alexa Fluor™ 647 channels, as well as features flagged bad, not found or absent by GenePix™

Pro 4.0 were removed from the analysis. Two different normalization methods were utilized in the analysis to adjust and balance for the technical or systemic variation between the features within an array and between arrays for differences not caused by treatment. Lowess (locally weighted Least squares regression) - global intensity normalization, was used to balance the variation associated with dye bias within each array (Yang et al., 2001; Yang et al., 2002). To balance the effect of the Alexa Fluor™ 546 and Alexa Fluor™ 647 dye bias intensity between arrays, quantile normalization was utilized (Bolstad et al., 2003). Following data preprocessing, the expression ratio for each feature (gene) was calculated using the following formula where a two-fold change is represented by a $\log_2$ ratio >1.0 (up-regulation) or < -1.0 (down-regulation) with M value ($\log_2$ expression ratio) = $\log_2$ (F647-B647$_{intensity}$/F546-B546$_{intensity}$). Using GPAP 3.2, a moderated t-test was used to identify the differentially expressed array elements along with their M value ($\log_2$ ratio), their P-value obtained from the moderated t-statistic after false discovery rate (FDR) adjustment using the Benjamini and Hochberg method (Benjamini and Hochberg, 1995), and the number of individual features ($\log_2$ ratio) used for each gene. Array elements where > 50% of the total features across arrays was used to calculate the average $\log_2$ ratio, a $|t| > 2$, an M-value $|M| > +0.9$ (representing a fold change of 1.87), and an adjusted P-value < 0.01 were considered significantly differentially expressed and included for further analysis using the Genome Functional Integrated Discoverer (GFINDer) (http://www.medinfopoli.polimi.it/GFINDer/) and Entrez Gene (http://www.ncbi.nlm.nih.gov/sites/entrez?db=gene).

Gene Ontology Analysis

The web based program GFINDer (Masseroli et al., 2004) was utilized in this study and is a program designed to retrieve annotations for a list of submitted genes, perform categorization and present the results for use in gene ontology and pathway analysis where possible. Entrez Gene is the National Center for Biotechnology Information (NCBI) database for gene-specific information (Maglott et al., 2005, 2007). The Entrez gene ID of the differentially expressed genes retrieved from NCBI was used for the ontology analysis. The annotation terms were generated with emphasis based on gene ontology assessment for molecular function and biological process rather than cellular component (Ashburner et al., 2000).

Ingenuity Pathway Analysis

To further understand the extent of how genes may interact within the context of metabolic or signaling pathways, Ingenuity Pathways Analysis (IPA) (Ingenuity® Systems, http://www.ingenuity.com) was utilized to identify the most relevant biological mechanisms, pathways, and functions of the differentially expressed genes identified through GPAP 3.2. IPA enables the visualization and exploration of gene interaction and relies on the most current known relationships among human, mouse and rat genes and proteins. A data set of differentially expressed genes from INT and diets of GP containing gene ID and corresponding expression values was uploaded into the IPA application. To gain a better understanding of the interactions between genes within a biological system, an arbitrary M-value of $|M| > +0.59$ (or a fold change of 1.50) and a P-value < 0.01 were assigned as parameters for this analysis. Each gene ID was mapped to its corresponding

gene object in the Ingenuity Pathways Knowledge Base (IPKB). These genes, called focus genes, were overlaid onto a global molecular network developed from information contained in the IPKB. Networks of these focus genes were algorithmically generated based on their connectivity and assigned a network score. IPA arbitrarily sets the maximum number of focus genes in each network at thirty-five. The functional analysis of an entire dataset or single network identifies the biological functions and/or diseases that were most significant to the genes in the dataset or network. IPA uses a Fischer's exact test to calculate a P-value determining the probability that each biological function and/or disease assigned to that dataset or network is due to chance alone. The network score is the negative log of this P-value and is a numerical value used to rank networks according to how relevant they are to the differentially expressed genes in the input dataset. The network score takes into account the number of focus genes in the network and the size of the network. The network score is not an indication of the quality or biological relevance of the network; it simply calculates the approximate "fit" between each network and the focus genes from the input data set. For example, a score of "6" would indicate a $P=10^{-6}$ chance of genes appearing in the network solely by chance. A network pathway is a graphical representation of the molecular relationships between genes/gene products. Genes or gene products are represented as nodes, and the biological relationship between two nodes is represented as an edge (line). All edges are supported by at least one reference from the literature, a textbook, or from information stored in the IPKB. The intensity of the node color indicates the degree of up- (red) or down- (green) regulation. Nodes are displayed using various shapes to represent the functional class of the gene product. Edges are displayed with various labels that describe the nature of the relationship

between the nodes. For a gene to be network eligible, it must meet the criteria specified in the analysis parameters and also have at least one other full-length, wild-type gene or protein in IPKB that interacts (directly or indirectly) with this gene. Ingenuity combines eligible genes into networks that maximize their specific interconnectedness with each other relative to all molecules to which they are connected. The network algorithm optimizes for specific connectivity, so when a "hub" molecule is included in a network it connects a higher fraction of network eligible molecules relative to all molecules to which the "hub" molecule is connected with additional molecules from IPKB used to specifically connect and merge two or more smaller networks.

IPA pathway analysis identifies the pathways from the IPA library most significant to the data set. The significance of the association between the data set and the pathway is measured in two ways: 1) a ratio of the number of genes from the data set that map to the pathway divided by the total number of genes that map to the pathway; and 2) Fischer's exact test is used to calculate a P-value determining the probability that the association between the genes in the dataset and the pathway is explained by chance alone.

Quantitative RT-PCR Validation of Microarray

Validation of the i.m. adipose tissue expression relative to s.c. adipose tissue expression values generated from the microarray experiment was carried out using two-step SYBR green qRT-PCR. Gene specific primers for thirteen different candidate genes selected for microarray data validation were designed using Primer 3 (Rozen and Skaletsky, 2000) and analyzed using Oligo Analyzer 3.1 (Integrated DNA Technologies),

http://www.idtdna.com/analyzer/Applications/OligoAnalyzer/. All primer sequences, annealing temperatures and product size are presented in Table 3.1.

Total RNA (1 ug) from s.c. and i.m. adipose tissue depots from each individual animal for the diet and phase randomly selected for validation was reverse transcribed using the QuantiTect® Reverse Transcription Kit (QIAGEN Inc., Valencia, CA) using oligo-dT and random primers in a total volume of 20 ul. RT- PCR reactions were carried out in duplicate, using a MyiQ Real-Time PCR detection system (Bio-Rad Laboratories, Hercules, CA) in a 15 ul reaction consisting of: 7.5 ul of 2X PerfeCTa™ SYBR Green SuperMix for iQ™ (Quanta BioSciences, Inc**.** Gaithersburg, MD), 400 nM forward primer, 400 nM reverse primer and 100 ng of cDNA. 18S ribosomal RNA was assayed as a normalization control for all samples assayed. A standard curve with five serial dilution points was included for each gene along with a no-template control. Thermal cycling conditions were 95º C for 2.5 min followed by 38 repetitive cycles of 95º C for 15 s, variable annealing temperature for 30 s, and 72º C for 30 s. Immediately following RT-PCR, a melt curve analysis was conducted by bringing the reaction to 95º C for 1 min, 55º C for 1 min, then increasing the temperature by 0.5º C from 55º C to 94.5º C. Gene expression between depots for the diet and phase selected for validation was evaluated using the comparative C_T method. A cycle threshold (C_T) value was assigned to each reaction at the beginning of the logarithmic phase of the PCR amplification. A ΔC_T value was calculated for each sample by subtracting the mean 18S ΔC_T value of each sample from the corresponding gene of interest mean ΔC_T value (Livak and Schmittgen, 2001). The $\Delta\Delta C_T$ was calculated by setting the i.m. ΔC_T value of the two depots as an arbitrary constant to subtract from the s.c. mean ΔC_T depot values (Hettinger et al., 2001). Relative

expression levels between the two adipose depots were calculated as fold changes, where each cycle of the PCR represented a two-fold change. The assay specific efficiency for each gene was not used in the calculation of the relative expression levels. Fold change (FC) gene expression was calculated using the formula: $FC = 2^{-\Delta\Delta CT}$.

Quantitative RT-PCR analysis for selected genes

Five genes from the adipose related category; acyl-CoA synthetase medium-chain family member 1 (ACSM1), CD36 molecule (thrombospondin receptor) (CD36), fatty acid binding protein 4 (FABP4), stearoyl-CoA desaturase (delta-9-desaturase) (SCD), hydroxyacyl-Coenzyme A dehydrogenase (HADH); three genes from the carbohydrate metabolism category, glucose phosphate isomerase (GPI), lactate dehydrogenase B (LDHB), and pyruvate kinase, muscle (PKM2); one gene from the binding category, four and a half LIM domains 1(FHL1); and one gene from the transcription/translation category, Y box binding protein 1 (YBX1), were measured for their mRNA expression between adipose depots across diets using quantitative RT-PCR and analyzed using the comparative C_T method. The $\Delta\Delta C_T$ was calculated by setting the highest mean ΔC_T value as an arbitrary constant to subtract from all other mean ΔC_T depot values (Hettinger et al., 2001). Relative expression levels between the depots across diets were calculated as fold changes, where each cycle of the PCR represented a two-fold change. Fold change (FC) gene expression was calculated using the formula: $FC = 2^{-\Delta\Delta CT}$. The ΔC_T values were analyzed by analysis of variance (ANOVA) and means were compared using the Least squares means (LSMEANS) of PROC MIXED of SAS 9.1.3 (SAS Institute Inc, Cary, North Carolina). The statistical model included the effects of depot, diet, and diet x depot interaction.

Results

Growing Phase

Performance and Carcass Merits

Performance and carcass merits previously reported by McCurdy (2006) indicated average daily gain (ADG) was greater for WP and PF steers than for SF steers ($P = 0.009$), with gains of 1.15, 1.10, and 1.18 kg/d for WP, SF, and PF steers, respectively. At the end of the GP, 12th-rib *Longissimus* muscle area was smaller for SF (60.3 cm^2) steers compared with WP (63.8 cm^2) and PF steers (65.0 cm^2) ($P < 0.05$). No other significant differences in carcass characteristics were observed.

Microarray and Ontology analysis

Three hundred sixty-eight of 1,089 array elements, or 34%, were observed to be differentially expressed between s.c. and i.m. adipose tissue depots in the INT and/or one of the diets of the GP. The Clone ID, Gene Symbol, Gene Name, Entrez Gene ID, dEST ID, GenBank Accession number, M-value, GO/KEGG ID, and GO term/KEGG pathway for the genes in INT and each diet of GP are presented in the appendices (Appendices Table A1).

Of the 368 array elements, 45 had a non-significant (E value >1e-15) or ambiguous match in the previously described NCBI databases and were grouped under the category "No Biological Data Available" (Rhee et al., 2008). Three hundred twenty-three array elements were observed to significantly (E value < 1e-15) correspond to specific annotated genes in the NCBI databases and were used for ontology analysis using GFINDer and Entrez Gene. One hundred sixteen array elements were not associated with any functional

or biological annotation, even though they had significant matches in the NCBI databases and were grouped under "Other". Based on results of the Bovine ontology analysis, 207 differentially expressed genes were organized into 15 functional/biological categories. Eighty-three of the 207 differentially expressed genes were detected in biochemical pathways for Bos Taurus defined by Kyoto Encyclopedia of Genes and Genomes (KEGG), http://www.genome.jp/kegg/, (Kanehisa and Goto, 2000).

Almost twice the number of differentially expressed genes were observed in the WP and PF diets than SF diet (200 and 196 vs. 104, respectively) with the number of differentially expressed genes in INT (146) being intermediate (Table 3.2). WP and PF diets had a greater number of differentially expressed genes involved in binding than INT or SF diet. Furthermore, WP steers had a greater number of differentially expressed genes involved in cell cytoskeletal/adhesion/extracellular matrix related functions than INT or SF and PF diets. Fewer differentially expressed genes in SF were involved in oxidoreductase, signal transduction and transporter functions than WP and PF, whereas the number of differentially expressed adipose related genes was similar between INT and WP, SF, and PF steers. The number of differentially expressed genes relating to transcription/translation was similar across INT and diets of the GP. The percent of differentially expressed genes not associated with any functional or biological annotation (those classified as "Other") for INT and WP, SF and PF steers was 32.19, 32.50, 25.0 and 37.24%, respectively.

Quantitative RT-PCR Validation of Microarray

Eleven differentially expressed genes were selected for microarray validation. Comparisons between the results of the expression profiles determined by microarray and

RT-PCR for each gene from diets of GP selected for validation are presented in Table 3.3. Microarray analysis indicated acyl-CoA synthetase medium-chain family member 1 (ACSL1), branched chain aminotransferase 2, mitochondrial (BCAT2), CD36 molecule (CD36), fatty acid binding protein 4 (FABP4), lactate dehydrogenase B (LDHB), and stearoyl-CoA desaturase (SCD), to be down-regulated in the i.m. adipose tissue in respective diets of GP. RT-PCR verified the down-regulated pattern of expression of these genes in i.m. adipose tissue. Microarray analysis indicated four and a half LIM domains 1 (FH1), glucose phosphate isomerase (GPI), N-myristoyltransferase 1 (NM1), pyruvate kinase, muscle (PKM2), and Y box binding protein 1 (YBX1) to be up-regulated in the i.m. adipose tissue in respective diets of the GP. The RT-PCR results verified the same up-regulated expression pattern of these genes in the i.m. adipose tissue in respective diets of the GP.

Quantitative RT-PCR Analysis for Selected Genes

Results for the RT-PCR analysis for mRNA expression measured for eleven differentially expressed genes for all experimental animals between depots across diets at the end of the growing phase are presented in (Figure 3.1 a-k). Four genes from the adipose related category, ACSM1, FABP4, HADH and SCD were significantly ($P < 0.05$) affected by depot, while CD36 had a tendency ($P < 0.065$) to be influenced by depot. FABP4 also had a tendency to be influenced by diet with mRNA expression approximately sevenfold higher in SF and PF steers compared to WP steers with no differences between INT and WP, SF, or PF steers. The mRNA expression for ACSM1, FABP4, SCD, and CD36 was down-regulated approximately 10 fold, 13 fold, 20 fold, and three fold,

respectively, in i.m. adipose tissue compared to s.c. adipose tissue. The mRNA expression for HADH was up-regulated approximately 3.5 fold in the i.m. adipose tissue compared to s.c. adipose tissue. Two genes from the carbohydrate metabolism category, GPI and PKM2, were significantly ($P < 0.05$) affected by depot, while LDHB had a tendency ($P < 0.09$) to be influenced by depot. GPI and PKM2 mRNA expression was up-regulated approximately seven and 96 fold, respectively, in i.m. adipose tissue compared to s.c. adipose tissue. LDHB mRNA expression was down-regulated approximately three fold in i.m. adipose tissue compared to s.c. adipose tissue. The mRNA expression for FHL1, from the binding category, and YBX1, from the transcription/translation category was also affected by depot as mRNA expression was up-regulated approximately eight fold and five fold in the i.m. adipose tissue compared to s.c. adipose tissue, respectively.

Ingenuity Pathway Analysis

The objective of IPA network generation is to hypothesize, using the most pertinent information available in the literature, how network eligible genes in a data set interact in a biological system. In this study, networks were generated through IPA using the dataset of differentially expressed genes identified through GPAP 3.2. An arbitrary M-value of $> +0.59$ or < -0.59 (representing a fold change of $> +1.50$ or < -1.50) and a P-value < 0.01 were implemented as cut-off parameters in the analysis. Of the 323 array elements observed to significantly correspond to specific annotated genes, 213 were IPA network eligible and 185 were eligible for functional/pathway analysis.

Networks are ranked by how relevant they are to the genes of the dataset with a higher score indicating a lower probability of finding the observed number of genes in a

given network by random chance. An abbreviated summary of the top networks generated by IPA for INT and WP, SF and PF diets of GP, including number of focus genes, network score and the top three network molecular/cellular functions, disease/disorder or physiological system development and function is presented in Table 3.4.

Eighteen networks were generated for INT with nine consisting of one focus gene. The most significant network for INT (IPA score: 52; focus genes: 26) had functions pertaining to cell-to-cell signaling and interaction (P-value, 3.83^{-3} to 4.75^{-8}) and lipid metabolism (P-value, 3.83^{-3} to 9.75^{-8}). Twenty-three networks were generated for WP, 12 of which had one focus gene. The principal network for WP (IPA score: 44; focus genes: 24) included functions associated with cell morphology (P-value, 3.95^{-2} to 1.92^{-3}) and cell death (P-value, 4.75^{-2} to 1.40^{-3}) with cell-to-cell signaling (P-value, 3.94^{-3} to 2.72^{-8}) and connective tissue disorders (P-value, 1.73^{-2} to 1.15^{-6}) foremost functions for network 2 (IPA score: 41; focus genes: 23). SF diet consisted of nineteen IPA generated networks with 11 consisting one focus gene. Lipid metabolism and small molecule biochemistry were functions pertaining to Network 1(IPA score: 52; focus genes: 26) (P-value, 3.95^{-2} to 3.69^{-4} and 3.95^{-2} to 3.69^{-4}), Network 2 (IPA score: 39; focus genes: 21) (P-value, 1.97^{-3} to 4.41^{-8} and 1.97^{-3} to 4.41^{-8}), and Network 3 (IPA score: 52; focus genes: 16) (P-value, 1.97^{-3} to 1.02^{-11} and 1.97^{-3} to 1.02^{-11}). Twenty-two networks were generated for PF steers, 13 of which contained one focus gene. Top functions of network 1 (IPA score: 51; focus genes; 26) encompassed DNA replication, recombination and repair (P-value, 4.82^{-2} to 1.69^{-4}) and cell death (P-value, 2.19^{-1} to 4.64^{-4}).

IPA currently listed 32 functions under the heading of “molecular and cellular functions” which were subdivided into lower level ancillary function “categories”. Figure

3.2 ranks, by significance, the top 10 global molecular and cellular functions associated across all generated networks for INT and each diet of GP, respectively. This represents a broad overview of the biology associated with each diet. In general, a P-value < 0.05 indicates a significant nonrandom association between genes of the dataset and a given function. Significance, expressed as the negative $\log_{10}$ of the P-value calculated for each function, is represented on the *y*-axis. Differences were observed between INT and diets of GP in the ranking of functions and the number of genes associated with those functions. Lipid metabolism, molecular transport and small molecule biochemistry were top-ranked functions for both SF and PF diets of GP. Cell death and cellular growth and proliferation were top-ranked functions for INT and WP diet, respectively, followed by lipid metabolism, molecular transport and small molecule biochemistry, respectively. Functional comparison, as well as metabolic and signaling pathway comparison between treatments, is a tool that allows for further determination of whether and to what extent a given function or pathway is affected by a treatment. Results of the comparative functional analysis between INT and diets of GP are presented in Figure 3.3. When evaluating these results, one must keep in mind the possibility of genes within the makeup of the function to be different between treatments without altering the significance of that function. Amino acid metabolism, energy production, free radical scavenging, gene expression, protein folding, protein synthesis, protein trafficking, and RNA post-transcriptional modification are functions displaying obvious variations between INT and diets of GP. IPA contains a total of 158 pathways in its library; 80 metabolic pathways and 78 signaling pathways. Metabolic pathway analysis and signaling pathway analysis comparing INT and diets of the GP are presented in Figures 3.4 and 3.5, respectively. Variations between diets ($P < 0.10$)

can be seen in a number of metabolic and signaling pathways. Using IPA comparison and network analysis, differentially expressed genes exclusive to INT and WP, SF and PF diets, respectively, were also investigated. These IPA identified genes along with their associated networks are presented in Tables 3.5 through 3.8, respectively.

Discussion

During the GP, ADG across diets were greater for WP and PF diets than for SF steers (P = 0.009), with gains of 1.15, 1.10, and 1.18 kg/d as previously reported by McCurdy (2006). However, results from a companion metabolism experiment showed similar metabolizable energy (ME) intake among treatment diets. Besides a smaller 12^{th}-rib *Longissimus* muscle being reported for WP steers compared with SF and PF steers, no other differences were observed in carcass characteristics at the end of the GP. Despite the fact that twice the number of differentially expressed genes were observed in WP and PF steers than SF steers and the top IPA generated functions for networks 1, 2, and 3 for SF steers pertained to lipid metabolism and small molecule biochemistry, the number of differentially expressed adipose related genes were similar between INT and diets of the GP with the majority being down-regulated in i.m. adipose tissue compared with s.c.

Adipose related genes (Figure 3.6) included those genes involved in lipid binding, transport, and metabolism as well as the metabolites secreted from adipose tissue. Gene expression of acyl-CoA synthetase medium-chain family member 1 (ACSM1), also known as butyrate-CoA ligase, was significantly altered by depot and was down-regulated nearly 10 fold in i.m. adipose tissue compared to s.c. adipose tissue. Synthetase refers to a reaction that utilizes an ATP and forms an acyl-AMP intermediate (Mashek et al., 2004)

and ACSM1 is involved in the reaction which is significant in the activation of fatty acids. Before fatty acids can be oxidized, they first must be "activated" or "primed" for the reaction by combining the fatty acid with Co-A to form fatty acyl Co-A. The fatty acyl group is then able to be transported into the mitochondrial matrix where it undergoes beta-oxidation. Acetyl-CoA can then feed directly into the TCA cycle, or if propionyl-CoA, be catabolized via a number of different pathways that convert it into pyruvate, acetate, or succinyl-CoA, which in turn, can enter the TCA cycle. However, acyl-CoA can function as ligands for transcription factors or enter several other pathways such as *de novo* synthesis of triacylglycerol and phospholipids, reacylation pathways, and cholesterol and retinal esterification (Coleman et al., 2002; Mashek et al., 2004). ACSM1 can also function as a GTP-dependent lipoate-activating enzyme that generates the substrate for lipoyltransferase (Fujiwara et al., 2001). There are six members of the medium-chain Acyl-Co A family (Mashek et al., 2004). These members catalyze the ligation of medium chain fatty acids, that is acids from C_4 to C_{11} and the corresponding 3-hydroxy- and 2,3- or 3,4-unsaturated acids (in vitro), with CoA to produce medium-chain Acyl-Co A (Inka Lindner, 2006). Though the most common substrates of the medium-chain acyl CoA synthetase family are fatty acids, xenobiotic carboxylic acids and bile salts can also serve as substrates (Mashek et al., 2004). In the mouse, medium chain acyl Co-A synthetase was found to be inhibited by nonsteroidal anti-inflammatory drugs (NSAIDs) (Kasuya et al., 2001). Also in the mouse, aspirin and salicylic acid were shown to decrease the mitochondrial activation and the β-oxidation of long chain fatty acids (palmitate) (*in vivo*) by 50 and 65%, respectively, (Deschamps et al., 1991).

Stearoyl-CoA desaturase (SCD) gene expression was also significantly affected by depot and was down-regulated nearly 20 fold in i.m. adipose tissue compared to s.c. adipose tissue. This is consistent with other finding in the literature where SCD activity appears to be essential for subsequent development of lipogenic activity of s.c. adipose tissue in growing steers (Smith et al., 2006b; Hausman et al., 2009), as s.c. adipose tissue was shown to have approximately twice the SCD catalytic activity as i.m. adipose tissue and also a greater concentration of MUFA than i.m. adipose tissue (Archibeque et al., 2005). However, in many breeds there has been shown to be nearly a linear increase in i.m. adipose tissue deposition over time on a finishing diet and in many breeds this increase in i.m. adipose deposition was consistent with the increase in adipose tissue MUFA and SCD activity (Hausman et al., 2009). Furthermore, when comparing s.c. adipose tissue from the mid-loin region of pasture-fed cattle or cattle placed in the feedlot fed a diet consisting of sorghum, roughage, and 5% whole cottonseed for 100, 200, or 300 d, SCD activity was shown to be 60 to 85% higher in cattle from a pasture-fed diet than cattle on the feedlot diet. This suggests that feeding whole cottonseed reduced the activity of SCD (Yang et al., 1999) as cattle from the pasture-fed diet had lower total saturated fatty acids and higher total unsaturated fatty acids in adipose tissue than cattle in the feedlot (Yang et al., 1999). No diet affects were observed for SCD mRNA gene expression in the present study.

CD36 molecule (thrombospondin receptor) (CD36) gene expression was significantly affected by depot and was shown to down-regulated over 3.5 fold in i.m. adipose tissue compared to s.c. adipose tissue. In *in vitro* studies using 3T3-L1 cells, no CD36 protein was detected in preadipocytes; however, CD36 was detected in 3 day post-differentiated cells (Qiao et al., 2008). CD36 has been identified as an important marker of

preadipocyte differentiation into adipocytes as CD36 mRNA expression was induced during the differentiation process and fatty acid uptake coincided with the up-regulated expression of CD36 (Abumrad et al., 1993; Sfeir et al., 1997). CD36 has been shown to be regulated by all three peroxisome proliferator receptors (PPAR) α, γ, and δ in a tissue specific manner (Hajri and Abumrad, 2002). More so, CD36 contains a CCAAT/enhancer binding protein (C/EBP) response element and C/EBP α and β were shown to increase CD36 expression with C/EBPα being a more potent inducer of CD36 than C/EBPβ indicating C/EBPα involvement in regulating CD36 expression at the transcriptional level (Qiao et al., 2008). One of the main functions of CD36 is to facilitate the translocation of fatty acids in adipocytes as well as in heart and muscle cells (Nicholson et al., 2000; Febbraio et al., 2001; Su and Abumrad, 2009). With CD36 being regulated by PPARγ and C/EBP; the up-regulation of expression of CD36 in the s.c. fat seems logical as it follows a similar pattern of expression as seen for other adipose related genes involved in fatty acid transport. Also, there is evidence that CD36 gene expression can differ between depots as CD36 gene expression in weaning piglets was shown to be higher in visceral adipose tissue as compared to s.c. and i.m. adipose tissue (Shu et al., 2008). Conversely, in a study using non-obese human subjects, CD36 gene expression was found to be up-regulated in s.c. adipose tissue as compared to omental adipose tissue (vanBeek et al., 2007).

In the present experiment FABP4 gene expression was shown to be significantly affected by depot, with a tendency to be influenced by diet. FABP4 gene expression was down-regulated over 14 fold in i.m. adipose tissue compared to s.c. adipose tissue with a tendency for gene expression to be higher in SF and PF diets as compared to the WP diet.

Similar findings were obsserved in porcine where FABP4 transcript and protein content was shown to be lower in i.m. adipocytes as compared to s.c. adipocytes when adipose cells were compared at the same size and same age (Gardan et al., 2007). Previous work by Moore al. (1991), showed activity of FABP4 in the *Longissimus* muscle not to be a good index for the determination of i.m. fat accretion in bovine. However, FABP4 polymorphisms have been shown to be associated with marbling and s.c. fat depth in cattle (Michal et al., 2006) and for fatness traits and i.m. fat accretion in pigs (Chmurzynska, 2006; Damon et al., 2006).

Hydroxyacyl-CoA dehydrogenase (HADH), an enzyme involved in the beta-oxidation of fatty acids through the oxidation of straight chain 3-hydroxyacyl CoA's (Rakheja et al., 2002; Song-Yu Yang, 2005), was altered by depot and was shown to be down-regulated over four fold in s.c. adipose tissue compared with i.m. adipose tissue. HADH is also present in the degradation pathways of the branched chain amino acids, valine, leucine, and isoleucine (Kanehisa and Goto, 2000), which can provide the acetyl CoA necessary for fatty acid biosynthesis in adipose tissue (Labrecque et al., 2009).

Lactate is formed from pyruvate, involving the enzyme lactate dehydrogenase. In the present experiment, lactate dehydrogenase B (LDHB) was shown to be down-regulated 3.5 fold in i.m. adipose tissue compared with s.c. adipose tissue. DiGirolamo et al. (1992) reviewed the role of adipose tissue lactate production and its physiological importance to the body's energy balance in the human and rat. Lactate production by the adipocyte was reported to be modulated, in part, by adipocyte size and density, anatomical location, glucose concentration, insulin levels, and nutrition and suggested the role of lactate production needed to be added to the evolving list of functions of the adipocyte tissue.

LDHB has been shown to be highly expressed in porcine s.c. adipose tissue (Chen et al., 2006) and has also been shown to be a precursor of fatty acid metabolism and glycerogenesis in bovine adipose tissue (Whitehurst et al., 1978). The rate of fatty acid synthesis, when either lactate or acetate was the precursor, was observed to be greater in subcutaneous adipose tissue than in intermuscular or intramuscular tissue (Whitehurst et al., 1981). *In vitro* studies have shown adipose tissue from steers fed a corn-based diet to have a greater conversion of glucose to lactate than a hay-based diet; however, there was no difference between s.c. and i.m. adipose depots in lactate production within the two diets (Rhoades et al., 2007).

Two genes involved in carbohydrate metabolism, glucose phosphate isomerase (GPI) and pyruvate kinase, muscle (PKM2) were both significantly altered by depot and were shown to up-regulated by seven fold and 90 fold, respectively, in i.m. adipose tissue compared to s.c. adipose tissue. IPA indicated other genes involved in carbohydrate metabolism including glyceraldehyde-3-phosphate dehydrogenase (GAPDH) and malate dehydrogenase 2 (MDH2), which displayed an up-regulated pattern of expression in i.m. adipose tissue compared to s.c. in respective diets (Figure 3.7). Glucose phosphate isomerase (GPI) is a dimeric enzyme involved in the second step of glycolysis which catalyzes the reversible isomerization of glucose-6-phosphate to fructose-6-phosphate (Voet and Voet, 2004a). Limitations in the GPI reaction or the phosphofructokinase (PFK) reaction can result in an increase in the glucose-6-phosphate level causing feedback inhibition of hexokinase and possibly a lower rate of glycolysis and fructose-6-phosphate being formed as a product of the pentose phosphate pathway resulting in the generation of NADPH for biosynthetic processes (Kugler and Lakomek, 2000; Voet and Voet, 2004c).

In ruminants, as much as 50 to 80% of NADPH needed for fatty acid synthesis in adipose tissue is produced by the pentose phosphate pathway (Vernon, 1981). Pyruvate kinase (PK) catalyzes the last step in the glycolysis pathway, which is the dephosphorylation of phosphoenolpyruvate to pyruvate and is responsible for producing the second ATP generated within the glycolytic pathway (Voet and Voet, 2004a). PK leads to either anaerobic fermentation or oxidative phosphorylation of pyruvate (Jurica et al., 1998) and can also serve as the control switch between the glycolysis and gluconeogenesis pathways in certain tissues (Voet and Voet, 2004a). IPA comparative metabolic pathway established genes involved in oxidative phosphorylation also displayed an up-regulated pattern of expression in i.m. adipose tissue of respective diets in four complexes of the electron transport chain (Figure 3.8). The down-regulation of LDHB and genes related to the beta-oxidation, synthesis, transport, and storage of fatty acids in i.m. adipose tissue, along with the up-regulation of glycolytic enzymes and components of oxidative phosphorylation in i.m. adipose tissue of respective diets, suggest that fatty acid and triglyceride synthesis and transport is attenuated in i.m. adipose tissue compared with s.c. Moreover, lactate is a possible substrate for glycerogenesis for use in triglyceride synthesis in s.c. adipose tissue. Acetyl-CoA, via beta oxidation, and the contribution of lactate allowing for anaerobic metabolism in s.c. may permit the sparing of glucose for repartitioning as an energy substrate for i.m. adipose tissue. Previous data reported by Smith and Crouse (1984) showed i.m. adipocytes used glucose as the primary substrate for fatty acid synthesis, whereas s.c. adipocytes utilized acetate and lactate for incorporation into fatty acids.

IPA showed the expression of other adipose related genes relevant to the synthesis of triglycerides and fatty acids such as diacylglycerol O-acyltransferase homolog 2

(DGAT2) (Yen et al., 2005), mitochondrial glycerol phosphate acyltransferase (GPAM) (Igal et al., 2001), adiponectin, C1Q and collagen domain containing (ADIPOQ) (Kadowaki and Yamauchi, 2005; Karbowska and Kochan, 2006) and prostaglandin-endoperoxide synthase 2 (PTGS2) (Williams and DuBois, 1996) to be down-regulated in i.m. adipose tissue compared with s.c. adipose tissue. Furthermore, adipose related genes involved in the transport of fatty acids and lipids including, clusterin (CLU) (Lee et al., 2008a), and macrophage scavenger receptor 1 (MSR1) (Wang et al., 2007) were also shown to be down regulated in i.m. adipose tissue compared with s.c. adipose tissue according to IPA.

IPA revealed transmembrane 7 superfamily member 2 (TM7SF2), isopentenyl-diphosphate delta isomerase 1 (IDI1), and niemann-pick disease, type C2 (NPC2) gene expression, up-regulated in i.m compared to s.c. in WP steers. These genes are shown to be involved with pre- and post-squalene intermediates in cholesterol homeostasis or the biosynthesis pathway (Ory, 2004; Bennati et al., 2006; Xu et al., 2007; Zheng et al., 2007). In humans, 3β-hydroxysterol Δ^{14}-reductase, encoded by the TM7SF2 gene, catalyzes the reduction of the Δ^{14}-double bond of post-squalene sterol intermediates during cholesterol biosynthesis pathway (Bennati et al., 2006). IDI1 is involved in the isomerization of the double bond of isopentenyl diphosphate to form dimethylallyl diphsophate which, through further successive reactions, forms squalene, a precursor to cholesterol (Zheng et al., 2007). NPC2 has been shown to bind cholesterol and is thought to be involved with the intracellular movement of cholesterol out of the lysosome throughout the cell extremities (Ory, 2004; Xu et al., 2007). In adipocytes, the intracellular level of cholesterol is controlled by two processes: biosynthesis and transport

into the cell from circulating lipoproteins complexes (Kouznetsova et al., 2006). Cholesterol is utilized in the synthesis of steroids and is an essential component of cell membranes (Villagra et al., 2007) with quiescent cells synthesizing very little cholesterol; however, in proliferating cells, synthesis can be detected in the G1 phase of the cell cycle (Chen, 1984). Furthermore, cells restricted of cholesterol have been shown to arrest at the G2 phase of the cell cycle (Martinez-Botas et al., 1999). However, in *in vitro* studies using human s.c. adipose tissue Tilvis et al. (1982) reported squalene to be synthesized and stored in high concentrations with only a small fraction converted to cholesterol with approximately 80% in the lipid droplet and 20% bound to microsomal membranes.

Spermidine/spermine N1-acetyltransferase 1 (SAT1), up-regulated in i.m. adipose tissue compared with s.c. in INT, WP and SF diets, is the regulatory enzyme that catalyzes the transfer of acetyl groups from acetyl-CoA to spermidine and spermine, which marks these polyamines for reutilization or export out of the cell (Casero et al., 1991; Wallace et al., 2003; Niranen, 2006; Pegg, 2008). The polyamines spermadine and spermine can influence transcription and translation (Parker and Gerner, 2002) and also play an essential role in cell growth and proliferation as well as amino acid synthesis and the synthesis of nucleic acids with a suggested role in programmed cell death, as inadequate polyamine concentrations lead to cell-cycle arrest (Wallace et al., 2003; Niranen, 2006). Strict regulatory control of polyamines is maintained between biosynthesis, degradation, and uptake of the amines (Wallace et al., 2003; Niranen, 2006). *In vitro* studies have also shown polyamines to negatively regulate the post-transcriptional expression of COX-2, as depletion of polyamines caused a time-dependent increase in COX-2 mRNA expression

(Parker and Gerner, 2002). RT-PCR showed no significant differences in prostaglandin-endoperoxide synthase 2 (PTGS2) mRNA expression between s.c. and i.m. adipose tissue depots. Mesenchymal stem cells (MCSs) are multi-potent stem cells which can serve as precursors for many cell types including bone, cartilage, adipocytes, and most connective tissues (Rosen and MacDougald, 2006; Chen et al., 2008). MSCs have been isolated from bone marrow as well as many other tissues, including adipose tissue (Zuk et al., 2002; Izadpanah et al., 2006). Tjabringa et al. (2008) reported treatment of adipose-tissue derived MSCs with the polyamine spermine, regulated the differentiation of these cells towards the osteogenic linage including an observed up-regulation of osteopontin. Interestingly, Jell et al. (2007) reported the over expression of SAT1 in mice decreased white adipose acetyl and malonyl CoA pools and increased glucose and palmitate oxidation whereas in SAT1–knockout mice, an increase in acetyl and malonyl CoA pools, a decrease in glucose and palmitate oxidation and an accumulation of body fat was observed.

In the present study, the principal IPA generated functions (Table 3.4) for networks 1 and 2 of WP diet pertained to cell morphology, cell death, cell-to-cell signaling and connective tissue disorders. The majority of differentially expressed genes involved in cell cytoskeletal/extracellular matrix related functions displayed a down-regulated pattern of expression in i.m. adipose tissue compared with s.c. including: collagen, type I, alpha 1(COL1Al); collagen, type I, alpha 2 (COL1A2); collagen, type III, alpha 1 (COL3Al); collagen, type IV, alpha 1 (COL4A1); collagen type VI, alpha 2 (COL6A1); fibronectin 1(FN1); and secreted protein, acidic, cysteine-rich (osteonectin) (SPARC). Adipocyte differentiation, or adipogenesis, is a multistep process regulated by a milieu of hormones and transcription factors and is paralleled by morphological changes as a result of

reorganization in the cytoskeletal network and alterations in components of the extracellular matrix (Nakajima et al., 1998; Rosen and Spiegelman, 2000; Kawaguchi et al., 2003). A basement membrane composed of collagens and other extracellular matrix components support each adipocyte (Pierleoni et al., 1998), the size of which varies dramatically under physiological conditions (Farnier et al., 2003). Simplistically, the adipocyte is a lipid storage container whose morphology is supported by components of the extracellular matrix (Pierleoni et al., 1998; Wang et al., 2008). Most adipose tissues form at sites of loose connective tissues (Rosen and Spiegelman, 2000).. More so, i.m. adipose tissue has been shown to develop within perimysium connective tissue alongside myofibers (Moody and Cassens, 1968). This study showed down-regulation in both adipogenic and extracellular matrix genes in i.m. adipose tissue and may be interpreted as support of previous work by Wang et al. (2008) who looked at genes to be used as potential biomarkers for i.m. adipose tissue development. The fore mentioned author suggested that expansion of the extracellular matrix might be a prerequisite for i.m. fat development since current work (Wang et al., 2008) showed the expression pattern of genes involved with connective tissue (COL1Al, COL1A2, COL3Al and FN1) and genes that influence the synthesis and interaction with the extracellular matrix (SPARC and FMOD) mirrored that of adipogenic related genes.

Insulin-like growth factor binding protein 6 (IGFBP6) and 5 (IGFBP5) were shown by IPA to be up-regulated in i.m. adipose tissue compared with s.c. in network 4 of WP (Table 3.6) and network 2 of PF (Table 3.8), respectively. IGFBP6 has been shown to have a ~50 fold higher affinity for IGF-II than for IGF-I (Rechler and Clemmons, 1998). IGF-I has been shown to not only be involved in the stimulation of cell proliferation and cell

differentiation in bone, muscle and cartilage but also in the differentiation of adipocytes (Boney et al., 1994). More recently, it has been suggested that IGF-I and IGF-II both play distinctive roles on the development of adipocytes (Gardan et al., 2008) The action of IGF-I and IGF-II can either be inhibited or enhanced by IGF-binding proteins depending on the cell type and binding protein involved (Clemmons, 1992). Furthermore, there have been considerable differences shown in the pattern of IGF-binding proteins produced by preadipocytes from different species (Butterwith, 1997).

The majority of genes categorized under signal transduction were down-regulated in i.m. adipose tissue compared with s.c. IPA signaling pathway analysis ascertained possible differences between diets in the notch signaling pathway. Further evaluation using IPA showed genes involved in this signaling pathway, MFNG-, RFNG-, and LFNG O-fucosylpeptide 3-beta-N-acetylglucosaminyltransferase (Moloney et al., 2000; Yang et al., 2005), and nicastrin (NCSTN) (Li et al., 2003), to be up-regulated in i.m. adipose tissue compared with s.c. adipose tissue in WP steers. Notch is a transmembrane protein involved in regulating cell signaling during development which functions to receive extracellular signals at the cell surface, and regulate gene expression in the nucleus (Lai, 2004; Nichols et al., 2007). Garces et al., (1997) reported the requirement of Notch-1 function for the commitment of *in vitro* 3T3-L1 preadipocyte cells to undergo adipogenesis. However, studies have concluded that Notch most likely blocks adipogenesis through the induction of Hes-1, which primarily functions as a transcription repressor in *in vitro* 3T3-L1 preadipocytes (Ross et al., 2004; Ross et al., 2006). In contrast to both the studies of Garces and Ross, Nichols et al. (2004) ruled out the possibility of Notch signaling playing

an essential role in adipogenesis in ES cells, as a deficiency for Notch-1 still allowed the ability to differentiate into adipocytes.

The number of differentially expressed genes relating to transcription/translation was attenuated in INT, WP and SF diets compared to PF. More so, IPA generated functions for network 1 of PF diet included DNA replication, recombination and repair and cell death (Figure 9). In the present study, RT-PCR revealed YBX1 expression to be up-regulated approximately five fold in i.m. adipose tissue compared with s.c. YBX1 has been shown to be a regulator of gene expression affecting transcription and translation in a positive and negative manner, as *in vitro* studies have shown translation stimulated by low concentrations of YBX1with high concentrations of YBX1 restricting translation (Davydova et al., 1997; Matsumoto and Wolffe, 1998; Nekrasov et al., 2003). YBX1 has been shown to directly bind the protein tyrosine phosphatase-1B (PTP1B) enhancer and induce PTP1B expression (Fukada and Tonks, 2003). PTP1B has been shown to act as a negative regulator of insulin signaling by dephosphorylating the phosphotryosine residues of insulin receptor kinase (Fukada and Tonks, 2003). YBX1 has also been reported to inhibit cell death through aberrant expression of protein 53 (p53) (Homer et al., 2005) and shown to have the strongest induction (130 fold) of the differently expressed genes in visceral adipose tissue of rats fed a high-fat diet (López et al., 2004). More recently, *in vitro* studies have shown YBX1 to stimulate microtubule assembly in the cell and through its interaction with tubulin, contribute to the regulation of mRNA's (Chernov et al., 2008). Proliferating cell nuclear antigen (PCNA) expression was up-regulated in i.m. adipose tissue compared with s.c in all diets in the present study. PCNA interacts with many p53 proteins and is involved in both DNA replication and DNA repair (Warbrick, 2000;

Paunesku et al., 2001). In the absence or aberration in levels of PCNA, cell apoptosis can occur. Furthermore, PCNA action in the cell is induced by p53 such that DNA replication occurs if PCNA is abundant in the cell and p53 is absent. Conversely, DNA repair takes place if PCNA is abundant and p53 presence is high in the cell (Paunesku et al., 2001). Another gene that plays a pivotal role in the regulation of transcription and suggested roles in cell cycle progression and cell proliferation is Histone deacetylase 3 (HDAC3) (Zhang et al., 2005; Villagra et al., 2007), which was found to be up-regulated in INT, WP and PF steers. HDAC3 has also been shown to deaceylate non-histone substances such as ReLA, which in turn regulates the duration of NKκB signaling action by allowing IκB to interact with RelA, allowing its export out of the nucleus (Karagianni and Wong, 2007).

RT-PCR revealed four-and-a-half-LIM Domains 1 (FHL1) expression to be up-regulated over 15 fold in i.m. adipose tissue compared with s.c. adipose tissue. Although FHL1 is highly expressed in skeletal and cardiac muscle (McGrath et al., 2006); FHL1 has been shown to be expressed in bovine, porcine, and human adipose tissue (Wang et al., 2005a; vanBeek et al., 2007; Labrecque et al., 2009). Although the exact function of FHL1 remains ambiguous, it does belong to a large family of LIM-proteins that function in cytoskeletal organization, cell lineage specification, the regulation of gene transcription, cell proliferation, cell differentiation and apoptosis (Bach, 2000; Kadrmas and Beckerle, 2004). As FHL1 has been shown to be highly expressed in adipocytes and not preadipocytes, it could serve as a marker for adipocyte differentiation (vanBeek et al., 2007). FHL1 has also been reported to interact with receptor interacting protein of 140 kDa (RIP140) which itself is known to interact with estrogen receptor-α (Lin et al., 2009). Recently, FHL1 and RIP140 were shown to synergistically inhibit the transcription of the

estrogen response element of the pS2 gene, whose expression is restricted to breast cancer cells (Lin et al., 2009). However, RIP140-null mice have shown to accumulate less fat in their adipose tissue and are resistant to high-fat diet-induced obesity and show improved glucose tolerance and insulin sensitivity (Leonardsson et al., 2004).

SF diet had the fewest number of differentially expressed genes relating to transporter functions with INT, WP and PF diet exhibiting about equal numbers of up- and down-regulated genes. Besides the transcripts mentioned in the above discussion, several others are worth mentioning which were differentially expressed between i.m. and s.c. adipose tissues in the different ontology categories including; casein kinase 1, alpha 1(CSNK1A1), growth hormone releasing hormone (GHRH), adrenergic, beta, receptor kinase 2 (ADRBK2), angiotensin II receptor, type 1(AGTR1), glutamate-cysteine ligase, catalytic subunit (GCLC), and asparagine-linked glycosylation 11 homolog (ALG11). These genes are only six of approximately 60 array elements shown to be down-regulated in all diets of the GP and up-regulated in only the WP diet of the finishing phase (Stein et al. unpublished data).

To our knowledge, the data presented is the first to use microarray analyses to evaluate the effect of different growing diets on adipose tissue depots at the end of the growing period in beef steers. The interactions between genes involved in adipocyte differentiation and diet differences still remain ambiguous. However, IPA metabolic and signaling pathway analysis generated in this study, has provided insight into possible differences in the molecular mechanisms affecting development of i.m. and s.c. adipose tissue in beef steers managed under different growing diets. As genes outside the dataset known to interact with the differentially expressed genes observed in this study were

included in the Ingenuity Pathway Analysis, elucidation of possible differences between diets and depots for future analysis is warranted as these genes may not have been included in the adipose specific microarray used in this study. Further investigation and validation is needed to evaluate network genes not included in the microarray and discern the differences observed between diets in the fore-mentioned functional analyses (Figure 3.3) and a number of the metabolic (Figure 3.4) and signaling (Figure 3.5) pathways such as; arachidonic acid metabolism, pyruvate metabolism, eicosinoid signaling and notch signaling.

In conclusion, almost 35% of the 323 array elements that had significant matches in the NCBI databases could not be associated with any functional or biological annotation. However, despite these insufficiencies, gene expression profiling suggests differences in the metabolic activity between s.c. and i.m. adipose tissue in the GP, even though there were no differences observed in carcass characteristics at the end of the GP. Most of the genes evaluated using RT-PCR seemed to be influenced by the main affect of depot and there seemed to be a similar pattern of expression observed within functional categories and depots. The data presented indicates the metabolic machinery for adipose tissue accretion was down-regulated in i.m. adipose tissue compared to s.c. adipose tissue and the main affect of diet can influence adipose tissue deposition at the end of the GP as FABP4 exhibited a tendency to be influenced by the main affect of diet. When using gene expression profiling as a measurement of cellular function, one must keep in mind that mRNA expression levels do not always correspond to the translated protein levels or active protein in the cell and further investigation and validation is needed to evaluate the candidate genes that might be influenced by depot, diet or their interaction.

Table 3.1. Sequences, accession number, and melting temperatures of the bovine specific primers for the selected target genes of interest. Accession number is from the national center for biotechnology information (NCBI) available at http://www.ncbi.nlm.nih.gov/.

Primer		Sequence	Size (bp)	Tm used	Product Size (bp)	GenBank Accession
ACSM1	Forward	AAGGAAACATTGGCATCAGG	20			
	Reverse	AGTCCCCACATTCCACTTCA	20	62 C	102 bp	BC109602.1
BCA2	Forward	TCCCTGTTCCTTGGTTTCTG	20			
	Reverse	GTGGTCGGTGAATGTCTTCC	20	62 C	149 bp	BC114055.1
CD36	Forward	CAATGGAAAGGACGACATAAG	21			
	Reverse	TGGAAATGAGGCTGCATCTGT	21	60 C	121 bp	NM_174010
FABP4	Forward	AAGCTGCACTTCTTTCTCACC	21			
	Reverse	GACCACACCCCCATTCAAAC	20	62 C	197 bp	NM_174314
FHL1	Forward	GCAACAAGGGTTTGGTAAAGG	21			
	Reverse	AGAGGGCAAGGACACAAGG	19	56 C	227 bp	BC102083.1
GPI	Forward	TGGGCATATTCTGGTGGACT	20			
	Reverse	GACCTCTGGCATCACATCCT	20	64 C	223 bp	NM_001040471.1
HADH	Forward	TCCGTTTGAGCTTCTCGATT	20			
	Reverse	CTTACAGGGCTTCGTCCTTG	20	55 C	210 bp	XM_001787625
LDHB	Forward	GCTGTGTGGAGTGGAGTGAA	20			
	Reverse	ATACACGGAAGGCTCAGGAA	20	56 C	287 bp	NM_174100.1
NM1	Forward	AGAGAAGGTTGGGCTGGTGT	20			
	Reverse	GTTCAGTTCTGCTCCCCTTG	20	60 C	148 bp	NM_177504.2
PKM2	Forward	TTGGGTCGGGTAGTTCAGAG	20			
	Reverse	ACAAAGGAAGGGAAGCAGGA	20	56 C	136 bp	XM_590109.4
PTGS2	Forward	ATGTATGAGTGTAGGATTTGACCAG	25			
	Reverse	GGGAGTGGGTTTCAGGAGTAA	21	55 C	234 bp	NM_174445.2
SCD	Forward	CCTGTGGAGTCACCGAACCT	20			
	Reverse	TGTTGCCAATGATCAGGAAGAC	22	60 C	66 BP	AB075020.1
YBX1	Forward	CGCAGTGTAGGAGATGGAGA	20			
	Reverse	CGTGGATAGCGTCTGTAATGG	21	56 C	149 bp	NM_174815.2

Table 3.2. The number of differentially expressed up- and down-regulated genes in each of the functional categories in Initial and Wheat Pasture, Silage Fed, and Program Fed diets of the Growing Phase.

			Growing Phase					
	Initial		Wheat Pasture		Silage Fed		Program Fed	
	Up	Down	Up	Down	Up	Down	Up	Down
Adipose Related	3	13	4	14	1	13	1	12
Apoptosis/Cell Death	2	1	1	1	1	1	2	1
Binding	12	7	15	12	9	7	15	10
Carbohydrate Metabolism	3	0	4	2	2	1	3	1
Cell Growth/Differentiation	0	1	1	5	0	1	1	4
Cell Cytoskeletal/ Adhesion/ ECM Related	2	3	2	7	1	1	2	2
Hydrolase/Transferase/Catalytic/Activity	0	6	5	4	1	5	3	6
Nucleic Acid Metabolism	0	1	0	2	0	1	0	2
Oxidative Phosphorylation	1	0	3	0	2	0	5	0
Oxidoreductase Activity	2	2	5	3	1	3	4	3
Protein Synthesis:Turn Over/AA Metabolism	3	3	4	5	3	4	5	2
Response to Stress/Stimuli	1	1	1	1	2	0	1	1
Signal Transduction	2	8	3	8	0	4	4	5
Transcription/Translation	9	5	9	7	5	8	12	6
Transporters	4	4	4	3	1	0	5	5
Other	17	30	32	33	8	18	33	40
	61	85	93	107	37	67	96	100
Total DE genes	146		200		104		196	

Table 3.3. Comparison of mRNA expression (i.m. relative to s.c.) detected in the cDNA microarray analysis to mRNA expression detected in RT-PCR. Fold change values represent i.m. adipose tissue expression relative to s.c. adipose tissue.

Gene Name	Diet	Fold Change	
		Microarray	RT-PCR
ACSM1	Wheat Pasture	-2.39 (±.07)	-8.81 (±.94)
BCA2	Wheat Pasture	-2.44 (±.09)	-4.31 (±1.5)
CD36	Program Fed	-4.78 (±.33)	-4.28 (±.32)
FABP4	Program Fed	-8.11 (±.16)	-16.79 (±.80)
FHL1	Silage Fed	5.13 (±.14)	68.59 (±1.36)
GPI	Wheat Pasture	2.34 (±.46)	9.06 (±.73)
LDHB	Wheat Pasture	-3.07 (±.44)	-5.93 (±.71)
NM1	Wheat Pasture	2.01 (±.20)	1.50 (±80)
PKM2	Silage Fed	4.40 (±.21)	2.53 (±.80)
SCD	Silage Fed	-5.69 (±.26)	-12.55 (±.97)
YBX1	Silage Fed	1.98 (±.16)	11.71 (±.98)

Figure 3.1.

(a) Relative fold difference in acyl-CoA synthetase medium-chain family member 1 (ACSM1) gene expression in s.c. (green) and i.m. (red) adipose tissue depots in steers at the end of the Growing Phase. The gene expression level for the i.m. adipose tissue was set as baseline and fold difference was calculated as described in Material and Methods. Columns with different superscripts differ significantly ($P < 0.001$).

(b) Relative fold difference in CD36 molecule (thrombospondin receptor) (CD36) gene expression in s.c. (green) and i.m. (red) adipose tissue depots in steers at the end of the Growing Phase. The gene expression level for the i.m. adipose tissue was set as baseline and fold difference was calculated as described in Material and Methods. Columns with different superscripts differ significantly ($P < 0.065$).

(c) Relative fold difference in stearoyl-CoA desaturase (SCD) gene expression in s.c. (green) and i.m. (red) adipose tissue depots in steers at the end of the Growing Phase. The gene expression level for the i.m. adipose tissue was set as baseline and fold difference was calculated as described in Material and Methods. Columns with different superscripts differ significantly ($P < 0.0002$)

(d) Relative fold difference in hydroxyacyl-Coenzyme A dehydrogenase (HADH) gene expression in s.c. (green) and i.m. (red) adipose tissue depots in steers at the end of the Growing Phase. The gene expression level for the s.c. adipose tissue was set as baseline and fold difference was calculated as described in Material and Methods. Columns with different superscripts differ significantly ($P < 0.05$).

(e) Relative fold difference in fatty acid binding protein 4, (FABP4) gene expression in s.c. (green) and i.m. (red) adipose tissue depots in steers at the end of the Growing Phase. The gene expression level for the i.m. adipose tissue was set as baseline and fold difference was calculated as described in Material and Methods. Columns with different superscripts differ significantly ($P < 0.001$).

(f) Relative fold difference in fatty acid binding protein 4, (FABP4) gene expression in Initial and Wheat Pasture, Silage-fed and Program-fed diets in steers at the end of the Growing Phase. The gene expression level for the Wheat Pasture diet was set as baseline and fold difference was calculated as described in Material and Methods. Columns with different superscripts differ significantly ($P < 0.09$).

(a)

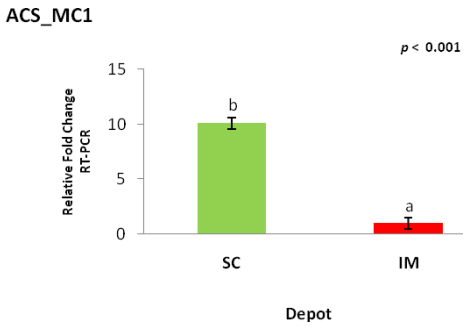
ACS_MC1
p < 0.001
Relative Fold Change RT-PCR
15
10
5
0
b
a
SC
IM
Depot

(b)

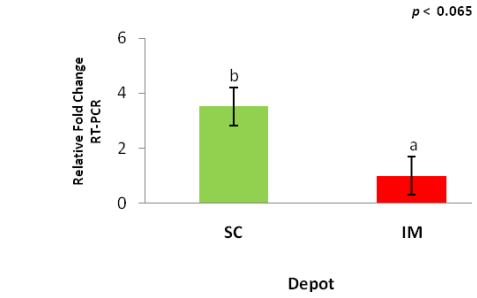
CD36
p < 0.065
Relative Fold Change RT-PCR
6
4
2
0
b
a
SC
IM
Depot

(c)

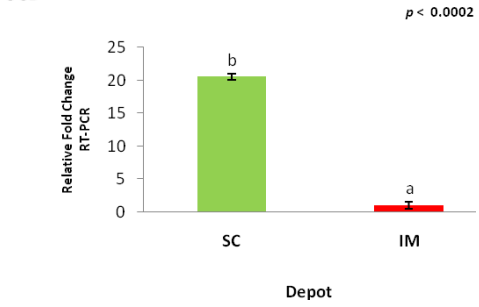
SCD
p < 0.0002
Relative Fold Change RT-PCR
25
20
15
10
5
0
b
a
SC
IM
Depot

(d)

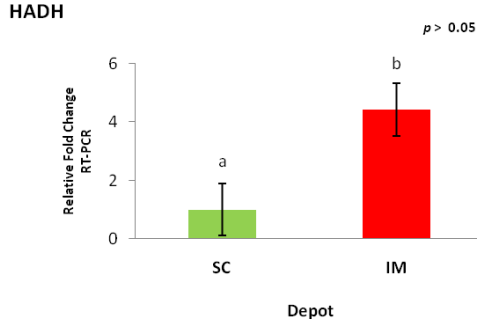
HADH
p > 0.05
Relative Fold Change RT-PCR
6
4
2
0
a
b
SC
IM
Depot

(e)

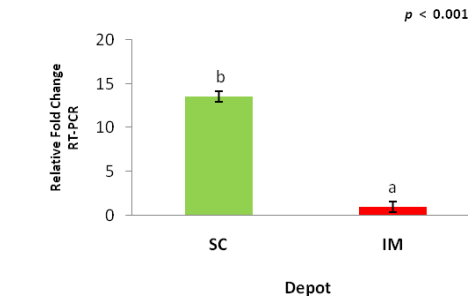
FABP4
p < 0.001
Relative Fold Change RT-PCR
20
15
10
5
0
b
a
SC
IM
Depot

(f)

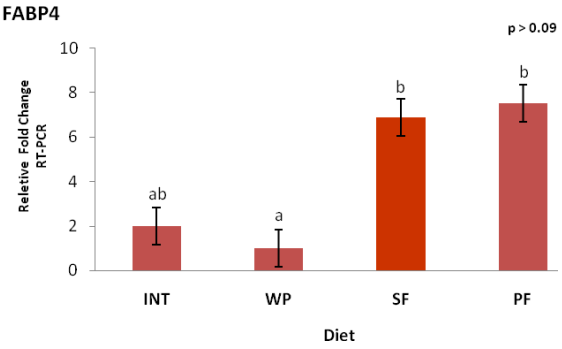
FABP4
p > 0.09
Relative Fold Change RT-PCR
10
8
6
4
2
0
ab
a
b
b
INT
WP
SF
PF
Diet

Figure 3.1.

(g) Relative fold difference in glucose phosphate isomerase (GPI) gene expression in s.c. (green) and i.m. (red) adipose tissue depots in steers at the end of the Growing Phase. The gene expression level for the s.c. adipose tissue was set as baseline and fold difference was calculated as described in Material and Methods. Columns with different superscripts differ significantly ($P < 0.004$).

(h) Relative fold difference in pyruvate kinase, muscle (PKM2) gene expression in s.c. (green) and i.m. (red) adipose tissue depots in steers at the end of the Growing Phase. The gene expression level for the s.c. adipose tissue was set as baseline and fold difference was calculated as described in Material and Methods. Columns with different superscripts differ significantly ($P< 0.001$).

(i) Relative fold difference in lactate dehydrogenase B (LDHB) gene expression in s.c. (green) and i.m. (red) adipose tissue depots in steers at the end of the Growing Phase. The gene expression level for the i.m. adipose tissue was set as baseline and fold difference was calculated as described in Material and Methods. Columns with different superscripts differ significantly ($P < 0.09$)

(j) Relative fold difference in Y box binding protein 1 (YBX1) gene expression in s.c. (green) and i.m. (red) adipose tissue depots in steers at the end of the Growing Phase. The gene expression level for the s.c. adipose tissue was set as baseline and fold difference was calculated as described in Material and Methods. Columns with different superscripts differ significantly ($P < 0.034$).

(k) Relative fold difference in four and a half LIM domains 1(FHL1) gene expression in s.c. (green) and i.m. (red) adipose tissue depots in steers at the end of the Growing Phase. The gene expression level for the s.c. adipose tissue was set as baseline and fold difference was calculated as described in Material and Methods. Columns with different superscripts differ significantly ($P < 0.005$).

(g)

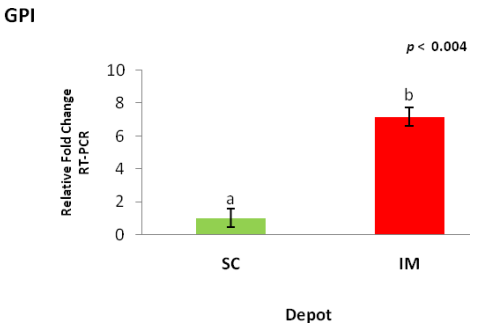
GPI
p < 0.004
Relative Fold Change RT-PCR
10
8
6
4
2
0
a
b
SC
IM
Depot

(h)

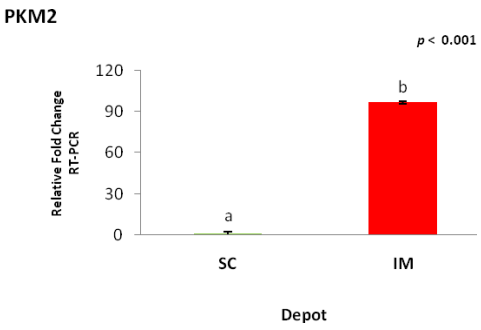
PKM2
p < 0.001
Relative Fold Change RT-PCR
120
90
60
30
0
a
b
SC
IM
Depot

(i)

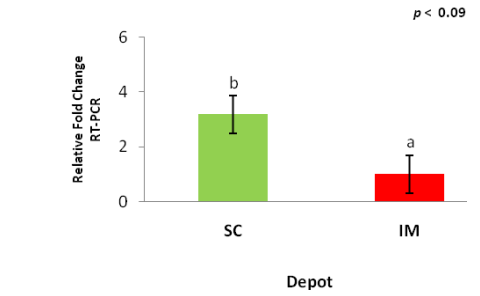
LDHB
p < 0.09
Relative Fold Change RT-PCR
6
4
2
0
b
a
SC
IM
Depot

(j)

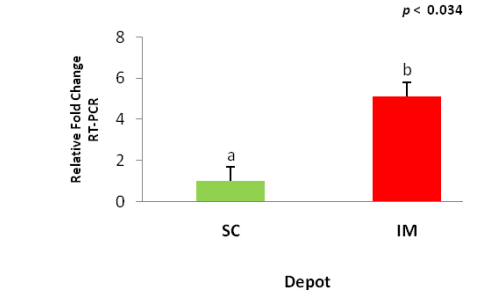
YBOX 1
p < 0.034
Relative Fold Change RT-PCR
8
6
4
2
0
a
b
SC
IM
Depot

(k)

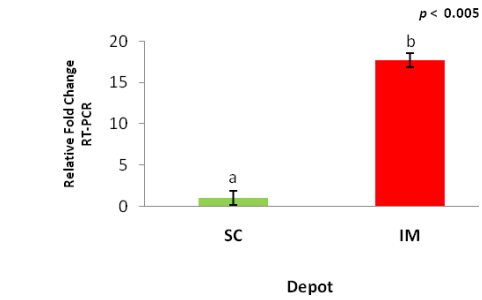
FHL1
p < 0.005
Relative Fold Change RT-PCR
20
15
10
5
0
a
b
SC
IM
Depot

Table 3.4. Principal Networks generated for Initial, Wheat Pasture, Silage-fed, and Program-fed diets of the Growing Phase using Inginuity Pathway Analysis. Focus genes were overlaid into a globular molecular network deveolped from information contained in the IPA Knowledge Base. Networks of these focus genes were then algorithmically generated based on their connectivity.

	Network ID	Score	Focus Molecules	Top Network Molecular or Cellular Function, Disease or Disorder, or Physiological System Development and Function
INT	1	51	26	Cell-To-Cell Signaling and Interaction, Immune and Lymphatic System Development and Function, Lipid Metabolism
	2	38	21	Cancer, Gastrointestinal Disease, Reproductive System Disease
	3	33	19	Immune Response, Hematological Disease, Infectious Disease
	4	28	17	Gene Expression, Free Radical Scavenging, Lipid Metabolism
	5	24	15	Amino Acid Metabolism, Post-Translational Modification, Small Molecule Biochemistry
	6	20	13	Cellular Assembly and Organization, Cell Cycle, DNA Replication, Recombination, and Repair
	7	18	12	Lipid Metabolism, Molecular Transport, Small Molecule Biochemistry
	8	15	11	Post-Translational Modification, Cell Death, Neurological Disease
	9	12	9	Cell Morphology, Dermatological Diseases and Conditions, Hair and Skin Development and Function
WP	1	44	24	Cell Morphology, Nervous System Development and Function, Cell Death
	2	41	23	Cell-To-Cell Signaling and Interaction, Connective Tissue Disorders, Dermatological Diseases and Conditions
	3	29	18	Cancer, Respiratory Disease, Reproductive System Disease
	4	27	17	Cellular Movement, Hematological System Development and Function, Lipid Metabolism
	5	23	15	RNA Post-Transcriptional Modification, Energy Production, Nucleic Acid Metabolism
	6	23	15	Free Radical Scavenging, Genetic Disorder, Neurological Disease
	7	21	14	Post-Translational Modification, Genetic Disorder, Skeletal and Muscular Disorders
	8	19	13	Cancer, Cell Death, Gene Expression
	9	19	13	Carbohydrate Metabolism, Small Molecule Biochemistry, Lipid Metabolism
	10	15	11	Cellular Assembly and Organization, Cellular Compromise, Hematological Disease
	11	8	7	Amino Acid Metabolism, Post-Translational Modification, Small Molecule Biochemistry
SF	1	52	26	Lipid Metabolism, Small Molecule Biochemistry, Ophthalmic Disease
	2	39	21	Lipid Metabolism, Small Molecule Biochemistry, Cell-To-Cell Signaling and Interaction
	3	27	16	Lipid Metabolism, Small Molecule Biochemistry, Carbohydrate Metabolism
	4	23	14	Drug Metabolism, Molecular Transport, Small Molecule Biochemistry
	5	21	13	Post-Translational Modification, Protein Folding, Cellular Assembly and Organization
	6	21	13	Cellular Assembly and Organization, Cell Cycle, DNA Replication, Recombination, and Repair
	7	21	13	Amino Acid Metabolism, Post-Translational Modification, Small Molecule Biochemistry
	8	11	8	Free Radical Scavenging, Genetic Disorder, Neurological Disease
PF	1	51	26	DNA Replication, Recombination, and Repair, Cell Death, Embryonic Development
	2	36	20	Lipid Metabolism, Small Molecule Biochemistry, Cardiovascular System Development and Function
	3	29	17	Hematological Disease, Immunological Disease, Respiratory Disease
	4	24	15	Gene Expression, Lipid Metabolism, Molecular Transport
	5	22	14	Genetic Disorder, Neurological Disease, Free Radical Scavenging
	6	20	13	Lipid Metabolism, Small Molecule Biochemistry, Organ Development
	7	18	12	Cellular Assembly and Organization, Cancer, Cellular Growth and Proliferation
	8	14	10	Genetic Disorder, Skeletal and Muscular Disorders, Cellular Assembly and Organization
	9	11	8	Protein Synthesis, Cellular Development, Cell Death

Table 3.5. Networks were generated for Initial using Inginuity Pathway Analysis. Genes differentially expressed only in Initial are highlighted in yellow. Genes highlighted in bold are focus genes. Genes in regular print were used to connect to other genes in the network.

Network ID	Genes in Network	Network Score	Focus Genes	Function
1	↑**A2M**, ↑**AARS**, ↓**ADIPOQ**, Ap1, ↓**APOE**, ↓**COL4A1**, ↓**CXCL16**, ↑**CYBB**, Cytochrome c, ↓**DCN**, ↓**FABP4**, ↓**FN1**, ↑**GAPDH**, ↓**GPAM**, ↓**GRN**, LDL, ↓**LPL**, ↓**MGP**, Mmp, ↓**MSR1**, NFkB, ↑**NPC2**, ↑**PCSK7**, peptidase, ↑**PKM2**, ↑**PLAT**, ↑**PRDX2**, ↓**RAP1A**, Rxr, ↑**SAT1**, ↑**SLC25A4**, ↑**SQSTM1**, Tgf beta, ↑**TMEM66**, Trypsin	51	26	Cell-To-Cell Signaling and Interaction, Immune and Lymphatic System Development and Function, Lipid Metabolism
2	↓**ACP5**, ↓**AGTR1**, Akt, ↑**ANKH**, ↑**ARL6IP5**, ↓**CCNL2**, ↓**CLU**, ↓**COL3A1**, Creb, Cyclin A, ERK1/2, FSH, ↓**GHRH**, hCG, ↑**HDAC3**, Histone h3, IK, Insulin, ↓**MAGED2**, Mek, ↓**NBN**, ↑**PCNA**, Pka, PLC, ↑**PPM1A**, ↓**PTGS2**, ↑**RASAL2**, RNA polymerase II, ↓**SETMAR**, ↑**SPP1**, ↓**THRSP**, ↑**UQCRC1**, Vegf, ↑**WDR36**, ↑**YBX1**	38	21	Cancer, Gastrointestinal Disease, Reproductive System Disease
5	ADAM10, amino acids, ARD1A, ARMC6, C6ORF211, CCT8, ↓**CPM**, DYRK1A, DYRK1B, FNTA, FNTB, ↑**GBAS**, ↓**GNL3**, HNF4A, KCNQ5 (includes EG:56479), MAP3K1, NIPSNAP1, ↓**NP**, ↑**PDK4**, PDZK1, ↑**PPM1A**, PRKCI, PTPRE, ↑**RPL10**, ↑**SAP18**, ↑**SH3PXD2A**, ↓**SHKBP1**, SMARCE1, SRC, SUB1, ↑**TM7SF2**, ↑**TMEM128**, ↑**TRUB2**, ↑**UBL7**, ↓**WDR68**	24	15	Amino Acid Metabolism, Post-Translational Modification, Small Molecule Biochemistry
6	↓**ABCG2**, ADCYAP1, ATP1B1, BAZ1A, ↑**BCAM**, beta-estradiol, ↓CDKN1C, ↓**CFB**, ↑**CHRAC1**, ↓**CRYZ**, CSF2, E2F1, ↑**EIF1**, ↑**FOXP1**, GHRHR, IL15, ITGAE, ITGAM, ↑**LYPLA1**, ↑**NACA**, PLA2R1, POLD1, POLE3, POLR1B, ↓**POLR1D**, ↓**PRDX6**, ↓**PTP4A2***, RFC3, RFC4, SFRS7, SMARCA5, ↑**SYAP1**, TAF1A, TBP, TK1	20	13	Cellular Assembly and Organization, Cell Cycle, DNA Replication, Recombination, and Repair

Table 3.6. Networks were generated for the Wheat Pasture diet of the Growing Phase using Inginuity Pathway Analysis. Genes differentially expressed only in the Wheat Pasture diet of the Growing Phase are highlighted in yellow. Genes highlighted in bold are focus genes. Genes in regular print were used to connect to other genes in the network.

Network ID	Genes in Network	Network Score	Focus Genes	Function
2	↑**A2M,** ↓**ADIPOQ,** Angiotensin II receptor type 1, Calpain, ↓**CD36,** ↓**CLU,** ↓**COL1A1,** ↓**COL1A2,** ↓**COL3A1,** ↓**COL4A1,** ↑**CYBB,** ↓**DCN,** ERK, Fibrin, ↓**FN1,** ↓**GCLC,** HDL, Integrin, LDL, ↓**MGP,** Mmp, ↓**MSR1,** ↑**NPC2,** ↑**PCSK7,** peptidase, ↑**PLAT,** ↓**PRNP,** ↓**SERPINE1,** ↑**SH3PXD2A,** Smad2/3-Smad4, ↓**SPARC,** Tgf beta, ↓**TLN1,** Vegf, ↑**YBX1**	41	23	Cell-To-Cell Signaling and Interaction, Connective Tissue Disorders, Dermatological Diseases and Conditions
3	↓**ACSL1,** ↑**ACTB,** Actin, ↓**ADRBK2,** Akt, ↑**CALM1,** Calmodulin, ↓**CAV1,** ↓**CD99 (includes EG:4267),** ↓**CDKN1C,** ↑**CFL2,** Cofilin, Cyclin A, E2f, F Actin, G-Actin, ↓**GHRH,** ↑**GPI,** ↓**GSN,** hCG, Hsp90, ↑**HSP90AA1,** Insulin, ↑**JUB,** ↓**NBN,** ↑**PCNA,** Pka, PLC, Pld, PP2A, ↑**PPM1A,** Proteasome, Rb, ↑**S100B,** ↑**SPTAN1**	29	18	Cancer, Respiratory Disease, Reproductive System Disease
4	Ap1, ↓**APOE,** Creb, ↓**CXCL16,** ERK1/2, ↓**FABP4,** ↓**GPAM,** ↑**IFI35,** Ifn gamma, ↑**IGFBP6,** IGF, IL1, IL12, Interferon alpha, ↓**LPL,** Mek, ↓**MYD88,** NCOR-LXR-Oxysterol-RXR-9 cis RA, Nfat, NFkB, Pdgf, Pkc(s), ↓**PLD1,** ↑**PRDX2,** ↓**PTGS2,** ↓**RIT1,** Rxr, ↓**S100G,** ↑**SLC25A4,** Sos, ↑**SPP1,** ↑**SQSTM1,** Tlr, ↓**TLR2,** VitaminD3-VDR-RXR	27	17	Cellular Movement, Hematological System Development and Function, Lipid Metabolism
5	ALDH2, ↓**ALDH1A1,** ARMC6, ATP5A1, ATP5L, ↑**ATP6V1H,** BCLAF1, C6ORF211, CCDC90B, ↓**CRYZ,** DDOST, EFTUD2, GLS, ↓**GNL3,** GSPT1, HNF4A, ↑**KIAA1704,** MAGOH, MAT2A, NCBP1 (includes EG:4686), ↓**NDFIP1,** ↓**NP,** PABPN1, ↑**RPL18,** RPL12 (includes EG:6136), ↓**RSRC1,** ↑**SAP18,** SFRS1, ↑**TM7SF2,** ↑**TMEM128,** ↑**TRUB2,** TUBB4, ↑**UBL7,** ↓**VEZT,** YWHAG	23	15	RNA Post-Transcriptional Modification, Energy Production, Nucleic Acid Metabolism
6	↑**APCDD1,** cholesterol, FNG, ↑**FOXP1,** ↑**IDI1,** ITGAM, ↓**LAP3,** ↑**LAPTM5,** ↑**LFNG,** ↑**MFNG,** NADH dehydrogenase, NADH2 dehydrogenase (ubiquinone), ND2, ND3, ND4, ND5, ND6, ↑**ND4L,** NDUFA13, NDUFS1, NDUFS2, NDUFS3, ↑**NDUFS4,** ↑NDUFS5, NDUFS8, NDUFS6 (includes EG:4726), ↑**NDUFV1,** NDUFV2, ↑**NPC2,** ↓**OAT,** ↑**PMPCA,** retinoic acid, ↑**RFNG,** SREBF1, ↑**TM7SF2**	23	15	Free Radical Scavenging, Genetic Disorder, Neurological Disease
7	↓**ABCG2,** APH1A (includes EG:226548), APH1A (includes EG:51107), APH1B, ASB9, ↓**BCAT2,** beta-estradiol, ↑**C1ORF21,** ↑**CCDC80,** ↓**CFB,** ↑**CHD2,** ↑**CKB,** CKM, CLEC3B, ↑**CNBP,** COL6A1, ↓**COL6A2,** COL6A3, CREB1, DGAT1, dihydrotestosterone, ↓**EHD2,** ERBB2, ↓**HADH,** HGF, ↑**NCSTN,** ↓**NID2,** PAM, PLA2R1, PSEN1, PSENEN, S100A6, ↓**SEC63,** SLC2A4, TMED2	21	14	Post-Translational Modification, Genetic Disorder, Skeletal and Muscular Disorders
8	↑AARS, ↓**ANLN,** C12ORF10, CEBPZ, CLIC4, ↑**EDEM2,** EIF2AK2, FASN, ↑**GAPDH,** ↑**GPI,** HSPH1, IARS2, ↓**ILF2 (includes EG:3608),** ↑**JTV1,** ↑**MRCL3,** MTHFD1, MYC, NANS, niacinamide, ↑**NMT1,** PIN4, ↑**PKM2,** PSAT1, ↑**RBMS1,** ↑**RNF139,** ↑**RPL10,** RPL23, ↑**RPL13A,** RPS3A, SGK1, TAF1A, TAF1B, TAF1C, TNFRSF1A, TPS3	19	13	Cancer, Cell Death, Gene Expression
9	ADIPOR2, BAZ1A, ↑**CHRAC1,** ↓**CIDEA,** CPT1, ↓**ELOVL5,** EWSR1, FABP3, GFPT1, ↑**GOT2,** ↓**GPBP1L1,** ↓**H1F0,** ILK, INS1, KCNJ11, lactic acid, ↓**LDHB,** LEP, ↑**LIMS2,** POLE3, ↓**POLR1D,** PPARA, ↓**PTRF*,** RB1, SERPINA12, SLC27A1, SMARCA5, TAF1A, TAF1C, TBP, ↓**THRSP,** UCP2, UCP3, ↑**UGP2,** ↑**ZDHHC3**	19	13	Carbohydrate Metabolism, Small Molecule Biochemistry, Lipid Metabolism
20	↓**CA5B,** Carbonic anhydrase	2	1	Genetic Disorder, Renal and Urological Disease, Infectious Disease

Table 3.7. Networks were generated for the Silage-fed diet of the Growing Phase using Inginuity Pathway Analysis. Genes differentially expressed only in the Silage-fed diet of the Growing Phase are highlighted in yellow. Genes highlighted in bold are focus genes. Genes in regular print were used to connect to other genes in the network.

Network ID	Genes in Network	Network Score	Focus Genes	Function
2	↓**ADIPOQ**, Ap1, ↓**APOE**, ↓**CD36**, ↓**COL4A1**, ↑**CYBB**, ↓**DCN**, ERK, ↓**FABP4**, ↓**GCLC**, ↓**GRN**, IKK, IL1, Insulin, LDL, ↓**LPL**, ↓**MSR1**, NCOR-LXR-Oxysterol-RXR-9 cis RA, Nfat, ↑**PCSK7**, Pdgf, ↑**PEA15**, peptidase, Pkc(s), ↓**PLD1**, ↑**PRDX2**, ↓**PRNP**, ↓**PTGS2**, ↓**RAP1A**, Rxr, ↓**SPARC**, ↑**SPARCL1**, ↑**SPP1**, Tgf beta, Vegf	39	21	Lipid Metabolism, Small Molecule Biochemistry, Cell-To-Cell Signaling and Interaction
3	ADIPOR1, ADIPOR2, AGXT, ↑**APCDD1**, ↑**C1ORF21**, ↓**CD36**, ↓**COL3A1**, D-glucose, dihydrotestosterone, ↑**EFEMP1**, ELN, ↓**ELOVL5**, ↓**FABP4**, FNG, INS1, KCNJ11, ↓**LAP3**, ↓**LDHB**, long chain fatty acid, ↓**MAGED2**, MDH2, ↑MFNG, ↓**NID2**, NOTCH1, ↓**OAT**, PPARA, ↓**PTRF***, retinoic acid, ↑**RFNG**, ↓**RPS26**, SCD, TK1, UCP3, ↑**UQCRC1**, UQCRC2	27	16	Lipid Metabolism, Small Molecule Biochemistry, Carbohydrate Metabolism

Table 3.8. Networks were generated for the Program-fed diet of the Growing Phase using Inginuity Pathway Analysis. Genes differentially expressed only in the Program-fed diet of the Growing Phase are highlighted in yellow. Genes highlighted in bold are focus genes. Genes in regular print were used to connect to other genes in the network.

Network ID	Genes in Network	Network Score	Focus Genes	Function
1	↓**AGTR1,** ↓**AQP4,** ↓**CCNL2,** ↓**CFB,** ↑**CHD8,** Ck2, ↓**CLIC1,** ↓**CXCL16,** ↑**FUS,** ↓**GHRH,** ↓**GPAM,** hCG, ↑**HDAC3,** Histone h3, ↓**HNRNPF,** ↓**MAGED2,** Mapk, ↑**MRCL3,** ↑**MYL6,** Myosin light chain, NFkB, ↓**NR2F2,** ↑**PCNA,** PDGF BB, ↑**PLAA,** ↑**PPM1A,** RNA polymerase II, ↑**S100B,** ↓**SETMAR,** ↑**SLC25A4,** ↓**SLC7A7,** ↑**UQCRC1,** Vegf, ↑**WDR36,** ↑**YBX1**	51	26	DNA Replication, Recombination, and Repair, Cell Death, Embryonic Development
2	↓**ACP5,** ↓**ADIPOQ,** Ap1, ↓**APOE,** Calpain, ↑**CAPN10,** ↓**CD36,** ↓**COL4A1,** ↑**CYBB,** ERK, ↓**FABP4,** ↓**GCLC,** ↑**IGFBP5,** IK, IL1, Insulin, LDL, ↓**LPL,** NCOR-LXR-Oxysterol-RXR-9 cis RA, Nfat, ↑**NPC2,** P38 MAPK, ↑**PCSK7,** Pdgf, peptidase, Pkc(s), ↑**PLAT,** ↑**PRDX2,** ↓**PRNP,** ↓**PTGS2,** ↓**RAP1A,** Rxr, ↑**SPP1,** Tgf beta, ↓**TLN1**	36	20	Lipid Metabolism, Small Molecule Biochemistry, Cardiovascular System Development and Function
4	ABCB1B, ADCYAP1, ↓**ANLN,** APPL1, ↑**BCAM,** ↑**C1ORF21,** CEBPB, ↑**COX3,** DGAT1, ↓**DGAT2,** dihydrotestosterone, E2F4, ↓**EHD2,** ↓**EXOSC9,** FABP, ↓**FABP4,** FNG, GFPT1, INS1, KIAA0101, ↑**LFNG,** ↑**MFNG,** ↑**NMT1,** ↓**NMT2,** NOTCH1, ↓**PRDX6,** ↓**PTRF*,** ↑RFNG, SERPINA12, SLC27A1, SLC2A4, ↑**SMPD4,** TNF, TP53, TTF1	24	15	Gene Expression, Lipid Metabolism, Molecular Transport
6	↓**ABCG2,** ACADVL, ACOX1, ↓ACSL1, ↑**APCDD1,** beta-estradiol, BMP4, ↑**C10ORF116,** ↑**CCDC80,** ↑**CHD2,** CHRD, ↑**CNBP,** CPT1A, CRYAA, ↓**CRYZ,** DAP3, dehydroisoandrosterone, ↓**ELOVL5,** ERH, FABP2, FABP5L2, FOXC2, GLS, ↓**GNL3,** ↓**HADH,** HGF, HSD11B1, ↓**NP,** NRL, ↑PDK4, PLA2R1, POU1F1, PPARA, ↓**PTP4A2*,** ↑**TWSG1**	20	13	Lipid Metabolism, Small Molecule Biochemistry, Organ Development
7	ANXA2, C19ORF57, ↓**CD99 (includes EG:4267),** ↑**EDEM2,** EGF, EWSR1, FASN, ↑**FOXP1,** FSTL1, ↓**GPBP1L1,** IDH1, ITGAM, ↑**JTV1,** lactic acid, MYC, PDPN, PIN4, ↑**PIP3-E,** POLR1B, ↓**POLR1D,** ↑**RBMS1,** RIBIN, ↑**RNF139,** ↑**RPL10,** RPL14, RPL19, RPL35, ↑**RPL13A,** RPS13 (includes EG:6207), RPS3A, TAF1A, TAF1B, TAF1C, TBP, ↑**ZDHHC3**	18	12	Cellular Assembly and Organization, Cancer, Cellular Growth and Proliferation
8	ABCD3, ANGPTL4, ARCN1, BAZ1A, ↓**BET1L,** ↓**BRP44L,** ↑**CHRAC1,** COL6A1, ↓**COL6A2,** COL6A3, COP I, COPA, COPB2, COPE, ↑**COPG,** COPZ1, COPZ2, DGAT1, ERBB2, GALNT1, ↓**H1F0,** IDH1, ILK, JARID1B, LEP, ↑**LIMS2,** PARVA, POLE2, POLE3, RB1, ↓**RNASET2,** SACM1L, SMARCA5, ↑**TMED9,** ↑**UGP2**	14	10	Genetic Disorder, Skeletal and Muscular Disorders, Cellular Assembly and Organization
9	ACOX1, ↑CALM1, CCT5, CEBPZ, CREB1, ↓**EMP3,** ETV6, ↑**FUS,** GHRHR, ↓**HNRNPF,** IL3, IL1RL1, KITLG (includes EG:4254), ↑**LAPTM5,** LATS2, ↑**MFNG,** MYO1C, ↑**NACA,** PAPPA2, PLA2G1B, retinoic acid, RPL3, RPL4, RPL6, ↑**RPL10,** RPL11, RPL23A, RPS16, SCYE1, ↓**SEC63,** TAF1C, TPM4, TPSB2, UCP2, ZBTB17	11	8	Protein Synthesis, Cellular Development, Cell Death
11	↓**EGFL7,** GFI1B	2	1	Cellular Development, Cellular Growth and Proliferation, Hematological
19	HS6ST1, ↑**HS6ST2**	2	1	Cellular Growth and Proliferation, Connective Tissue Development and

Figure 3.2. The top ten molecular and cellular functions associated with all generated networks for Intital and Wheat Pasture,Silage-fed, and Program-fed diets of the Growing Phase. Threshold signifiacnce($P < 0.05$) expressed as the negative $\log_{10}$ of the P-value calculated using the right-tailed Fischer's exact test is represented by the orange bar. Numbers at top of each graph are the number of genes associated with that function.

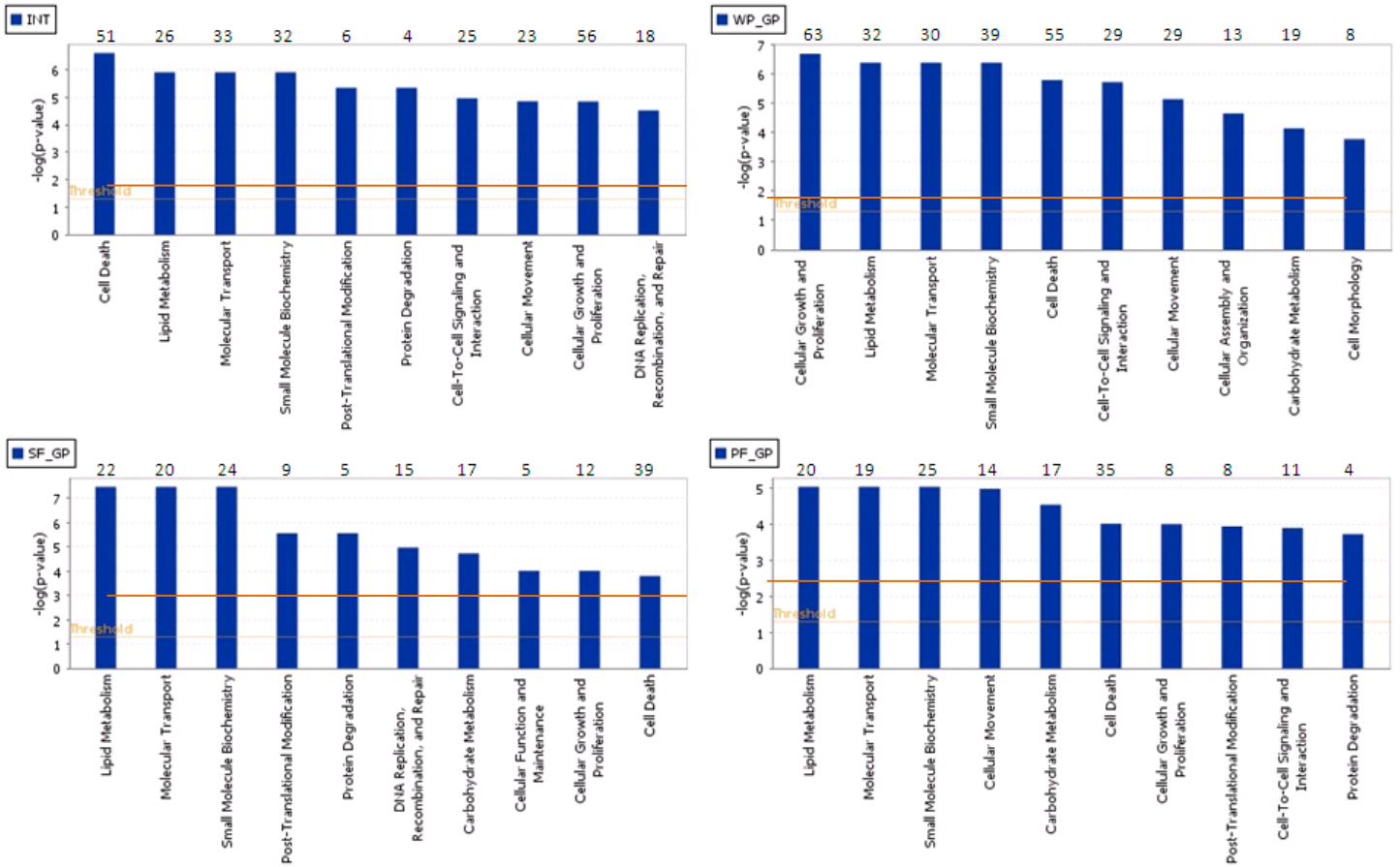

Figure 3.3. Comparative Functional Analysis of differentialy expressed genes comparing Initial,Wheat Pasture, Silage-fed, and Program-fed diets of the Growing Phase. Significance ($P < 0.05$), expressed as the negative $\log_{10}$ of the P-value calculated for each function using the right- tailed Fischer's exact test, is represented by the orange bar.

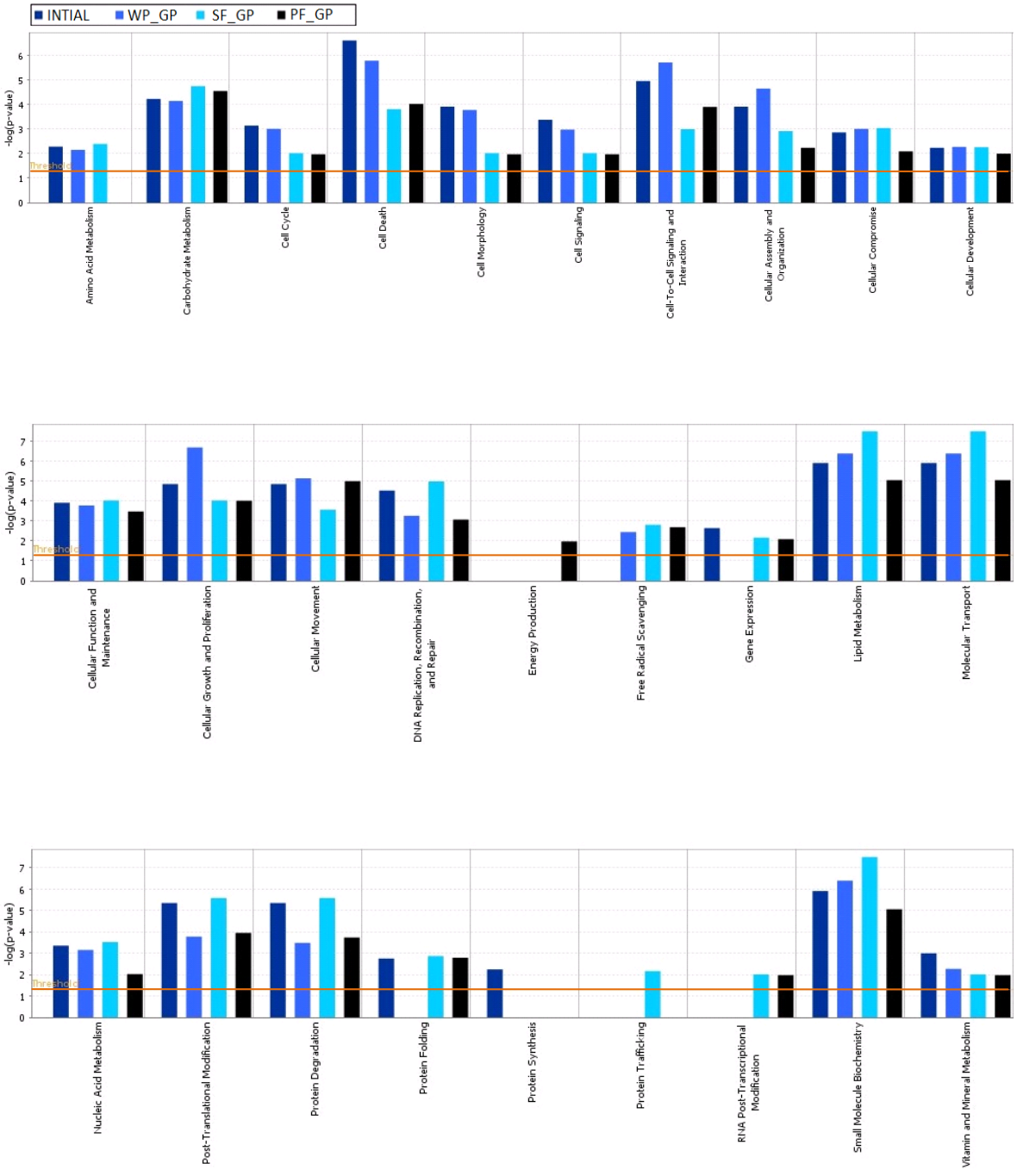

Figure 3.4. Metabolic pathway comparison between Initial, Wheat Pasture, Silage-fed, and Program-fed diets of the Growing Phase. Significance ($P < 0.10$), expressed as the negative $\log_{10}$ of the P-value calculated for each function using the right-tailed Fischer's exact test, is represented by the orange bar.

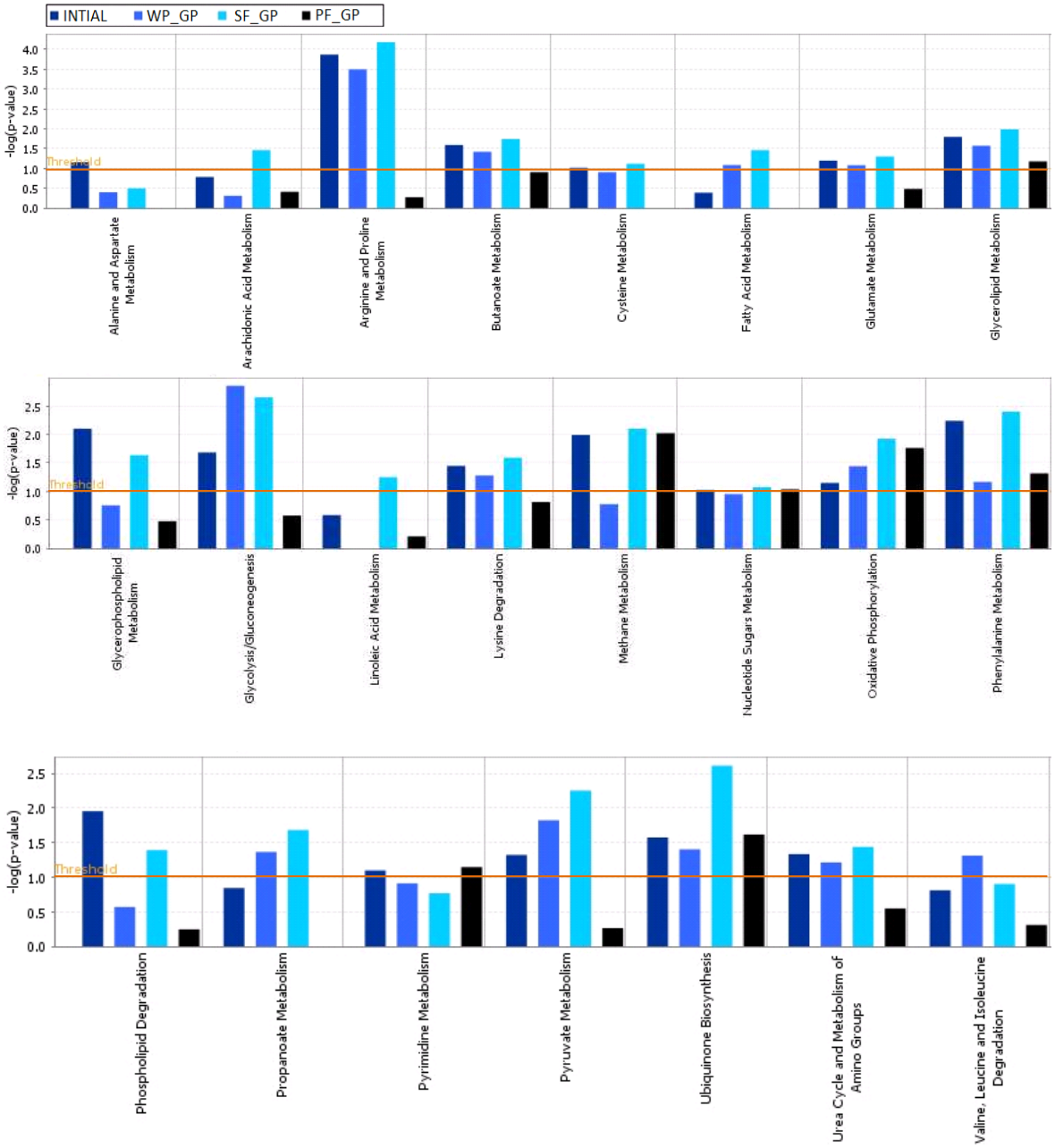

Figure 3.5. Signaling pathway comparison between Initial, Wheat Pasture, Silage-fed, and Program-fed diets of Growing Phase. Significance ($P < 0.10$), expressed as the negative $\log_{10}$ of the P-value calculated for each function using the right-tailed Fischer's exact test, is represented by the orange bar.

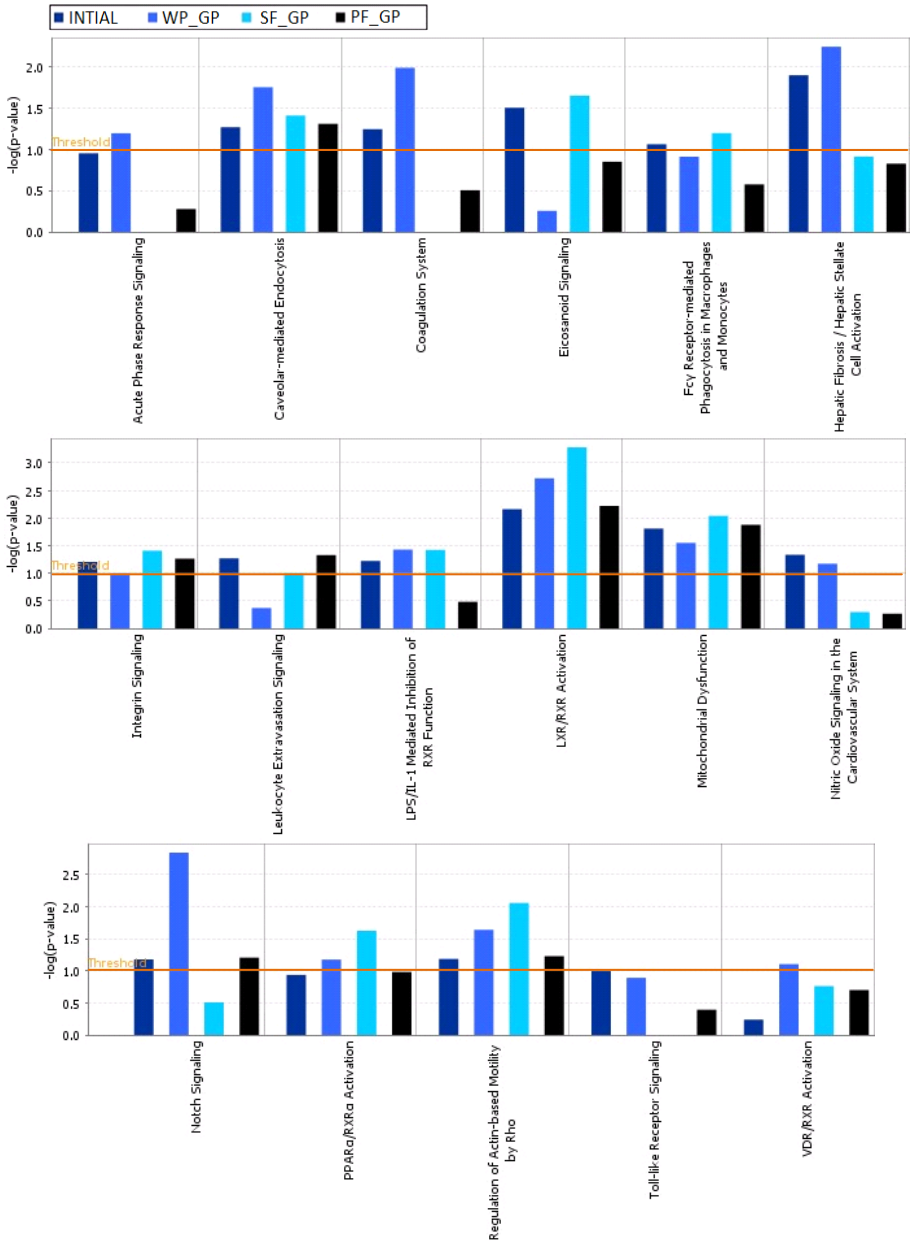

Figure 3.6. Heat map of genes in the Adipose Related ontology category. Boxes colored with shades of red represent genes up-regulated in i.m. adipose tissue compared to s.c. adipose tissue and boxes with shades of green represent down-regulted genes in i.m. adipose tissue compared to s.c. adipose tissue. Black boxes represent no observed change in gene expression.

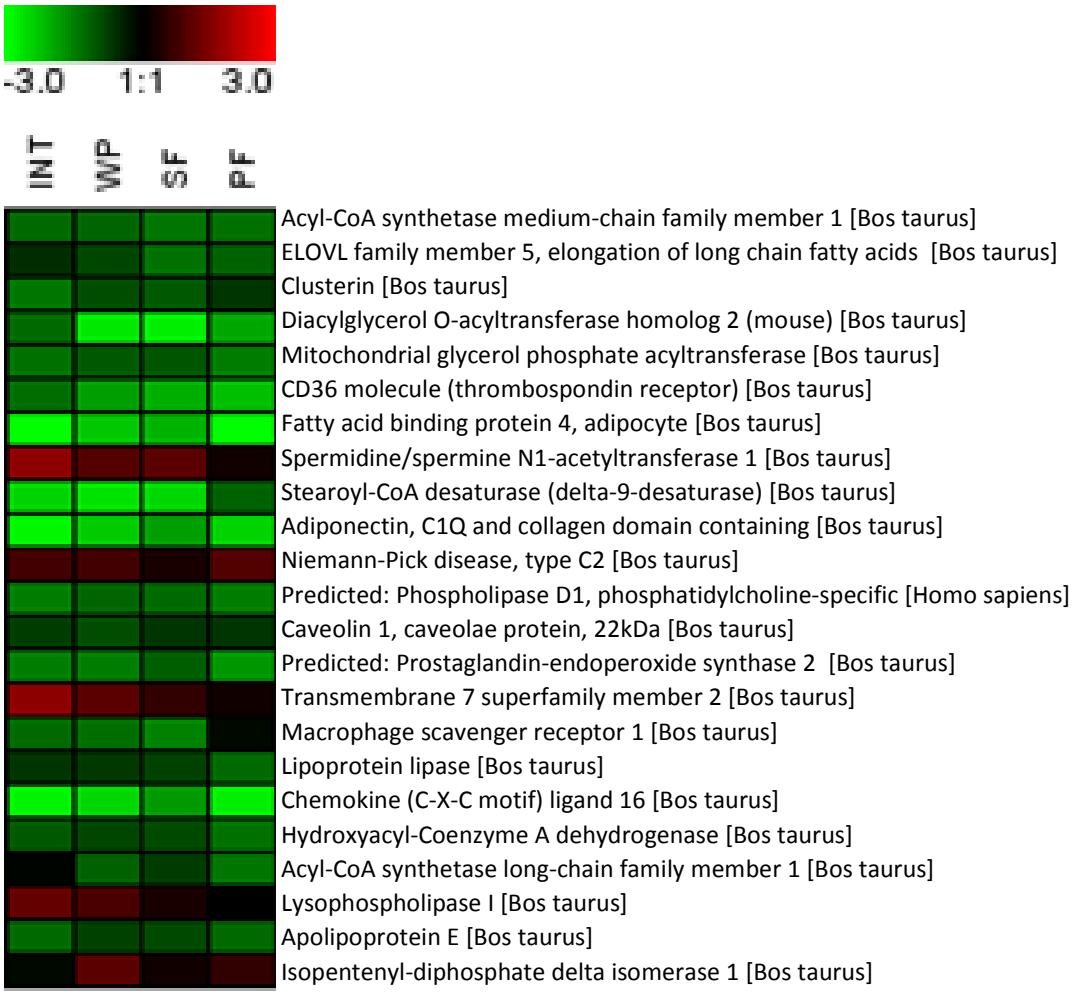

Figure 3.7. Heat map of genes in the Carbohydrate Metabolism ontology category. Boxes colored with shades of red represent genes up-regulated in i.m. adipose tissue compared to s.c. adipose tissue and boxes with shades of green represent down-regulted genes in i.m. adipose tissue compared to s.c. adipose tissue. Black boxes represent no observed change in gene expression.

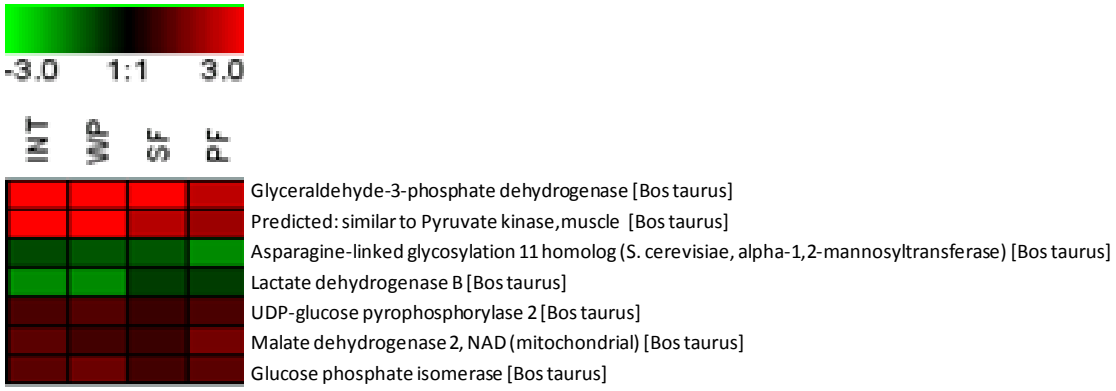

Figure 3.8. Heat map of genes in the Oxidative Phosphorylation ontology category. Boxes colored with shades of red represent genes up-regulated in i.m. adipose tissue compared to s.c. adipose tissue and boxes with shades of green represent down-regulted genes in i.m. adipose tissue compared to s.c. adipose tissue . Black boxes represent no observed change in gene expression.

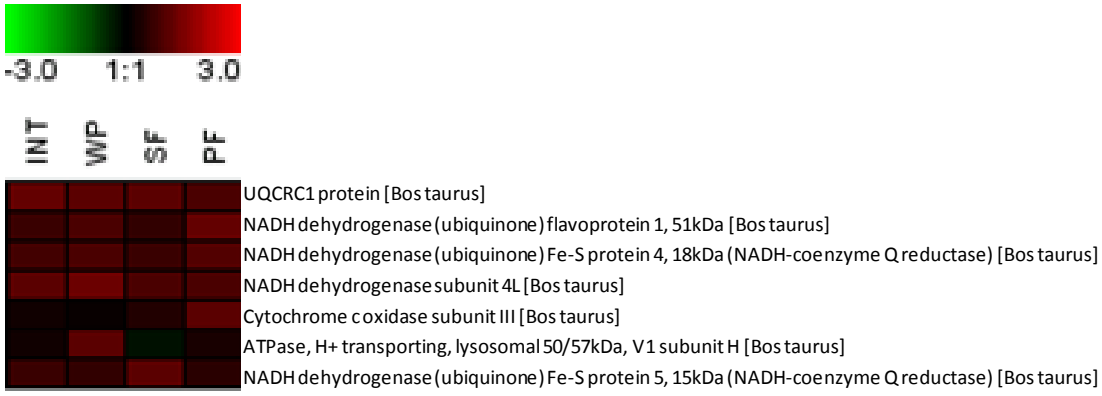

Figure 3.9. Network 1 of theWheat Pasture diet of the Growing Phase depiciting genes involved in apoptosis of eukaryotic cells and cell morphology. Dataset was analyzed by the Ingenuity Pathways Analysis software. Node color indicates the expression level of the genes; green = down-regulation in i.m. adipose tissue when compared to s.c. adipose tissue and red = up-regulated in i.m. when compared to s.c. adipose tissue.

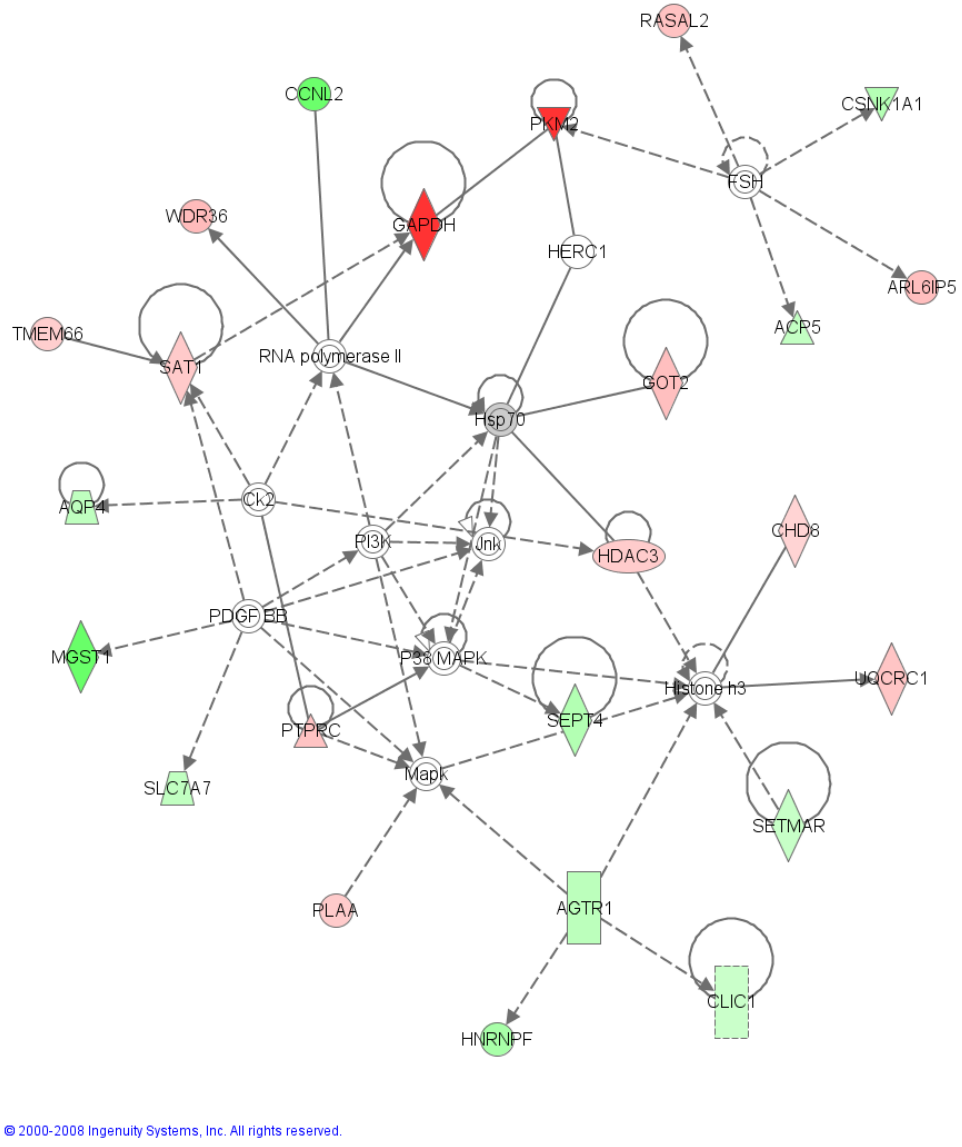

Figure 3.10. Network 1 of the Program Fed diet of the Growing Phase depiciting genes involved in DNA Replication, Recombination, and Repair. Dataset was analyzed by the Ingenuity Pathways Analysis software. Node color indicates the expression level of the genes; green = down-regulation in i.m. adipose tissue when compared to s.c. adipose tissue and red = up-regulated in i.m. when compared to s.c. adipose tissue.

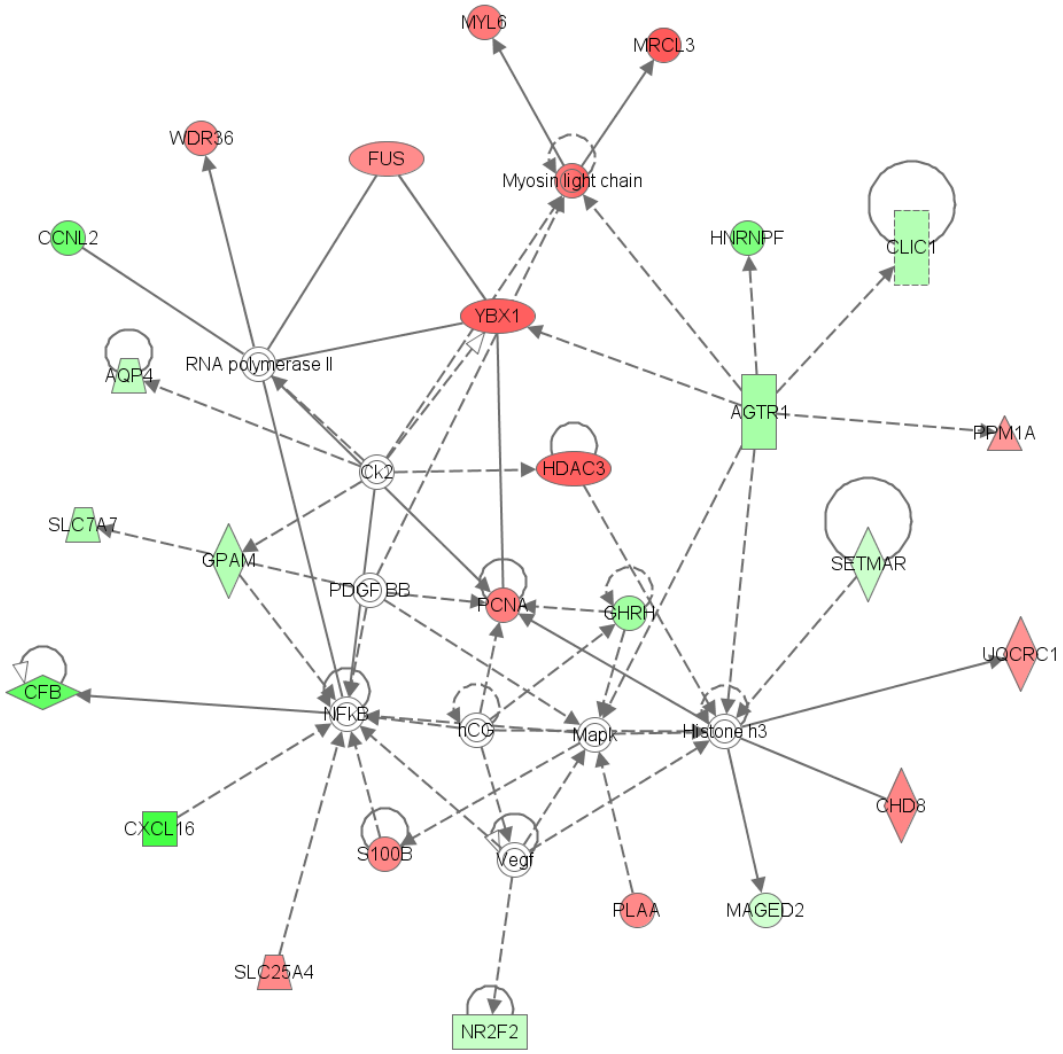

CHAPTER IV

Effects of winter growing programs on gene expression in different adipose tissue depots in beef steers at the end of the finishing phase

D.R. Stein[1], A. Pillai[1], C.R. Krehbiel[1], G.W. Horn[1], M. McCurdy[2], J. J. Wagner[3], J.B. Morgan[1], R.D. Geisert[5] P.J. Ayoubi[4] and U.E. DeSilva[1]

[1] OSU Dept. of Animal Science, [2]Nutrition Service Associates, Kenmore, QLD, Australia, [3]Southeast Colorado Research Center, Colorado State University, Lamar, CO, [4] OSU Dept. of Biochemistry & Mol. Biology, and [5]Dept. of Animal Science, University of Missouri, Columbia

Abstract

Previous research in our laboratory demonstrated that nutrition during the growing phase affects the performance of beef cattle during the finishing phase. More so, the nutritional background in beef steers (i.e., steers on supplemented native range or steers on high-gain wheat pasture) altered gene expression in s.c. and i.m. adipose tissue depots during the finishing phase in the feedlot. Microarray analyses, validated by RT-PCR, was utilized to investigate the effects of different winter growing programs on gene expression in s.c. and i.m. adipose tissue depots in beef steers at the end of the subsequent finishing phase (FP). Steers of similar breed, type, and age were assigned to initial harvest or one of four treatment diets; steers placed in the feedlot after weaning and fed a high-concentrate diet (CF); steers grazed on wheat pasture (WP); steers fed a sorghum silage-based growing diet (SF); or steers program fed a high-concentrate diet (PF). SF and PF were fed to gain BW similar to WP. At the end of a 112-d growing phase (GP), 6 steers from WP, SF, and PF were harvested, with the remaining steers of each diet placed in the feedlot. At the end

of FP, steers from all treatment groups were harvested at a common 12^{th} rib fat (1.27 cm) as determined by ultrasound. Days on feed were 123, 104, and 104, for WP, SF, and PF steers, respectively. CF steers were on feed for a total of 196 d, 112 of which coincides with the time the WP, SF, and PF steers were on respective diets of the GP. A 7.6 cm^3 section was dissected from the *Longissimus* muscle at the 12^{th} rib from which s.c. and i.m. adipose tissue were collected. Total RNA was extracted and cDNA microarray hybridizations performed. Preprocessing and normalization of data was accomplished utilizing GenePix AutoProcessor (GPAP 3.2). Ontology analysis was carried out using GFINDer. Ingenuity Pathways Analysis (IPA) was also used to identify the most relevant biological mechanisms, pathways and functions of the annotated genes. A total of 248 genes were differentially expressed (DE) between s.c. and i.m. adipose tissue depots in at least one of the four treatment diets of FP. The number of differentially expressed genes observed in WP steers was almost four times greater than SF steers (145 vs. 41), almost three times greater than PF steers (145 vs. 55) and almost twice the number in CF steers (145 vs. 82). WP steers had a greater number of differentially expressed genes involved in binding, cell growth and differentiation, signal transduction and transcription/translation functions than steers on the SF, PF and CF diets. However, the number of differentially expressed adipose related genes was only slightly attenuated in SF and PF steers as compared to WP and CF steers. The data presented indicates the metabolic machinery for adipose tissue accretion was down-regulated in the i.m. adipose tissue depot compared to the s.c. adipose tissue depot and the main affect of previous diet could possibly influence gene expression at the end of the FP as HADH, GPI, PKM2, and FHL1 were influenced or had a tendency to be influenced by diet, with PTGS2 having a tendency to be influenced by a diet x depot interaction. IPA metabolic and signaling pathway analysis also provided

insight into possible differences in the molecular mechanisms affecting gene expression in s.c. and i.m. adipose tissue depots in beef steers managed under different growing diets at the end of the subsequent finishing phase.

Key words: beef cattle, microarray, adipose tissue, gene expression

Introduction

The terms backgrounding and stockers are synonymous (Peel, 2000) and describe the production phase between the time a calf is weaned until placement into a feedlot for finishing (Bock et al., 1991; Thomson and White, 2006). Stockers are raised primarily on forage or pasture diets in the south central and southern U.S., while silage is the primary diet fed in backgrounding lots in the north central and northern U.S. (McCurdy, 2006). Lack of available forage or pasture due to inclement weather or market conditions may warrant the confinement of animals to a drylot and fed a grain-based ration (Thomson and White, 2006). Two alternatives to roughage or pasture based programs are; 1) program feeding, defined by Galyean (1999) as the use of net energy equations to calculate the quantities of feed required to meet the needs of maintenance plus a specific ADG, and 2) calf-fed programs, a system where cattle are placed on an *ad libitum* finishing diet immediately following weaning (Lardy, 1998). Due to geographical regions in the U. S., backgrounding/stocker programs involve a wide range of production environments and management skills, such that not all programs and systems are feasible for producers in the various locations in the U.S. (Peel, 2006). Nutrition during the growing phase has been shown to affect the performance of cattle during their finishing phase as hot carcass weight, *Longissimus* muscle area, and marbling score were greater for steers grazing winter wheat compared to steers grazing native range prior to feedlot placement (Choat et al., 2003). Cattle fed grain-based diets have been shown to have increased i.m. fat compared with

those fed forage-based diets as marbling scores were significantly lower for steers grazed on summer pasture and then fed for either 45 or 75 d in the feedlot compared to steers taken to the feedlot immediately after weaning (Schaake et al., 1993). Furthermore, steers fed a diet consisting of 68% high-moisture corn and 25% alfalfa silage had increased i.m. fat compared to cattle fed a 95% alfalfa silage diet for the same number of days on feed (Mandell et al., 1998). Additionally, grazing-based growing programs prior to feedlot entry resulted in cattle with lower marbling scores compared to calves placed directly in a drylot and fed a silage-based diet followed by a corn diet (Hedrick et al., 1983). Using suppressive subtractive hybridization, we have reported different nutritional background in beef steers (i.e., steers on supplemented native range or steers on high-gain wheat pasture) altered gene expression in s.c. and i.m. adipose tissue depots during the feedlot phase (Ross et al., 2005). Thus, it is important to determine the effects of background, previous nutrition and management systems throughout the production phases on marbling and subsequent quality of the carcass. Therefore, the objective in the present study was to determine the effects of different winter growing programs on gene expression in s.c. and i.m. adipose tissue depots in beef steers at the end of the finishing phase.

Materials and Methods

Animals and Treatment Groups (Diet)

Adipose tissue samples used in the present study were collected from previous work by McCurdy (2006). A total of 260 British crossbred steers were used for this study which included 50 steers from the Oklahoma State University cow herd and 210 steers purchased by Colorado Beef (Lamar, CO) of similar breed, type, and age (average initial BW=236 ± 22.0 kg). Four steers were randomly selected for initial serial slaughter (INT) and were transported to the Robert M. Kerr Food & Agricultural Products Center abattoir (FAPC),

located on the campus of Oklahoma State University, Stillwater, OK. The remaining steers were blocked by initial weight and randomly allotted to one of four treatment groups for winter feeding or growing phase (GP). One group of steers was placed in the feedlot (CF**;** n = 8 pens; 8 steers/pen) immediately on arrival and adapted to an *ad libitum* high-concentrate finishing diet. Steers in this treatment group underwent a three tier adaptation period consisting of a 49% and 74% concentrate diet, each fed for 5 d, followed by an 88% concentrate (finisher) diet. The three remaining treatment groups were managed under three different growing systems. One treatment group (WP; n = 64) was grazed as a single group on wheat pasture with unrestricted forage availability; the second treatment group (SF; n = 8 pens; 8 steers/pen) was fed a sorghum silage-based growing diet; and the third treatment group (PF; n = 8 pens; 8 steers/pen) was program fed a high-concentrate diet. Steers in the SF and PF groups were fed to gain BW at a similar rate as WP steers. All steers were implanted with progesterone (USP 200 mg) and estradiol benzoate (20 mg) (Component E-S, VetLife, West Des Moines, IA) at the start of the GP. Steers from all treatment groups were weighed at 28 d intervals. Wheat pasture grazing took place at the Oklahoma State University Wheat Pasture Research Unit in Logan County, OK, while all pen feeding was conducted at the Southeastern Colorado Research Center, Lamar, CO. Steers at OSU allocated to the SF, PF, and CF groups were transported from Stillwater, OK to Lamar, CO (688 km), while purchased steers allocated to the WP group were transported from Lamar to Stillwater prior to the beginning of the trial. At the end of the growing phase (112 d), six randomly selected steers from each of the WP, SF, and PF treatment groups were transported to the Robert M. Kerr Food & Agricultural Products Center **(**FAPC) abattoir in Stillwater, OK for slaughter. The remaining steers in the WP group were shipped from Stillwater, OK to Lamar, CO.

Finishing Phase

Steers from the WP, SF, and PF treatment groups shipped to Lamar CO were adapted to the same high-concentrate finishing diet as the CF steers and placed in the feedlot (n = 8 pens; 8 steers/pen). Steers in the WP and SF groups were adapted to the finishing diet as previously described for the CF treatment group; PF steers immediately received the 74% concentrate diet for 5 d followed by the 88% concentrate finisher. Steers on the growing diets (WP, SF, and PF) were re-implanted with Revalor-S at the start of the finishing program. Calf-fed steers were re-implanted with Revalor-S at d 84 of the finishing period. Days on feed were 123, 104, and 104, for WP, SF, and PF steers, respectively. CF steers were on feed for a total of 196 d, 112 of which coincided with the time the WP, SF, and PF steers were on respective diets of the GP. At the end of the finishing phase, steers from all treatment groups were harvested at a common 12^{th} rib fat (1.27 cm) as determined by ultrasound. Six randomly selected steers from each of the WP, SF, PF and CF treatment groups were transported to the FAPC abattoir for the final serial slaughter group. The remaining steers in all treatments were slaughtered commercially at the Swift plant in Cactus, TX and complete carcass data was collected by the National Cattleman's Beef Association's carcass data collection service.

Sample Collection and RNA Extraction

At slaughter, steers harvwested at FAPC were stunned with captive bolt and exsanguinated. Following exsanguination, a 7.6 cm^3 section was dissected from the *Longissimus* muscle between the 12^{th} and 13^{th} rib, from which s.c. and i.m. adipose tissue was collected and frozen at -80º C. Total RNA was extracted using TRIzol reagent (Invitrogen, Carlsbad, CA) (4 ml TRIzol per 1 g of adipose tissue). The adipose tissue, in

TRIzol, was homogenized and centrifuged at 3,500 x g at 4º C for 15 min to separate insoluble material and excess fat. The lower aqueous (TRIzol) phase was transferred to a fresh tube and 0.2 ml chloroform/ml of TRIzol was added. Samples were centrifuged at 3,500 x g at 4º C for 30 min and the upper aqueous phase was transferred to a fresh tube. Isopropyl alcohol (0.5 ml/ml of TRIzol) was added and samples were maintained at -20º C overnight followed by centrifugation at 3,500 x g at 4º C for 10 min. The supernatant was removed and the RNA pellet washed with 75% chilled ethanol and suspended in DNase/RNase free water. A subsequent phenol:chloroform:isoamyl alcohol (25:24:1; pH 5.2) extraction of the RNA (1:1 ratio, respectively) was carried out. The RNA/phenol:chloroform:isoamyl alcohol mixture was centrifuged at 10,600 x g at 4º C for 5 min and the upper aqueous phase was transferred to a fresh tube and precipitated with 0.01 volumes of sodium acetate (3M; pH 5.2) and 2.5 volumes of chilled 98% ethanol. The samples were then maintained at -20º C overnight and centrifuged at 10,600 x g at 4º C for 30 min. The supernatant was removed and the RNA pellet was washed with 70% chilled ethanol and suspended in DNase/RNase free water and stored at -80º C. The integrity of the RNA was analyzed using gel electrophoresis (1.5%) and the RNA was quantified using a NanoDrop® ND-100 Spectrophotometer (NanaDrop Technologies, Willington, DE). Four steers from each diet were selected for microarray comparison.

Microarray Experiment

A bovine specific adipose tissue cDNA array prepared by Dr. Udaya DeSilva, Animal Molecular Genetics, Oklahoma State University, was used in this study. The printed array consisted of a 1,089 cDNA non-redundant clone library constructed from subcutaneous and visceral adipose tissue spotted onto Corning® UltraGAPS™ Coated

Slides (Corning, NY). Array printing procedures were adapted from published literature (Hegde et al., 2000). The library was sequenced, with the EST sequences submitted to GenBank. GenBank accession numbers and dbEST IDs are presented in a supplementary table available at http://www.ansi.okstate.edu/faculty/desilva/papers/table.html. Library annotation was accomplished, with EST sequences queried against the Peptide, Unigene, and nr GenBank database (Bos Taurus) with unknown EST sequences queried against the nr GenBank database (Mammalian).

The OmniGrid 100 microarrayer (Genomic Solutions Ann Arbor, MI) used to print the microarray slide was equipped with a print head containing 16 print tips in a 4 by 4 fashion, with subarrays printed by the print head representing a block. The array consisted of 16 blocks in a 4 by 4 design with each probe (sequence) being printed once per array. The array was printed in triplicate on each slide to give a final 4 by 12 block slide design; accordingly each probe was represented three times on the microarray slide. The adipose microarray contained a positive control consisting of a pooled sample of cDNA used to create the library and a negative control consisting of the printing buffer. The slides were left in a humidified atmosphere after printing for 6 to 8 h to facilitate probe attachment to the slide. The slides were then baked at 80º C overnight and then stored in a vacuum desiccator at room temperature until the implementation of the hybridization protocol. The microarray slides were rinsed in 0.1% SDS for 5 min and then rinsed in sterile ddH_2O for 15 s and immediately dried for 2 min using a slide centrifuge. The microarray slides were then placed into a screw-top 50 ml conical vial containing a pre-warmed (48º C) commercial pre-hybridization buffer (BlockIt Microarray Blocking Solution, TeleChem Int., Sunnyvale, CA) and incubated at 48º C for 4 h. Slides were removed and rinsed in sterile ddH_2O for 15 s and immediately dried for 2 min using a slide centrifuge.

To compare i.m. adipose tissue expression relative to s.c. adipose tissue, total RNA (2.5 μg) from s.c. (reference sample) and i.m. (test sample) adipose tissue was reverse transcribed into cDNA in separate tubes using both random and dT primers and reverse transcriptase (Superscript II RT, Invitrogen, Carlsbad, CA). The reaction was carried out at 42º C for 6 h and the cDNA was subsequently labeled using the 3DNA Array 900MPX Expression Array Detection Kit (Genisphere, Hatfield, PA). The cDNA was then purified using the Qiagen MinElute PCR Purification Kit (Qiagen Inc., Valencia, CA). Following a poly-T tailing reaction, the "tagged" cDNA was ligated to the 3DNA Capture Sequence, a 31-mer sequence specific for each the Alexa Fluor™ 546 and Alexa Fluor™ 647 and subsequently purified as previously described. For the primary hybridization (hybridizing the tagged cDNA to the array), the hybridization solution (75 ul) consisting of: 10.0 μl of cDNA/3DNA Capture Sequence of each the Alexa Fluor™ 546 and Alexa Fluor™ 647; 40.0 μl of the supplied 2X formamide-based hybridization buffer; 2.0 μl LNA dT blocker and 13μl nuclease-free water was denatured at 80º C for 10 min and deposited to a pre-hybridized array slide under a 24 x 60 mm lifterslip (Erie Scientific, Portsmouth, NH). The array was then incubated at 48º C for 18 h in a humidified hybridization cassette. Following incubation the lifterslip was allowed to wash off in a 2X sodium chloride/sodium citrate (SSC)/0.2% sodium dodecyl sulfate (SDS) solution prewarmed to 48 º C. The array slides were then washed in 2X SSC/0.2% SDS, 60º C,15 min; 2X SSC, RT,15 min; and 0.2X SSC, RT, 15 min. Following the final wash, the array slide was immediately dried for 2 min using a slide centrifuge. For the secondary hybridization, the hybridization solution (75 ul) consisting of 2.5 μl of the fluorescent 3DNA Capture Reagent (capture reagent is complement to the capture sequence of the primary hybridization) of each the Alexis Fluor™ 546 (reference sample) and Alexa Fluor™ 647

(test sample), 40.0 µl of the supplied 2X formamide-based hybridization buffer and 30 µl nuclease-free water was deposited to the array under a 24 x 60 mm LifterSlip (Erie scientific, Portsmouth, NH). The array was then incubated at 48º C for 4 h in a hybridization cassette. The array slide was washed and dried as previously described and stored in a light-proof container until image acquisition.

Microarray Data Analysis

To compare i.m. adipose tissue expression (Alexa 647) relative to s.c. adipose tissue (Alexa 546), hybridization signals were captured by scanning the microarray slides with lasers at two wavelengths, Alexa 546 (s.c.) and Alexa 647 (i.m.), using a ScanArray™ Express confocal laser scanner (PerkinsElmer Life Sciences Inc., Boston, MA) at a pixel size resolution of 10 microns with the resulting images saved as 16 bit TIFF images. For each slide, the laser power and photomultiplier tube (PMT) gain were adjusted to minimize variation between channels. Using a local background subtraction method (spots with foreground intensity minus background intensity), the commercial software package GenePix™ Pro 4.0 (Axon Instruments Inc., Union City, CA) was used to analyze the signal intensity values of each feature (spot) in the Alexa Fluor™ 546 and Alexa Fluor™ 647 channels. The GenePix Pro Result (GPR) files generated from the results of the image analysis from each biological and technical replication were used for further downstream analysis and ratio calculations. Preprocessing and normalization of data was accomplished utilizing the R-project statistical environment (http://www.r-project.org) with the Bioconductor and LIMMA packages (http://www.bioconductor.org) through the GenePix AutoProcessor (GPAP 3.2) website (http://darwin.biochem.okstate.edu/gpap32/) (Weng and Ayoubi, 2004). Background correction was performed using Robust Multi-array

Average (RMA) algorithm (Allison et al., 2006) available in the Bioconductor/LIMMA package. Following background correction, poor quality features were removed by filtering. Such poor quality features were defined as features displaying an intensity value of 200 Relative Fluorescence Units or less in both the Alexa Fluor™ 546 and Alexa Fluor™ 647 channels, as well as features flagged bad, not found, or absent by GenePix™ Pro 4.0 and were removed from the analysis. Two different normalization methods were utilized in the analysis to adjust and balance for the technical or systemic variation between the features within an array and between arrays for differences not caused by treatment. Lowess (locally weighted Least squares regression) - global intensity normalization, was used to balance the variation associated with dye bias within each array (Yang et al., 2001; Yang et al., 2002). To balance the effect of the Alexa Fluor™ 546 and Alexa Fluor™ 647 dye bias intensity between arrays, quantile normalization was utilized (Bolstad et al., 2003). Following data preprocessing, the expression ratio for each feature (gene) was calculated using the following formula where a two-fold change is represented by a $\log_2$ ratio >1.0 (up-regulation) or < -1.0 (down-regulation): M value ($\log_2$ expression ratio) = $\log_2$ (F647-B647$_{intensity}$ /F546-B546$_{intensity}$). Using GPAP 3.2, a moderated t-test was used to identify the differentially expressed array elements along with their M value ($\log_2$ ratio), their P-value obtained from the moderated t-statistic after false discovery rate (FDR) adjustment using the Benjamini and Hochberg method (Benjamini and Hochberg, 1995), and the number of individual features ($\log_2$ ratio) used for each gene. Array elements where > 50% of the total features across arrays was used to calculate the average $\log_2$ ratio, a $|t| > 2$, an M-value $|M| > +0.9$ (representing a fold change of 1.87), and an adjusted P-value < 0.01 were considered significantly differentially expressed and included for further analysis using the Genome Functional Integrated Discoverer (GFINDer)

(http://www.medinfopoli.polimi.it/GFINDer/) and Entrez Gene (http://www.ncbi.nlm.nih.gov/sites/entrez?db=gene).

Gene Ontology Analysis

The web based program GFINDer (Masseroli et al., 2004) was used in this study and is a program designed to retrieve annotations for a list of submitted genes, perform categorization and present the results for use in gene ontology and pathway analysis where possible. Entrez Gene is the National Center for Biotechnology Information (NCBI) database for gene-specific information (Maglott et al., 2005, 2007). The Entrez gene ID of the differentially expressed genes retrieved from NCBI was used for the ontology analysis. The annotation terms were generated with emphasis based on gene ontology assessment for molecular function and biological process rather than cellular component (Ashburner et al., 2000).

Ingenuity Pathway Analysis

To further understand the extent of how genes may interact within the context of metabolic or signaling pathways, Ingenuity Pathways Analysis (IPA) (Ingenuity® Systems, http://www.ingenuity.com) was utilized to identify the most relevant biological mechanisms, pathways and functions of the differentially expressed genes identified through GPAP 3.2. IPA enables the visualization and exploration of gene interaction and relies on the most current known relationships among human, mouse and rat genes and proteins.

A data set of differentially expressed genes from the four diets of FP containing gene ID and corresponding expression values was uploaded into the IPA application. To

gain a better understanding of the interactions between genes within a biological system, an arbitrary M-value of $|M| > +0.59$ (or a 1.50 fold change) and a P-value < 0.01 were assigned as parameters for this analysis. Each gene ID was mapped to its corresponding gene object in the Ingenuity Pathways Knowledge Base (IPKB). These genes, called focus genes, were overlaid onto a global molecular network developed from information contained in the IPKB. Networks of these focus genes were algorithmically generated based on their connectivity and assigned a network score. IPA arbitrarily sets the maximum number of focus genes in each network at thirty-five. The functional analysis of an entire dataset or single network identifies the biological functions and/or diseases that were most significant to the genes in the dataset or network. IPA uses a Fischer's exact test to calculate a P-value determining the probability that each biological function and/or disease assigned to that dataset or network is due to chance alone. The network score is the negative log of this P-value and is a numerical value used to rank networks according to how relevant they are to the differentially expressed genes in the input dataset. The network score takes into account the number of focus genes in the network and the size of the network. The network score is not an indication of the quality or biological relevance of the network; it simply calculates the approximate "fit" between each network and the focus genes from the input data set. For example, a score of "6" would indicate a $P=10^{-6}$ chance of genes appearing in the network solely by chance. A network pathway is a graphical representation of the molecular relationships between genes/gene products. Genes or gene products are represented as nodes, and the biological relationship between two nodes is represented as an edge (line). All edges are supported by at least one reference from the literature, a textbook, or from information stored in the IPKB. The intensity of the node color indicates the degree of up- (red) or down- (green) regulation.

Nodes are displayed using various shapes to represent the functional class of the gene product. Edges are displayed with various labels that describe the nature of the relationship between the nodes. For a gene to be network eligible, it must meet the criteria specified in the analysis parameters and also have at least one other full-length, wild-type gene or protein in IPKB that interacts (directly or indirectly) with this gene. Ingenuity combines eligible genes into networks that maximize their specific interconnectedness with each other relative to all molecules to which they are connected. The network algorithm optimizes for specific connectivity, so when a "hub" molecule is included in a network it connects a higher fraction of network eligible molecules relative to all molecules to which the "hub" molecule is connected with additional molecules from IPKB used to specifically connect and merge two or more smaller networks.

IPA pathway analysis identifies the pathways from the IPA library that were most significant to the data set. The significance of the association between the data set and the pathway is measured in two ways; 1) a ratio of the number of genes from the data set that map to the pathway divided by the total number of genes that map to the pathway; and 2) Fischer's exact test is used to calculate a P-value determining the probability that the association between the genes in the dataset and the pathway is explained by chance alone.

Quantitative RT-PCR Validation of Microarray

Validation of the i.m. adipose tissue expression relative to s.c. adipose tissue expression values generated from the microarray experiment was carried out using two-step SYBR green qRT-PCR. Gene specific primers for ten different candidate genes selected for microarray data validation were designed using Primer 3 (Rozen and Skaletsky, 2000) and analyzed using Oligo Analyzer 3.1 (Integrated DNA Technologies),

http://www.idtdna.com/analyzer/Applications/OligoAnalyzer/. Primer sequences, annealing temperatures and product size are presented in Table 4.1. Total RNA (1 ug) from s.c. and i.m. adipose tissue depots from each individual animal for the diet and phase selected for validation was reverse transcribed using the QuantiTect® Reverse Transcription Kit (QIAGEN Inc., Valencia, CA) using oligo-dT and random primers in a total volume of 20 ul. RT- PCR reactions were carried out in duplicate, using a MyiQ Real-Time PCR detection system (Bio-Rad Laboratories, Hercules, CA) in a 15 ul reaction consisting of: 7.5 ul of 2X PerfeCTa™ SYBR Green SuperMix for iQ™ (Quanta BioSciences, Inc**.** Gaithersburg, MD), 400 nM forward primer, 400 nM reverse primer and 100 ng of cDNA. 18S ribosomal RNA was assayed as a normalization control for all samples assayed. A standard curve with five serial dilution points was included for each gene along with a no-template control. Thermal cycling conditions were 95º C for 2.5 min followed by 38 repetitive cycles of 95º C for 15 s, variable annealing temperature for 30 s, and 72º C for 30 s. Immediately following RT-PCR, a melt curve analysis was conducted by bringing the reaction to 95º C for 1 min, 55º C for 1 min, then increasing the temperature by 0.5º C from 55º C to 94.5º C. Gene expression between depots for the diet and phase selected for validation was evaluated using the comparative C_T method. A cycle threshold (C_T) value was assigned to each reaction at the beginning of the logarithmic phase of the PCR amplification. A ΔC_T value was calculated for each sample by subtracting the mean 18S ΔC_T value of each sample from the corresponding gene of interest mean ΔC_T value (Livak and Schmittgen, 2001). The $\Delta\Delta C_T$ was calculated by setting the IM ΔC_T value of the two depots as an arbitrary constant to subtract from the SC mean ΔC_T depot values (Hettinger et al., 2001). Relative expression levels between the two depots were calculated as fold changes, where each cycle of the PCR represented a two-

fold change. The assay specific efficiency for each gene was not used in the calculation of the relative expression levels. Fold change (FC) gene expression was calculated using the formula: $FC = 2^{-\Delta\Delta CT}$.

Quantitative RT-PCR Analysis for Selected Genes

Five genes from the adipose related category; acyl-CoA synthetase medium-chain family member 1 (ACSL1), CD36 molecule (CD36), fatty acid binding protein 4, (FABP4), stearoyl-CoA desaturase (SCD), and prostaglandin-endoperoxide synthase 2 (PTGS2); three genes from the carbohydrate metabolism category; glucose phosphate isomerase (GPI), lactate dehydrogenase B (LDHB), and pyruvate kinase, muscle (PKM2); and one gene from the binding category, four and a half LIM domains 1 (FH1) were measured for their mRNA expression between depots across diets using quantitative RT-PCR and analyzed using the comparative C_T method. The $\Delta\Delta C_T$ was calculated by setting the highest mean ΔC_T value as an arbitrary constant to subtract from all other mean ΔC_T depot values (Hettinger et al., 2001). Relative expression levels between the depots across diets were calculated as fold changes, where each cycle of the PCR represented a two-fold change. Fold change (FC) gene expression was calculated using the formula: $FC = 2^{-\Delta\Delta CT}$. The ΔC_T values were analyzed by analysis of variance (ANOVA) and means were compared using the Least squares means (LSMEANS) of PROC MIXED of SAS 9.1.3 (SAS Institute Inc, Cary, North Carolina)

Results

Finishing Phase

Performance and Carcass Merits

Performance and carcass merits previously reported by McCurdy (2006) showed ADG during the FP to be greater ($P < 0.05$) for steers in SF than PF (2.02 vs. 1.85 kg/d, respectively, and ADG for steers in PF greater ($P < 0.01$) than steers in WP or CF (1.85 vs. 1.64 and 1.63 kg/d, respectively). Final weight was greater ($P < 0.001$) for steers that were managed in a growing program than for calf-fed steers (avg. =579 vs. 559 kg, respectively); however, hot carcass weight did not differ among treatment diets ($P = 0.12$). Dressing percentage was greater ($P < 0.05$) for WP, PF, and CF steers than for SF steers and *Longissimus* muscle area was smaller ($P < 0.05$) for CF than SF and PF steers, with WP steers intermediate. Yield grades were lower for WP and CF steers, 3.19 and 3.39 respectively, than for SF and PF steers, 2.76 and 2.94, respectively. Steers in SF group had higher ($P < 0.01$) marbling scores compared with WP and CF with PF steers being intermediate. Days on feed during the finishing phase were 123, 104, and 104, for WP, SF, and PF steers, respectively. CF steers were on feed for a total of 196 d, 112 of which coincides with the time the WP, SF, and PF steers were on respective diets of the GP.

Microarray and Ontology Analysis

Two hundred forty-eight of 1089 array elements, or 23%, were found to be differentially expressed (DE) between s.c. and i.m. adipose tissue depots in at least one of the four treatment diets of the FP. Clone ID, gene symbol, gene name, Entrez gene ID, dEST ID, GenBank accession number, M-value, GO/KEGG ID, and GO term/KEGG pathway for genes in each diet of FP are presented in the appendices (Appendices Table A2).

Of the 248 array elements of FP, 29 had a non-significant (E value >1e-15) or ambiguous match in the previously described NCBI databases and were grouped under the category "No Biological Data Available" (Rhee et al., 2008). Two hundred nineteen array elements were observed to significantly (E value < 1e-15) correspond to specific annotated genes in the NCBI database and were used for ontology analysis using GFINDer and Entrez Gene. Seventy-nine array elements were not associated with any functional or biological annotation even though they had significant matches in the NCBI databases and were grouped under "Other". Based on results of the Bovine ontology analysis, 140 differentially expressed genes were organized into 15 functional/biological categories. Fifty-six of the 140 differentially expressed genes were detected in biochemical pathways for Bos Taurus defined by Kyoto Encyclopedia of Genes and Genomes (KEGG), http://www.genome.jp/kegg/, (Kanehisa and Goto, 2000). The number of differentially expressed genes observed in WP steers was almost four times greater than SF steers (145 vs. 41), almost three times greater than PF steers (145 vs. 55) and almost twice the number in CF diet (145 vs. 82) (Table 4.2). WP steers had a greater number of differentially expressed genes involved in binding, cell growth and differentiation, signal transduction and transcription/translation functions than SF, PF and CF steers. However, the number of differentially expressed adipose related genes was slightly attenuated in SF and PF steers as compared to WP and CF steers. The percent of differentially expressed genes not associated with any functional or biological annotation (those classified as "Other") for WP, SF, PF and CF steers was 39.3, 21.9, 29.1and 29.3%, respectively.

Quantitative RT-PCR Validation of Microarray

Nine differentially expressed genes were selected for microarray validation. Comparisons between the results of the expression profiles determined by microarray and RT-PCR for each gene from diets of FP selected for validation are presented in Table 4.3. Microarray analysis indicated acyl-CoA synthetase medium-chain family member 1 (ACSL1), CD36 molecule (CD36), fatty acid binding protein 4 (FABP4), lactate dehydrogenase B (LDHB), and stearoyl-CoA desaturase (SCD) to be down-regulated in i.m. adipose tissue in respective diets of the FP. RT-PCR verified the down-regulated pattern of expression of these genes in i.m. adipose tissue. Microarray analysis indicated four and a half LIM domains 1 (FH1), glucose phosphate isomerase (GPI), pyruvate kinase, muscle (PKM2), and prostaglandin-endoperoxide synthase 2 (PTGS2) to be up-regulated in i.m. adipose tissue depot in respective diets of the FP. RT-PCR verified the up-regulated expression pattern of these genes in i.m. adipose tissue depot with the exception of GPI in CF steers where RT-PCR results indicated an opposite direction of expression from the microarray analysis.

Quantitative RT-PCR Analysis of Selected Genes

Results of the RT-PCR analysis of mRNA expression measured for all experimental animals between depots across diets at the end of the FP for ACSM1, CD36, SCD, HADH, FABP4, PTGS2, LDHB, GPI, PKM2, and FHL1 and are shown in (Figure 4.1 a-m). Four genes from the adipose related category, ACSM1, CD36, FABP4, and SCD were significantly ($P < 0.05$) affected by depot and were down-regulated approximately four, five, four, and 20 fold, respectively, in the i.m. adipose tissue compared to s.c. adipose tissue. HADH had a tendency ($P < 0.09$) to be influenced by diet where mRNA expression

was greater in SF and PF steers compared to WP steers with CF steers not significantly different from the SF, PF or WP steers. PTGS2 had a tendency ($P < 0.09$) to be influenced by a diet x depot interaction where mRNA expression was greater in the i.m. adipose tissue of WP steers than the other adipose tissue depots in the other steers except the i.m. adipose tissue of PF steers. Three genes from the carbohydrate metabolism category, GPI, PKM2, and LDHB were significantly affected by depot ($P < 0.05$). PKM2 was also significantly affected by diet with GPI having a tendency to be influenced by diet ($P < 0.06$). GPI and LDHB mRNA expressions were down-regulated approximately three and four fold, respectively, in i.m. adipose tissue compared to s.c. adipose tissue. PKM2 mRNA expression was up-regulated over 15 fold in the i.m. adipose tissue compared to s.c. adipose tissue. PKM2 mRNA expression was greater in SF and PF steers compared to WP steers with the CF steers not significantly different from either the SF and PF or WP steers. GPI mRNA expression was greater in PF steers compared to WP steers, with SF and CF steers not significantly different from either the PF or WP steers.

FHL1 mRNA expression was affected by depot ($P < 0.03$) with a tendency to be influenced by diet ($P < 0.06$). The mRNA expression was up-regulated approximately four fold in i.m. adipose tissue compared to s.c. adipose tissue. FHL1 mRNA expression was greater in SF and PF steers compared to the WP steers with CF steers not significantly different from either the SF and PF or WP steers.

Ingenuity Pathway Analysis

The objective of IPA network generation is to hypothesize, using the most pertinent information available in the literature, how network eligible genes in a data set interact in a biological system. In this study, networks were generated through IPA using the dataset of

differentially expressed genes identified through GPAP 3.2. An arbitrary M-value of > +0.59 or < -0.59 (representing a fold change of > +1.50 or < -1.50) and a P-value < 0.01 were implemented as cut-off parameters in the analysis. Of the 219 array elements shown to significantly correspond to specific annotated genes, 146 were network eligible while 132 were eligible for functional/pathway analysis.

Networks are ranked by how relevant they are to the genes of the dataset with a higher score indicating a lower probability of finding the observed number of genes in a given network by random chance. A summary of the top networks generated by IPA for diets of FP, including number of focus genes, network score and the top three network molecular/cellular functions, disease/disorder or physiological system development and function is presented in Table 4.4.

Fourteen networks were generated for WP diet with six containing one focus gene while five major networks were generated for CF diet with five possessing only one gene. The most significant networks of both the WP (IPA score=45; 23 focus genes) and CF (IPA score=34; 17 focus genes) diets included functions pertaining to cellular movement (P-value, 2.82^{-3} to 1.08^{-8}) (P-value, 5.91^{-3} to 2.47^{-7}) and cellular growth and proliferation (P-value, 1.75^{-1} to 1.55^{-8}) (P-value, 1.41^{-1} to 5.87^{-7}). The down-regulated nuclear factor of kappa light polypeptide gene enhancer in B-cells 1 (p105) (NFKB1), along with ERK and AP1, were central to both networks of WP and CF diet. Eight networks, four of which contained only one focus gene, were generated for SF and PF diets. The most significant network in both SF (IPA score=39; 18 focus genes) and PF (IPA score=44; 20 focus genes) diets included functions associated with lipid metabolism (P-value, 4.02^{-3} to 6.54^{-6}; P-value, 4.02^{-3} to 6.54^{-6}) and molecular transport (P-value, 5.08^{-3} to 2.52^{-7}; P-value, 3.94^{-3} to 2.52^{-7}). ERK, H3F3A, AP1, and P38 MAP-K were central molecules to these networks.

IPA currently listed 32 functions under the heading of "molecular and cellular functions" which are subdivided into lower level ancillary function "categories". Figure 4.2 ranks, by significance, the top 10 global molecular and cellular functions associated across all generated networks for each respective diet of the FP, respectively. This represents a broad overview of the biology associated with each diet. In general, a P-value < 0.05 indicates a significant nonrandom association between genes of the dataset and a given function. Significance, expressed as the negative $\log_{10}$ of the P-value calculated for each function, is represented on the *y*-axis. Differences were observed between diets of FP in the ranking of those functions and also in the number of genes and the pattern of expression associated with those functions. Lipid metabolism was the top-ranked function for both SF and PF diets while cellular growth and proliferation and cellular movement were top-ranked for both WP and CF diets with lipid metabolism being ranked fourth in both WP and CF diets. Functional comparison, as well as metabolic and signaling pathway comparison between treatments, is a tool that allows for further determination of whether and to what extent a given function or pathway is affected by a treatment. Results of the comparative functional analysis between diets of FP are presented in Figure 4.3. The possibility does exist for genes within the makeup of the function to change between treatments without altering the significance value for that function. Amino acid metabolism, energy production, protein synthesis, RNA post-translational modification and vitamin and mineral metabolism are functions displaying obvious variations between diets of the FP.

IPA contains a total of 158 pathways in its library, 80 metabolic pathways and 78 signaling pathways. Metabolic pathway analysis and signaling pathway analysis comparing diets of the FP are presented in Figures 4.4 and 4.5, respectively. Metabolic and

signaling pathways exhibited a number of significant variations ($P < 0.10$) in gene expression between diets of the FP.

Using IPA comparison and network analysis, differentially expressed genes exclusive to WP, SF, PF and CF diets, respectively, were also investigated. Fifty-three differentially expressed genes were exclusive to WP steers with no differentially expressed genes exclusive to SF steers. These IPA identified genes along with their associated networks are presented in Tables 4.5 through 4.7, respectively.

Discussion

Steers from all treatment diets were harvested at a common 12^{th} rib fat (1.27 cm) as determined by ultrasound. Days on feed for WP, SF, and PF steers of FP were 123, 104, and 104, respectively. CF steers were on feed for a total of 196 d, 112 of which coincides with the time WP, SF, and PF steers were on respective diets of the GP. Steers in the SF group had higher marbling scores compared with WP and CF, with PF steers being intermediate. Dressing percentage was greater for WP, PF, and CF steers than for SF steers while yield grades were lower for WP and CF steers, 3.19 and 3.39 respectively, than for SF and PF steers, 2.76 and 2.94, respectively.

The number of differentially expressed genes observed in WP steers of the FP was over four times greater than SF diet (146 vs. 35), almost three times greater than PF diet (146 vs. 54) and almost twice the number as CF diet (146 vs. 82). Interestingly, the number of differentially expressed adipose related genes was slightly attenuated in SF and PF diet as compared to WP and CF diets. The WP and CF diets shared common functions in their most significant network, respectively, which included cellular movement and cellular growth and proliferation. SF and PF diets shared common functions in their most

significant network, respectively, which included lipid metabolism and molecular transport. More so, SF and PF diets shared common functions for networks 2 and 4 as well; network 2 included lipid metabolism, carbohydrate metabolism and small molecule biochemistry while network 4 included cell cycle, cellular assembly and organization, and DNA replication, recombination and repair.

Adipose related genes (Figure 4.6) included those involved in lipid binding, transport, and metabolism as well as the metabolites secreted from adipose tissue. Acyl-CoA synthetase medium-chain family member 1 (ACSM1) is involved in a key reaction in the activation of fatty acids. RT-PCR revealed gene expression for ACSM1, also known as butyrate-CoA ligase, to be significantly altered by depot and was down-regulated over 4 fold in i.m. adipose tissue compared to s.c. adipose tissue. The term synthetase or ligase, refers to a reaction that utilizes an ATP and forms an acyl-AMP intermediate (Mashek et al., 2004). Before fatty acids can be oxidized they first must be "activated" for the reaction by combining the fatty acid with Co-A to form fatty acyl Co-A. The fatty acyl group can then be transported into the mitochondrial matrix, where it undergoes beta-oxidation. Acetyl-CoA can feed directly into the TCA cycle, or if propionyl-CoA, it can be catabolized via a number of different pathways that convert it into pyruvate, acetate, or succinyl-CoA, which in turn, can enter the TCA cycle. However, acyl-CoA can also function as ligands for transcription factors or enter several other pathways such as *de novo* synthesis of triacylglycerol and phospholipids, reacylation pathways, and cholesterol and retinal esterification (Coleman et al., 2002; Mashek et al., 2004). ACSM1 can also function as a GTP-dependent lipoate-activating enzyme that generates the substrate for lipoyltransferase (Fujiwara et al., 2001). There are six members of the medium-chain Acyl-Co A family (Mashek et al., 2004) which catalyze the ligation of medium chain fatty

acids, [acids from C_4 to C_{11} and the corresponding 3-hydroxy- and 2,3- or 3,4-unsaturated acids (*in vitro*)] with CoA to produce medium-chain Acyl-Co A (Inka Lindner, 2006). Though the most common substrates of the medium-chain acyl CoA synthetase family are fatty acids, xenobiotic carboxylic acids and bile salts can also serve as substrates (Mashek et al., 2004). In the mouse, medium chain acyl Co-A synthetase was shown to be inhibited by nonsteroidal anti-inflammatory drugs (NSAIDs) (Kasuya et al., 2001). Also in the mouse, aspirin and salicylic acid were shown to decrease the mitochondrial activation and the β-oxidation of long chain fatty acids (palmitate) *in vivo* by 50 and 65%, respectively, (Deschamps et al., 1991).

In the present experiment, CD36 molecule (CD36) gene expression was significantly affected by depot and was down-regulated over 5 fold in i.m. adipose tissue compared to s.c. adipose tissue. In *in vitro* studies using 3T3-L1 cells, no CD36 protein was detected in preadipocytes; however, CD36 was detected in cells 3 days post-differentiation (Qiao et al., 2008). CD36 has been identified as an important marker of preadipocyte differentiation into adipocytes as CD36 mRNA expression was induced during the differentiation process and fatty acid uptake coincided with the up-regulated expression of CD36 (Abumrad et al., 1993; Sfeir et al., 1997). CD36 has been shown to be regulated by all three peroxisome proliferator receptors (PPAR), α, γ, and δ, in a tissue specific manner (Hajri and Abumrad, 2002). More so, CD36 contains a CCAAT/enhancer binding protein (C/EBP) response element and C/EBP α and β were shown to increase CD36 expression with C/EBPα being a more potent inducer of CD36 than C/EBPβ indicating C/EBPα involvement in regulating CD36 expression at the transcriptional level (Qiao et al., 2008). One of the main functions of CD36 is to facilitate the translocation of fatty acids in adipocytes as well as in heart and muscle cells (Nicholson

et al., 2000; Febbraio et al., 2001; Su and Abumrad, 2009). With CD36 being regulated by PPARγ and C/EBP; the up-regulation of expression of CD36 in the s.c. seems consistent, as it follows a similar pattern of expression as seen for other adipose related genes involved in fatty acid transport. Also, there is evidence that CD36 gene expression can differ between depots, as CD36 gene expression in weaning piglets was shown to be higher in visceral adipose tissue as compared to s.c. and i.m adipose tissue (Shu et al., 2008). Conversely, in a human study using non-obese subjects, CD36 gene expression was shown to be up-regulated in s.c. adipose tissue as compared to omental adipose tissue (vanBeek et al., 2007)

Stearoyl-CoA desaturase (SCD) gene expression was also shown to be significantly affected by depot in the present experiment, and was down-regulated over 20 fold in i.m. adipose tissue compared to s.c. adipose tissue. This is consistent with other findings in the literature where SCD activity appears to be essential for subsequent development of lipogenic activity of s.c. adipose tissue in growing steers (Smith et al., 2006b; Hausman et al., 2009). Subcutaneous adipose tissue was shown to have approximately twice the SCD catalytic activity as i.m. adipose tissue and a greater concentration of MUFA than i.m. adipose tissue (Archibeque et al., 2005). However, in many breeds a nearly linear increase in i.m. adipose deposition has been shown with time on a finishing diet, with this increase in i.m. adipose deposition being consistent with an increase in adipose tissue MUFA and SCD activity (Hausman et al., 2009).

Furthermore, in comparing s.c. adipose tissue from the mid-loin region of pasture-fed cattle or cattle placed in the feedlot and fed a diet consisting of sorghum, roughage, and 5% whole cottonseed for 100, 200, or 300 d SCD activity was observed to be 60 to 85% higher in cattle from the pasture-fed diet than cattle on the feedlot diet suggesting that

feeding whole cottonseed reduced the activity of SCD (Yang et al., 1999). Cattle from the pasture-fed diet had lower total saturated fatty acids and higher total unsaturated fatty acids in adipose tissue than cattle in the feedlot (Yang et al., 1999). No diet affects were observed for SCD mRNA gene expression in the present study.

Hydroxyacyl-CoA dehydrogenase (HADH), an enzyme involved in the beta-oxidation of fatty acids through the oxidation of straight chain 3-hydroxyacyl CoA's (Rakheja et al., 2002; Song-Yu Yang, 2005), was significantly altered by diet and was shown to be up-regulated in both SF and PF diets compared to WP diet. There was not a significant difference observed between the CF and WP diets. HADH is also present in the degradation pathways of the branched chain amino acids, valine, leucine, and isoleucine (Kanehisa and Goto, 2000), which can provide the acetyl-CoA necessary for fatty acid biosynthesis in adipose tissue (Labrecque et al., 2009).

In the present experiment, FABP4 gene expression was shown to be significantly affected by depot with gene expression down-regulated over 4 fold in i.m. adipose tissue compared to s.c. adipose tissue. Similar findings were found in porcine where FABP4 transcript and protein content were shown to be lower in i.m. adipocytes as compared to s.c. adipocytes when adipose cells were compared at the same size and same age (Gardan et al., 2007). Previous work by Moore et al., (1991) showed the activity of FABP4 in the *Longissimus* muscle not to be a good index for the determination of i.m. fat accretion in bovine. However, FABP4 polymorphisms have been shown to be associated with marbling and s.c. fat depth in cattle (Michal et al., 2006), and for fatness traits and i.m. fat accretion in pigs (Chmurzynska, 2006; Damon et al., 2006).

Prostaglandin-endoperoxide synthase 2 (PTGS2), also known as cyclooxygenase (COX), had a tendency to be affected by a diet x depot interaction where mRNA

expression was greater in the i.m. adipose tissue of WP than other adipose tissue depots in other diets except the i.m. adipose tissue of PF diet. The i.m. adipose tissue depot of PF was greater than the s.c. adipose depot of WP diet with no difference in the other adipose tissue depots in the other diets. There are two isoforms of PTGS: a constitutive PTGS1 (or COX-1) and an inducible PTGS2 (or COX-2) which differs in their regulation of expression and tissue distribution (Petersen et al., 2003; Yan et al., 2003). PTGS2 catalyzes the conversion of arachidonic acid to prostaglandin H_2 and is the rate-limiting step in the formation of prostanoids which include $PGF_2\alpha$, PGJ_2, PGI_2, and PGE_2 (Morita, 2002; Yan et al., 2003; Lu et al., 2004). Three classes of enzymes essentially regulate the numerous signaling pathways of arachidonic acid; the first being COX, which initiates the synthesis of prostaglandins (PG's); the second are the lipooxygenases, which initiate the synthesis of leukotrienes (LK); and the third, cytochrome P450's, which initiate the synthesis of hydroxyeicosatetraenoic acids (HETE) and epoxyeicosatetraenoic acids (EET). The differences in the biological activity of the products generated by these enzymes are due to the insertion of oxygen at different positions in the arachidonic acid molecule.

Arachidonic acid has been shown to inhibit adipocyte differentiation (Petersen et al., 2003) and is itself, along with the prostinoids, a ligand for PPARγ. The inhibition of *in vitro* adipocyte differentiation by arachidonic acid was reversed by the addition of COX inhibitors suggesting that prostaglandins may be the key to mediating this inhibition of adipocyte differentiation. Also, when adipocyte differentiation was inhibited by arachidonic acid, COX-2 expression was sustained at an elevated level with the inhibition being reversed by the addition of the nonselective COX inhibitor, indomethacin (Petersen et al., 2003). COX isoforms being involved in the inhibition of *in vitro* of adipocyte differentiation, with COX-2 isoform appearing to be the mediator of the inhibition, has also

been shown by other researchers (Yan et al., 2003). Furthermore, *de novo* fatty acid synthesis, diacylglycerol acyltransferase (DGAT) activity, and triacylglycerol accumulation were suppressed in adipocytes *in vitro* treated with arachidonic acid. The nonselective COX inhibitor indomethacin, restored DGAT activity and the accumulation of triacylglycerol; however, *de novo* fatty acid synthesis was not restored which resulted in the increased incorporation of arachidonic acid into cellular triacylglycerols (Petersen et al., 2003).

The function of PTGS (COX) and prostaglandins in the regulation of adipocyte differentiation is difficult to understand as the different prostaglandins exert distinct effects on adipocyte differentiation. Early work revealed rapidly growing cultures of 3T3-L1 preadipocyte cells produced significant amounts of prostaglandins, mainly PGE_2, when incubated with arachidonic acid; however, PGE_2 synthesis declined when cells reached confluency, suggesting the involvement in either the induction or maintenance of differentiation (Hymann et al., 1982). PGI_2 and PGE_2 have been shown to behave in an autocrine/paracrine manner (Aubertv et al. 2000; Boone et al., 2000) with the PGI_2 receptor present mainly in preadipocytes while the PGE_2 receptor is mostly present in mature adipocytes (Boone et al., 2000). PGI_2 is an efficient activator of cAMP production in preadipocytes and can enhance cell differentiation (Négrel et al., 1989), while PGE_2 decreases cAMP concentrations and avoids lipolysis (Boone et al., 2000). Thus, PGI_2 and PGE_2 may increase adipose tissue accretion through the enhancement of hyperplasia and hypertrophy (Boone et al., 2000). More so, PGI_2 and its analogue carbacyclin ($cPGI_2$) have been shown to up-regulate the expression of C/EBPβ and C/EBPα in OB1771 and 3T3-F442A preadipocytes (Aubertv et al., 2000). Vassaux et al. (1992) described PGI_2, which is able to activate the three PPAR isoforms, γ,α,δ, (Brun et al., 1996; Hertz et al., 1996), as

an adipogenic-hyperplastic effector of adipocyte precursor cells, and PGE_2 as an anti-lipolytic-hypertrophic effector of adipocytes and also suggested the two might contribute in concert in adipose tissue development. More recently, Sugimoto et al. (2004) suggested that PGE_2 inhibited adipocyte differentiation by acting on the EP4 receptors as PGE_2 was shown to inhibit or suppress the differentiation-associated expression of certain genes such as GHRH, ADIPOQ, DGAT1, G3PDH, and HADH. In the present study, HADH was not influenced by depot but was influenced by diet and was up-regulated in both SF and PF steers compared to WP steers with no significant difference observed between the CF and WP steers. Adipose tissue is an important source of angiotensinogen, the precursor of the vasoconstrictor angiotensin II (Lu et al., 2007). Angiotensin II plays an important role in the cell cycle progression in human preadipocytes (Crandall et al., 1992) and can stimulate the production of PGI_2 and PGE_2 (Boone et al., 2000). It is worth noting that in the present study, the microarray analysis showed angiotensin II receptor, type-1 to be up-regulated in the i.m. adipose tissue in the WP steers and down-regulated in the SF, PF, and CF steers. The pattern of expression for angiotensin II receptor, type-1 seen in the microarray needs to be verified by RT-PCR.

$PGF_2\alpha$ is also unable to affect cAMP production (Négrel et al., 1989) and has been reported to inhibit adipocyte differentiation (Serrero et al., 1992; Miller et al., 1996; Petersen et al., 2003). PGD_2, whose hydration products are PGJ_2, Δ^{12}-PGJ2, and 15-deoxy-$\Delta^{12,14}$-PGJ2 (Lu et al., 2004), is also unable to affect cAMP production (Négrel et al., 1989). However, PGJ_2 and $PGF_2\alpha$ have been reported to have opposing effects on PPARγ, the central regulator of adipogenesis (Reginato et al., 1998; Fajas et al., 2003), with PGJ2 functioning as an activating ligand for PPARγ, and $PGF_2\alpha$ functioning in the inhibitory phosphorylation of PPARγ through activation of mitogen-actived protein kinase (Kliewer

et al., 1995; Reginato et al., 1998). Furthermore, the treatment of 3T3-L1 cells with aspirin, a COX inhibitor, attenuated triacylglycerol accumulation, with the addition of PGD_2, 15d-PGJ_2 and PGE_2 reversing the effect, while $PGF_2\alpha$ had an additional inhibitory effect on triacylglycerol accumulation (Lu et al., 2004). In characterizing depot differences in mRNA expression of enzymes involved in prostaglandin D and J2 synthesis between different adipose tissue depots in humans, prostaglandin synthase-1 (PGHS1 or COX-1) and prostaglandin D synthase (PTGDS) were shown to be up-regulated 2.1 and 3.2 fold, respectively, in omental (OM) adipose tissue as compared to s.c. adipose tissue while human prostaglandin transporter (hPGT) was expressed in OM adipose tissue and was undetectable in s.c. adipose tissue (Quinkler et al., 2006). Also,the expression of 17β-hydroxysteroid dehydrogenase 5 (ARK1C3), which catalyzes PGD_2 to $PGF_2\alpha$, was down-regulated in OM adipose tissue compared to s.c. adipose tissue by 3.2 fold, further adding complexity to differences seen in depots in the generation of prostaglandin metabolites that can act as agonists or antagonists of PPARγ (Quinkler et al., 2006).

The COX enzyme is the target of many nonsteroidal anti-inflammatory drugs (NSAIDs) including aspirin (Fajas et al., 2003). Some NSAIDs inhibit both COX-1 and COX-2 while others are selective only for COX-2. Celecoxib (Celebrex ®), an NSAID that is highly selective for COX-2 inhibition, is approximately 7.6 times more selective for COX-2 inhibition over COX-1 (Silverstein et al., 2000). In rats fed a high fat diet for 14 weeks, Celecoxib was found to reduce fat accumulation by decreasing fatty acid synthase expression through the down-regulation of the c-Jun N-terminal kinase-1 (JNK1) (Lu and Archer, 2007). Rofecoxib (Vioxx), another COX-2 selective NSAID, administered for a six week period in mice fed a high fat diet resulted in a reduction in body weight and a reduction in s.c. and gonadal adipose tissue mass with no significant difference in food

intake (Lijnen et al., 2008). Also, the adipocytes were smaller in the gonadal adipose tissue after Vioxx treatment compared to placebo, with no differences in adipocyte size being observed in the s.c. adipose tissue (Lijnen et al., 2008).

The IPA analysis revealed possible variations between diets of the FP in arachidonic acid metabolism and the eicosanoid signaling pathway (Figure 4.4 and 4.5, respectively). Genes involved in arachidonic acid metabolism generated by IPA included; acyl-CoA synthetase short-chain family member 2; cytochrome P450, family 2, subfamily D, polypeptide 6; cytochrome P450 subfamily 2B; glutathione peroxidase 3 (plasma); and granulin. As previously mentioned, cytochrome P450 metabolizes arachidonic acid to HETE and EET which are intermediate compounds in the conversion of arachidonic acid to a number of biological active compounds including prostaglandins, thromboxanes, and leukotrienes (Kroetz and Zeldin, 2002). Genes involved in eicosanoid signaling generated by IPA included PTGS2 and granulin. There are four families of eicosanoids; the prostaglandins, the prostacyclins, the thromboxanes and the leukotrienes (Wolfe, 1982). Besides the presence of multiple forms of the COX enzyme, COX-1, COX-2 COX-3, and two smaller COX-1-derived proteins (Chandrasekharan et al., 2002) that can generate functional diversity in the COX enzyme class, there are multiple isoforms of other enzymes in these signaling pathways. For example, two PGE_2 synthase enzymes, one constitutively expressed and one induced (Martel-Pelletier et al., 2004), two enzymes that catalyze the synthesis of PGD_2, several lipooxygenases isoforms, (Soberman and Christmas, 2003) and thirteen different isoforms of the cytochrome P450 family of enzymes (Roman and Alonso-Galicia, 1999) have been reported in the literature. Each of these isoforms can function differently by being coupled with different stimuli in different tissues (Soberman and Christmas, 2003). This functional diversity also carries over into the prostaglandin

receptors as eight types and subtypes of receptors are conserved in mammals, each with a distinct tissue- and cell-specific function (Soberman and Christmas, 2003).

Several of the differentially expressed genes in the adipose related and carbohydrate metabolism functional categories can be placed in the PPAR γ signaling pathway (Figure 4.7). Besides the previously discussed genes, CD36, FABP4, SCD, and ACMC1, which were shown to be down-regulated in i.m adipose tissue compared to s.c. adipose tissue, the microarray analysis showed adiponectin (ADIPOQ) and phosphoenolpyruvate carboxykinase 2 (PCK2) to be down regulated in the i.m. adipose tissue in all diets or not differentially expressed between adipose tissue depots, respectively. PPARγ is a ligand dependent transcription factor which is the master regulator of adipogenesis (Rosen and MacDougald, 2006; Tontonoz and Spiegelman, 2008). PPARγ is also a regulator of other cellular functions and biological processes such as carbohydrate and lipid metabolism and immune cell activation and is abundantly expressed in adipose tissue as well as skeletal muscle, heart, liver, and intestine (Lopez-Liuchi and Meier, 1998; Fernyhough et al., 2007; Minge et al., 2008; Nettles, 2008). Endogenous ligands for PPARγ, which can bind at μM levels, include unsaturated and oxidized fatty acids, eicosanoids and prostaglandins (Nettles, 2008). PPARγ functions as a heterodimer with the retinoid X receptor (RXR) with the required dimerization promoted by ligand binding to either PPARγ or anyone of the three RXR isotypes; α, β, or γ, with which PPARγ is able to dimerize (Metzger et al., 2005; Nettles, 2008; Tontonoz and Spiegelman, 2008). The RXR is activated by 9-cis retinoic acid (Metzger et al., 2005). Three types of PPAR have identified, α, δ, and γ; with four isoforms of PPARγ arising from differential promoter action and alternate gene splicing (PPARγ(1-4); Metzger et al., 2005; Fernyhough et al., 2007). PPARγ3 and 4

produce translated proteins identical to PPARγ1; thus, only two receptors result in the biological system, PPARγ1and 2 (Fernyhough et al., 2007). Ligand activation of PPARγ is required for the induction of adipogenesis, as no factors have been discovered that promote adipogenesis in the absence of PPARγ. Although PPARγ is required to maintain the adipocyte in its differentiated state, it is not required to maintain PPARγ–dependent gene expression in mature adipocytes (Rosen and MacDougald, 2006).

Glucose phosphate isomerase (GPI), the dimeric enzyme involved in the second step of glycolysis which catalyzes the reversible isomerization of glucose-6-phosphate to fructose-6-phosphate (Voet and Voet, 2004a), was significantly affected by depot ($P < 0.004$). RT-PCR indicated mRNA expression was down-regulated approximately three fold in the i.m. adipose tissue compared to the s.c. adipose tissue; which is opposite from what was reported at the end the GP (Stein et al., 2009, article in preparation). Also, GPI mRNA expression had a tendency to be influenced by diet ($P < 0.06$) and was found to be greater in PF steers compared to WP steers, with SF and CF steers not significantly different from either the PF or WP steers. Limitations in the GPI reaction or the phosphofructokinase (PFK) reaction could result in an increase in the glucose-6-phosphate level causing feedback inhibition of hexokinase possibly resulting in a lower rate of glycolysis and a shift to fructose-6-phosphate being produced through the pentose phosphate pathway resulting in the generation of NADPH for biosynthetic processes such as fatty acid synthesis (Kugler and Lakomek, 2000; Voet and Voet, 2004c). In ruminants, as much as 50 to 80% of NADPH needed for fatty acid synthesis in adipose tissue is produced by the pentose phosphate pathway (Vernon, 1981). However, PFK in the microarray analysis was shown not to be differentially expressed between adipose tissue depots in respective diets. The phosphofructokinase reaction is the rate-limiting step of

glycolysis that is highly regulated. Pyruvate kinase (PK) catalyzes the last step in the glycolysis pathway, which is the dephosphorylation of phosphoenolpyruvate to pyruvate and is responsible for producing the second ATP generated within the glycolytic pathway (Voet and Voet, 2004a). PK leads to either anaerobic fermentation or oxidative phosphorylation of pyruvate (Jurica et al., 1998) and can also serve as the control switch between the glycolysis and gluconeogenesis pathways in certain tissues (Voet and Voet, 2004a). PKM2 was significantly affected by depot ($P < 0.001$) and by diet ($P < 0.04$). PKM2 mRNA expression was up-regulated over 15 fold in the i.m. adipose tissue compared to s.c. adipose tissue. PKM2 mRNA expression was greater in SF and PF steers compared to WP steers with CF steers not significantly different from either the SF and PF or WP steers. PKM2 is one of four pyruvate kinase isoenzymes, M1, M2, L and R, with the M1 isoform being the only one of the four not allosterically controlled (Noguchi et al., 1986; Mattevi et al., 1996; Christofk et al., 2008). Mammalian PK is active as a tetramer of four identical or very similar subunits with a high affinity for the substrate, phosphoenolpyruvate. The dimeric form of PK is characterized by a low affinity for phosphoenolpyruvate. Fructose-1,6-bisphophate, the allosteric activator of PKM2, induces the inactive dimeric form to the active tetramer form. PKM2 is the only PK isoform that binds phosphotyrosine peptides, which have the ability to release the allosteric activator, fructose-1,6-bisphophate, leading to the inhibition of the enzymatic activity of PKM2 (Mattevi et al., 1996; Wooll et al., 2001; Christofk et al., 2008).

The down-regulation of LDHB and genes involved in the synthesis, transport, and storage of fatty acids in i.m. adipose tissue along with the up-regulation of some glycolytic enzymes in i.m. adipose tissue of respective diets suggest that fatty acid and triglyceride synthesis and transport is attenuated in i.m. adipose tissue compared with s.c.. Also, lactate

is a possible substrate for glycerogenesis for use in triglyceride synthesis in s.c. adipose tissue. The rate of fatty acid synthesis, when either lactate or acetate was the precursor, was shown to be greater in subcutaneous adipose tissue than in intermuscular or intramuscular tissue (Whitehurst et al., 1981). Furthermore, the contribution of lactate allowing for anaerobic metabolism in s.c. may permit the sparing of glucose for repartitioning as an energy substrate for i.m. adipose tissue. Previous data reported by Smith and Crouse (1984) showed i.m. adipocytes to utilize glucose as the primary substrate for fatty acid synthesis, whereas s.c. adipocytes utilized acetate and lactate incorporation into fatty acids. However, without further investigation into other genes involved in the glycolytic pathway, pentose phosphate pathway, or in oxidative phosphorylation, it is difficult to speculate what implications this has on these metabolic pathways.

In the present study, RT-PCR revealed four-and-a-half-LIM domains 1 (FHL1) expression to be up-regulated almost four fold in i.m. adipose tissue compared with s.c. adipose tissue. FHL1 also had a tendency to be affected by diet where mRNA expression was greater in SF and PF steers compared to WP steers, with CF steers not significantly different from SF, PF, or WP steers. Although FHL1 is highly expressed in skeletal and cardiac muscle (McGrath et al., 2006), FHL1 has been shown to be expressed in bovine, porcine, and human adipose tissue (Wang et al., 2005a; vanBeek et al., 2007; Labrecque et al., 2009). Although the exact function of FHL1 remains ambiguous, it does belong to a large family of LIM-proteins that function in cytoskeletal organization, cell lineage specification, the regulation of gene transcription, cell proliferation, cell differentiation and apoptosis (Bach, 2000; Kadrmas and Beckerle, 2004). As FHL1 has been shown to be highly expressed in adipocytes and not preadipocytes, it could serve as a marker for adipocyte differentiation (vanBeek et al., 2007). FHL1 has also been reported to interact

with receptor interacting protein of 140 kDa (RIP140), which itself is known to interact with estrogen receptor-α (Lin et al., 2009). Recently, FHL1 and RIP140 were shown to synergistically inhibit the transcription of the estrogen response element of the pS2 gene, whose expression is restricted to breast cancer cells (Lin et al., 2009). However, RIP140-null mice have been shown to accumulate less fat in their adipose tissue and are resistant to high-fat diet-induced obesity, and show improved glucose tolerance and insulin sensitivity (Leonardsson et al., 2004).

Most economic relevant traits in the bovine are complex traits and are under the control of an interacting network of genes, each with a small effect, and the environment (Wu and Lin, 2006). The present study clearly demonstrates that previous growing diet significantly influences gene expression in beef steers at the end of the subsequent finishing phase. It was interesting to observe the similarities between the SF and PF diets at the end of the FP as compared to WP and CF diets. The top function from the respective list of the top ten molecular and cellular functions associated across all generated networks for the SF and PF diets of FP was lipid metabolism. More so, SF and PF diets shared common functions for IPA generated network 1 which included lipid metabolism and molecular transport; network 2 which included lipid metabolism, carbohydrate metabolism and small molecule biochemistry; and network 4 which included cellular assembly; cellular assembly and repair, and DNA recombination, recombination, and repair. Days on feed were 104 for each the SF and PF steers compared to 123 d for WP steers. Steers in the SF group had higher marbling scores compared with WP and CF steers, with PF steers being intermediate. Yield grades were lower for WP and CF steers than for SF and PF steers. ADG during the FP was greater for steers in SF than PF and ADG for steers in PF was greater than steers in WP or CF. The number of differentially expressed genes was greatly

attenuated in the SF and PF steers compared to the WP and CF steers, as the number of differentially expressed genes in the WP steers was almost four times greater than SF steers (145 vs. 41), almost three times greater than PF steers (145 vs. 55), and almost twice the number as CF steers (145 vs. 82) (Table 4.2). Also, 53 differentially expressed genes were exclusive to WP steers, with no differentially expressed genes exclusive to SF steers. These IPA identified genes along with their associated networks are presented in Tables 4.5 through 4.7, respectively. In five of the ten genes evaluated using RT-PCR, mRNA expression was influenced by diet or a diet x depot interaction. A similar pattern of expression was observed in the four genes influenced by diet. Interestingly the SF and PF steers had greater mRNA expression than WP steers. In order for beef quality to be improved, it is important to understand the effect of diet on the regulation of preadipocyte proliferation and differentiation in beef cattle as the accretion of adipose tissue is controlled by a balance of preadipocyte (hyperplasia) and differentiation (hypertrophy) (Wan et al., 2009). *In vitro* studies showed propionate had selective adipogenic effects on bovine i.m. preadipocytes and s.c. adipocytes as propionate contributed to the hypertrophy of adipocytes within i.m. adipose tissue and to the recruitment of new adipocytes in s.c. adipose tissue (Wan et al., 2009). Propionate was also shown to induce the mRNA expression of PPARγ and C/EBPα in both i.m. preadipocytes and s.c. adipocytes (Wan et al., 2009).

In conclusion, to our knowledge, the data presented is the first to use microarray analyses to evaluate the effect of different growing diets on adipose tissue depots at the end of the finishing period in beef steers. The interactions between genes involved in adipocyte differentiation and diet differences still remain ambiguous. However, IPA metabolic and signaling pathway analysis generated in this study has provided insight into possible

differences in the molecular mechanisms affecting development of i.m. and s.c. adipose tissue in beef steers at the end of the finishing phase managed under different growing diets. As genes outside the dataset known to interact with the differentially expressed genes observed in this study were included in the Ingenuity Pathway Analysis, elucidation of possible differences between diets and depots for future analysis is warranted, as these genes may not have been included in the adipose specific microarray used in this study. Further investigation and validation is needed to evaluate network genes not included in the microarray and discern the differences observed between diets in the fore-mentioned functional analyses (Figure 4.3) and a number of the metabolic (Figure 4.4) and signaling (Figure 4.5) pathways.

In addition, over 35% of the 219 array elements that had significant matches in the NCBI databases could not be associated with any functional or biological annotation. However, despite these insufficiencies, gene expression profiling suggests differences in the metabolic activity between s.c. and i.m. adipose tissue between diets at the end of the FP. The data presented indicates the metabolic machinery for adipose tissue accretion was down-regulated in the i.m. adipose tissue depot compared to s.c. adipose tissue depot and the main affect of previous diet can influence adipose tissue deposition at the end of the FP as HADH, GPI, PKM2, and FHL1 were influenced by diet with PTGS2 influenced by a diet x depot interaction. When using gene expression profiling as a measurement of cellular function, one must keep in mind that mRNA expression levels do not always correspond to the translated protein levels or active protein in the cell and further investigation and validation is needed to evaluate the candidate genes that might be influenced by depot, diet or their interaction.

Table 4.1. Sequences, accession number, and melting temperatures of the bovine specific primers for the selected target genes of interest. Accession number is from the national center for biotechnology information (NCBI) available at http://www.ncbi.nlm.nih.gov/.

Primer		Sequence	Size (bp)	Tm used	Product Size (bp)	GenBank Accession
ACSM1	Forward	AAGGAAACATTGGCATCAGG	20			
	Reverse	AGTCCCCACATTCCACTTCA	20	62 C	102 bp	BC109602.1
CD36	Forward	CAATGGAAAGGACGACATAAG	21			
	Reverse	TGGAAATGAGGCTGCATCTGT	21	60 C	121 bp	NM_174010
FABP4	Forward	AAGCTGCACTTCTTTCTCACC	21			
	Reverse	GACCACACCCCCATTCAAAC	20	62 C	197 bp	NM_174314
FHL1	Forward	GCAACAAGGGTTTGGTAAAGG	21			
	Reverse	AGAGGGCAAGGACACAAGG	19	56 C	227 bp	BC102083.1
GPI	Forward	TGGGCATATTCTGGTGGACT	20			
	Reverse	GACCTCTGGCATCACATCCT	20	64 C	223 bp	NM_001040471.1
HADH	Forward	TCCGTTTGAGCTTCTCGATT	20			
	Reverse	CTTACAGGGCTTCGTCCTTG	20	55 C	210 bp	XM_001787625
LDHB	Forward	GCTGTGTGGAGTGGAGTGAA	20			
	Reverse	ATACACGGAAGGCTCAGGAA	20	56 C	287 bp	NM_174100.1
PKM2	Forward	TTGGGTCGGGTAGTTCAGAG	20			
	Reverse	ACAAAGGAAGGGAAGCAGGA	20	56 C	136 bp	XM_590109.4
PTGS2	Forward	ATGTATGAGTGTAGGATTTGACCAG	25			
	Reverse	GGGAGTGGGTTTCAGGAGTAA	21	55 C	234 bp	NM_174445.2
SCD	Forward	CCTGTGGAGTCACCGAACCT	20			
	Reverse	TGTTGCCAATGATCAGGAAGAC	22	60 C	66 BP	AB075020.1

Table 4.2. The number of differentially expressed up- and down-regulated genes in each of the functional categories in Initial and Wheat Pasture, Silage Fed, and Program Fed diets of the Growing Phase

	Finishing Phase							
	Wheat Pasture		Silage Fed		Program Fed		Calf Fed	
	Up	Down	Up	Down	Up	Down	Up	Down
Adipose Related	5	10	0	10	0	10	1	12
Apoptosis/Cell Death	2	2	0	0	1	0	1	0
Binding	15	4	5	4	7	1	6	2
Carbohydrate Metabolism	3	1	2	0	3	0	3	1
Cell Growth/Differentiation	4	2	0	0	0	1	0	0
Cell Cytoskeletal/ Adhesion/ ECM Related	2	1	1	1	1	1	1	4
Hydrolase/Transferase/ Catalytic/Activity	2	1	0	1	0	1	0	1
Nucleic Acid Metabolism	2	0	0	0	0	0	0	1
Oxidative Phosphorylation	1	0	1	0	0	0	1	0
Oxidoreductase Activity	3	2	0	1	0	1	2	2
Protein Synthesis:Turn Over/AA Metabolism	2	4	1	2	0	3	2	5
Response to Stress/Stimuli	1	0	0	0	0	0	1	0
Signal Transduction	10	3	0	1	2	3	2	2
Transcription/Translation	6	4	0	1	1	2	3	3
Transporters	3	2	0	1	0	1	1	1
Other	29	28	1	8	4	12	8	16
	90	64	11	30	19	36	32	50
Total DE genes	154		41		55		82	

Table 4.3. Comparison of mRNA expression (i.m. relative to s.c.) detected in the cDNA microarray analysis to mRNA expression detected in RT-PCR. Fold change values represent i.m. adipose tissue expression relative to s.c. adipose tissue.

Gene Name	Diet	Fold Change	
		Microarray	RT-PCR
ACSM1	Calf Fed	-2.18 (±.11)	-6.23 (±1.23)
CD36	Wheat Pasture	-4.40 (±.47)	-9.89 (±.58)
FABP4	Wheat Pasture	-3.09 (±.28)	-3.84 (±.46)
FHL1	Program Fed	2.94 (±.18)	4.76 (±.55)
GPI	Calf Fed	2.11 (±.22)	-2.77 (±.58)
LDHB	Calf Fed	-2.14 (±.69)	-14.72 (±.15)
PKM2	Program Fed	4.00 (±.47)	3.43 (±.79)
SCD	Program Fed	-5.13 (±.22)	-21.40 (±.70)
PTGS2	Wheat Pasture	2.11 (±.33)	14.12 (±.69)

Figure 4.1.

(a) Relative fold difference in acyl-CoA synthetase medium-chain family member 1 (ACSM1) gene expression in s.c. (green) and i.m. (red) adipose tissue depots in steers at the end of the Finishing Phase. The gene expression level for the i.m. adipose tissue was set as baseline and fold difference was calculated as described in Material and Methods. Columns with different superscripts differ significantly ($P < 0.01$).

(b) Relative fold difference in CD36 molecule (thrombospondin receptor) (CD36) gene expression in s.c. (green) and i.m. (red) adipose tissue depots in steers at the end of the Finishing Phase. The gene expression level for the i.m. adipose tissue was set as baseline and fold difference was calculated as described in Material and Methods. Columns with different superscripts differ significantly ($P < 0.02$).

(c) Relative fold difference in stearoyl-CoA desaturase (SCD) gene expression in s.c. (green) and i.m. (red) adipose tissue depots in steers at the end of the Finishing Phase. The gene expression level for the i.m. adipose tissue was set as baseline and fold difference was calculated as described in Material and Methods. Columns with different superscripts differ significantly ($P < 0.001$).

(d) Relative fold difference in hydroxyacyl-Coenzyme A dehydrogenase (HADH) gene expression in Wheat Pasture, Silage-fed, Program-fed, and Calf-fed diets in steers at the end of the Finishing Phase. The gene expression level for the Wheat Pasture diet was set as baseline and fold difference was calculated as described in Material and Methods. Columns with different superscripts differ significantly ($p < 0.09$).

(e) Relative fold difference in fatty acid binding protein 4 (FABP4) gene expression in s.c. (green) and i.m. (red) adipose tissue depots in steers at the end of the Finishing Phase. The gene expression level for the i.m. adipose tissue was set as baseline and fold difference was calculated as described in Material and Methods. Columns with different superscripts differ significantly ($P < 0.019$).

(f) Relative fold difference in prostaglandin-endoperoxide synthase 2 (PTGS2) gene expression in Wheat Pasture, Silage-fed, Program-fed and Calf-fed depot x diet in steers at the end of the Finishing Phase. The gene expression level for the Wheat Pasture diet was set as baseline and fold difference was calculated as described in Material and Methods. Columns with different superscripts differ significantly ($P < 0.09$).

(g) Relative fold difference in lactate dehydrogenase B (LDHB) gene expression in s.c. (green) and i.m. (red) adipose tissue depots in steers at the end of the Finishing Phase. The gene expression level for the i.m. adipose tissue was set as baseline and fold difference was calculated as described in Material and Methods. Columns with different superscripts differ significantly ($P < 0.05$).

(a)

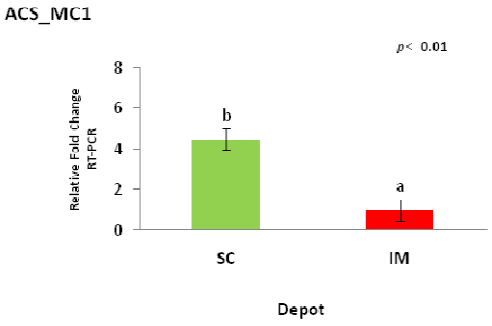
ACS_MC1
p< 0.01
Relative Fold Change RT-PCR
8
6
4
2
0
b
a
SC
IM
Depot

(b)

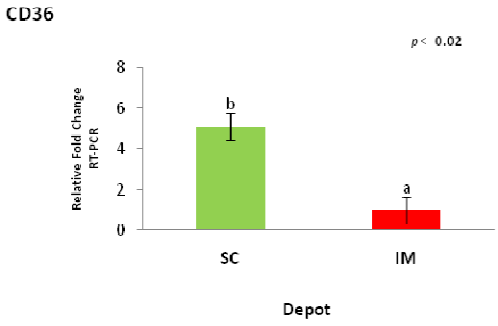
CD36
p< 0.02
Relative Fold Change RT-PCR
8
6
4
2
0
b
a
SC
IM
Depot

(c)

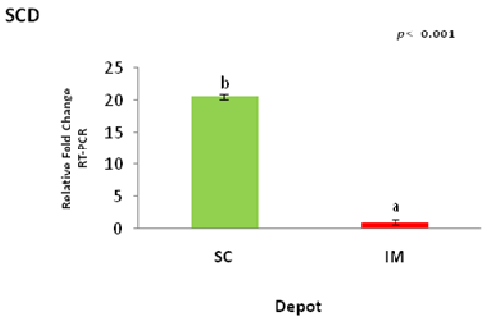
SCD
p< 0.001
Relative Fold Change RT-PCR
25
20
15
10
5
0
b
a
SC
IM
Depot

(d)

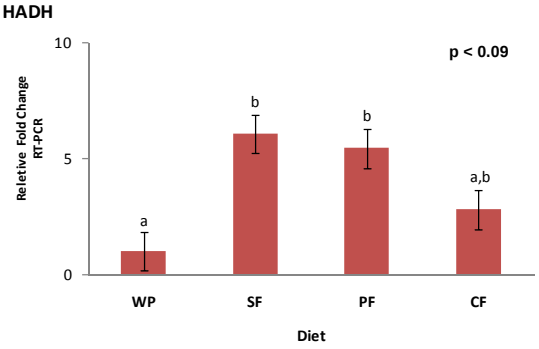
HADH
p < 0.09
Reletive Fold Change RT-PCR
10
5
0
a
b
b
a,b
WP
SF
PF
CF
Diet

(e)

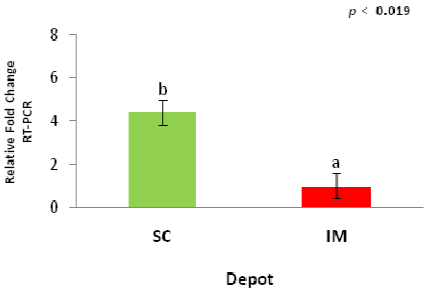
FABP4
p < 0.019
Relative Fold Change RT-PCR
8
6
4
2
0
b
a
SC
IM
Depot

(f)

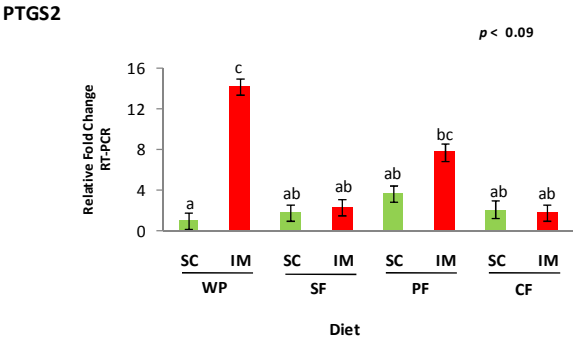
PTGS2
p< 0.09
Relative Fold Change RT-PCR
16
12
8
4
0
a
c
ab
ab
ab
bc
ab
ab
SC
IM
WP
SF
PF
CF
Diet

(g)

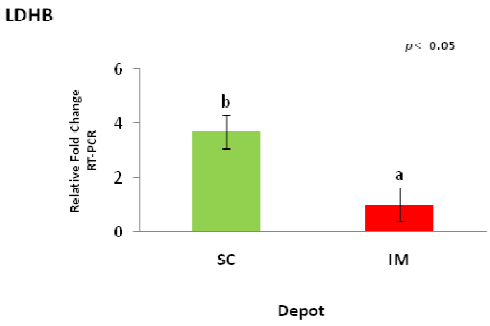
LDHB
p< 0.05
Relative Fold Change RT-PCR
6
4
2
0
b
a
SC
IM
Depot

Figure 4.1.

(h) Relative fold difference in glucose phosphate isomerase (GPI) gene expression in s.c. (green) and i.m. (red) adipose tissue depots in steers at the end of the Finishing Phase. The gene expression level for the i.m. adipose tissue was set as baseline and fold difference was calculated as described in Material and Methods. Columns with different superscripts differ significantly ($P < 0.004$).

(i) Relative fold difference in glucose phosphate isomerase (GPI) gene expression in Wheat Pasture, Silage-fed, Program-fed, and Calf-fed diets in steers at the end of the Finishing phase. The gene expression level for the Wheat Pasture diet was set as baseline and fold difference was calculated as described in Material and Methods. Columns with different superscripts differ significantly ($P < 0.06$).

(j) Relative fold difference in pyruvate kinase, muscle (PKM2) gene expression in s.c. (green) and i.m. (red) adipose tissue depots in steers at the end of the Finishing Phase. The gene expression level for the s.c. adipose tissue was set as baseline and fold difference was calculated as described in Material and Methods. Columns with different superscripts differ significantly ($P < 0.0001$).

(k) Relative fold difference in pyruvate kinase, muscle (PKM2) gene expression in Wheat Pasture, Silage-fed, Program-fed and Calf-fed diets in steers at the end of the Finishing Phase. The gene expression level for the Wheat Pasture diet was set as baseline and fold difference was calculated as described in Material and Methods. Columns with different superscripts differ significantly ($P < 0.04$).

(l) Relative fold difference in four and a half LIM domains 1(FHL1) gene expression in s.c. (green) and i.m. (red) adipose tissue depots in steers at the end of the Finishing Phase. The gene expression level for the s.c. adipose tissue was set as baseline and fold difference was calculated as described in Material and Methods. Columns with different superscripts differ significantly ($P < 0.03$).

(m) Relative fold difference in four and a half LIM domains 1(FHL1) gene expression in Wheat Pasture, Silage-fed, Program-fed, and Calf-fed diets in steers at the end of the Finishing Phase. The gene expression level for the Wheat Pasture diet was set as baseline and fold difference was calculated as described in Material and Methods. Columns with different superscripts differ significantly ($P < 0.06$).

(h)

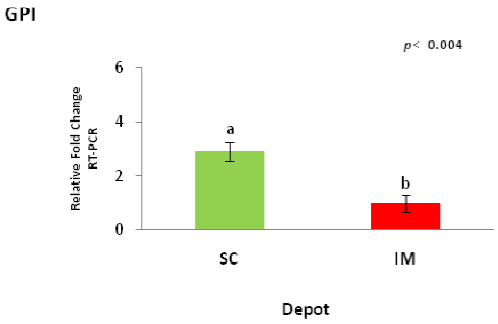
GPI
p< 0.004
Relative Fold Change RT-PCR
6
4
2
0
a
b
SC
IM
Depot

(i)

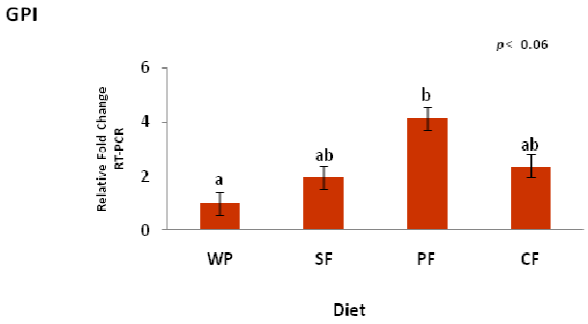
GPI
p< 0.06
Relative Fold Change RT-PCR
6
4
2
0
a
ab
b
ab
WP
SF
PF
CF
Diet

(j)

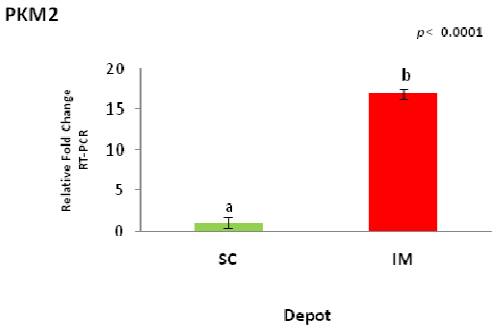
PKM2
p< 0.0001
Relative Fold Change RT-PCR
20
15
10
5
0
a
b
SC
IM
Depot

(k)

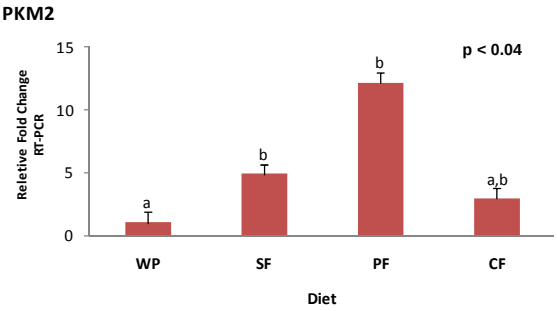
PKM2
p < 0.04
Reletive Fold Change RT-PCR
15
10
5
0
a
b
b
a,b
WP
SF
PF
CF
Diet

(l)

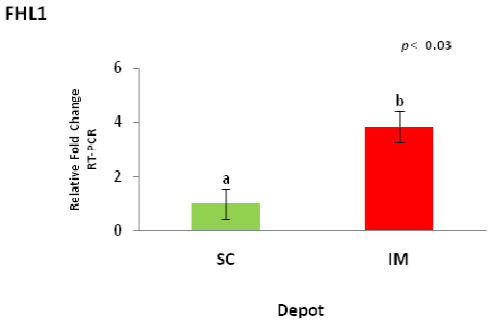
FHL1
p< 0.03
Relative Fold Change RT-PCR
6
4
2
0
a
b
SC
IM
Depot

(m)

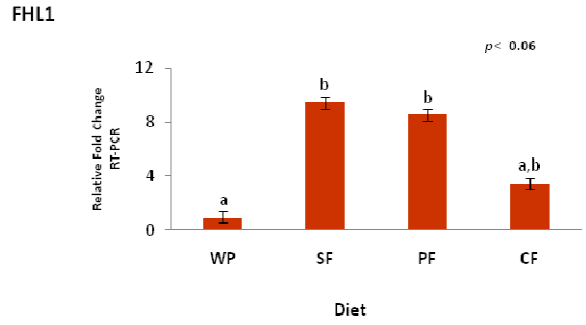
FHL1
p< 0.06
Relative Fold Change RT-PCR
12
8
4
0
a
b
b
a,b
WP
SF
PF
CF
Diet

Table 4.4. Principle Networks generated for Wheat Pasture, Silage-fed, Program-fed, and Calf-fed diets of the Finishing Phase using Inginuity Pathway Analysis. Focus genes were overlaid into a globular molecular network deveolped from information contained in the IPA Knowledge Base. Networks of these focus genes were then algorithmically generated based on their connectivity.

Network ID	Score	Focus Molecules	Top Network Molecular or Cellular Function, Disease or Disorder, or Physiological System Development and Function
1	45	23	Cellular Movement, Cellular Growth and Proliferation, Skeletal and Muscular System Development and Function
2	35	19	DNA Replication, Recombination, and Repair, Carbohydrate Metabolism, Cell Morphology
3	26	15	Amino Acid Metabolism, Post-Translational Modification, Small Molecule Biochemistry
4	26	15	Carbohydrate Metabolism, Small Molecule Biochemistry, Cancer
5	24	14	Cell Morphology, Cellular Assembly and Organization, Cellular Compromise
6	21	13	Cell Cycle, Cellular Assembly and Organization, Cellular Function and Maintenance
7	15	10	Molecular Transport, RNA Trafficking, Cell Cycle
8	11	8	DNA Replication, Recombination, and Repair, Energy Production, Nucleic Acid Metabolism
1	39	18	Cardiovascular Disease, Lipid Metabolism, Molecular Transport
2	36	17	Carbohydrate Metabolism, Small Molecule Biochemistry, Lipid Metabolism
3	23	12	Cellular Compromise, Developmental Disorder, Embryonic Development
4	23	12	Cellular Assembly and Organization, Cell Cycle, DNA Replication, Recombination, and Repair
1	44	20	Cardiovascular Disease, Lipid Metabolism, Molecular Transport
2	28	14	Lipid Metabolism, Small Molecule Biochemistry, Carbohydrate Metabolism
3	25	13	Cell Cycle, Hair and Skin Development and Function, Immunological Disease
4	16	9	Cell Cycle, Cellular Assembly and Organization, DNA Replication, Recombination, and Repair
1	34	17	Cardiovascular Disease, Cellular Growth and Proliferation, Cellular Movement
2	34	17	Cellular Assembly and Organization, Cardiovascular Disease, Neurological Disease
3	26	14	Cellular Function and Maintenance, Cellular Movement, Hair and Skin Development and Function
4	24	13	Cellular Growth & Proliferation, Skeletal & Muscular System Development & Function, Connective Tissue Development & Function
5	24	13	Cell Cycle, Embryonic Development, Tissue Development

Table 4.5. Networks were generated for the Wheat Pasture diet of the Finishing Phase using Inginuity Pathway Analysis. Genes differentially expressed only in the Wheat Pasture diet of the Finishing Phase are highlighted in yellow. Genes highlighted in bold are focus genes. Genes in regular print were used to connect to other genes in the network.

Network ID	Genes in Network	Network Score	Focus Genes	Function
1	↓**ADIPOQ**, ↑**ANXA5**, Ap1, ↓**CD36**, ↓**CDH13**, ERK, ↓**FABP4**, ↑**GCLC**, ↓**IGFBP5**, LDL, ↑**LRG1**, Mek, ↓**MRAS**, ↓**MSR1**, ↑**MYLK**, ↑**NBN**, Nfat, ↓**NFKB1**, ↑**NOD1**, Pdgf, PDGF BB, peptidase, ↓**PLAU**, ↑**PLD1**, ↑**PTGS2**, ↑**RAP1A**, Ras, Rxr, ↓**S100G**, ↓**SPARC**, ↑**SPP1**, ↓**STRN3**, Tgf beta, ↓**TXNIP**, VitaminD3-VDR-RXR	45	23	Cellular Movement, Cellular Growth and Proliferation, Skeletal and Muscular System Development and Function
2	↑**ADRBK2**, ↑**AGTR1**, Akt, ↑**AQP4**, Calmodulin, Caspase, ↓**CFB**, Ck2, Creb, ↓**CXCL16**, ↑**CYCS (includes EG:54205)**, ↑**FKBP3**, ↑**GHRH**, ↑**GPAM**, ↓**HNRNPF**, Hsp90, Ikk, IL1, Insulin, Interferon alpha, ↓**ITM2B**, ↑**MYL6**, Myosin light chain, NFkB, P38 MAPK, ↑**PCSK7**, PLC, ↑**PRNP**, Proteasome, ↓**PSAP**, ↑**SEPT4**, ↑**SPARCL1**, ↑**STAT1**, ↓**THRSP**, Ubiquitin	35	19	DNA Replication, Recombination, and Repair, Carbohydrate Metabolism, Cell Morphology
3	↑**ABCG2**, amino acids, beta-estradiol, BTG1, ↓**C10ORF116**, CDC2L2, ↑**CPM**, CRYAA, ↑**CRYZ**, ↑**CSNK1A1**, CSNK1E, ↓**CSTB**, CTSH, DUSP6, DYRK2, DYRK1A, DYRK1B, ↓**EIF3B**, EIF3D, EIF3G, EIF3J, FNTA, ↑**GCLC**, ↑**GNL3**, ↓**GPX3**, ↑**HADH**, MAP3K1, ↓**MGST1**, ↑**NP**, ↓PDK4, PINK1, PTPN2, TGFBR1, ↓**TGFBRAP1**, ↓**WDR68**	26	15	Amino Acid Metabolism, Post-Translational Modification, Small Molecule Biochemistry
4	↓**ACSS2**, APC2, Cbp/p300, CD40LG, ↓**CDH13**, CDKN1A, ↓CIDEA, CLIP2, CTNNB1, ↑**CYP2B6 (includes EG:1555)**, ↓**DGAT2**, ↑**EHBP1**, ↓**EHD2**, ↓**ELOVL5**, FABP5L2, ↑GOT2, IL1B, ↑**LCP1**, ↑**MAPRE1**, palmitic acid, ↓**PCK2**, ↓**POLR1D**, PPARA, RXRA, SAT1, SLC2A4, ↓**SNF8**, TBP, ↑**TMEM66**, ↓**TRAF3IP1**, TSG101, TYMP, ↑**VEZT**, VPS36, WNT3	26	15	Carbohydrate Metabolism, Small Molecule Biochemistry, Cancer
5	↑**ACTB**, Actin, ↓**CCNL2**, CENTA1, CFL2, ↓**CHD8**, ↓**COL3A1**, ↑**CSNK1A1**, ↓**DNASE1**, DSTN, F Actin, FMNL1, FSH, G-Actin, ↑**GAPDH**, hCG, HIST2H3D, Histone h3, HPCAL1, IL12, Jnk, KCNJ8, ↑**MAGED2**, Mapk, ↑**PFN1**, PHACTR1, PI3K, Pkc(s), ↑**PKM2**, RNA polymerase II, ↑**ROR2**, ↑**SETMAR**, ↑**TLN1**, XPO6, ↓**YY1**	24	14	Cell Morphology, Cellular Assembly and Organization, Cellular Compromise
6	↓**AHCYL1**, BET1, ↑**BET1L**, BTG1, COPE, EPB41L1, ↓**FAM160B1**, GOLGB1, GOSR2, ↓**HPRT1**, IFITM1, IL15, ITPR1, ITPR2, JUNB, KIF1B, ↑**LAP3**, ↓**NDFIP1**, ↑**NP**, ↓**OAT**, PDIA2, ↑**PFN1**, ↓**PTP4A2***, PXN, RABGGTB, retinoic acid, RHOA, RPL3, ↓**SBDS**, ↑**STARD13**, TAX1BP1, testosterone, TK1, ↑**TM7SF2**, XBP1	21	13	Cell Cycle, Cellular Assembly and Organization, Cellular Function and Maintenance
7	ABCD3, BAZ1A, ↑**CHRAC1**, ↓**DHX16**, ↓**DPT**, E2F1, ↑**EIF1**, EZH2, FBL, HOXB4, IFNG, IL10RA, LOX, MNDA, MYC, NUP98, ↓**NUP107**, NUP133, NUP160, OAS1, PAM, PARP9, POLE3, PSAT1, ↑**RBMS1**, ↑**SASH3**, SCAMP1, ↑**SCAMP2**, ↑**SCPEP1**, SFRS2, SMARCA5, SUMO2 (includes EG:6613), TGTP, TPR, ↓**ZMYM4**	15	10	Molecular Transport, RNA Trafficking, Cell Cycle
8	↑**ANLN**, ARRB1, ATP5A1, ATP5B, ATP5C1, ATP5D, ↑**ATP5O**, BCLAF1, CFL1, DDX5, ↓**DNASE1**, H2AFX, HIST1H1C, HSPA9, ILF3, ↑**ILF2 (includes EG:3608)**, KCTD3, KIF23, KIF1B, LBR, LIMA1, MYH1, ↑**NBN**, ↓**NMT2**, poly(ADP-ribose), PPM1A, PRKDC, RAB11FIP5, RPA2, ↓**RSRC1**, ↓**RTN3**, SRRM2, TP53, TUBB4, YWHAG	11	8	DNA Replication, Recombination, and Repair, Energy Production, Nucleic Acid Metabolism
9	BMYC, ↑**LOC257407**	2	1	Cellular Development, Cellular Growth and Proliferation, Renal and
10	LSM8, ↑**THUMPD3**	2	1	
11	↑**ALG11**, UBE2G2	2	1	Connective Tissue Disorders, Dermatological Diseases and Conditions,
12	↑**NLRX1**, VISA	2	1	Viral Function, Embryonic Development, Immune and Lymphatic System
13	ZP3, ↑**ZP3R** = **LOC506707**	2	1	Cell-To-Cell Signaling and Interaction, Reproductive System

Table 4.6. Networks were generated for the Program-fed diet of the Finishing Phase using Inginuity Pathway Analysis. Genes differentially expressed only in the Program-fed diet of the Finishing Phase are highlighted in yellow. Genes highlighted in bold are focus genes. Genes in regular print were used to connect to other genes in the network.

Network ID	Genes in Network	Network Score	Focus Genes	Function
2	↓**ACSS2,** ASB9, beta-estradiol, ↑**C10RF21,** CEBPB, ↓**CIDEA,** ↑**CKB,** ↓**DGAT2,** dihydrotestosterone, ↓**ELOVL5,** FABPSL2, ↓**HPRT1,** IL1B, MGP, MIA, ND4, ↑**NDUFS5,** ↑**PDK4,** ↑**PFKL,** ↓**POLR1D,** PPARA, RHOA, S100A6, SAT1, SERPINB9, ↑**STARD13,** TAF1A, TAF1B, TAF1C, TBP, TGFBR1, ↓**TGFBRAP1,** TM4SF1, ↑**TMEM66,** TMF1	28	14	Lipid Metabolism, Small Molecule Biochemistry, Carbohydrate Metabolism
4	↓**AHCYL1,** BAZ1A, BCL2, BCLAF1, CDC2L1 (includes EG:984), ↓**CFB,** ↑**CHRAC1,** DYRK1A, E2F1, FHL1, ↓**GOLGA7,** HOXA9, HRAS, ↓ITM2B, KIF1B, lactic acid, LIMA1, MAP3K1, MFN2, MTHFD1, MYC, ↓**NMT2,** POLE3, PSAT1, Pyruvate kinase, ↑**RBMS1,** RPS13 (includes EG:6207), ↓**RSRC1,** SFRS2, SMARCA5, ↑**SRPR,** TOMM20, ↓**WDR68,** YWHAG, ZDHHC9	16	9	Cell Cycle, Cellular Assembly and Organization, DNA Replication, Recombination, and Repair

Table 4.7. Networks were generated for the Calf-fed diet of the Finishing Phase using Inginuity Pathway Analysis. Genes differentially expressed only in the Calf-fed diet of the Finishing Phase are highlighted in yellow. Genes highlighted in bold are focus genes. Genes in regular print were used to connect to other genes in the network.

Network ID	Genes in Network	Network Score	Focus Genes	Function
2	↑**ACTB,** ↓**AHCYL1,** Akt, ALP, ↓**CCNL2,** ↓**CFB,** ↓**CLU,** ↓**CXCL16,** Cyclin A, Cytochrome c, ↓**DCN,** ↓**FN1,** FSH, ↑**GAPDH,** ↑**GPI,** hCG, Histone h3, Hsp90, IFN Beta, ↓**IGFBP5,** IL12, Insulin, Interferon alpha, Mapk, NFkB, P38 MAPK, ↑**PCNA,** PI3K, ↑**PKM2,** Proteasome, RNA polymerase II, ↑**SLC25A4,** ↑**STAT1,** ↓**THRSP,** ↑**UQCRC1**	34	17	Cellular Assembly and Organization, Cardiovascular Disease, Neurological Disease
3	↓**ACSS2,** APH1B, Cbp/p300, CCT5, CLIC4, COL6A1, ↓**COL6A2,** COMP, ↓**DPT,** ↓**ELOVL5,** FIGF, FNTA, ↑**GAPDH,** ↓**GOLGA7,** ↓**GRN,** HRAS, MMP2, MMP17, ↑**MYL6,** ↓**NMT2,** PAFAH1B3, PCDHA4, ↑**PCSK7,** PPARA, PXN, ↓**RSRC1,** SAT1, SLC4A1, ↓**STRN3,** TGFB1, ↑**TM7SF2,** ↑**TMEM66,** TP53, YWHAG, ZDHHC9	26	14	Cellular Function and Maintenance, Cellular Movement, Hair and Skin Development and Function
4	ABL1, Actin, ↑**C10RF21,** CEACAM1, ↓**DHX16,** dihydrotestosterone, DSTN, ↓**FAM160B1,** FBL, FNTA, ↑**GAPDH,** ↓**GPX3,** HTR2C, IL15, INS1, KCNJ11, KIF1B, LDHA, ↓**LDHB,** MYC, ↓**NCSTN,** ND3, ND4, NDUFS4, ↑**NDUFS5,** ↑PFN1, PGK1, ↓**PTP4A2*,** ↑**RBMS1,** RHOA, ↑**SCPEP1,** SGK1, ↑**STARD13,** TGFBR1, ↓**TGFBRAP1**	24	13	Cellular Growth and Proliferation, Skeletal and Muscular System Development and Function, Connective Tissue Development and Function

Figure 4.2. The top ten molecular and cellular functions associated with all generated networks for the Wheat Pasture, Silage-fed, Program-fed, and Calf-fed diets of the Finishing Phase. Threshold signifiacnce ($P < 0.05$) expressed as the negative $\log_{10}$ of the P-value calculated using the right-tailed Fischer's exact test, is represented by the orange bar. Numbers at top of each graph are the number of genes associated with that function.

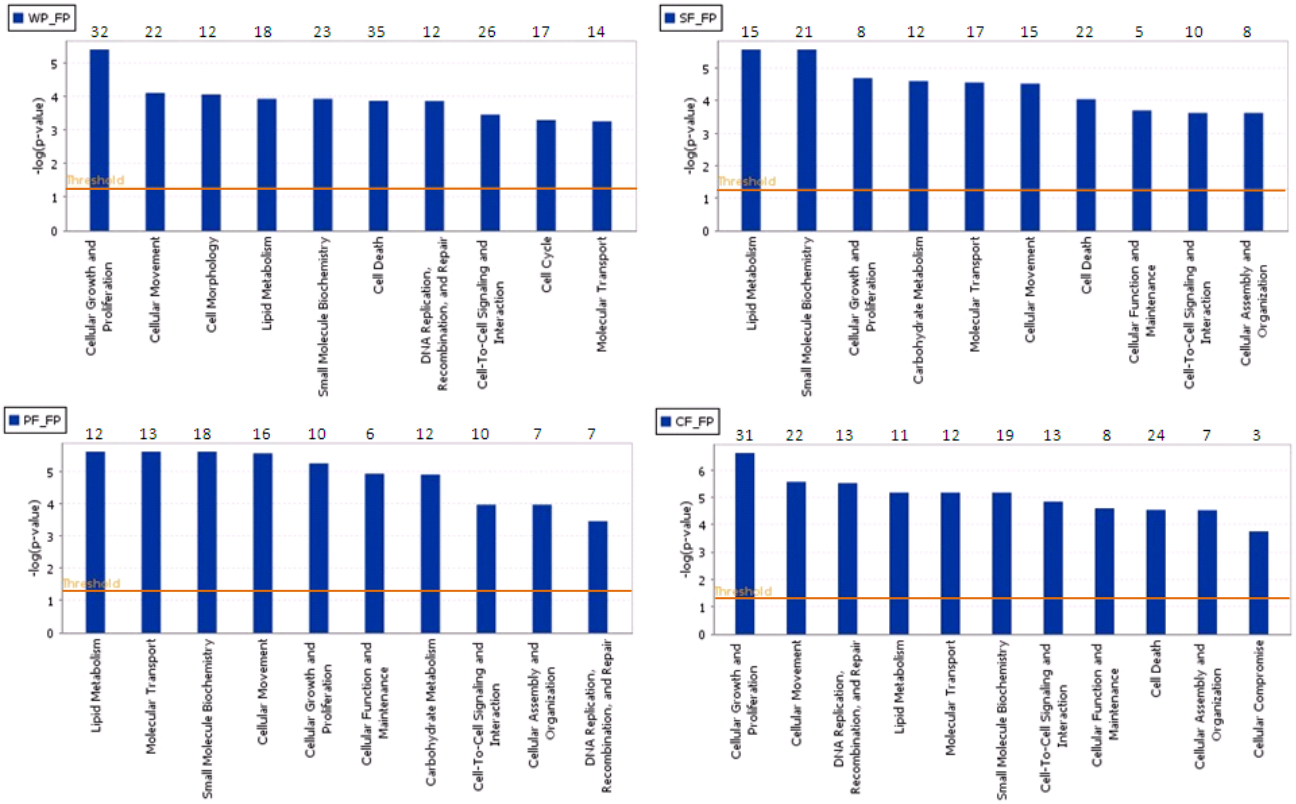

Figure 4.3. Comparative Functional Analysis of differentialy expressed genes comparing the Wheat Pasture, Silage-fed, Program-fed, and Calf-fed diets of the Finishing Phase. Significance ($P < 0.05$), expressed as the negative $\log_{10}$ of the P-value calculated for each function using the right- tailed Fischer's exact test, is represented by the orange bar.

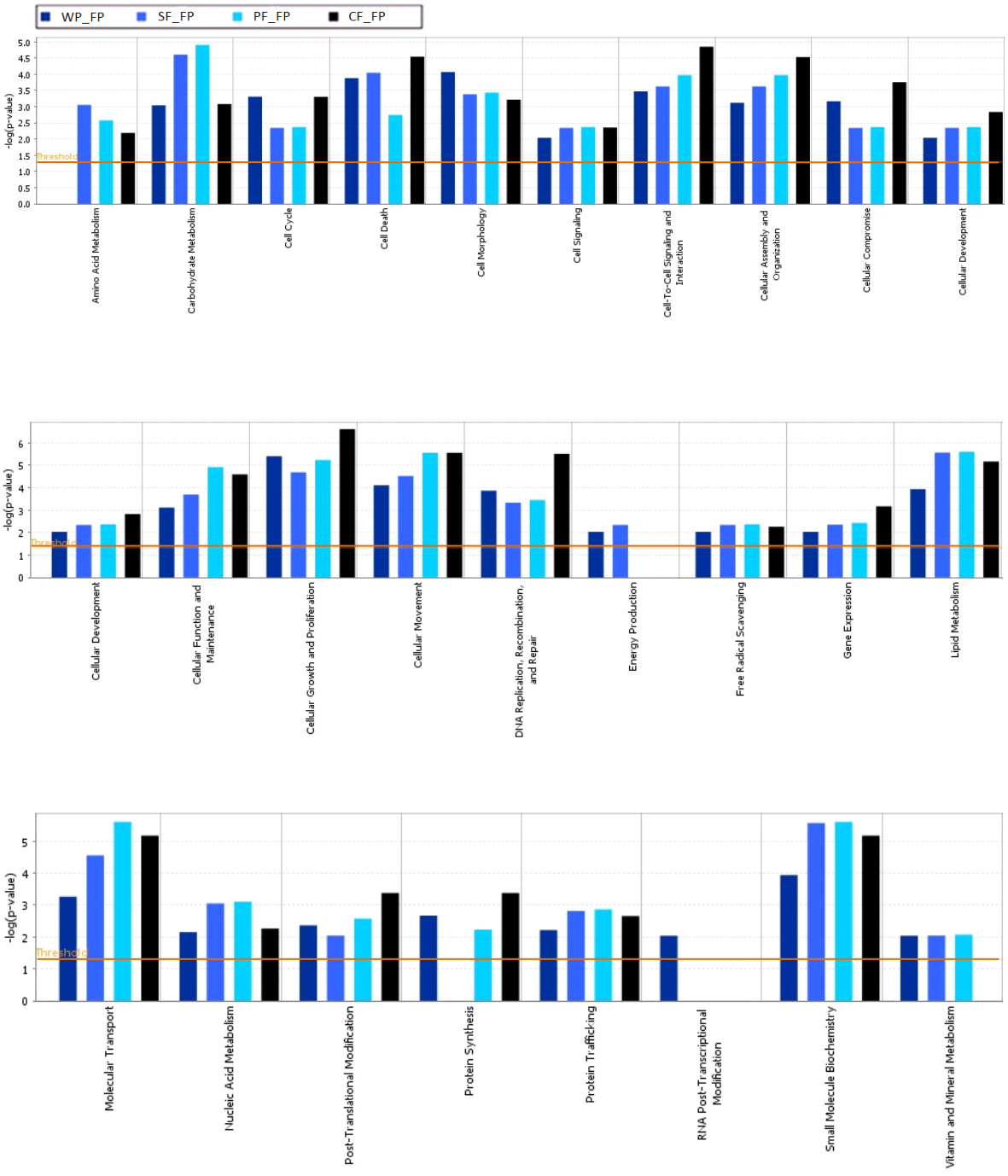

Figure 4.4. Metabolic pathway comparison between the Wheat Pasture, Silage-fed, Program-fed, and Calf-fed diets of theFinishing Phase. Significance ($P < 0.10$), expressed as the negative $\log_{10}$ of the P-value calculated for each function using the right- tailed Fischer's exact test, is represented by the orange bar.

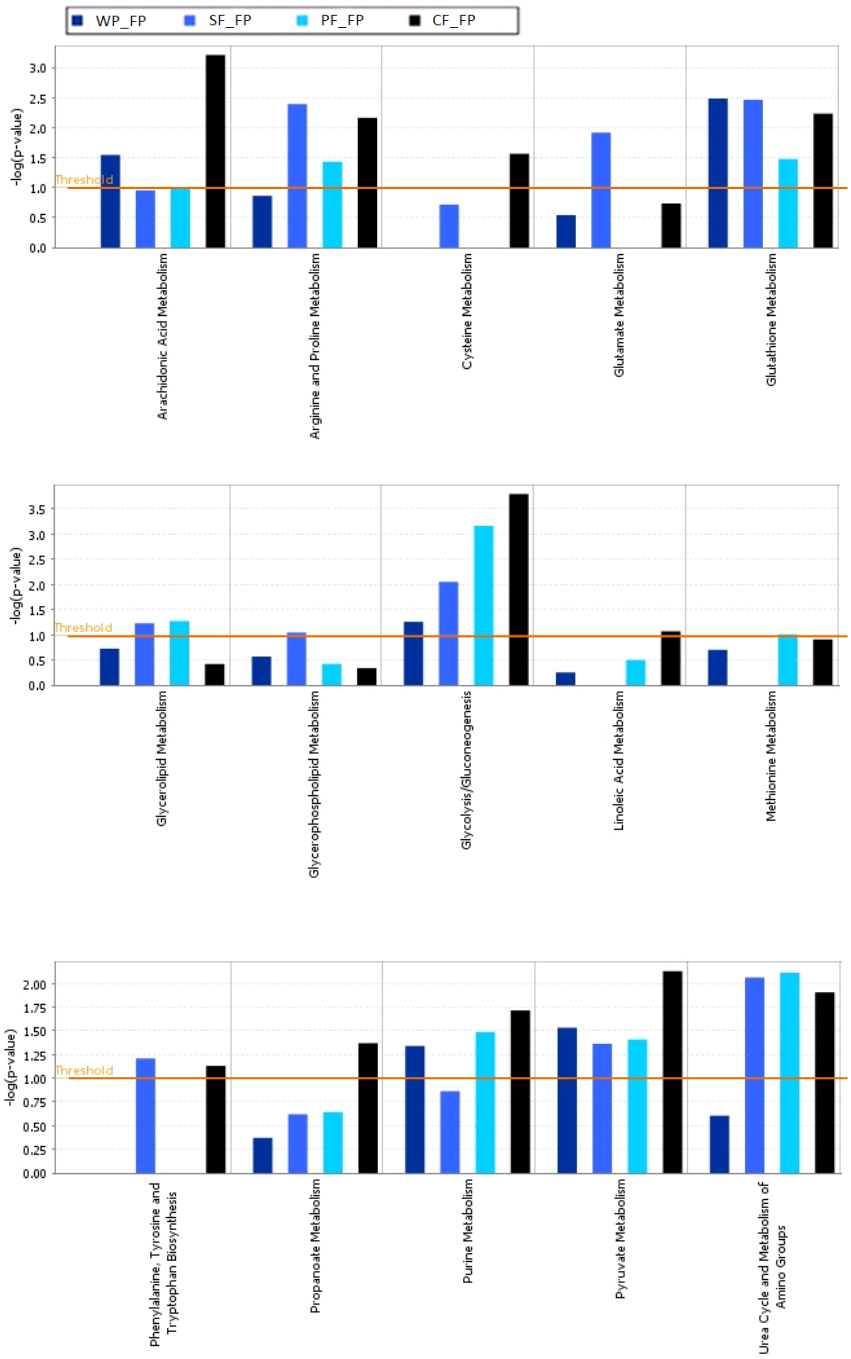

Figure 4.5. Signaling pathway comparison between the Wheat Pasture, Silage-fed, Program-fed, and Calf-fed diets of the Finishing Phase. Significance ($P < 0.10$), expressed as the negative $\log_{10}$ of the P-value calculated for each function using the right-tailed Fischer's exact test, is represented by the orange bar.

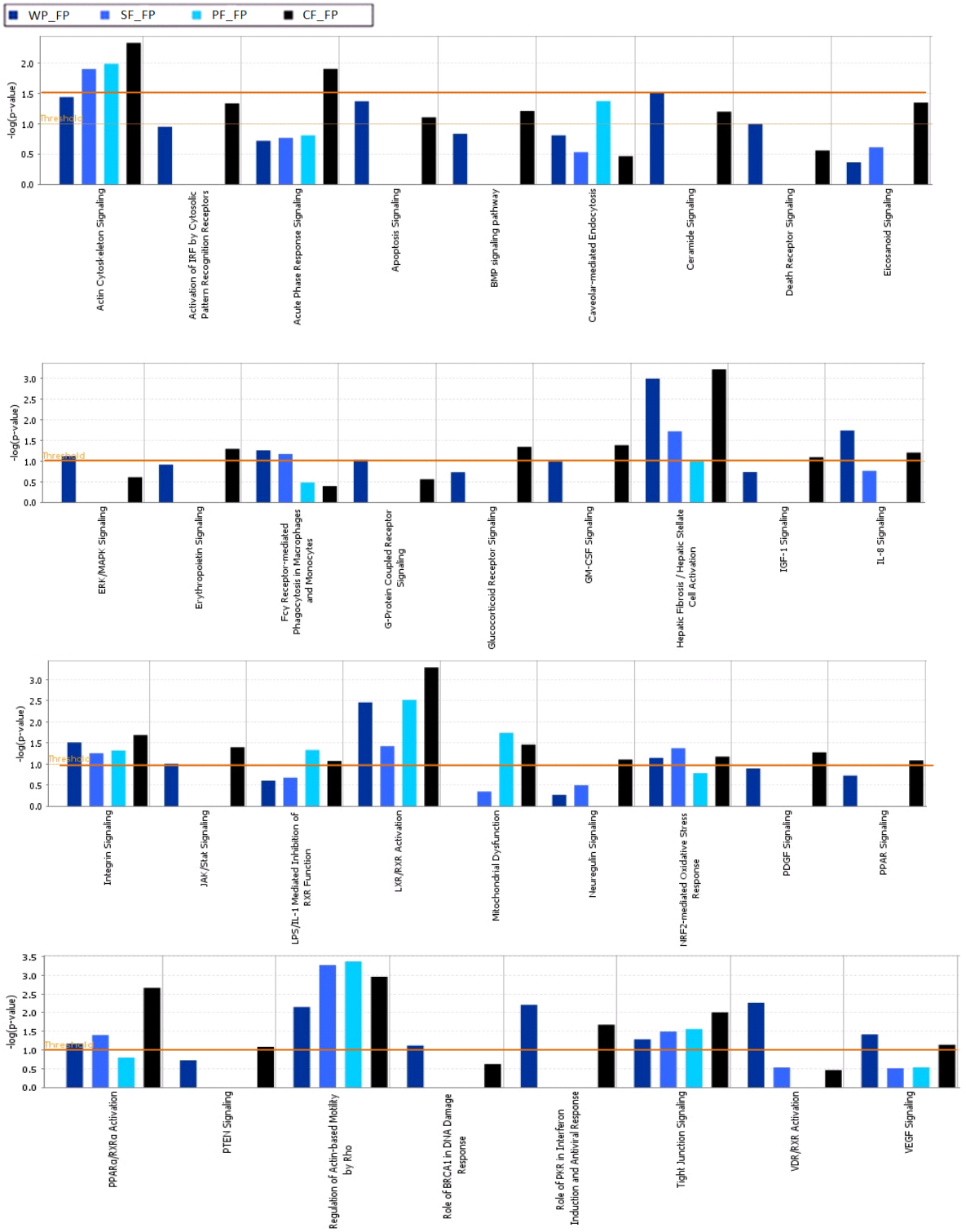

Figure 4.6. Heat map of genes in the Adipose Related ontology category. Boxes colored with shades of red represent genes up-regulated in i.m. adipose tissue compared to s.c. adipose tissue and boxes with shades of green represent down-regulted genes in i.m. adipose tissue compared to s.c. adipose tissue. Black boxes represent no observed change in gene expression.

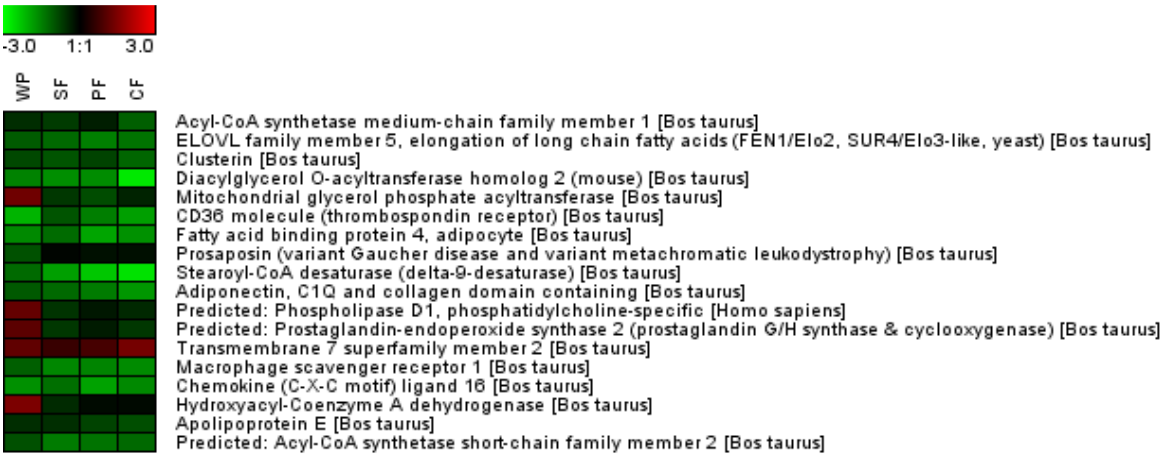

Figure 4.7. Diagram of the KEGG Bovine PPAR signaling pathway. Genes highlighted in red are those genes found differntiallyexpressed in at least one of the diets of the finshing phase.

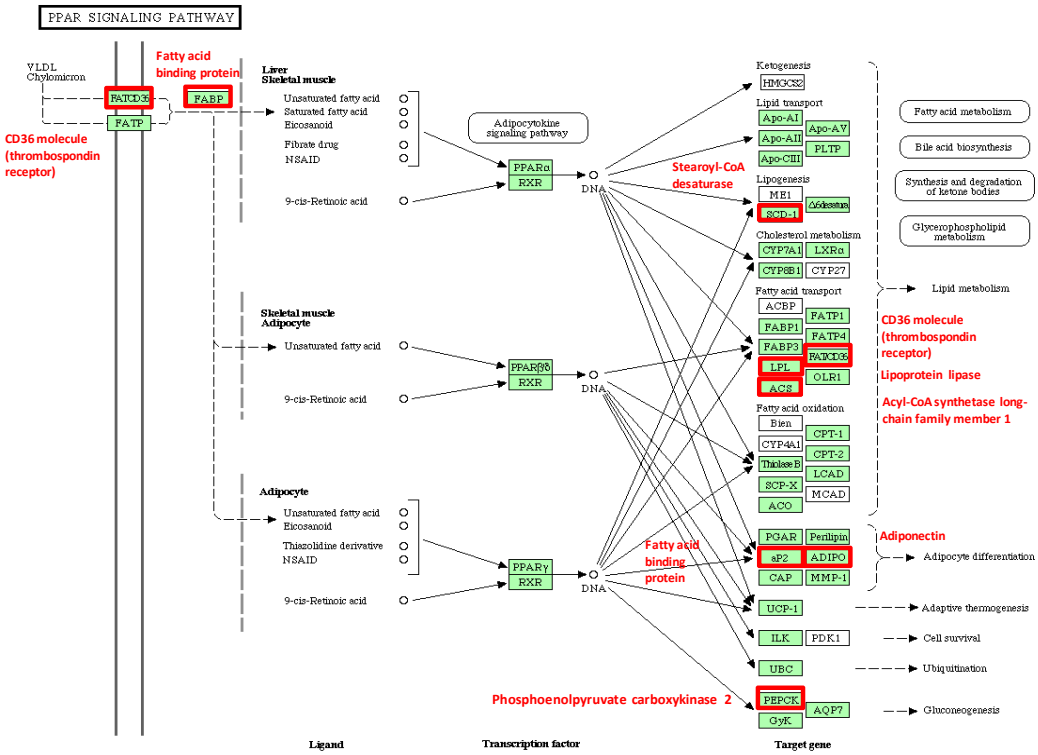

Figure 4.8. Network 1 of theSilage-fed diet of the Finishing Phase depiciting genes involved in lipid metabolism and molecular transport. Dataset was analyzed by the Ingenuity Pathways Analysis software. Node color indicates the expression level of the genes; green = down-regulation in i.m. adipose tissue when compared to s.c. adipose tissue and red = up-regulated in i.m. when compared to s.c. adipose tissue.

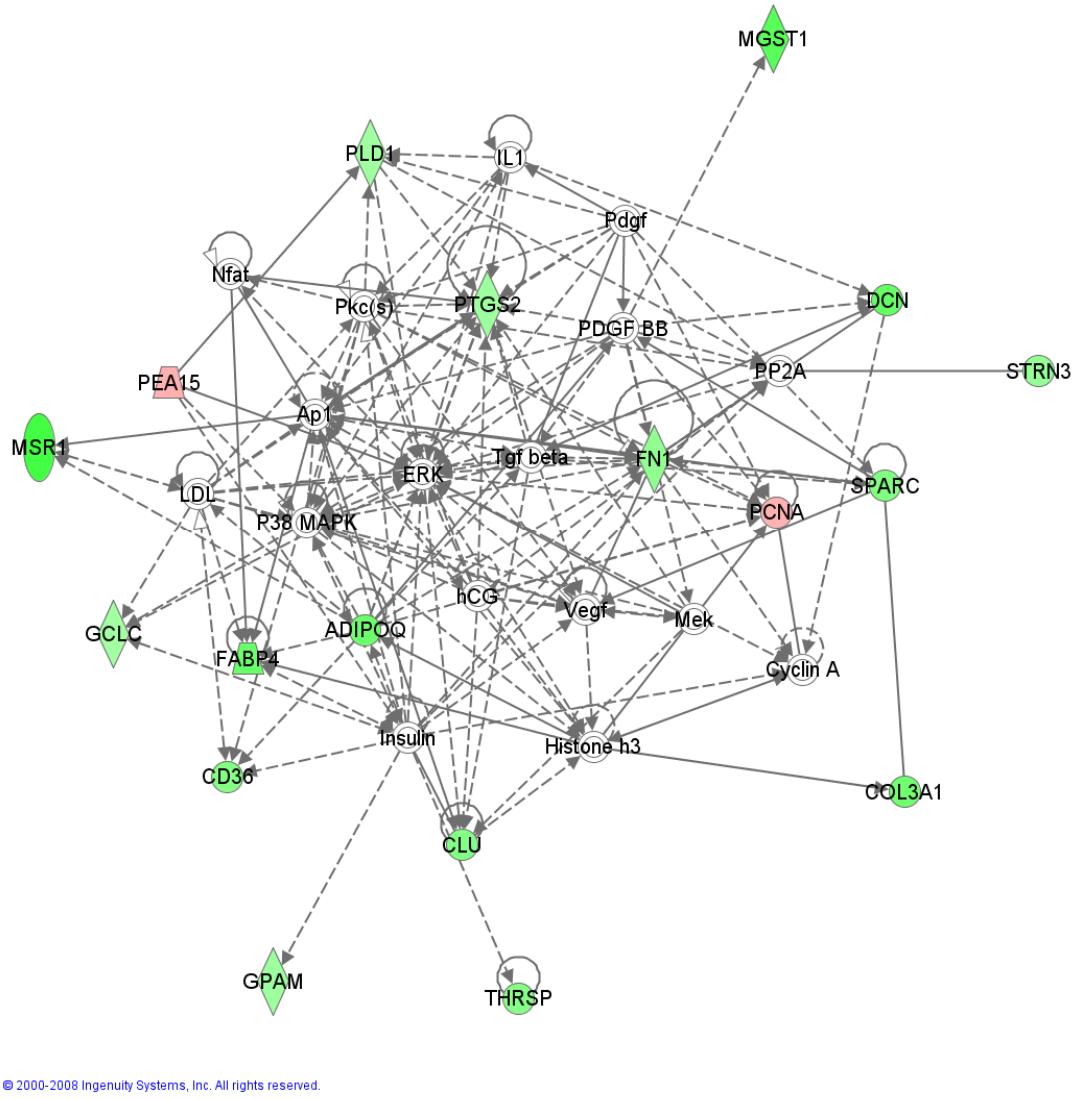

Figure 4.9. Network 1 of theProgram-fed diet of the Finishing Phase depiciting genes involved in lipid metabolism and molecular transport. Dataset was analyzed by the Ingenuity Pathways Analysis software. Node color indicates the expression level of the genes; green = down-regulation in i.m. adipose tissue when compared to s.c. adipose tissue and red = up-regulated in i.m. when compared to s.c. adipose tissue.

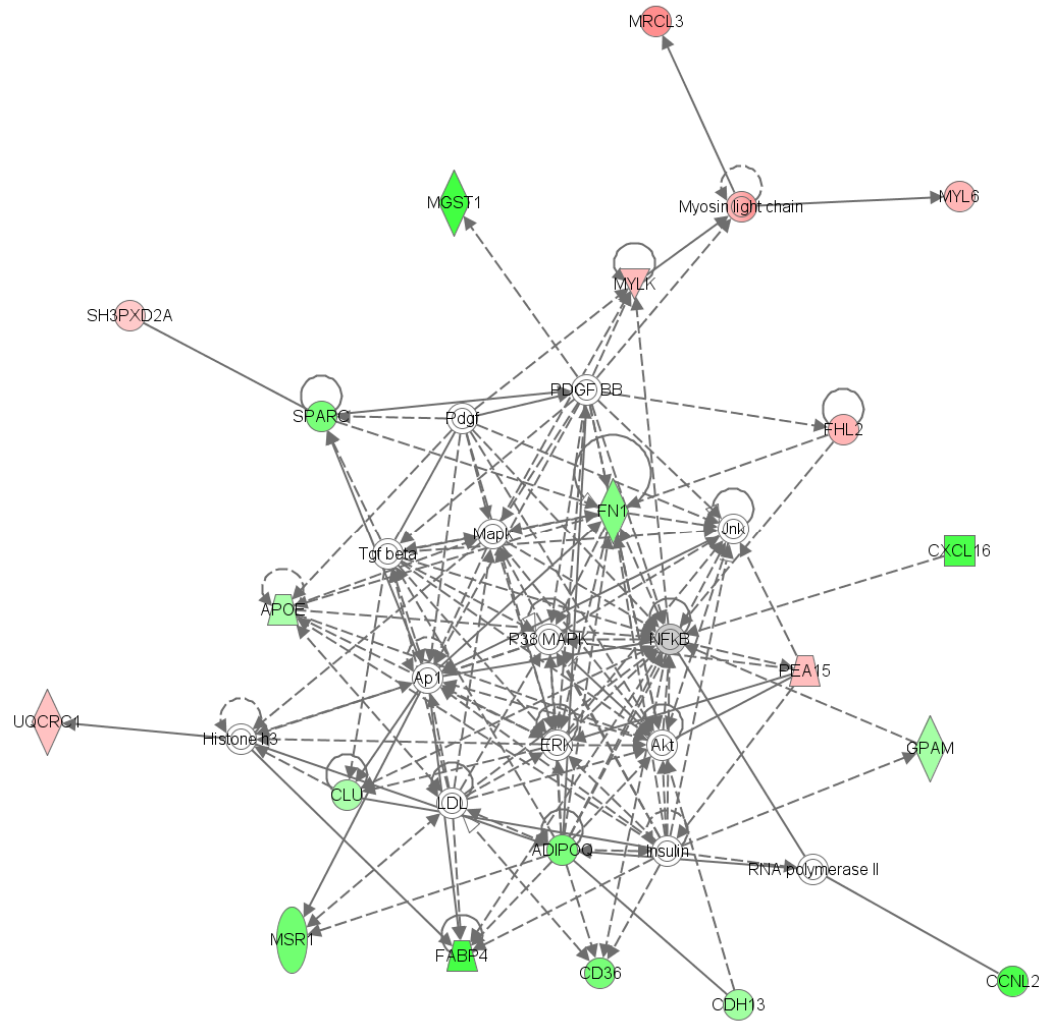

CHAPTER V

Effects of the β–adrenergic agonist, zilpaterol hydrochloride, on gene expression in muscle and adipose tissue depots in beef steers

D.R. Stein[1], B.P. Holland[1], C.R., Krehbiel[1], G.G. Hilton[1], D.L. VanOverbeke[1], P.J. Ayoubi [2], and U.E. DeSilva[1]

[1]OSU Dept. of Animal Science and [2]OSU Dept. of Biochemistry & Mol. Biology

Abstract

Microarray analysis, validated by RT-PCR, was utilized to investigate the effects of the β–adrenergic agonist, zilpaterol hydrochloride, on gene expression in i.m., s.c., and visceral adipose tissue depots and muscle tissue in beef steers. The β-adrenergic agonist was fed for 20 d at the end of the feeding period with a 3-d withdrawal period. Ninety-six crossbred beef steers were blocked by weight and randomly allocated into 16 pens (6 steers/pen). Pens were assigned to treatments in a randomized complete block design. Main effects were the addition of 0 (CON) or 8.3 mg/kg zilpaterol hydrochloride (ZH; DM basis) to the finishing diet for 20 d before estimated average harvest date plus a 3-d withdrawal period prior to harvest. Individual BW was measured initially, 1 d prior to ZH feeding, and 1 d prior to harvest. At slaughter a 7.6 cm^3 section was dissected from the *Longissimus* muscle between the 12^{th} and 13^{th} rib, from which muscle tissue and s.c. and i.m. adipose tissue was collected. Visceral adipose tissue was collected at the region of the pyloric sphincter.

Total RNA was extracted and microarray hybridizations performed. The array contained a total of 24,000 oligonucleotide probes, 70 bases in length. Annotation for the genes on the array can be downloaded from Bovine Oligo Microarray Consortium (BOMC) at www.bovineoligo.org. Preprocessing and normalization of data was accomplished utilizing GenePix AutoProcessor (GPAP 3.2). Ontology analysis was carried out using GFINDer. Carcass data were collected at harvest.

Average daily gain (ADG) was shown not to increase during the 20-d ZH supplementation plus 3-d withdrawal period or over the entire feeding period. Dry matter intake (DMI) and gain:feed (G:F) was not affected by ZH supplementation over the entire feeding period. For the ZH supplementation plus 3 d withdrawal period, there was a tendency ($P = 0.09$) for DMI to be decreased by ZH supplementation. Carcass adjusted G:F was greater ($P = 0.009$) and G:F had a tendency ($P = 0.08$) to be greater in ZH-supplemented steers. Carcass merit at the end of the 3-d withdrawal showed hot carcass weight (HCW), dressing percentage and *Longissimus* muscle (LM) area to be greater in ZH-supplemented steers. No other significant differences in carcass characteristics were observed. No array elements were found to be differentially expressed (DE) between the CON steers and ZH-supplemented steers in the i.m., s.c., and visceral adipose tissue depots or muscle tissue when the following criteria for significant differential expression were used; array elements where greater than 50% of the total features across arrays were used to calculate the average $\log_2$ ratio; a 't' > 2 (regardless of sign); an M-value > +0.9 or < -0.9 (representing a fold change of > 1.87 or < -1.87); and an adjusted P-value < 0.01. Of the eight genes selected for validation by RT-PCR in respective tissues and the six selected as genes of interest in respective tissues, CYC1 and βAR_2 in i.m. adipose

tissue and βAR_1 in s.c. adipose tissue were shown not to support the results of the microarray analysis. RT-PCR revealed CYC1, βAR_1 and βAR_2 mRNA expression to be up-regulated three fold, four fold and four fold, respectively, in steers supplemented with ZH.

Key words: beef cattle, beta-adrenergic agonists; carcass merit, microarray, performance, zilpaterol hydrochloride

Introduction

The pursuit to optimize the response of β-adrenergic agonists (β-AA) and to define their effects on feed efficiency and carcass composition in the various livestock species has been an ongoing and a well documented undertaking since the early 1980's. β-adrenergic agonists can be defined as "organic molecules" which bind the β-adrenergic receptor (β-AR) such that the agonist-receptor complex activates the stimulatory G-protein (G_s protein) (Mersmann, 1998), a member of the superfamily of regulatory GTP-ases that are collectively known as G-proteins (Voet and Voet, 2004d). Cattle and sheep seem to have a greater response to β-AA compared to swine, while poultry appear to be the least responsive (Moody et al., 2000). However, feeding β-AA to cattle, pigs, poultry, and sheep has resulted in an increase in muscle mass and a decrease in fat mass (Mersmann, 2001; Sillence, 2004), as β-adrenergic agonists seem to act by increasing the efficiency of growth by preferentially stimulating skeletal muscle growth as compared to adipose tissue. In general, this repartitioning affect is thought to be brought about by an increase in protein synthesis, a decrease in muscle protein degradation or a combination of both or by the release of free fatty acids from adipose tissue, which then could be used

as a source of energy for protein synthesis (muscle mass) (Ricks et al., 1984, Mersmann, 2001; Sillence, 2004, Baxa, 2008; Chung and Johnson, 2008).

The β-AA is effective only for a limited period of time as the efficacy of adrenergic agonists can be altered by desensitization caused by the continuous exposure of the β- adrenergic receptor to the β-AA (Hausdorff et al., 1990b; Lynch and Ryall, 2008). There are three mechanisms of desensitization. The first, the functional uncoupling of the β-AR from G_s, involves the phosphorylation of the β-AR which occurs very rapidly (usually within seconds or minutes) when agonist exposure occurs and decreases the β-AR affinity for the agonist, and is considered a completely reversible process (Mills, 2002b; Badino et al., 2005). The second mechanism is physical sequestration of the receptor away from the cell surface by targeting the receptor for internalization where the receptor can be either targeted for degradation or recycled back to the plasma membrane (Gurevich and Gurevich, 2006; Moore et al., 2007). β-AR sequestration is a reversible process which is not a significant mechanism underlying rapid desensitization (Hausdorff et al., 1990a; Yu et al., 1993). The third is down-regulation of the total number of receptors (Yu et al., 1993; Mills, 2002b; Badino et al., 2005). Down-regulation develops more slowly, taking hours or days to occur, with the decline in binding sites related to potency and efficacy of the agonist. Down-regulation of the β-AR is not rapidly overcome and is slower to overcome than the event of uncoupling (Mills, 2002b). However, following down-regulation, transcription and translational processes are required to restore membrane receptor numbers (Johnson, 2006b). Though an abundance of information regarding β-AR desensitization and down-

regulation exists in the literature, the body of information about the regulation of β-AR synthesis is somewhat lacking (Lynch and Ryall, 2008).

Different species of animals seem to have different responses to β-AA (Mersmann, 1995, 1998) as a particular β-AA may not activate the target β-AR or the target tissue as well in one species as another. This may involve differences in the number of receptors in the tissue, the agonist affinity towards the receptor, the coupling of the agonist-receptor complex to the signal transduction system, the differences in delivery of the agonist to the receptor site, the differences in agonist or receptor deactivation, or the β-AR subtype may change with the phase of differentiation or the hormone environment of the cell (Mersmann, 1998). β_2-AR is the primary receptor (75%) found in bovine adipose tissue as compared to β_1-AR (25%) (Van Liefde et al., 1994). β_2-AR was also reported as the primary receptor in perirenal adipose tissue and the *Longissimus* muscle (Sillence and Matthews, 1994). Messenger RNA of all three β-AR subtypes has been shown to be expressed in bovine adipose tissue; however, β_3-AR mRNA expression was very small or undetectable in animals after three months of age (Casteilla et al., 1994; Van Liefde et al., 1994). The β_2-AA zilpaterol hydrochloride (ZH) has a greater affinity for the β_2-AR subtype receptor compared to the β_1-AR subtype but is capable of binding both the β_1-AR subtype (Ki = 1.0 x 10-5) and β_2-AR subtype (Ki = 1.1 x 10-6) receptor (Verhoeckx et al., 2005).

Baxa (2008) hypothesized ZH supplementation could possibly alter the expression of myosin isoforms. Myosin, the most abundant protein present in striated muscle cells, is one of the major proteins involved in protein synthesis, constituting approximately 25% of the total protein pool (Baldwin and Haddad, 2001). The four

major myosin heavy chain (MHC) isoforms found in adult mammalian skeletal muscles are MHC type I; slow fiber type and MHC type II, and fast fiber type, IIA (MYH2), IIX/D (MYH1), and IIB (MHY4) (Schiaffino and Reggiani, 1994; Pette and Staron, 2000)

Zilmax® (Intervet/Schering-Plough Animal Health, Millsboro, DE) is a synthetic β_2-AA used for increased rate of weight gain, improved feed efficiency, and increased carcass leanness in cattle fed in confinement for slaughter (Dikeman, 2007; Kern et al., 2009) and contains the active ingredient zilpaterol hydrochloride. In 2006, ZH was approved by the U.S. Food and Drug Administration (FDA) as a feed ingredient for cattle during the last phase of the feeding period to improve production efficiency but it has been used since the 1990's in Mexico and South Africa (Avendano-Reyes et al., 2006). Zilmax is administered through the feed the last 20 to 40 days of the feeding period at levels of 60 to 90 mg/animal/d and is required to be withdrawn 3 d prior to harvest. In 2008, the FDA approved ZH for use in cattle feeds in five different combinations with MGA® (melengestrol acetate), Rumensin® (monensin, USP), and Tylan® (tylosin phosphate). Zilpaterol residue levels in cattle have been below the threshold that poses any human health risk (Moody et al., 2000; Anderson et al., 2004), which are 0.02, 0.05, 0.10, and 0.10 ppm for muscle, liver, kidney, and fat, respectively (Intervet, Inc. 2006).

Currently, no data in the literature addresses the global pattern of gene expression in i.m., s.c., visceral, adipose tissue depots and muscle tissue in ZH-supplemented cattle, which may give insight into the mechanism(s) of action of βAA. The purpose of the present study was to investigate, using microarray analysis validated by RT-PCR, the effects of the β–AA, ZH, on gene expression in i.m., s.c., and visceral adipose tissue

depots and muscle tissue in beef steers fed for 20 days at the end of the feeding period with a 3-d withdrawal.

Methods and Materials

Animals and Treatment Groups

Ninety-six crossbred beef steers were blocked by weight and randomly allocated into 16 pens (6 steers/pen). Pens were assigned to treatments in a randomized complete block design. Steers were implanted with Zeranol (Ralgro, Schering-Plough Animal Health, Kenilworth, NJ) and adapted to an 88% concentrate diet over a 21-d period, at which time they were program-fed to gain 1.13 kg/d (NRC, 2000) for a period of 78 d. Following the preconditioning/growing period, steers were weighed and reimplanted with Revalor S (120 mg of trenbolone acetate and 24 mg of estradiol; Intervet) and assigned to treatment pens. Steers were then fed for either 95 or 123 d before ZH supplementation. Main effects were the addition of 0 (CON) or 8.3 mg/kg zilpaterol hydrochloride (ZH; DM basis) supplemented for 20 d at the end of the feeding period plus a 3-d withdrawal period prior to harvest. Steers were initially fed 2% (as-fed) of initial BW a 75% concentrate ration and "stepped up" to a final total mixed ration over 16 d, feeding the 75% concentrate ration and an 85% concentrate ration for seven days each. The final finishing ration contained 94% concentrate. The final finishing diet, CON, (Table 5.2) was formulated to meet or exceed NRC (1996) requirements and contained monensin and tylosin at 33.06 mg/kg and 9.92 mg/kg, respectively, on a 90% DM basis. The final diet fed to the ZH pens was identical to the CON, with the exclusion of monensin and tylosin and the addition of zilpaterol HCl. The animal whose final BW was closest to the pen

average from each pen assigned to the CON and ZH treatments, was selected for intensive sampling at slaughter. These animals were loaded in the evening and hauled less than 5 km to the Robert M. Kerr Food & Agricultural Products Center abattoir (FAPC), located on the campus of Oklahoma State University, Stillwater, OK for harvest.

Sample Collection and RNA Extraction

At slaughter, steers were stunned with captive bolt and exsanguinated. Following exsanguination, a 7.6 cm^3 section was dissected from the *Longissimus* muscle between the 12^{th} and 13^{th} rib, from which muscle tissue and s.c. and i.m. adipose tissue was collected. Visceral adipose tissue was collected at the region of the pyloric sphincter. The i.m. adipose tissue was placed in 50 ml conical vials containing RNA*later*® (Applied Biosystems/Ambion, Austin, TX) until further separation using an Olympus SZ30 stereomicroscope (9x - 40x zoom range). All other tissues were frozen at -80º C. Total RNA was extracted using TRIzol reagent (Invitrogen, Carlsbad, CA). The tissue, in TRIzol, was homogenized and centrifuged at 3,500 x g at 4º C for 15 min to separate insoluble material and excess fat. The lower aqueous (TRIzol) phase was transferred to a fresh tube and 0.2 ml chloroform/ml of TRIzol was added. Samples were centrifuged at 3,500 x g at 4º C for 30 min and the upper aqueous phase was transferred to a fresh tube. Isopropyl alcohol (0.5 ml/ml of TRIzol) was added and samples were maintained at -20º C overnight followed by centrifugation at 3,500 x g at 4º C for 10 min. The supernatant was removed and the RNA pellet washed with 75% chilled ethanol and suspended in DNase/RNase free water. A subsequent phenol:chloroform:isoamyl alcohol (25:24:1; pH 5.2) extraction of the RNA (1:1 ratio, respectively) was carried out. The

RNA/phenol:chloroform:isoamyl alcohol mixture was centrifuged at 10,600 x g at 4º C for 5 min and the upper aqueous phase was transferred to a fresh tube and precipitated with 0.01 volumes of sodium acetate (3M; pH 5.2) and 2.5 volumes of chilled 98% ethanol. The samples were then maintained at -20º C overnight and centrifuged at 10,600 x g at 4º C for 30 min. The supernatant was removed and the RNA pellet was washed with 70% chilled ethanol and suspended in DNase/RNase free water and stored at -80º C. The integrity of the RNA was analyzed utilizing gel electrophoresis (1.5%) and the RNA was quantified using a NanoDrop® ND-100 Spectrophotometer (NanaDrop Technologies, Willington, DE).

Microarray Experiment

A bovine oligo array designed by the Bovine Oligonucleotide Microarray Consortium was used in this study (Elsik et al. 2006) containing a total of 24,000 oligonucleotide probes**,** 70 bases in length, which were printed in singlet on the slide. The array included 16,846 probes designed from ESTs that were aligned to homologous vertebrate proteins and to the 6X bovine genome assembly (BGA). The probe set was supplemented with oligos designed from 703 predicted RefSeq genes, 5,943 reproductive tissue ESTs with a BGA but no protein alignment, and 504 positive and negative controls. The following criteria were used in EST selection and probe design: 1) predicted constitutive exon, 2) polymorphism avoidance, 3) minimal distance to 3' end of protein coding region, and 4) optimal Tm and specificity. Probe sequences and annotations are available at http://www.bovineoligo.org.

Global amplification (Nygaard and Hovig, 2006) of mRNA in this experiment was accomplished using the TargetAmp™ 1-Round Aminoallyl-aRNA Amplification Kit 101 (Epicentre® Biotechnologies, Madison, WI). The poly(A) RNA component of total RNA (500 ng) from each the reference sample (CON) and test sample (ZH) was reversed transcribed into first strand cDNA in separate tubes using oligo-dT primers and reverse transcriptase (Superscript III RT, Invitrogen, Carlsbad, CA). The reaction was carried out at 50º C for 30 min. The RNA fragments, produced from the cDNA:RNA hybrid using RNase H, were used to prime the second strand cDNA synthesis reaction carried out at 65º C for 10 min. Aminoallyl anti-sense RNA (AA-aRNA) was then produced during the subsequent *in vitro* transcription reaction at 42º C for 4 h where 5-(3-aminoallyl)-UTP was partially substituted for the UTP nucleotide. The AA-aRNA was then purified using the Qiagen RNeasy Mini Kit (Qiagen Inc., Valencia, CA) and eluted with 20 ul of DNase/RNase free water. The reference and test AA-aRNA (12.5 ul) was then coupled with a 15 ul aliquot of Invitrogen's succinimidyl ester Alexa Fluor 546 and 647 dyes (Molecular Probes Inc., Eugene, OR), respectively, in separate tubes along with 3 ul of 1M sodium bicarbonate buffer, pH 9.0. One vial of Alexa Fluor dye was resuspended in 150 ul of dimethylsulfoxide (DMSO) and divided into aliquots of 15 ul and stored at -80º C. This coupling reaction was allowed to continue for 1 h in the dark at room temperature. To quench the coupling reaction, 3 μl of 100 mM Tris-HCl, pH 8.0 was added to the mixture. The dye-labeled AA-aRNA was then purified using the Qiagen RNeasy Mini Kit (Qiagen Inc., Valencia, CA) and eluted with 25 ul of DNase/RNase free water. The concentration of the AA-aRNA was determined using a NanoDrop® ND-100 Spectrophotometer (NanaDrop Technologies, Willington, DE).

Fold amplification of the reaction was calculated using the assumption that the Poly (A) RNA constitutes approximately 1% of the RNA in the total RNA. For each sample, the total picomoles of Alexa Fluor 546 and 647 dye incorporation (pmol/μg) was also calculated. For hybridizing the Alexa Fluor dye-labeled AA-aRNA to the array, the hybridization solution (80 ul) consisting of: 20.0 μl of dye-labeled AA-aRNA of each the Alexa Fluor™ 546 and Alexa Fluor™ 647; 40.0 μl of 2X formamide-based hybridization buffer was denatured at 65º C for 10 min and deposited to a pre-hybridized array slide under a 24 x 60 mm lifterslip (Erie Scientific, Portsmouth, NH). The array was then incubated at 42º C for 18 h in a humidified hybridization cassette. Following incubation the lifterslip was allowed to wash off in a 2X Sodium Chloride/Sodium Citrate (SSC) /0.2% sodium dodecyl sulfate (SDS) solution prewarmed to 42º C. The array slides were then washed in 2X SSC/0.2% SDS, 42º C,15 min; 2X SSC, RT,15 min; and 0.2X SSC, RT, 15 min. Following the final wash, the array slide was immediately dried for 2 min using a slide centrifuge and stored in a light-proof container until image acquisition.

Microarray Data Analysis

To compare zilpaterol hydrochloride supplemented animals (Alexa 647) relative to control animals (Alexa 546) in respective adipose and muscle tissues, hybridization signals were captured by scanning the microarray slides with lasers at two wavelengths, Alexa 546 and Alexa 647, using a ScanArray™ Express confocal laser scanner (PerkinsElmer Life Sciences Inc., Boston, MA) at a pixel size resolution of 10 microns with the resulting images saved as 16 bit TIFF images. For each slide, the laser power and photomultiplier tube (PMT) gain were adjusted to minimize variation between

channels. Using a local background subtraction method (spots with foreground intensity minus background intensity), the commercial software package GenePix™ Pro 4.0 (Axon Instruments Inc., Union City, CA) was used to analyze the signal intensity values of each feature (spot) in the Alexa Fluor™ 546 and Alexa Fluor™ 647 channels. The GenePix Pro Result (GPR) files generated from the results of the image analysis from each biological and technical replication were used for further downstream analysis and ratio calculations. Preprocessing and normalization of data was accomplished utilizing the R-project statistical environment (http://www.r-project.org) with the Bioconductor and LIMMA packages (http://www.bioconductor.org) through the GenePix AutoProcessor (GPAP 3.2) website (http://darwin.biochem.okstate.edu/gpap32/) (Weng and Ayoubi, 2004). Background correction was performed using Robust Multi-array Average (RMA) algorithm (Allison et al., 2006) available in the Bioconductor/LIMMA package. Following background correction, poor quality features were removed by filtering. Such poor quality features were defined as features displaying an intensity value of 200 relative fluorescence units (RFU) or less in both the Alexa Fluor™ 546 and Alexa Fluor™ 647 channels, as well as features flagged bad, not found, or absent by GenePix™ Pro 4.0 and were removed from the analysis. Two different normalization methods were utilized in the analysis to adjust and balance for the technical or systemic variation between the features within an array and between arrays for differences not caused by treatment. Lowess (locally weighted Least squares regression) - global intensity normalization, was used to balance the variation associated with dye bias within each array (Yang et al., 2001; 2002). To balance the effect of the Alexa Fluor™ 546 and Alexa Fluor™ 647 dye bias intensity between arrays, quantile normalization was utilized

(Bolstad et al., 2003). Following data preprocessing, the expression ratio for each feature (gene) was calculated using the following formula where a two-fold change is represented by a $\log_2$ ratio >1.0 (up-regulation) or < -1.0 (down-regulation) with M value ($\log_2$ expression ratio) = $\log_2$ (F647-B647$_{intensity}$ /F546-B546$_{intensity}$). Using GPAP 3.2, a moderated T-test was used to identify the differentially expressed array elements along with their M value ($\log_2$ ratio), their P-value obtained from the moderated t-statistic after false discovery rate (FDR) adjustment using the Benjamini and Hochberg method (Benjamini and Hochberg, 1995), and the number of individual features ($\log_2$ ratio) used for each gene. Array elements where > 50% of the total features across arrays was used to calculate the average $\log_2$ ratio, a $|t| > 2$, an M-value $|M| > +0.9$ (representing a fold change of 1.87), and an adjusted P-value < 0.01 were considered significantly differentially expressed and included for further analysis using the Genome Functional Integrated Discoverer (GFINDer) (http://www.medinfopoli.polimi.it/GFINDer/) and Entrez Gene (http://www.ncbi.nlm.nih.gov/sites/entrez?db=gene).

Gene Ontology Analysis

The web based program GFINDer (Masseroli et al., 2004) was used in this study and is a program designed to retrieve annotations for a list of submitted genes, perform categorization, and present the results for use in gene ontology and pathway analysis. Entrez Gene is the National Center for Biotechnology Information (NCBI) database for gene-specific information (Maglott et al., 2005, 2007). The Entrez gene ID of the differentially expressed genes retrieved from NCBI was used for the ontology analysis. The annotation terms were generated with emphasis based on gene ontology assessment

for molecular function and biological process rather than cellular component (Ashburner et al., 2000).

Quantitative RT-PCR Validation of Microarray

Validation of the expression values comparing ZH-supplemented animals (Alexa 647) relative to control animals (Alexa 546) in i.m., s.c., and visceral adipose tissue depots and muscle tissue generated from the microarray experiment was carried out using two-step SYBR green qRT-PCR. Gene specific primers for candidate genes selected for microarray data validation were designed using Primer 3 (Rozen and Skaletsky, 2000) and analyzed using Oligo Analyzer 3.1 (Integrated DNA Technologies), http://www.idtdna.com/analyzer/Applications/OligoAnalyzer/. All primer sequences, annealing temperatures and product size are presented in Table 5.1.

Total RNA (1 ug) from the i.m., s.c., visceral adipose tissues and muscle tissue from each individual animal from CON and ZH supplementation was reverse transcribed using the QuantiTect® Reverse Transcription Kit (QIAGEN Inc., Valencia, CA) using oligo-dT and random primers in a total volume of 20 ul. RT- PCR reactions were carried out, in duplicate, utilizing a MyiQ Real-Time PCR detection system (Bio-Rad Laboratories, Hercules, CA) in a 15 ul reaction consisting of: 7.5 ul of 2X PerfeCTa™ SYBR Green SuperMix for iQ™ (Quanta BioSciences, Inc**.** Gaithersburg, MD), 400 nM forward primer, 400 nM reverse primer and 100 ng of cDNA. 18S ribosomal RNA was assayed as a normalization control for all samples assayed. A standard curve with five serial dilution points was included for each gene along with a no-template control. Thermal cycling conditions were 95º C for 2.5 min followed by 35 repetitive cycles of

95º C for 15 s, variable annealing temperature for 30 s, and 72º C for 30 s. Immediately following RT-PCR, a melt curve analysis was conducted by bringing the reaction to 95º C for 1 min, 55º C for 1 min, then increasing the temperature by 0.5º C from 55º C to 94.5º C. Gene expression between depots for the diet and phase selected for validation was evaluated using the comparative C_T method. A cycle threshold (C_T) value was assigned to each reaction at the beginning of the logarithmic phase of the PCR amplification. A ΔC_T value was calculated for each sample by subtracting the mean 18S ΔC_T value of each sample from the corresponding gene of interest mean ΔC_T value (Livak and Schmittgen, 2001). The $\Delta\Delta C_T$ was calculated by setting the highest mean ΔC_T value as an arbitrary constant to subtract from all other mean ΔC_T depot values (Hettinger et al., 2001). Relative expression levels between the control and ZH treatment were calculated as fold changes, where each cycle of the PCR represented a two-fold change. The assay specific efficiency for each gene was not used in the calculation of the relative expression levels. Fold change (FC) gene expression was calculated using the formula: $FC = 2^{-\Delta\Delta CT}$.

Quantitative RT-PCR Analysis for Selected Genes

The adrenergic beta-1-receptor (βAR_1), adrenergic beta-2-receptor (βAR_2), and adrenergic beta-3-receptor (βAR_3) genes in the i.m., s.c., and visceral adipose tissue depots and MHC type II; fast fiber type IIA (MYH2) and IIX/D (MYH1) and calpastatin (CAST) genes in muscle tissue were measured for mRNA expression between CON and ZH supplementation using quantitative RT-PCR and analyzed using the comparative C_T method. The $\Delta\Delta C_T$ was calculated by setting the highest mean ΔC_T value as an arbitrary

constant to subtract from all other mean ΔC_T depot values (Hettinger et al., 2001). Relative expression levels between the CON and ZH supplementation were calculated as fold changes, where each cycle of the PCR represented a two-fold change. Fold change (FC) gene expression was calculated using the formula: $FC = 2^{-\Delta\Delta CT}$. The ΔC_T values were analyzed by analysis of variance (ANOVA) and means were compared using the Least squares means (LSMEANS) of PROC MIXED of SAS 9.1.3 (SAS Institute Inc, Cary, North Carolina).

Statistical Analysis for Performance and Growth

Data were analyzed as a completely randomized block design, with pen considered the experimental unit. There were two weight blocks with 4 pens/treatment in each weight block. Least squares means were calculated using the MIXED procedure of SAS. The dietary inclusion of ZH was the fixed effect and weight block was included as a random effect.

Results

Performance and Carcass Merits

Average daily gain (ADG) was not increased by ZH supplementation plus 3 d withdrawal period or over the entire feeding period (Table 5.3). However, carcass adjusted ADG was greater for ZH-supplemented steers than for CON steers ($P < 0.02$) from the time of ZH supplementation to end of withdrawal, with gains of 1.89 and 1.42 kg/d, respectively. In addition, there was a tendency ($P < 0.06$) for ZH supplementation to increase carcass adjusted ADG over the entire feeding period with gains of 1.71 and 1.60

kg/d, respectively, for ZH supplementation and CON. From the time of ZH supplementation to end of withdrawal, there was a tendency ($P < 0.09$) for DMI to be decreased in ZH-supplemented steers (9.42 kg/d) compared with CON steers (9.93 kg/d) while carcass adjusted G:F was greater ($P < 0.009$) in ZH-supplemented steers (0.202 kg/hd) than CON steers (0.143 kg/hd) (Fig. 5.3). The unadjusted G:F had a tendency ($P < 0.08$) to be greater in ZH-supplemented steers (0.187 kg/kg) compared with CON steers (0.143 kg/kg). DMI and G:F were not affected by ZH supplementation over the entire feeding period in the present study; however, carcass adjusted G:F was greater in ZH-supplemented steers (0.179 kg/kg) compared with CON steers (0.166 kg/kg) (Table 5.3).

Carcass merit at the end of the three day withdrawal showed hot carcass weight (HCW) to be greater ($P < 0.005$) in ZH-supplemented steers than CON steers, 374 kg/d vs. 360 kg/d, respectively. Dressing percentage was greater ($P < 0.05$) for ZH-supplemented steers than CON steers, 64.46% and 63.57%, respectively. *Longissimus* muscle area was greater ($P < 0.02$) in ZH-supplemented steers than CON steers, 93.95 cm vs. 89.68 cm, respectively. No other significant differences in carcass characteristics were observed (Table 5.4).

Microarray and Ontology Analysis

No array elements were shown to be differentially expressed (DE) between the CON steers and ZH-supplemented steers in the i.m., s.c., and visceral adipose tissue depots or muscle tissue when the criteria for significant differential expression were used.

Quantitative RT-PCR Validation of Microarray

Even though no array elements were shown to be significantly differentially expressed between the CON steers and ZH-supplemented steers in the i.m., s.c., and visceral adipose tissue depots or muscle tissue using our stringent criteria; two genes, one up-regulated and one down-regulated, from each the i.m., s.c., and visceral adipose tissues and muscle tissue were selected for microarray validation when the level of significance was placed at P-value < 0.05. In i.m. adipose tissue, the microarray analysis did not find cytochrome C-1 (CYC1) or tumor necrosis factor receptor superfamily, member 1B (TNFRSF1B) to be differentially expressed between the CON and ZH-supplemented steers (data not shown). However, RT-PCR analysis of i.m. adipose tissue revealed CYC1 mRNA expression (Figure 5.1a) to be up-regulated threefold in ZH-supplemented steers compared with CON steers. TNFRSF1B was shown not to be significantly affected by ZH supplementation (Figure 5.1b). In s.c. adipose tissue, heat shock 70kDa protein 4 (HSPA4) and SAPS domain family, member 1 (SAPS1) were not shown to be differentially expressed in the microarray analysis (data not shown). RT-PCR analysis revealed HSPA4 mRNA expression with a tendency (P < 0.09) (Figure 5.1c) to be up-regulated in the ZH-supplemented steers compared with CON steers. SAPS1 was shown not to be significantly affected by ZH supplementation (Figure 5.1d). Angiotensin II receptor, type 1 (AGTR1) and SH3 domain binding glutamic acid-rich protein like 3 (SH3BGRL3) in the visceral adipose tissue and S-adenosylhomocysteine hydrolase (AHCY) and deoxyguanosine kinase (DGUOK) in muscle tissue were not differentially expressed in the microarray analysis (data not shown). RT-PCR analysis

confirmed mRNA expression for AGTR1, SH3BGRL3, AHCY, and DGUOK not to be significantly influenced by ZH supplementation (Figures 5.1e-h).

Quantitative RT-PCR Analysis for Selected Genes of Interest

The microarray analysis did not reveal adrenergic β-1-receptor (βAR_1), adrenergic β-2-receptor (βAR_2), and adrenergic β-3-receptor (βAR_3) genes in the i.m., s.c., and visceral adipose tissue depots and muscle tissue or the MHC type II; fast fiber type IIA (MYH2) and IIX/D (MYH1) and calpastatin (CAST) genes in muscle tissue to be differentially expressed between the CON steers and ZH-supplemented steers (data not shown). RT-PCR analysis indicated that βAR_1 mRNA expression was not influenced by ZH supplementation in the i.m. (Figure 5.1i) or visceral (Figure 5.1k) adipose tissue. However, in the s.c. adipose tissue, RT-PCR revealed βAR_1 mRNA expression to be up-regulated fourfold ($P < 0.01$; Figure 5.1j) in ZH-supplemented steers vs. CON steers. βAR_1 mRNA expression in muscle tissue was detected in only two of the six animals of each the CON and ZH-supplemented treatment groups and no further statistical analysis was performed.

RT-PCR revealed βAR_2 mRNA expression to be significantly affected by treatment in the i.m. adipose tissue ($P < 0.006$; Figure 5.1l) with nearly a fourfold greater expression level in ZH-supplemented steers than CON steers. βAR_2 mRNA expression was not significantly influenced by ZH supplementation in the s.c. (Figure 5.1m) and visceral (Figure 5.1n) adipose tissue depots or the muscle tissue (Figure 5.1o).

RT-PCR revealed that βAR_3 was not significantly influenced by ZH supplementation in i.m. (Figure 5.1p) or visceral (Figure 5.1q) adipose tissue. Under the

RT-PCR parameters utilized in the experiment, βAR_3 mRNA expression was detected in s.c. adipose tissue and muscle tissue in all ZH-supplemented-steers but in only two steers in the CON group and no further statistical analysis was performed. RT-PCR revealed that MHC type II; fast fiber type IIA (MYH2) and IIX/D (MYH1) and calpastatin (CAST) mRNA expression were not significantly influenced by ZH supplementation in muscle tissue (Figures 5.1r, 5.1s, and 5.1t, respectively).

Discussion

Effect of Zilpaterol Hydrochloride on Carcass Characteristics

In the present study, ZH supplementation did not increase ADG during the 20 d ZH supplementation plus 3-d withdrawal period or over the entire feeding period. These findings are not in agreement with previous studies as ADG was increased 0.19 kg/d in steers supplemented with ZH for 30 d plus 5-d withdrawal (Montgomery et al., 2009b). Furthermore, Avendano-Reyes et al. (2006) reported an increase in ADG of 0.56 kg/d during ZH supplementation for 33 d plus 3 d withdrawal period, and an increase of 0.52 kg/d was observed by Plascencia et al. (1999) for steers supplemented with ZH for 42 d plus 2-d withdrawal with an increase of 0.16 kg/d reported for the average of ZH-supplemented for 20, 30, or 40 d with a 3-d withdrawal (Vasconcelos et al., 2008). Montgomery et al. (2009a) reported increases of 0.40 kg/d in steers and 0.215 kg/d in heifers for the average of ZH-supplemented for 20 and 40 d with a 5-d withdrawal. More so, Baxa (2008) reported an increase in ADG of 0.11 kg/d over the entire 91 d feeding period which included the ZH supplementation of 30 d plus 3-d withdrawal period. In the present study, when calculated using carcass adjusted final BW, ZH supplementation

significantly increased ADG by 0.47 kg/d during the ZH supplementation and 3 d withdrawal period and tended to increase ADG by 0.11 kg/d over the entire feeding period.

ZH supplementation has been shown to affect DMI and G:F in different ways. During the ZH supplementation plus 3-d withdrawal period in the present study, G:F had a tendency to be greater (29%) and the carcass adjusted G:F was 41% greater in ZH-supplemented steers compared with the CON steers with a tendency for DMI to be decreased by 6% by ZH supplementation. Plascencia et al. (1999) and Avendano-Reyes et al. (2006) reported a 28% and 11% greater G:F, respectively, in ZH-supplemented steers with no differences in DMI observed. Similarly, Baxa (2008) reported a 6.8% greater G:F in ZH-supplemented steers with no difference in DMI over a 91 d feeding period which included the ZH supplementation and 3-d withdrawal. Montgomery et al. (2009b) reported a 15% greater G:F and a 3.5% decrease in DMI in ZH-supplemented steers. Montgomery et al. (2009a) reported a 28% greater G:F in steers with a tendency for DMI to be decreased (2.3%) in the average of ZH-supplemented for 20 and 40 d with a 5-d withdrawal; while in heifers, a 21.2% greater G:F for ZH supplementation was reported with a 6% decrease in DMI. Furthermore, Vasconcelos et al. (2008) reported a 15% greater G:F for the average of ZH-supplemented for 20, 30, or 40 d and a linear increase in G:F was observed from d 20 to d 40 of ZH supplementation; also, a linear decrease in DMI was observed from d 20 to d 40 of ZH supplementation.

In the present study, ZH supplementation for 20 d with a 3-d withdrawal period increased HCW 14 kg, *Longissimus* muscle area by 4.27 cm and dressing percentage by 0.89 percentage units. Previous studies have reported similar increases in HCW, dressing

percentage and *Longissimus* muscle area in carcasses from cattle supplemented with ZH compared to non-supplemented controls. Montgomery et al. (2009b) and Plascencia et al. (1999) reported increases in HCW of 13 kg, respectively, in steers supplemented with ZH with Montgomery et al. (2009b) reporting increases in *Longissimus* muscle area of 7.95 cm and dressing percentage of 1.2 percentage units and Plascencia et al. (1999) reporting an increase in dressing percentage of 2.2 percentage units with a tendency for *Longissimus* muscle area to be increased by 2.2 cm. More so, Avendano-Reyes et al. (2006) reported increases in HCW of 21.9 kg, *Longissimus* muscle of 8.48 cm, and dressing percentage of 2.01 percentage units in ZH-supplemented steers. Vasconcelos et al. (2008) reported an average increase of 17.2 kg in HCW, 9.56 cm in *Longissimus* muscle area, and 1.9 percentage units in dressing percentage when ZH was fed for 20, 30, or 40 d. Montgomery et al. (2009a) reported an average increase in HCW of 16.45 kg in steers supplemented for 20 or 40 d, with the length of ZH supplementation affecting *Longissimus* muscle area and dressing percentage as increases in *Longissimus* muscle area of 7.9 and 8.6 cm and dressing percentage of 1.13 and 1.8 percentage units were observed for ZH-supplemented steers for 20 and 40 d, respectively. In heifers, the length of ZH supplementation affected HCW, *Longissimus* muscle area, and dressing percentage as HCW was increased 11 and 13 kg, *Longissimus* muscle area was increased 5.8 and 6.9 cm, and dressing percentage increased 1.5 and 1.6 was percentage units for ZH-supplemented for 20 and 40 d, respectively. Baxa (2008) reported increases in HCW of 21 kg, *Longissimus* muscle area of 11.9 cm, and dressing percentage of 2.37 percentage units over a 91-d feeding period, which included a 30-d ZH supplementation and 3 d withdrawal period.

ZH supplementation has also been shown to affect %KPH, marbling score, and 12th rib fat in different ways. In the present study, no differences in %KPH, marbling score or 12th rib fat were observed. Similar findings were reported by Plascencia et al. (1999) and Avendano-Reyes et al. (2006) who observed no differences in %KPH and marbling score. However, Plascencia et al. (1999) reported no differences in 12th rib fat while Avendano-Reyes et al. (2006) reported a 0.29 cm decrease in 12th rib fat. ZH supplementation decreased marbling score 46.5 degrees for the average of ZH-supplemented for 20 and 40 d in steers, with a tendency for marbling score to be decreased in heifers (Montgomery et al., 2009a). No differences were observed in %KPH and 12th rib fat in steers or heifers. Montgomery et al. (2009b) reported that feeding ZH decreased %KPH by 0.07%, marbling score by 24 degrees, and 12th rib fat by 0.095 cm. Vasconcelos et al. (2008) reported a decrease in %KPH of 0.10% for the average of ZH supplementation for 20, 30, and 40 d, and a linear decrease in %KPH observed from d 20 to d 40 of ZH supplementation. Also, a reduction in marbling score of 44 degrees was observed along with 12th rib fat reduced by 0.22 cm for the average of ZH supplementation for 20, 30, and 40 d. A linear decrease in 12th rib fat was also observed from d 20 to d 40 of ZH supplementation. Baxa (2008) reported decreases in %KPH of 0.16%, decreases in marbling score of 29.75 degrees, and decreases in 12th rib fat of 0.14 cm over a 91 d feeding period which included the ZH supplementation and 3-d withdrawal period.

β-AA seem to act by increasing the efficiency of growth by preferentially stimulating skeletal muscle growth as compared to adipose tissue. This repartitioning affect is thought to be brought about by an increase in protein synthesis, a decrease in

muscle protein degradation or a combination of both or also by the release of free fatty acids from adipose tissue, which then could be used as a source of energy for amino acids (muscle mass) (Baxa, 2008; Chung and Johnson, 2008). The greater G:F observed in the ZH-supplemented animals could possibly, to a degree, be due to the decreased DMI with similar or increased ADG. In studies where no changes in DMI were observed and no changes in %KPH, marbling or 12th rib fat were observed, it is possible, ZH supplementation increased carcass protein accretion and improved performance by improving the efficiency by which nutrients are converted to gain. In studies where no changes in DMI were observed and decreases in %KPH, marbling or 12th rib fat were observed, a decrease in fat synthesis and/or an increase in fat degradation with a repartitioning of nutrients could have resulted in increased muscle accretion; when the ratio of lean to fat deposition is improved, so is feed conversion efficiency (Sillence, 2003) This is supported, in part, by Greife et al. (1989), where the β-AA, clenbuterol, decreased perirenal fat in rats and when administered to rats of different initial BW resulted in greater weight gains in the heavier weight rats; possibly a result of an increase in protein deposition from energy that was released through the mobilization of body fat stores caused by clenbuterol. Dressing percentage can increase as live weight increases and/or as fat depth increases. In the present study, carcass adjusted live weight was increased in ZH-supplemented steers with no changes in %KPH, marbling score or 12th rib fat between CON and ZH-supplemented steers observed. As β-AA have been shown to increase blood flow in cattle (Byrem et al., 1998), β-AA may have an indirect effect on muscle hypertrophy by increasing the nutrient availability to specific tissues or the increased blood flow may allow for non-esterified fatty acids to be carried away from

adipose tissue increasing lipid degradation (Mersmann, 1998). Also, Page et al. (2004) reported a significant increase in apoptosis in epididymal and parametrial adipose tissue in rats treated with different β-AA, suggesting the activation of β-AR's can trigger the apoptotic process in adipocytes. Furthermore, β-AR signaling has been implicated in the apoptotic process in other tissues such as heart and skeletal muscle; however, there is deliberation over whether apoptosis is promoted or inhibited in these tissues (Lynch and Ryall, 2008).

Microarray Analysis and RT-PCR Analysis for Selected Genes

Amplified RNA has been shown to generate highly reliable microarray expression data of comparable quality to data generated by microarray methods that use non-amplified mRNA samples (Jenson et al., 2003). RT-PCR is commonly used to confirm the gene expression results obtained from microarray analysis. However, no standard definition of validation exists and microarray and RT-PCR data often result in disagreement (Morey et. al., 2006). In the present study using the TargetAmp™ 1-Round Aminoallyl-aRNA Amplification Kit 101 (Epicentre® Biotechnologies, Madison, WI), no array elements were shown to be differentially expressed (DE) between CON and ZH-supplemented steers in the i.m., s.c., and visceral adipose tissue depots or muscle tissue. By adjusting the level of significance to $P < 0.05$, eight genes were selected for validation using RT-PCR in respective tissues and six genes were selected as genes of interest. Only CYC1 and β_2-AR in i.m. adipose tissue and β_1-AR in s.c. adipose tissue did not support the results of the microarray analysis. RT-PCR revealed CYC1, β_1-AR and β_2-

AR mRNA expression to be up-regulated threefold, fourfold and fourfold in ZH-supplemented steers vs. CON, respectively.

Phenothalamines developed for use in the livestock industry target the β_1- and β_2-subtype receptors (Moody et al., 2000). The distribution of the receptor subtypes depends on tissue type with the β_1-AR subtype and β_2-AR subtype co-expressed in most tissues with the ratio of these subtypes varying according to tissue type. The β_3-AR subtype has a more limited pattern of expression, but is found in both white and brown adipose tissue (Mills, 2002a). The β_2-adrenergic agonist ZH has a greater affinity for the β_2-AR subtype receptor compared to the β_1-AR subtype but is capable of binding both the β_1-AR (Ki = 1.0 x 10-5) and β_2-AR subtype (Ki = 1.1 x 10-6) receptor (Verhoeckx et al., 2005). In the present study, β_1-AR, β_2-AR, and β_3-AR were selected as genes of interest as mRNA of all three β-AR subtypes has been shown to be expressed in bovine adipose tissue; however, β_3 -AR mRNA expression has been reported to be very small or undetectable in animals after three months of age (Casteilla et al., 1994). More so, Van Liefde et al. (1994) reported β_2-AR as the primary receptor (75%) compared to β_1-AR (25%) in bovine (calf) adipose tissue with both involved in lipolysis and the atypical β–AR (β_3-AR) not present. However, mRNA of all three β-AR subtypes has been shown to be expressed and involved in the regulation of lipolysis in dairy cattle (Sumner and McNamara, 2007). β_3-AR is the strongest of the three subtypes in its ability to induce lipolysis and the β_2-AR is the weakest of the three subtypes in its ability to induce lipolysis, while the β_1-AR subtype is intermediate to the β_3-AR and β_2-AR subtypes (Sumner and McNamara, 2007). In Holstein steers, *in vitro* basal lipolytic rates, expressed as pmol glycerol released per mg protein, were greatest in s.c. adipose tissue

compared to omental, perirenal and intermuscular adipose tissue (Rule et al., 1992). β_2-AR was also reported as the primary receptor in perirenal adipose tissue and the *Longissimus* muscle in bovine (Sillence and Matthews, 1994). Transcript mRNA for β_1-AR, β_2-AR, and β_3-AR were present in adipocytes of porcine (McNeel and Mersmann, 1995) and in adipocytes in humans (Seydoux et al., 1996). β_1-AR and β_2-AR were reported to comprise nearly 95% of the β-AR in swine adipocytes with β_1-AR representing 80% of the total β-AR (McNeel and Mersmann, 1999) and the primary subtype mediating lipolysis (Mills et al., 2003). However, β_2-AR was reported to be the predominately expressed receptor in muscle while in the adipocyte, β_1-AR and β_2-AR were reported to be expressed in almost an equal percentage (Spurlock et al., 1994; Sillence et al., 2005).

In the present study, the distribution of the receptor subtypes varied between tissue types as RT-PCR analysis indicated β_1-AR mRNA expression not to be significantly influenced by ZH supplementation in i.m. or visceral adipose tissue depots; however, β_1-AR mRNA expression in the s.c. adipose tissue was up-regulated in ZH-supplemented steers vs. CON steers. β_2-AR expression in i.m. adipose tissue was up-regulated in ZH-supplemented steers vs. CON steers with β_2-AR mRNA expression not influenced by ZH supplementation in the s.c. and visceral adipose tissue. β_3-AR mRNA expression was not influenced by ZH supplementation in i.m. or visceral adipose tissue with β_3-AR mRNA expression detected in s.c. adipose tissue of ZH-supplemented steers and in only two steers in the CON group. Also, the increased mRNA levels may not have been the magnitude needed to initiate the signaling cascade to bring about lipolysis as no changes in %KPH, marbling score, or 12^{th} rib fat between CON and ZH-supplemented

steers were observed. ZH may be weakly binding its respective receptors on respective tissue types triggering only the synthesis of new protein, thus the observed increase in respective mRNA expression. It is unclear from the data whether β_1-AR was triggering a response only in s.c. adipose tissue and β_2-AR only in i.m. adipose tissue as in some studies, the β-AA is only effective for a limited period of time as the efficacy of β-AA can be altered by desensitization caused by the continuous exposure of the β-AR to the β-AA (Hausdorff et al., 1990b; Lynch and Ryall, 2008).

The increased growth in muscle tissue reported with the use of ZH in other studies may be through mechanisms associated with changes in the expression levels of β-AR. However, in *Longissimus* muscle of the present study, β_1-AR mRNA expression was detected in only two of the six steers in the CON and ZH-supplemented groups, while β_2-AR mRNA expression was detected in all steers of CON and ZH-supplemented groups, although ZH supplementation did not influence mRNA expression. β_3-AR mRNA expression was detected only in ZH-supplemented steers. Similarly, Rathmann et al. (2009) reported no effects of ZH supplementation on β_1-AR or β_2-AR mRNA in semimembranous muscle in steers fed 0, 20, 30, or 40 d plus 3-d withdrawal; however, a tendency for a linear increase in β_2-AR mRNA expression as DOF increased was observed. These results contradict other findings in the literature. For example, Baxa (2008) reported no effects of ZH supplementation on β_1-AR in semimembranous muscle of steers supplemented with ZH over a 91-d feeding period, which included a 30-d ZH supplementation and 3-d withdrawal period. However, mRNA expression of β_2-AR was significantly increased with levels nearly 1,000 times greater than β_1-AR. β_3-AR mRNA expression was not reported in the study. The addition of ZH to proliferating myoblasts,

in vitro, resulted in decreased mRNA in β_1-AR, β_2-AR, and β_3-AR levels (Miller et al., 2009). In addition, Walker et al. (2007) reported β_1-AR, β_2-AR, and β_3-AR mRNA levels present in *Longissimus* muscle and semimembranous muscle of steers supplemented with ractopamine for 28 d; however, β_1-AR and β_2-AR mRNA expression was decreased by ractopamine supplementation in the *Longissimus* muscle with no affect on β_3-AR mRNA levels. Winterholler et al. (2007) reported the most abundant β-AR mRNA in semimembranous muscle of finishing steers supplementation with ractopamine the last 28 d on feed was β_2-AR; ractopamine supplementation had no effect on the abundance of β_1-AR or β_3-AR mRNA, but tended to increase β_2-AR mRNA. Similar to Winterholler et al. (2007), Sissom et al. (2007) reported that ractopamine had no effect on β_1-AR mRNA expression in heifers supplemented with ractopamine the last 28 d on feed; however, there was a tendency for ractopamine supplementation to increase expression of β_2-AR mRNA expression. In *Longissimus* muscle of beef steers, Winterholler et al. (2008) reported ractopamine tended to increase ($P = 0.09$) the abundance of β_1-AR mRNA, but did not affect β_2-AR or β_3-AR.

In the present study, MHC type II, fast fiber type IIA (MYH2) and IIX/D (MYH1), and calpastatin (CAST) were selected as genes of interest even though the microarray analysis did not reveal them to be differentially expressed in *Longissimus* muscle tissue. Baxa (2008) hypothesized ZH supplementation could possibly alter the expression of myosin isoforms. The four major myosin heavy chain (MHC) isoforms observed in adult mammalian skeletal muscles are MHC type I, slow fiber type and MHC type II, fast fiber type, IIA (MYH2), IIX/D (MYH1), and IIB (MHY4) (Schiaffino and Reggiani, 1994; Pette and Staron, 2000). As Baxa (2008) and Rathmann et al. (2009)

reported that MHC-I mRNA expression was not influenced by ZH supplementation and Chikuni et al. (2004) was not able to detect MHC type IIB (MHY4) in bovine skeletal muscle, they were not evaluated in the present study. RT-PCR revealed MHC type II, fast fiber type IIA (MYH2) and IIX/D (MYH1) mRNA expression were not significantly influenced by ZH supplementation in the *Longissimus* muscle tissue. These findings do not agree with Baxa (2008) where ZH supplementation increased MHC-IIX (MYH1) mRNA expression while MHC-IIa (MYH2) mRNA expression had a tendency to be decreased in semimembranous muscle. Similarly, Rathmann et al. (2009) reported a days on feed (DOF) x ZH duration interaction in MHC IIA (MYH2) and IIX (MYH1). MHC IIA (MYH2) expression was decreased by ZH supplementation within the 177 and 198 DOF groups. MHC IIX (MYH1) expression was increased in the 20-d ZH group within the 157 DOF group and the 40-d ZH group within the 177 and 198 DOF groups.
In pigs fed ractopamine for 42 d, MHC IIA (MYH2) and IIX (MYH1) fiber types were decreased while MHC IIB (MYH4) fiber type, the fastest and most glycolytic fiber type, was increased. In contrast, MHC IIA (MYH2) and IIX (MYH1) fiber types were increased in control pigs (Depreux et al., 2002).

In studies where lambs (Pringle et al., 1993) and steers (Wheeler and Koohmaraie, 1992) were fed the β-AA, $L_{644,969}$ the modification of muscle growth was closely related to the activity of the calpain-calpastatin system. In steers supplemented with 3 ppm of the β-AA, $L_{644,969}$, for 6 wk, Wheeler and Koohmaraie (1992) reported higher calpastatin activity in muscle from the β-AA-fed steers at 0 and 7-d postmortem than control steers. Furthermore, in steers supplemented with the β-AA cimaterol, calpastatin mRNA and calpain II large subunit mRNA was increased 96% and 30%,

respectively, vs. nonsupplemented steers (Parr et al., 1992). In the current study, RT-PCR revealed calpastatin (CAST) mRNA expression not significantly influenced by ZH supplementation in the *Longissimus* muscle tissue. These findings are in agreement with Baxa (2008), as CAST mRNA expression was not altered by ZH supplementation in semimembranous muscle. Rathmann et al. (2009) reported similar findings as CAST mRNA expression was not altered by ZH supplementation in semimembranous muscle; however, a tendency for a linear decrease in CAST mRNA expression as ZH duration increased and an increase in CAST mRNA expression as DOF increased was observed.

The Freedom of Information Summary for Zilmax (Intervet, Inc. 2006), indicates when cattle were fed 0.15 mg/kg BW (or 6.8 g/ton in the diet) of ^{14}C-zilpaterol, levels of total residues (unchanged zilpaterol and the major metabolite, deisopropyl-zilpaterol) in muscle and fat after a 12 hr withdrawal to be 19±2.1 and 9.2 ppb, respectively. Levels at the 24 hr withdrawal were 11±2.3 ppb and non-detectable (ND), respectively. Levels at the 48 hr and 96 hour withdrawal were nondetectable in muscle and fat. Stachel et al. (2003) reported similar findings when 0.15 mg of ZH per kg body weight was fed for 14 days. After a one day withdrawal, zilpaterol concentrations in muscle were 6.93 ug/kg (ppb) and after a ten day withdrawal were 0.01 ug/kg (ppb). In sheep fed 0.15 mg of ZH per kg body weight for 10 d, muscle residues after a 0, 2, 5, and 9-d withdrawal were 13.3, 0.86, 0.12, and 0.08 ng/g (ppb), respectively (Shelver and Smith, 2006). As the minimum concentration of ZH, or its metabolic products, in adipose tissue and muscle tissues to elicit a positive growth response is unclear and the ability to detect βAR expression due to ZH supplementation after withdrawal periods greater than 3 d is

uncertain, further investigation into the mechanisms of action of ZH supplementation is warranted.

Table 5.1. Sequences, accession number and melting temperatures of the bovine specific primers for the selected target genes of interest. Accession number is from the national center for biotechnology information (NCBI) available at http://www.ncbi.nlm.nih.gov/.

Primer		Sequence	Size (bp)	Tm used	Product Size (bp)	GenBank Accession
BAR1	Forward	ACGCTCACCAACCTCTTCAT	20			
	Reverse	CACACAGGGTCTCAATGCTG	20	57 C	181 bp	AF188187
BAR2	Forward	GGGGCTGCTATGTTTTGATG	20			
	Reverse	AAATAAGAGGGGCGAGGAGA	20	57 C	185 bp	NM_174231
BAR3	Forward	GGTTGCCTTTCTTTGTGGTC	20			
	Reverse	GTAGATGAGCGGGTTGAAGG	20	59 C	125 bp	NM_174232.2
MYH1	Forward	GCTCCTAATCACCACCAACC	20			
	Reverse	TCAGCAACTTCAGTGCCATC	20	56 C	246 bp	NM_174117.1
MYH2	Forward	GCTGCGTCTTCTCACTTGGT	20			
	Reverse	CCACCTTCTCTGCTCTGGAT	20	56 C	219 bp	XM_001255271.2
CAST	Forward	GGAAGCAGATCCAGAAGACG	20			
	Reverse	GACAGAGCATCGAGGAGGAC	20	56 C	216 bp	NM_174003.2
TNFRSF1B	Forward	GCAGGAATGAAGCCCAGTTA	20			
	Reverse	ACCAAGACAGGACCCATCAG	20	61 C	205 bp	NM_001040490
CYC1	Forward	CCAGGTAGCCAAGGATGTGT	20			
	Reverse	CTTTCGGCTCTTGAGGACTG	20	55 C	163 bp	NM_001038090
SAPS1	Forward	ATCTGAAGGGAGCAGAGTGG	20			
	Reverse	AGCTGAAAGGTCGAGTGTGG	20	61 C	187 bp	XM_870871
HSPA4	Forward	GGCTTGCATTTCTTTTGGAC	20			
	Reverse	TTGGATTTTTCTGCCTCCAC	20	58 C	150 bp	XM_001790383
SH3	Forward	CTGTAAGCCCCCTCTTCTCC	20			
	Reverse	AATCAACAAAGGTGCCCATC	20	61 C	153 bp	NM_001034763
AGTR1	Forward	ATCCTCTGTCGTCCCCTTCT	20			
	Reverse	GAGATCCAACCAGTCCATCC	20	55 C	174 bp	NM_174233
AHCY	Forward	AGCCCATGCACTTTACCATC	20			
	Reverse	GAGCATTCAAACACCCACAG	20	58 C	151 bp	NM_001034315
DGUOK	Forward	CCAGTGCTCGTGTTGGATGT	20			
	Reverse	TGGGTGGCTTGGTATTTTCT	20	58 C	171 bp	NM_001014888

Table 5.2. Ingredient and nutrient composition of experimental diets (DM basis)

	Treatment[1]	
Item	Control	ZH
Ingredient		
Dry rolled corn	68.5	68.5
Corn DDGS	16.0	16.0
Ground alfalfa hay	6.0	6.0
Liquid supplement[2]	5.0	5.0
Control dry supplement[3]	4.5	-
ZH dry supplement[4]	-	4.5
Nutrient composition[5]		
DM, %	81.7	82.6
CP, %	14.6	14.0
ADF, %	7.4	8.7
NDF, %	16.9	17.1
Ca, %	0.59	0.55
P, %	0.38	0.36
Zilpaterol HCl, mg/kg	None Detected	7.47[6]

[1]Zilpaterol hydrochloride diet was formulated to contain 7.50 mg/kg (90% DM basis) of zilpaterol hydrochloride (Intervet/Schering-Plough, DeSoto, KS).
[2]Synergy 19/14 (Westway Feed Products, New Orleans, LA).
[3]Pelleted supplement contained the following (DM basis): 44.44% ground corn, 15.68% wheat middlings, 28.89% limestone, 5.33% salt, 2.22% magnesium oxide, 0.07% manganous oxide, 2.44% potassium chloride, 0.13% zinc sulfate, 0.07% vitamin A (30,000 IU/g), 0.05% vitamin E (50%), 0.42% Rumensin 80 (Elanco Animal Health, Indianapolis, IN), and 0.25% Tylan 40 (Elanco Animal Health).
[4]Pelleted supplement contained the following (DM basis): 44.73% ground corn, 15.68% wheat middlings, 28.89% limestone, 5.33% salt, 2.22% magnesium oxide, 0.07% manganous oxide, 2.44% potassium chloride, 0.13% zinc sulfate, 0.07% vitamin A (30,000 IU/g), 0.05% vitamin E (50%), and 0.39% zilpaterol hydrochloride premix (Intervet).
[5]All values are from laboratory analyses and are presented on a 100% DM basis (except DM).
[6]Determined from the average of three samples (approximately 20 kg; collected June 18, 2007) dispensed from a Roto-Mix 184-8 mixer (Roto-Mix, Dodge City, KS) after 25%, 50%, and 75% of the batch had been fed. From the large samples, 4 sub-samples were analyzed for zilpaterol HCl content (Intervet Pharmaceutical Laboratory, Lawrence, KS).

Table 5.3. Effect of Zilpaterol hydrochloride supplementation (30 d plus 3 d withdrawal) on performance of steers.

Item	Control	ZH	S.E.M.	*Probability*
BW, kg				
Initial	357.0	356.0	19.14	0.17
Final	566.0	577.0	5.62	0.19
Carc. Adj. BW	565.0	579.0	4.65	0.05
Performance, ZH to end				
ADG, kg/d	1.43	1.77	0.164	0.17
Adj. ADG, kg/d	1.42	1.89	0.186	0.02
DMI, kg/d	9.93	9.42	0.201	0.09
G:F, kg/kg	0.144	0.187	0.017	0.08
Carc. Adj. G:F, kg/kd	0.143	0.202	0.021	0.009
Performance, d 0 to end				
ADG, kg/d	1.60	1.69	0.045	0.19
Adj. ADG, kg/d	1.60	1.71	0.044	0.06
DMI, kg/d	9.62	9.54	0.197	0.72
G:F, kg/kg	0.167	0.177	0.005	0.15
Carc. Adj. G:F, kg/kg	0.166	0.179	0.004	0.04

Table 5.4. Effect of Zilpaterol hydrochloride supplementation (30 d plus 3 d withdrawal) on carcass characteristics of steers.

Item	Control	ZH	S.E.M.	*Probability*
HCW, kg	359.50	373.60	3.027	0.005
Dressing %	63.57	64.46	0.324	0.056
LM area, cm	89.68	93.95	1.812	0.02
12th-rib fat, cm	1.24	1.25	0.103	0.96
KPH, %	1.90	1.91	0.230	0.87
Marbling	37.15	37.45	0.956	0.83
Preliminary YG	3.19	3.15	0.077	0.69
Adj. preliminary YG	3.22	3.23	0.101	0.96
Calculated YG	2.66	2.58	0.234	0.57
USDA YG	2.24	2.14	0.094	0.41
Skeletal maturity	70.04	72.42	4.818	0.31
Lean maturity	62.04	63.38	9.722	0.64
Overall maturity	67.38	69.04	5.824	0.38
Color score	4.96	5.08	0.072	0.26

Figure 5.1.

(a) Relative fold difference in cytochrome C-1 gene expression in control (green) and zilpaterol treatment (red) i.m. adipose tissue depots in steers at the end of the Finishing Phase. The gene expression level for control i.m. adipose tissue was set as baseline and fold difference was calculated as described in Material and Methods. Columns with different superscripts differ significantly ($P < 0.002$).

(b) Relative fold difference in tumor necrosis factor receptor superfamily, member 1B gene expression in control (green) and zilpaterol treatment (red) i.m. adipose tissue depots in steers at the end of the Finishing Phase. The gene expression level for zilpaterol treatment i.m. adipose tissue was set as baseline and fold difference was calculated as described in Material and Methods. No significant difference was observed between control and zilpaterol treatment ($P < 0.26$).

(c) Relative fold difference in heat shock 70kDa protein 4 gene expression in control (green) and zilpaterol treatment (red) s.c. adipose tissue depots in steers at the end of the Finishing Phase. The gene expression level for control s.c. adipose tissue was set as baseline and fold difference was calculated as described in Material and Methods. No significant difference was observed between control and zilpaterol treatment ($P < 0.09$).

(d) Relative fold difference in SAPS domain family, member 1 gene expression in control (green) and zilpaterol treatment (red) s.c. adipose tissue depots in steers at the end of the Finishing Phase. The gene expression level for control s.c. adipose tissue was set as baseline and fold difference was calculated as described in Material and Methods. No significant difference was observed between control and zilpaterol treatment ($P < 0.14$).

(a)

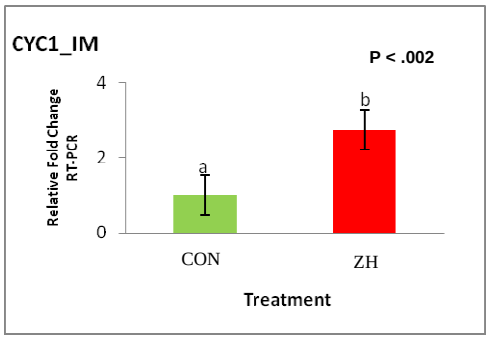
CYC1_IM
P < .002
Relative Fold Change RT-PCR
4
2
0
a
b
CON
ZH
Treatment

(b)

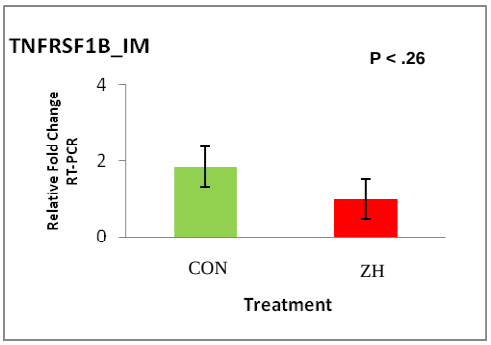
TNFRSF1B_IM
P < .26
Relative Fold Change RT-PCR
4
2
0
CON
ZH
Treatment

(c)

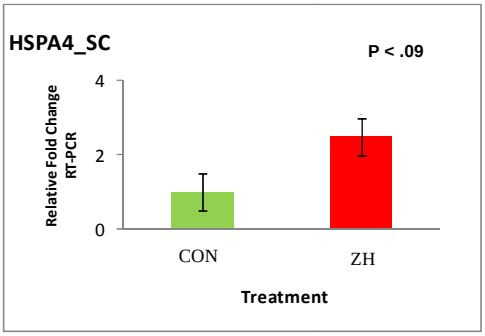
HSPA4_SC
P < .09
Relative Fold Change RT-PCR
4
2
0
CON
ZH
Treatment

(d)

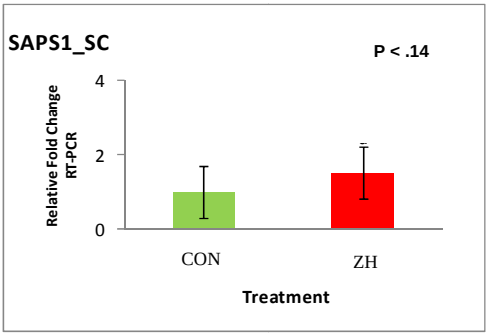
SAPS1_SC
P < .14
Relative Fold Change RT-PCR
4
2
0
CON
ZH
Treatment

Figure 5.1.

(e) Relative fold difference in angiotensin II receptor, type 1 in control (green) and zilpaterol treatment (red) visceral adipose tissue depots in steers at the end of the Finishing Phase. The gene expression level for control visceral adipose tissue was set as baseline and fold difference was calculated as described in Material and Methods. Columns with different superscripts differ significantly ($P < 0.002$).

(f) Relative fold difference in SH3 domain binding glutamic acid-rich protein like 3 gene expression in control (green) and zilpaterol treatment (red) visceral adipose tissue depots in steers at the end of the Finishing Phase. The gene expression level for the control visceral adipose tissue was set as baseline and fold difference was calculated as described in Material and Methods. No significant difference was observed between control and zilpaterol treatment ($P < 0.21$).

(g) Relative fold difference in S-adenosylhomocysteine hydrolase gene expression in control (green) and zilpaterol treatment (red) LM depots in steers at the end of the Finishing Phase. The gene expression level for control muscle depot was set as baseline and fold difference was calculated as described in Material and Methods. No significant difference was observed between control and zilpaterol treatment ($P < 0.75$).

(h) Relative fold difference in deoxyguanosine kinase gene expression in control (green) and zilpaterol treatment (red) LM depots in steers at the end of the Finishing Phase. The gene expression level for the zilpaterol treatment muscle depot was set as baseline and fold difference was calculated as described in Material and Methods. No significant difference was observed between control and zilpaterol treatment ($P < 0.91$).

(e)

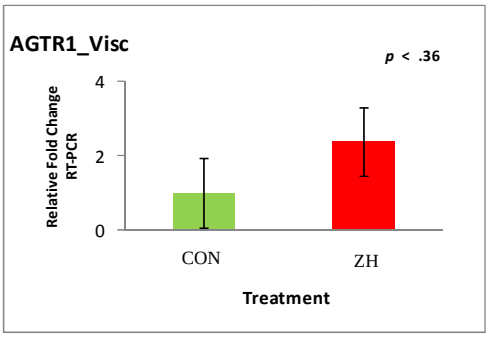
AGTR1_Visc
p < .36
Relative Fold Change RT-PCR
4
2
0
CON
ZH
Treatment

(f)

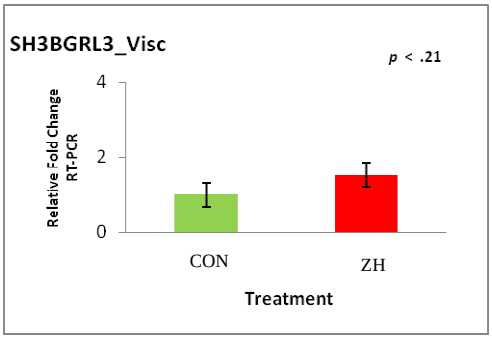
SH3BGRL3_Visc
p < .21
Relative Fold Change RT-PCR
4
2
0
CON
ZH
Treatment

(g)

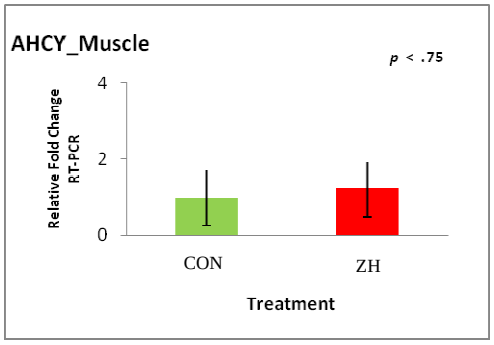
AHCY_Muscle
p < .75
Relative Fold Change RT-PCR
4
2
0
CON
ZH
Treatment

(h)

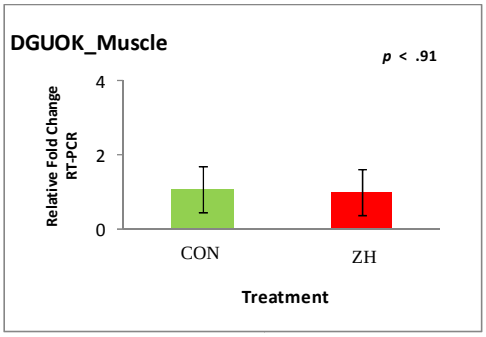
DGUOK_Muscle
p < .91
Relative Fold Change RT-PCR
4
2
0
CON
ZH
Treatment

Figure 5.1.

(i) Relative fold difference in adrenergic, beta-1- receptor expression in control (green) and zilpaterol treatment (red) i.m. adipose tissue depots in steers at the end of the Finishing Phase. The gene expression level for the control i.m. adipose tissue was set as baseline and fold difference was calculated as described in Material and Methods. No significant difference was observed between control and zilpaterol treatment ($P < 0.27$).

(j) Relative fold difference in adrenergic, beta-1- receptor gene expression in control (green) and zilpaterol treatment (red) s.c. adipose tissue depots in steers at the end of the Finishing Phase. The gene expression level for the control s.c. adipose tissue was set as baseline and fold difference was calculated as described in Material and Methods. Columns with different superscripts differ significantly ($P < 0.01$).

(k) Relative fold difference in adrenergic, beta-1- receptor gene expression in control (green) and zilpaterol (red) visceral adipose tissue depots in steers at the end of the Finishing Phase. The gene expression level for the control visceral adipose tissue was set as baseline and fold difference was calculated as described in Material and Methods. No significant difference was observed between control and zilpaterol treatment ($P < 0.38$).

(i)

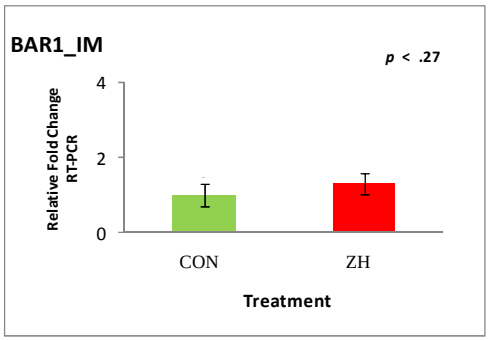
BAR1_IM
p < .27
Relative Fold Change RT-PCR
4
2
0
CON
ZH
Treatment

(j)

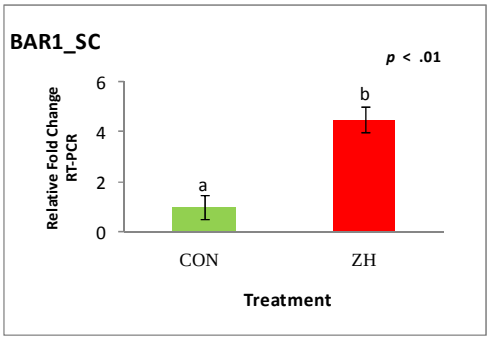
BAR1_SC
p < .01
Relative Fold Change RT-PCR
6
4
2
0
a
b
CON
ZH
Treatment

(k)

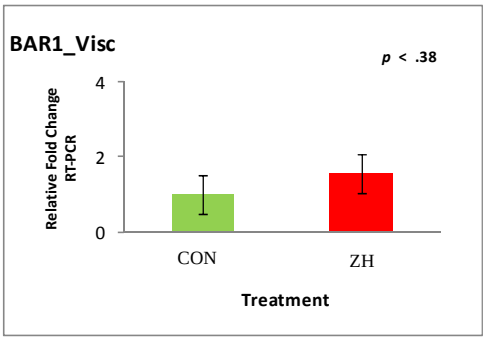
BAR1_Visc
p < .38
Relative Fold Change RT-PCR
4
2
0
CON
ZH
Treatment

Figure 5.1.

(l) Relative fold difference in adrenergic, beta-2- receptor gene expression in control (green) and zilpaterol treatment (red) i.m. adipose tissue depots in steers at the end of the Finishing Phase. The gene expression level for the control i.m. adipose tissue was set as baseline and fold difference was calculated as described in Material and Methods. Columns with different superscripts differ significantly ($P < 0.006$).

(m) Relative fold difference in adrenergic, beta-2- receptor gene expression in control (green) and zilpaterol treatment (red) s.c. adipose tissue depots in steers at the end of the Finishing Phase. The gene expression level for the control s.c. adipose tissue was set as baseline and fold difference was calculated as described in Material and Methods. No significant difference was observed between control and zilpaterol treatment ($P < 0.10$).

(n) Relative fold difference in adrenergic, beta-2- receptor gene expression in control (green) and zilpaterol treatment (red) visceral adipose tissue depots in steers at the end of the Finishing Phase. The gene expression level for the control visceral adipose tissue was set as baseline and fold difference was calculated as described in Material and Methods. No significant difference was observed between control and zilpaterol treatment ($P < 0.55$).

(o) Relative fold difference in adrenergic, beta-2- receptor (green) and zilpaterol treatment (red) muscle depots in steers at the end of the Finishing Phase. The gene expression level for the control muscle depot was set as baseline and fold difference was calculated as described in Material and Methods. No significant difference was observed between control and zilpaterol treatment ($P < 0.72$).

(p) Relative fold difference in adrenergic, beta-3- receptor gene expression in control (green) and zilpaterol treatment (red) i.m. adipose tissue depots in steers at the end of the Finishing Phase. The gene expression level for the control i.m. adipose tissue was set as baseline and fold difference was calculated as described in Material and Methods. No significant difference was observed between control and zilpaterol treatment ($P < 0.41$).

(q) Relative fold difference in adrenergic, beta-3- receptor gene expression in control (green) and zilpaterol treatment (red) visceral adipose tissue depots in steers at the end of the Finishing phase. The gene expression level for the control visceral adipose tissue was set as baseline and fold difference was calculated as described in Material and Methods. No significant difference was observed between control and zilpaterol treatment ($P < 0.40$).

(l)

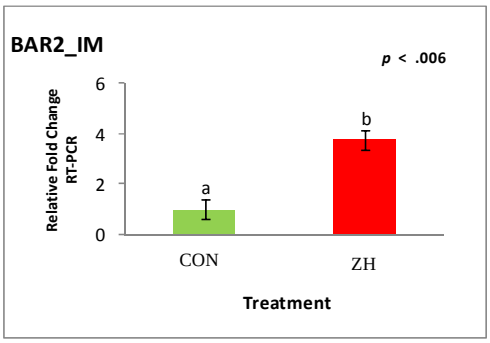
BAR2_IM
p < .006
Relative Fold Change RT-PCR
6
4
2
0
a
b
CON
ZH
Treatment

(m)

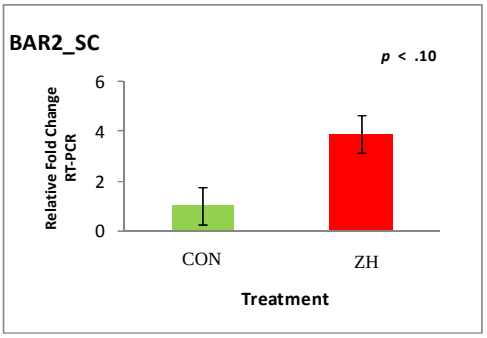
BAR2_SC
p < .10
Relative Fold Change RT-PCR
6
4
2
0
CON
ZH
Treatment

(n)

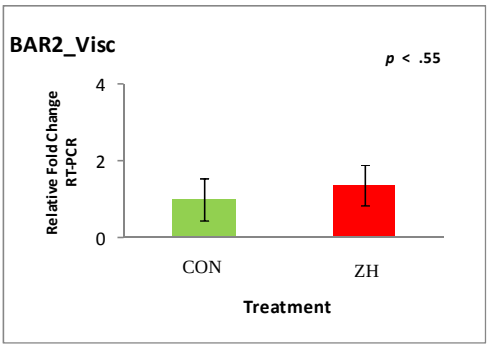
BAR2_Visc
p < .55
Relative Fold Change RT-PCR
4
2
0
CON
ZH
Treatment

(o)

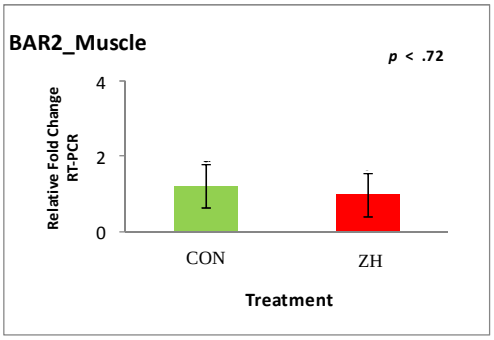
BAR2_Muscle
p < .72
Relative Fold Change RT-PCR
4
2
0
CON
ZH
Treatment

(p)

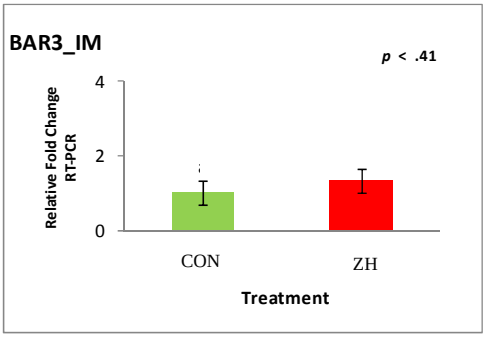
BAR3_IM
p < .41
Relative Fold Change RT-PCR
4
2
0
CON
ZH
Treatment

(q)

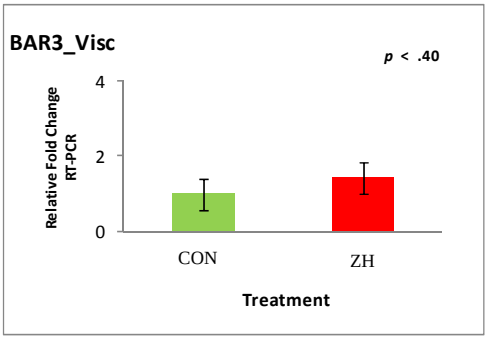
BAR3_Visc
p < .40
Relative Fold Change RT-PCR
4
2
0
CON
ZH
Treatment

Figure 5.1.

(r) Relative fold difference in myosin heavy chain 1 (green) and zilpaterol treatment (red) muscle depot in steers at the end of the Finishing Phase. The gene expression level for zilpaterol treatment muscle depot was set as baseline and fold difference was calculated as described in Material and Methods. No significant difference was observed between control and zilpaterol treatment ($P < 0.83$).

(s) Relative fold difference in myosin heavy chain 2 gene expression in control (green) and zilpaterol treatment (red) muscle depot in steers at the end of the Finishing Phase. The gene expression level for zilpaterol treatment muscle depot was set as baseline and fold difference was calculated as described in Material and Methods. No significant difference was observed between control and zilpaterol treatment ($P < 0.60$).

(t) Relative fold difference in calpastatin gene expression in control (green) and zilpaterol treatment (red) muscle depot in steers at the end of the Finishing Phase. The gene expression level for the control muscle depot was set as baseline and fold difference was calculated as described in Material and Methods. No significant difference was observed between control and zilpaterol treatment ($P < 0.74$).

(r)

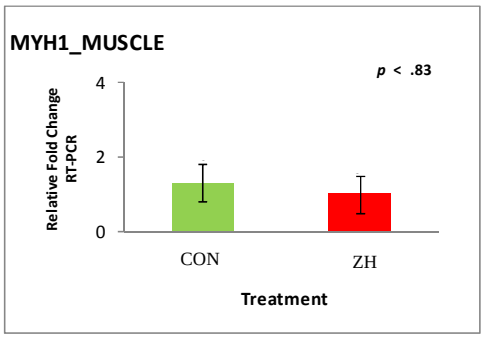
MYH1_MUSCLE
p < .83
Relative Fold Change RT-PCR
4
2
0
CON
ZH
Treatment

(s)

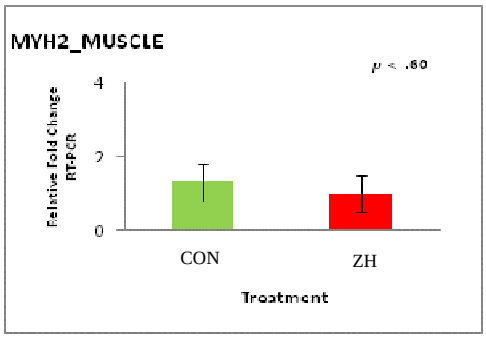
MYH2_MUSCLE
Relative Fold Change RT-PCR
4
0
CON
ZH
Treatment

(t)

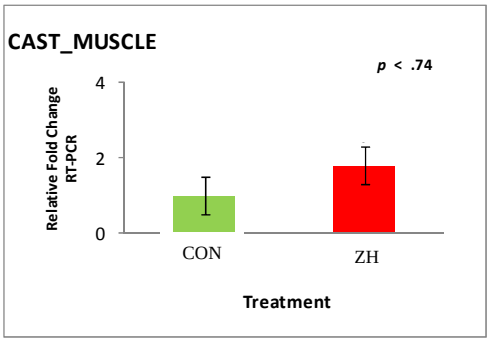
CAST_MUSCLE
p < .74
Relative Fold Change RT-PCR
4
2
0
CON
ZH
Treatment

ABBREVIATIONS

ADG	average daily gain
β-AA	β-adrenergic agonists
β-AR	β-adrenergic receptor
βARK1	β-adrenergic receptor kinase1
BW	body weight
CF	calf-fed diet
C/EBP/α	CCAAT/enhancer binding protein alpha
CRE	cAMP response element
CREB	cAMP response element binding
CLA	conjugated linoleic acid
DE	differentially expressed
DMI	dry matter intake
DOF	days on feed
ECM	extracellular matrix
FABP4	fatty acid binding protein 4
FAS	fatty acid synthase
FDA	food and drug administration
F:G	feed to gain
FP	finishing phase
GP	growing phase
GRK	G-coupled receptor kinases
HOL	Holstein
HCW	hot carcass weight
HSL	hormone-sensitive lipase
i.m.	intramuscular
INT	initial
JB	Japanese Black
KPH	kidney, pelvic and heart
LM	*Longissimus* muscle
LCFA	long chain fatty acid
MAT	malonyl/acetyl-CoA transacylase
ME	metabolizable energy
MUFA	monounsaturated fatty acids
PF	program-fed diet
PPARγ	peroxisome proliferator-activated receptor-gamma
PUFA	polyunsaturated fatty acids
PKA	protein kinase A
s.c.	subcutaneous
SCD	stearoyl-CoA desaturase
SF	silage-fed diet
SNPs	single nucleotide polymorphisms
TE	thioesterase
VEGF	vascular endothelial growth factor
WP	wheat-pasture diet

Literature Cited

Abumrad, N. A., M. R. el-Maghrabi, E. Z. Amri, E. Lopez, and P. A. Grimaldi. 1993. Cloning of a rat adipocyte membrane protein implicated in binding or transport of long-chain fatty acids that is induced during preadipocyte differentiation. Homology with human CD36. J Biol Chem 268: 17665-17668.

Ailhaud, G., P. Grimaldi, and R. Negrel. 1992. Cellular and molecular aspects of adipose tissue development. Annu Rev Nutr 12: 207-233.

Albright, A. L., and J. S. Stern. 1998. Adipose tissue. In: Fay T.D. (ed.) Encyclopedia of sports medicine and science, Internet society for sport science, Available from: http://sportsci.org.

Allison, D. B., X. Cui, G. P. Page, and M. Sabripour. 2006. Microarray data analysis: From disarray to consolidation and consensus. Nat Rev Genet 7: 55-65.

Anderson, D. B., D. E. Moody, and D. L. Hancock. 2004. Beta adrenergic agonists. In Pond W. G. and Bell A. W. (ed.), Encyclopedia of Animal Science: pg. 104-107.

Archibeque, S. L., D. K. Lunt, C. D. Gilbert, R. K. Tume, and S. B. Smith. 2005. Fatty acid indices of stearoyl-CoA desaturase do not reflect actual stearoyl-CoA desaturase enzyme activities in adipose tissues of beef steers finished with corn-, flaxseed-, or sorghum-based diets. J Anim Sci 83: 1153-1166.

Ashburner, M., C. A. Ball, J. A. Blake, D. Botstein, H. Butler, J. M. Cherry, A. P. Davis, K. Dolinski, S. S. Dwight, J. T. Eppig, M. A. Harris, D. P. Hill, L. Issel-Tarver, A. Kasarskis, S. Lewis, J. C. Matese, J. E. Richardson, M. Ringwald, G. M. Rubin, and G. Sherlock. 2000. Gene ontology: Tool for the unification of biology. Nature Genetics 25: 25-29.

Asturias, F. J. 2006. Mammalian fatty acid synthase: X-ray structure of a molecular assembly line. ACS Chem Biol 1: 135-138.

Asturias, F. J., J. Z. Chadick, I. K. Cheung, H. Stark, A. Witkowski, A. K. Joshi, and S. Smith. 2005. Structure and molecular organization of mammalian fatty acid synthase. Nat Struct Mol Biol 12: 225-232.

Aubertv J., P. Saint-Marc, N. Belmonte, C. Dani, R. Négrel and G. Ailhaud. 2000. Prostacyclin IP receptor up-regulates the early expression of C/EBPβ and C/EBPδ in preadipose cells. Mol and Cell Endocrin160: 149-156.

Avendano-Reyes, L., V. Torres-Rodriguez, F. J. Meraz-Murillo, C. Perez-Linares, F. Figueroa-Saavedra, and P. H. Robinson. 2006. Effects of two beta-adrenergic agonists on finishing performance, carcass characteristics, and meat quality of feedlot steers. J. Anim Sci. 84: 3259-3265.

Bach, I. 2000. The LIM domain: Regulation by association. Mech Dev 91: 5-17.

Badino, P., R. Odore, and G. Re. 2005. Are so many adrenergic receptor subtypes really present in domestic animal tissues? A pharmacological perspective. The Veterinary Journal 170: 163-174.

Baker, J. G. 2005. The selectivity of beta-adrenoceptor antagonists at the human beta 1, beta 2 and beta 3 adrenoceptors. Br J Pharmacol 144: 317-322.

Baldwin, K. M., and F. Haddad. 2001. Effects of different activity and inactivity paradigms on myosin heavy chain gene expression in striated muscle. J Appl Physiol 90: 345-357.

Barnes, P. J. 1995. Beta-adrenergic receptors and their regulation. Am J Respir Crit Care Med 152: 838-860.

Bauman, D. E., J. W. Perfield, M. J. deVeth, and A. L. Lock. 2003. New perspectives on lipid digestion and metabolism in ruminants. In: Cornell Nutrition Conference for Feed Manufacturers, Syracuse, NY. pg. 175-189.

Baxa, T. 2008. Effect of zilpaterol hydrochloride and steroid implantation on yearling steer feedlot performance, carcass characteristics, and skeletal muscle gene expression. Kansas State University, Manhattan, KS. PhD dissertation. http://krex.k-state.edu/dspace/handle/2097/936.

Benjamini, Y., and Y. Hochberg. 1995. Controlling the false discovery rate: A practical and powerful approach to multiple testing. Journal of the Royal Statistical Society. Series B (Methodological) 57 (1): 289-300.

Bennati, A. M., M. Castelli, M. A. Della Fazia, T. Beccari, D. Caruso, G. Servillo, and R. Roberti. 2006. Sterol dependent regulation of human tm7sf2 gene expression: Role of the encoded 3 β-hydroxysterol Δ14-reductase in human cholesterol biosynthesis. Biochimica et Biophysica Acta (BBA) - Molecular and Cell Biology of Lipids 1761: 677-685.

Bennett, G. L., and C. B. Williams. 1994. Implications of genetic changes in body composition on beef production systems. J Anim Sci 72: 2756-2763.

Bock, B. J., S. M. Hannah, F. K. Brazle, L. R. Corah, and G. L. Kuhl. 1991. Stocker cattle management and nutrition. Kansas State University Agricultural Experiment Station and Cooperative Extension Service: C723.

Bolstad, B. M., R. A. Irizarry, M. Astrand, and T. P. Speed. 2003. A comparison of normalization methods for high density oligonucleotide array data based on variance and bias. Bioinformatics 19: 185-193.

Bonen, A., S. E. Campbell, C. R. Benton, A. Chabowski, S. L. Coort, X. X. Han, D. P. Koonen, J. F. Glatz, and J. J. Luiken. 2004. Regulation of fatty acid transport by fatty acid translocase/CD36. Proc Nutr Soc 63: 245-249.

Boney, C. M., B. M. Moats-Staats, A. D. Stiles, and A. J. D'Ercole. 1994. Expression of insulin-like growth factor-I (IGF-I) and IGF-binding proteins during adipogenesis. Endocrinology 135: 1863-1868.

Boone, C., J. Mourot, F. Gregoire, and C. Remacle. 2000. The adipose conversion process: Regulation by extracellular and intracellular factors. Reprod Nutr Dev 40: 325-358.

Brun, R. P., P. Tontonoz, B. M. Forman, R. Ellis, J. Chen, R. M. Evans, and B. M. Spiegelman. 1996. Differential activation of adipogenesis by multiple PPAR isoforms. Genes Dev 10: 974-984.

Burrow, H. M., S. S. Moore, D. J. Johnston, W. Barendse, and B. M. Bindon. 2001. Quantitative and molecular genetic influences on properties of beef: A review. Aust. J. Exp. Agric 41: 893-920.

Butterwith, S. C. 1997. Regulators of adipocyte precursor cells. Poult Sci 76: 118-123.

Bylund, D. B. 2007. Alpha- and beta-adrenergic receptors: Ahlquist's landmark hypothesis of a single mediator with two receptors. Am J Physiol Endocrinol Metab 293: E1479-1481.

Byrem, T. M., D. H. Beermann, and T. F. Robinson. 1998. The beta-agonist cimaterol directly enhances chronic protein accretion in skeletal muscle. J Anim Sci 76: 988-998.

Cameron, P. J., M. Rogers, J. Oman, S. G. May, D. K. Lunt, and S. B. Smith. 1994. Stearoyl Coenzyme A desaturase enzyme activity and mRNA levels are not different in subcutaneous adipose tissue from Angus and American Wagyu steers. J Anim Sci 72: 2624-2628.

Cartwright, M. J., T. Tchkonia, and J. L. Kirkland. 2007. Aging in adipocytes: Potential impact of inherent, depot-specific mechanisms. Experimental Gerontology 42: 463-471.

Casero, R. A., Jr., P. Celano, S. J. Ervin, N. B. Applegren, L. Wiest, and A. E. Pegg. 1991. Isolation and characterization of a cDNA clone that codes for human spermidine/spermine n1-acetyltransferase. J Biol Chem 266: 810-814.

Casteilla, L., P. Muzzin, J. P. Revelli, D. Ricquier, and J. P. Giacobino. 1994. Expression of beta 1- and beta 3-adrenergic-receptor messages and adenylate cyclase beta-adrenergic response in bovine perirenal adipose tissue during its transformation from brown into white fat. Biochem J 297 (Pt 1): 93-97.

Chakravarty, B., Z. Gu, S. S. Chirala, S. J. Wakil, and F. A. Quiocho. 2004. Human fatty acid synthase: Structure and substrate selectivity of the thioesterase domain. Proc Natl Acad Sci U.S.A. 101: 15567-15572.

Chandrasekharan, N. V., H. Dai, K. L. Roos, N. K. Evanson, J. Tomsik, T. S. Elton, and D. L. Simmons. 2002. COX-3, a cyclooxygenase-1 variant inhibited by acetaminophen and other analgesic/antipyretic drugs: Cloning, structure, and expression. Proc Natl Acad Sci U.S.A. 99: 13926-13931.

Chen, C. H., E. C. Lin, W. T. Cheng, H. S. Sun, H. J. Mersmann, and S. T. Ding. 2006. Abundantly expressed genes in pig adipose tissue: An expressed sequence tag approach. J Anim Sci 84: 2673-2683.

Chen, H. W. 1984. Role of cholesterol metabolism in cell growth. Fed Proc 43: 126-130.

Chen, Y., J.-Z. Shao, L.-X. Xiang, X.-J. Dong, and G.-R. Zhang. 2008. Mesenchymal stem cells: A promising candidate in regenerative medicine. The International Journal of Biochemistry & Cell Biology 40: 815-820.

Cherezov, V., D. M. Rosenbaum, M. A. Hanson, S. G. Rasmussen, F. S. Thian, T. S. Kobilka, H. J. Choi, P. Kuhn, W. I. Weis, B. K. Kobilka, and R. C. Stevens. 2007. High-resolution crystal structure of an engineered human beta2-adrenergic G protein-coupled receptor. Science 318: 1258-1265.

Chernov, K., A. Mechulam, N. Popova, D. Pastre, E. Nadezhdina, O. Skabkina, N. Shanina, V. Vasiliev, A. Tarrade, J. Melki, V. Joshi, S. Baconnais, F. Toma, L. Ovchinnikov, and P. Curmi. 2008. YB-1 promotes microtubule assembly *in vitro* through interaction with tubulin and microtubules. BMC Biochemistry 9: 23.

Chirala, S. S., and S. J. Wakil. 2004. Structure and function of animal fatty acid synthase. Lipids 39: 1045-1053.

Chmurzynska, A. 2006. The multigene family of fatty acid-binding proteins (FABPs): Function structure and polymorphisms. J Appl Genet 47 (1) 39-48.

Choat, W. T., C. R. Krehbiel, G. C. Duff, R. E. Kirksey, L. M. Lauriault, J. D. Rivera, B. M. Capitan, D. A. Walker, G. B. Donart, and C. L. Goad. 2003. Influence of grazing dormant native range or winter wheat pasture on subsequent finishing cattle performance, carcass characteristics, and ruminal metabolism. J Anim Sci 81: 3191-3201.

Christofk, H. R., M. G. Vander Heiden, N. Wu, J. M. Asara, and L. C. Cantley. 2008. Pyruvate kinase M2 is a phosphotyrosine-binding protein. Nature 452: 181-186.

Chung, K. Y., and B. J. Johnson. 2007. Cellular aspects of intramuscular adipogenesis: Competition for cells between muscle and marbling. In: Plains Nutrition Council, Publication No. AREC 07-20, Texas A&M University Agricultural Research and Extension Center, San Antonio TX, March 29-30

Chung, K. Y., and B. J. Johnson. 2008. Application of cellular mechanisms to growth and development of food producing animals. J Anim Sci 86: E226-235.

Church, D. C. 1988. The ruminant animal; digestive and physiology and nutrition. Waveland Press, Prospect Heights, Ill.

Cianzio, D. S., D. G. Topel, G. B. Whitehurst, D. C. Beitz, and H. L. Self. 1985. Adipose tissue growth and cellularity: Changes in bovine adipocyte size and number. J Anim Sci 60: 970-976.

Cinti, S. 2005. The adipose organ. Prostaglandins, Leukotrienes and Essential Fatty Acids 73: 9-15.

Clarke, S. D. 1993. Regulation of fatty acid synthase gene expression: An approach for reducing fat accumulation. J Anim Sci 71: 1957-1965.

Clemmons, D. R. 1992. IGF binding proteins: Regulation of cellular actions. Growth Regul 2: 80-87.

Coburn, C. T., T. Hajri, A. Ibrahimi, and N. A. Abumrad. 2001. Role of CD36 in membrane transport and utilization of long-chain fatty acids by different tissues. J Mol Neurosci 16: 117-121.

Coburn, C. T., F. F. Knapp, Jr., M. Febbraio, A. L. Beets, R. L. Silverstein, and N. A. Abumrad. 2000. Defective uptake and utilization of long chain fatty acids in muscle and adipose tissues of CD36 knockout mice. J Biol Chem 275: 32523-32529.

Colbert, W. E., P. D. Williams, and G. D. Williams. 1991. Beta-adrenoceptor profile of ractopamine HCL in isolated smooth and cardiac muscle tissues of rat and guinea-pig. J Pharm Pharmacol 43: 844-847.

Coleman, R. A., T. M. Lewin, C. G. Van Horn, and M. R. Gonzalez-Baro. 2002. Do long-chain acyl-CoA synthetases regulate fatty acid entry into synthetic versus degradative pathways? J Nutr 132: 2123-2126.

Crandall,D., D. Armellino, D. Busler, B. McHendry-Rinde and J. Kral. 1992. Angiotensin II receptors in human preadipocytes: Role in cell cycle regulation. Endocrin 140: 154-158

Corino, C., A. Di Giancamillo, R. Rossi, and C. Domeneghini. 2005. Dietary conjugated linoleic acid affects morphofunctional and chemical aspects of subcutaneous adipose tissue in heavy pigs. J Nutr 135: 1444-1450.

Cronan, J. E., Jr. 2004. The structure of mammalian fatty acid synthase turned back to front. Chem Biol 11: 1601-1602.

Damon, M., I. Louveau, L. Lefaucheur, B. Lebret, A. Vincent, P. Leroy, M. P. Sanchez, P. Herpin, and F. Gondret. 2006. Number of intramuscular adipocytes and fatty acid binding protein-4 content are significant indicators of intramuscular fat level in crossbred Large White x Duroc pigs. J Anim Sci 84: 1083-1092.

Daniel, Z. C., R. J. Wynn, A. M. Salter, and P. J. Buttery. 2004. Differing effects of forage and concentrate diets on the oleic acid and conjugated linoleic acid content of sheep tissues: The role of stearoyl-CoA desaturase. J Anim Sci 82: 747-758.

Dave, M., M. J. Sauer, and R. J. Fallon. 1998. Clenbuterol plasma pharmacokinetics in cattle. Analyst 123: 2697-2699.

Davydova, E. K., V. M. Evdokimova, L. P. Ovchinnikov, and J. W. Hershey. 1997. Over expression in COS cells of p50, the major core protein associated with mRNA, results in translation inhibition. Nucleic Acids Res 25: 2911-2916.

Deng, T., S. Shan, P. P. Li, Z. F. Shen, X. P. Lu, J. Cheng, and Z. Q. Ning. 2006. Peroxisome proliferator-activated receptor-gamma transcriptionally up-regulates hormone-sensitive lipase via the involvement of specificity protein-1. Endocrinology 147: 875-884.

Depreux, F. F., A. L. Grant, D. B. Anderson, and D. E. Gerrard. 2002. Paylean alters myosin heavy chain isoform content in pig muscle. J Anim Sci 80: 1888-1894.

Deschamps, D., C. Fisch, B. Fromenty, A. Berson, C. Degott, and D. Pessayre. 1991. Inhibition by salicylic acid of the activation and thus oxidation of long chain fatty acids. Possible role in the development of Reye's syndrome. J Pharmacol Exp Ther 259: 894-904.

DiGirolamo, M., F. Newby, and J. Lovejoy. 1992. Lactate production in adipose tissue: A regulated function with extra- adipose implications. FASEB J. 6: 2405-2412.

Dikeman, M. E. 2007. Effects of metabolic modifiers on carcass traits and meat quality. Meat Science 77: 121-135.

Dobrzyn, A., and J. M. Ntambi. 2005. The role of stearoyl-CoA desaturase in the control of metabolism. Prostaglandins Leukot Essent Fatty Acids 73: 35-41.

Dobrzyn, P., J. M. Ntambi, and A. Dobrzyn. 2008. Stearoyl-CoA desaturase: A novel control point of lipid metabolism and insulin sensitivity. European Journal of Lipid Science and Technology 110: 93-100.

Dodson, M. V., and M. E. Fernyhough. 2008. Mature adipocytes: Are there still novel things that we can learn from them? Tissue and Cell 40 (4): 307-308.

Dolezal, H. G. 2000. Relevance of results of the national beef quality audits, conducted in 1991 and 1995, to the beef industry. National Beef Quality Audit, Englewood, CO.

Duckett, S. K. 2001. Effect of nutrition and management practices on marbling deposition and composition. http://www.cabpartners.com/news/research/index.php: accessed 8/14/08.

Ehehalt, R., J. Fullekrug, J. Pohl, A. Ring, T. Herrmann, and W. Stremmel. 2006. Translocation of long chain fatty acids across the plasma membrane--lipid rafts and fatty acid transport proteins. Mol Cell Biochem 284: 135-140.

Ehehalt, R., R. Sparla, H. Kulaksiz, T. Herrmann, J. Fullekrug, and W. Stremmel. 2008. Uptake of long chain fatty acids is regulated by dynamic interaction of fat/CD36 with cholesterol/sphingolipid enriched microdomains (lipid rafts). BMC Cell Biol 9:45.

Elsik, C. G., E., Antoniou, S. C. Fahrenkrug, J. M. Reecy, R. D Wolfinger, and J. F. Taylor. 2006. A bovine whole genome long oligonucleotide expression array. In 'Proceedings of the 30th International Conference on Animal Genetics'. #C224. p. 68. (International Society for Animal Genetics:Brazil.)

Evans, B. A., M. Papaioannou, S. Hamilton, and R. J. Summers. 1999. Alternative splicing generates two isoforms of the beta3-adrenoceptor which are differentially expressed in mouse tissues. Br J Pharmacol 127: 1525-1531.

Fajas, L., S. Miard, M. R. Briggs, and J. Auwerx. 2003. Selective cyclo-oxygenase-2 inhibitors impair adipocyte differentiation through inhibition of the clonal expansion phase. J Lipid Res 44: 1652-1659.

Farnier, C., S. Krief, M. Blache, F. Diot-Dupuy, G. Mory, P. Ferre, and R. Bazin. 2003. Adipocyte functions are modulated by cell size change: Potential involvement of an integrin/ERK signaling pathway. Int J Obes Relat Metab Disord 27: 1178-1186.

Febbraio, M., D. P. Hajjar, and R. L. Silverstein. 2001. CD36: A class B scavenger receptor involved in angiogenesis, atherosclerosis, inflammation, and lipid metabolism. J Clin Invest 108: 785-791.

Fernyhough, M. E., E. Okine, G. Hausman, J. L. Vierck, and M. V. Dodson. 2007. PPARγ and Glut-4 expression as developmental regulators/markers for preadipocyte differentiation into an adipocyte. Domest Anim Endocrinol.

Feuz, D. M., S. W. Fausti, and J. J. Wagner. 1993. Analysis of the efficiency of four marketing methods for slaughter cattle. Agribusiness 9: 453-463.

Fliers, E., F. Kreier, P. J. Voshol, L. M. Havekes, H. P. Sauerwein, A. Kalsbeek, R. M. Buijs, and J. A. Romijn. 2003. White adipose tissue: Getting nervous. J Neuroendocrinol 15: 1005-1010.

Frank, P. G., S. Pavlides, M. W. Cheung, K. Daumer, and M. P. Lisanti. 2008. Role of caveolin-1 in the regulation of lipoprotein metabolism. Am J Physiol Cell Physiol 295: C242-248.

Fujiwara, K., S. Takeuchi, K. Okamura-Ikeda, and Y. Motokawa. 2001. Purification, characterization, and cDNA cloning of lipoate-activating enzyme from bovine liver. J Biol Chem 276: 28819-28823.

Fukada, T., and N. K. Tonks. 2003. Identification of YB-1 as a regulator of PTP1B expression: Implications for regulation of insulin and cytokine signaling. Embo J 22: 479-493.

G. P. Holloway, J. J. F. P. Luiken., J. F. C. Glatz, L. L. Spriet, A. Bonen,. 2008. Contribution of fat/CD36 to the regulation of skeletal muscle fatty acid oxidation: An overview. Acta Physiologica 194: 293-309.

Gaillard, D., M. Wabitsch, B. Pipy, and R. Negrel. 1991. Control of terminal differentiation of adipose precursor cells by glucocorticoids. J Lipid Res 32: 569-579.

Galyean, G., L,. 1999. Restricted and programmed feeding of beef cattle - definitions, application, and research results. The Professional Animal Scientist 15: 1-6.

Garces, C., M. J. Ruiz-Hidalgo, J. Font de Mora, C. Park, L. Miele, J. Goldstein, E. Bonvini, A. Porras, and J. Laborda. 1997. Notch-1 controls the expression of fatty acid-activated transcription factors and is required for adipogenesis. J Biol Chem 272: 29729-29734.

Garcia, L. G., K. L. Nicholson, T. W. Hoffman, T. E. Lawrence, D. S. Hale, D. B. Griffin, J. W. Savell, D. L. Vanoverbeke, J. B. Morgan, K. E. Belk, T. G. Field, J. A. Scanga, J. D. Tatum, and G. C. Smith. 2008. National beef quality audit-2005: Survey of targeted cattle and carcass characteristics related to quality, quantity, and value of fed steers and heifers. J Anim Sci 86: 3533-3543.

Gardan, D., I. Louveau, and F. Gondret. 2007. Adipocyte- and heart-type fatty acid binding proteins are both expressed in subcutaneous and intramuscular porcine (sus scrofa) adipocytes. Comparative Biochemistry and Physiology Part B: Biochemistry and Molecular Biology 148: 14-19.

Gardan, D., J. Mourot, and I. Louveau. 2008. Decreased expression of the IGF-II gene during porcine adipose cell differentiation. Mol Cell Endocrinol 292: 63-68.

Glatz, J. F., and G. J. van der Vusse. 1996. Cellular fatty acid-binding proteins: Thier function and physiological significance. Prog. Lipid Res 35: 243-282.

Glaubiger, G., and R. J. Lefkowitz. 1977. Elevated beta-adrenergic receptor number after chronic propranolol treatment. Biochem Biophys Res Commun 78: 720-725.

Granneman, J. G. 1992. Effects of agonist exposure on the coupling of beta 1 and beta 3 adrenergic receptors to adenylyl cyclase in isolated adipocytes. J Pharmacol Exp Ther 261: 638-642.

Granneman, J. G. 2001. The putative beta4-adrenergic receptor is a novel state of the beta1-adrenergic receptor. Am J Physiol Endocrinol Metab 280: E199-202.

Granneman, J. G., and H. P. Moore. 2008. Location, location: Protein trafficking and lipolysis in adipocytes. Trends Endocrinol Metab 19: 3-9.

Gregoire, F. M., C. M. Smas, and H. S. Sul. 1998. Understanding adipocyte differentiation. Physiological Reviews 78: 783-809.

Greife, H. A., G. Klotz, and F. Berschauer. 1989. Effects of the phenethanolamine clenbuterol on protein and lipid metabolism in growing rats. J. Appl. Physiol. 61:19–27.

Gurevich, E. V., and V. V. Gurevich. 2006. Arrestins: Ubiquitous regulators of cellular signaling pathways. Genome Biol 7: 236.

Gwartney, B. L., C. R. Calkins, R. J. Rasby, R. A. Stock, B. A. Vieselmeyer, and J. A. Gosey. 1996. Use of expected progeny differences for marbling in beef: Carcass and palatability traits. J Anim Sci 74: 1014-1022.

Hajri, T., and N. A. Abumrad. 2002. Fatty acid transport across membranes: Relevance to nutrition and metabolic pathology. Annu Rev Nutr 22: 383-415.

Harper, G. S., and D. W. Pethick. 2004. How might marbling begin? Australian Journal of Experimental Agriculture 44: 653-662.

Hausdorff, W. P., M. G. Caron, and R. J. Lefkowitz. 1990a. Turning off the signal: Desensitization of beta-adrenergic receptor function. FASEB J 4: 2881-2889.

Hausdorff, W. P., M. G. Caron, and R. J. Lefkowitz. 1990b. Turning off the signal: Desensitization of beta-adrenergic receptor function [published erratum appears in FASEB J, 1990 Sep;4(12):3049]. The FASEB Journal 4: 2881-2889.

Hausman, G. J., M. V. Dodson, K. Ajuwon, M. Azain, K. M. Barnes, L. L. Guan, Z. Jiang, S. P. Poulos, R. D. Sainz, S. Smith, M. Spurlock, J. Novakofski, M. E. Fernyhough, and W. G. Bergen. 2009. Board-invited review: The biology and regulation of preadipocytes and adipocytes in meat animals. J Anim Sci 87: 1218-1246.

Hausman, G. J., and R. L. Richardson. 2004. Adipose tissue angiogenesis. J Anim Sci 82: 925-934.

Hausman, G. J., and G. B. Thomas. 1984. The development of the inner layer of backfat in fetal and young pigs. J Anim Sci 58: 1550-1560.

Hedrick, H. B., J. A. Paterson, A. G. Matches, J. D. Thomas, R. E. Morrow, W. G. Stringer, and R. J. Lipsey. 1983. Carcass and palatability characteristics of beef produced on pasture, corn silage and corn grain. J Anim Sci 57: 791-801.

Hegde, P., R. Qi, K. Abernathy, C. Gay, S. Dharap, R. Gaspard, J. E. Hughes, E. Snesrud, N. Lee, and J. Quackenbush. 2000. A concise guide to cDNA microarray analysis. BioTechniques 29 (3): 548-562.

Hertz, R., I. Berman, D. Keppler, and J. Bar-Tana. 1996. Activation of gene transcription by prostacyclin analogues is mediated by the peroxisome-proliferators-activated receptor (PPAR). Eur J Biochem 235: 242-247.

Hettinger, A. M., M. R. Allen, B. R. Zhang, D. W. Goad, J. R. Malayer, and R. D. Geisert. 2001. Presence of the acute phase protein, bikunin, in the endometrium of gilts during estrous cycle and early pregnancy. Biol Reprod 65: 507-513.

Hilton, G. G., J. L. Montgomery, C. R. Krehbiel, D. A. Yates, J. P. Hutcheson, W. T. Nichols, M. N. Streeter, J. R. Blanton, Jr., and M. F. Miller. 2009. Effects of feeding zilpaterol hydrochloride with and without monensin and tylosin on carcass cutability and meat palatability of beef steers. J Anim Sci 87: 1394-1406.

Homer, C., D. A. Knight, L. Hananeia, P. Sheard, J. Risk, A. Lasham, J. A. Royds, and A. W. Braithwaite. 2005. Y-box factor YB1 controls p53 apoptotic function. Oncogene 24: 8314-8325.

Hood, R. L., and C. E. Allen. 1973. Cellularity of bovine adipose tissue. J Lipid Res 14: 605-610.

Hyman, B., L. Stool, A. Spector. 1982. Prostaglandin production by 3T3-L1 cells in culture. Biochem Biophys Acta 713: 375-385.

Igal, R. A., S. Wang, M. Gonzalez-Baro, and R. A. Coleman. 2001. Mitochondrial glycerol phosphate acyltransferase directs the incorporation of exogenous fatty acids into triacylglycerol. J Biol Chem 276: 42205-42212.

Inka Lindner, D. R., Ulf Helwig, Inke Nitz, Jochen Hampe, Stefan Schreiber, Jürgen Schrezenmeir, Frank Döring. 2006. The l513s polymorphism in medium-chain acyl-CoA synthetase 2 (MACS2) is associated with risk factors of the metabolic syndrome in a caucasian study population. Molecular Nutrition & Food Research 50: 270-274.

Intervet. Inc. 2006. Freedom of information summary original new animal drug application, Zilmax (zilpaterol hydrochloride), NADA 141-258, Millsboro, DE, http://www.fda.gov/cvm/FOI/141-258o08102006.pdf.

Intervet. Inc. 2007. Material safety data sheet number 01173, Zilmax, product code 708481, Millsboro, DE.

Izadpanah, R., C. Trygg, C. Kriedt, and B. Bunnell. 2006. Biological comparison of mesenchymal stem cells derived from bone marrow and adipose tissue. Mol Ther 13: S134-S135.

Michal J.J., Z.W. Zhang , C.T. Gaskins , Z. Jiang. 2006. The bovine fatty acid binding protein 4 gene is significantly associated with marbling and subcutaneous fat depth in Wagyu and Limousin F2 crosses. Animal Genetics 37: 400-402.

Jayakumar, A., S. S. Chirala, and S. J. Wail. 1997. Human fatty acid synthase: Assembling recombinant halves of the fatty acid synthase subunit protein reconstitutes enzyme activity. Proceedings of the National Academy of Science 94 (23): 123326-112330.

Jell, J., S. Merali, M. L. Hensen, R. Mazurchuk, J. A. Spernyak, P. Diegelman, N. D. Kisiel, C. Barrero, K. K. Deeb, L. Alhonen, M. S. Patel, and C. W. Porter. 2007. Genetically altered expression of spermidine/spermine n1-acetyltransferase affects fat metabolism in mice via acetyl-CoA. J Biol Chem 282: 8404-8413.

Jenkins-Kruchten, A. E., A. Bennaars-Eiden, J. R. Ross, W. J. Shen, F. B. Kraemer, and D. A. Bernlohr. 2003. Fatty acid-binding protein-hormone-sensitive lipase interaction. Fatty acid dependence on binding. J Biol Chem 278: 47636-47643.

Jenkins, T. 1992. Symposium: Advances in ruminant lipid metabolism. J Dairy Sci 76: 3851-3863.

Jenson, S.D., R. S. Robetorye, S.D. Bohling, J. A. Schumacher, J. W. Morgan, M. S. Kim, K. S. J. Elenitoba-Johnson. 2003. Validation of cDNA microarray gene expression data obtained from linearly amplified RNA. J Clin Pathol: Mol Pathol 56: 307-312.

Jiang, Z., J. Michal, D. Tobey, T. Daniels, D. Rule, and M. MacNeil. 2008. Significant associations of stearoyl-CoA desaturase (SCD1) gene with fat deposition and composition in skeletal muscle. Int J Biol Sci 4: 345-351.

Johnson, H. C. 2006a. Impact of beef quality on market signals transmitted by grid pricing. Journal of Agricultural and Applied Economics 38(1), http://findarticles.com/p/articles/mi_qa4051/is_200604/ai_n17172165.

Johnson, H. C., and C. E. Ward. 2005. Market signals transmitted by grid pricing. Journal of Agricultural and Resource Economics 30; 561-579.

Johnson, M. 2006b. Molecular mechanisms of beta(2)-adrenergic receptor function, response, and regulation. J Allergy Clin Immunol 117: 18-24.

Joshi, A. K., A. Witkowski, and S. Smith. 1997. Mapping of functional interactions between domains of the animal fatty acid synthase by mutant complementation in vitro. Biochemistry 36: 2316-2322.

Joshi, A. K., A. Witkowski, and S. Smith. 1998. The malonyl/acetyltransferase and beta-ketoacyl synthase domains of the animal fatty acid synthase can cooperate with the acyl carrier protein domain of either subunit. Biochemistry 37: 2515-2523.

Jurica, M. S., A. Mesecar, P. J. Heath, W. Shi, T. Nowak, and B. L. Stoddard. 1998. The allosteric regulation of pyruvate kinase by fructose-1,6-bisphosphate. Structure 6: 195-210.

Jurie, C., I. Cassar-Malek, M. Bonnet, C. Leroux, D. Bauchart, P. Boulesteix, D. W. Pethick, and J. F. Hocquette. 2007. Adipocyte fatty acid-binding protein and mitochondrial enzyme activities in muscles as relevant indicators of marbling in cattle. J Anim Sci 85: 2660-2669.

Kadowaki, T., and T. Yamauchi. 2005. Adiponectin and adiponectin receptors. Endocr Rev 26: 439-451.

Kadrmas, J. L., and M. C. Beckerle. 2004. The LIM domain: From the cytoskeleton to the nucleus. Nat Rev Mol Cell Biol 5: 920-931.

Kanehisa, M., and S. Goto. 2000. Kegg: Kyoto encyclopedia of genes and genomes. Nucleic Acids Res 28: 27-30.

Karagianni, P., and J. Wong.2007. HDAC3: Taking the SMRT-N-CoRrect road to repression. Oncogene 26: 5439-5449.

Karbowska, J., and Z. Kochan. 2006. Role of adiponectin in the regulation of carbohydrate and lipid metabolism. Journal of Physiology and Pharmacology 57, Supp 6: 103-113.

Kasuya, F., M. Hiasa, Y. Kawai, K. Igarashi, and M. Fukui. 2001. Inhibitory effect of quinolone antimicrobial and nonsteroidal anti-inflammatory drugs on a medium chain acyl-CoA synthetase. Biochemical Pharmacology 62: 363-367.

Kawaguchi, N., C. Sundberg, M. Kveiborg, B. Moghadaszadeh, M. Asmar, N. Dietrich, C. K. Thodeti, F. C. Nielsen, P. Moller, A. M. Mercurio, R. Albrechtsen, and U. M. Wewer. 2003. Adam12 induces actin cytoskeleton and extracellular matrix reorganization during early adipocyte differentiation by regulating {beta}1 integrin function. Journal of Cell Science 116: 3893-3904.

Kern, C., T. Meyer, S. Droux, D. Schollmeyer, and C. Miculka. 2009. Synthesis and pharmacological characterization of beta-2-adrenergic agonist enantiomers: Zilpaterol. Journal of Medicinal Chemistry 52: 1773-1777.

Kliewer, S. A., J. M. Lenhard, T. M. Willson, I. Patel, D. C. Morris, and J. M. Lehmann. 1995. A prostaglandin J2 metabolite binds peroxisome proliferator-activated receptor gamma and promotes adipocyte differentiation. Cell 83: 813-819.

Kobilka, B. K., and X. Deupi. 2007. Conformational complexity of G-protein-coupled receptors. Trends Pharmacol Sci 28: 397-406.

Kohout, T. A., and R. J. Lefkowitz. 2003. Regulation of G protein-coupled receptor kinases and arrestins during receptor desensitization. Mol Pharmacol 63: 9-18.

Kouznetsova, T. N., E. V. Ignatieva, D. Y. Oshchepkov, Y. V. Kondrakhin, A. V. Katokhin, M.Y.Shamanina, and V. A. Mordvinov. 2006. A gene network of adipocyte lipid metabolism: Coordinated interactions between the transcription factors SREBP, LXRα and PPARγ. In: The Fifth International Conference on Bioinformatics of Genome Regulation and Structure, Novosibirsk, Russia, July 16-22, 2006. p 137-140.

Kraemer, F. B., and W. J. Shen. 2002. Hormone-sensitive lipase: Control of intracellular tri-(di-) acylglycerol and cholesteryl ester hydrolysis. J Lipid Res 43: 1585-1594.

Kroetz, D. L., and D. C. Zeldin. 2002. Cytochrome p450 pathways of arachidonic acid metabolism. Curr Opin Lipidol 13: 273-283.

Kugler, W., and M. Lakomek. 2000. Glucose-6-phosphate isomerase deficiency. Best Practice & Research Clinical Haematology 13: 89-101.

Labrecque, B., O. Mathieu, V. Bordignon, B. D. Murphy, and M.-F. Palin. 2009. Identification of differentially expressed genes in a porcine *in vivo* model of adipogenesis using suppression subtractive hybridization. Comparative Biochemistry and Physiology Part D: Genomics and Proteomics 4: 32-44.

Lai, E. C. 2004. Notch signaling: Control of cell communication and cell fate. Development 131: 965-973.

Lane, M. D., Q. Q. Tang, and M. S. Jiang. 1999. Role of the CCAAT enhancer binding proteins (C/EBPS) in adipocyte differentiation. Biochem Biophys Res Commun 266: 677-683.

Langin, D., G. Travernier, M. Lafontan. 1995. Regulation of beta3-adrenoceptor expression in white fat cells. Fundam Clin Pharmacol 9: 97-106.

Lanzara, R. 2005. Optimal agonist/antagonist combinations maintain receptor response by preventing rapid beta1-adrenergic receptor desensitization. International Journal of Pharmacolcogy 1 (2): 122-131.

Lardy, G. 1998. Systems of backgrounding beef cattle. publication no. AS-1151, North Dakota State University. http://www.ag.ndsu.edu/pubs/beef.html.

Lee, K. B., J. H. Jeon, I. Choi, O. Y. Kwon, K. Yu, and K. H. You. 2008a. Clusterin, a novel modulator of TGF-beta signaling, is involved in smad2/3 stability. Biochem Biophys Res Commun 366: 905-909.

Lee, S. H., Y. M. Cho, B. S. Kim, N. K. Kim, Y. H. Choy, K. H. Kim, D. Yoon, S. K. Im, S. J. Oh, and E. W. Park. 2008b. Identification of marbling-related candidate genes in m. Longissimus dorsi of high- and low marbled Hanwoo (Korean native cattle) steers. BMB Rep 41: 846-851.

Lee, S. H., E. W. Park, Y. M. Cho, S. K. Kim, J. H. Lee, J. T. Jeon, C. S. Lee, S. K. Im, S. J. Oh, J. M. Thompson, and D. Yoon. 2007. Identification of differentially expressed genes related to intramuscular fat development in the early and late fattening stages of Hanwoo steers. J Biochem Mol Biol 40: 757-764.

Lefkowitz, R. J., B. K. Kobilka, J. L. Benovic, M. Bouvier, S. Cotecchia, W. P. Hausdorff, H. G. Dohlman, J. W. Regan, and M. G. Caron. 1988. Molecular biology of adrenergic receptors. Cold Spring Harb Symp Quant Biol 53 Pt 1: 507-514.

Lefkowitz, R. J., J.-P. Sun, and A. K. Shukla. 2008. A crystal clear view of the [beta]2-adrenergic receptor. Nat Biotech 26: 189-191.

Leheska, J. M., J. L. Montgomery, C. R. Krehbiel, D. A. Yates, J. P. Hutcheson, W. T. Nichols, M. Streeter, J. R. Blanton, Jr., and M. F. Miller. 2009. Dietary zilpaterol hydrochloride. Carcass composition and meat palatability of beef cattle. J Anim Sci 87: 1384-1393.

Lehnert, S. A., A. Reverter, K. A. Byrne, Y. Wang, G. S. Nattrass, N. J. Hudson, and P. L. Greenwood. 2007. Gene expression studies of developing bovine Longissimus muscle from two different beef cattle breeds. BMC Dev Biol 7: 95.

Lengi, A., and B. Corl. 2007. Identification and characterization of a novel bovine stearoyl-CoA desaturase isoform with homology to human scd5. Lipids 42: 499-508.

Lengi, A. J., and B. A. Corl. 2008. Comparison of pig, sheep and chicken SCD5 homologs: Evidence for an early gene duplication event. Comparative Biochemistry and Physiology Part B: Biochemistry and Molecular Biology 150: 440-446.

Leonardsson, G. R., J. H. Steel, M. Christian, V. Pocock, S. Milligan, J. Bell, P.-W. So, G. Medina-Gomez, A. Vidal-Puig, R. White, and M. G. Parker. 2004. Nuclear receptor corepressor RIP140 regulates fat accumulation. Proc Natl Acad Sci U.S.A.101: 8437-8442.

Li, T., G. Ma, H. Cai, D. L. Price, and P. C. Wong. 2003. Nicastrin is required for assembly of presenilin/gamma-secretase complexes to mediate notch signaling and for processing and trafficking of beta-amyloid precursor protein in mammals. J Neurosci 23: 3272-3277.

Lijnen, H. R., B. Van Hoef, H. R. Lu, and D. J. Gallacher. 2008. Rofecoxib impairs adipose tissue development in a Murine model of nutritionally induced obesity. Thromb Haemost 100: 338-342.

Lin, J., L. Ding, R. Jin, H. Zhang, L. Cheng, X. Qin, J. Chai, and Q. Ye. 2009. Four and a half LIM domains 1 (fhl1) and receptor interacting protein of 140 kda (rip140) interact and cooperate in estrogen signaling. The International Journal of Biochemistry & Cell Biology 41: 1613-1618.

Lin, K. C., H. R. Cross, and S. B. Smith. 1992. Esterification of fatty acids by bovine intramuscular and subcutaneous adipose tissues. Lipids 27: 111-116.

Liu, J., S. M. DeYoung, M. Zhang, M. Zhang, A. Cheng, and A. R. Saltiel. 2005. Changes in integrin expression during adipocyte differentiation. Cell Metabolism 2: 165-177.

Livak, K. J., and T. D. Schmittgen. 2001. Analysis of relative gene expression data using real-time quantitative PCR and the $2^{-\Delta\Delta ct}$ method. Methods 25: 402-408.

Lopez-Liuchi, J. V., and C. A. Meier. 1998. PPARgamma: From adipose tissue to the atherosclerotic plaque. Eur J Endocrinol 139: 363-364.

López, I. P., F. I. Milagro, A. Martí, M. J. Moreno-Aliaga, J. A. Martínez, and C. De Miguel. 2004. Gene expression changes in rat white adipose tissue after a high-fat diet determined by differential display. Biochemical and Biophysical Research Communications 318: 234-239.

Lu, H., C. Boustany-Kari, A. Daugherty and L. Cassis. 2007. Angiotensin II increases adipose angiotensinogen expression. Am J Physiol Endocrinol Metab 292: E1280-E1287

Lu, S., K. Nishimura, M. Hossain, M. Jisaka, T. Nagaya, K. Yokota. 2004. Regulation and role of arachidonate cascade during changes in life cycle of adipocytes. Appl Biochem and Biotech 118: 133-153.

Lu, S., and M. C. Archer. 2007. Celecoxib decreases fatty acid synthase expression via down-regulation of c-JUN n-terminal kinase-1. Exp Biol Med 232: 643-653.

Luiken, J. J., D. J. Dyck, X. X. Han, N. N. Tandon, Y. Arumugam, J. F. Glatz, and A. Bonen. 2002. Insulin induces the translocation of the fatty acid transporter fat/CD36 to the plasma membrane. Am J Physiol Endocrinol Metab 282: E491-495.

Lynch, G., and J. Ryall. 2008. Role of beta-adrenoceptor signaling in skeletal muscle: Implications for muscle wasting disease. Physiol Rev 88: 729-767.

MacDougald, O. A., and M. D. Lane. 1995. Transcriptional regulation of gene expression during adipocyte differentiation. Annual Review of Biochemistry 64: 345-373.

Maglott, D., J. Ostell, K. D. Pruitt, and T. Tatusova. 2005. Entrez gene: Gene-centered information at NCBI. Nucleic Acids Res 33: D54-58.

Maglott, D., J. Ostell, K. D. Pruitt, and T. Tatusova. 2007. Entrez gene: Gene-centered information at NCBI. Nucleic Acids Res 35: D26-31.

Maier, T., S. Jenni, and N. Ban. 2006. Architecture of mammalian fatty acid synthase at 4.5 Å resolution. Science 311: 1258-1262.

Majerus, P. W. 1967. Acyl carrier protein; structural requirements for function in fatty acid synthesis. J Biol Chem 242: 2325-2332.

Majerus, P. W., A. W. Alberts, and P. R. Vagelos. 1965. Acyl carrier protein. VII. The primary structure of the substrate-binding site. J Biol Chem 240: 4723-4726.

Mandell, I. B., J. G. Buchanan-Smith, and C. P. Campbell. 1998. Effects of forage vs. grain feeding on carcass characteristics, fatty acid composition, and beef quality in Limousin-cross steers when time on feed is controlled. J Anim Sci 76: 2619-2630.

Marcinkiewicz, A., D. Gauthier, A. Garcia, and D. L. Brasaemle. 2006. The phosphorylation of serine 492 of Perilipin A directs lipid droplet fragmentation and dispersion. J Biol Chem 281: 11901-11909.

Martel-Pelletier, J., J. P. Pelletier, and H. Fahmi. 2004. New insights into prostaglandin biology. J Rheumatol 31: 14-16.

Martinez-Botas, J., Y. Suarez, A. J. Ferruelo, D. Gomez-Coronado, and M. A. Lasuncion. 1999. Cholesterol starvation decreases p34(cdc2) kinase activity and arrests the cell cycle at G2. Faseb J 13: 1359-1370.

Mashek, D. G., K. E. Bornfeldt, R. A. Coleman, J. Berger, D. A. Bernlohr, P. Black, C. C. DiRusso, S. A. Farber, W. Guo, N. Hashimoto, V. Khodiyar, F. A. Kuypers, L. J. Maltais, D. W. Nebert, A. Renieri, J. E. Schaffer, A. Stahl, P. A. Watkins, V. Vasiliou, and T. T. Yamamoto. 2004. Revised nomenclature for the mammalian long-chain acyl-CoA synthetase gene family. J Lipid Res 45: 1958-1961.

Masseroli, M., D. Martucci, and F. Pinciroli. 2004. GFINDer: Genome function integrated discoverer through dynamic annotation, statistical analysis, and mining. Nucleic Acids Res 32: W293-300.

Matsumoto, K., and A. P. Wolffe. 1998. Gene regulation by Y-box proteins: Coupling control of transcription and translation. Trends in Cell Biology 8: 318-323.

Mattevi, A., M. Bolognesi, and G. Valentini. 1996. The allosteric regulation of pyruvate kinase. FEBS Letters 389: 15-19.

May, S. G., J. W. Savell, D. K. Lunt, J. J. Wilson, J. C. Laurenz, and S. B. Smith. 1994. Evidence for preadipocyte proliferation during culture of subcutaneous and intramuscular adipose tissues from Angus and Wagyu crossbred steers. J. Anim Sci. 72: 3110-3117.

McCurdy, M. P. 2006. Effect of winter growing programs on subsequent feedlot performance, body composition, carcass merit, organ mass and oxygen consumption in beef steers, Ph.D. Dissertation, Animal Science Department, Oklahoma State University, Stillwater, OK.

McDonald, P., R. A. Edwards, J. F. D. Greenhalgh, and C. A. Morgan. 2002. Animal nutrition. 6th ed. Pearson/ Prentice Hall, Edinburgh Gate, Harlow, England.

McGrath, M. J., D. L. Cottle, M. A. Nguyen, J. M. Dyson, I. D. Coghill, P. A. Robinson, M. Holdsworth, B. S. Cowling, E. C. Hardeman, C. A. Mitchell, and S. Brown. 2006. Four and a half LIM protein 1 binds myosin-binding protein c and regulates myosin filament formation and sarcomere assembly. J Biol Chem 281: 7666-7683.

McNeel, R. L., and H. J. Mersmann. 1995. Beta-adrenergic receptor subtype transcripts in porcine adipose tissue. J Anim Sci 73: 1962-1971.

McNeel, R. L., and H. J. Mersmann. 1999. Distribution and quantification of beta1-, beta2-, and beta3-adrenergic receptor subtype transcripts in porcine tissues. J Anim Sci 77: 611-621.

Mehats, C., C. B. Andersen, M. Filopanti, S. L. C. Jin, and M. Conti. 2002. Cyclic nucleotide phosphodiesterases and their role in endocrine cell signaling. Trends in Endocrinology and Metabolism 13: 29-35.

Mersmann, H. J. 1995. Species variation in mechanisms for modulation of growth by beta-adrenergic receptors. J. Nutr. 125: 1777S-1782S.

Mersmann, H. J. 1998. Overview of the effects of beta-adrenergic receptor agonists on animal growth including mechanisms of action. J Anim Sci 76: 160-172.

Mersmann, H. J. 2001. Beta-adrenergic receptor modulation of adipocyte metabolism and growth. J. Anim Sci. 80 (E Suppl. 1): E24-E29.

Mersmann, H. J. 2002. Beta-adrenergic receptor modulation of adipocyte metabolism and growth. J. Anim Sci. 80: E24-29.

Metzger, D., T. Imai, M. Jiang, R. Takukawa, B. Desvergne, W. Wahli, and P. Chambon. 2005. Functional role of RXRS and PPARγ in mature adipocytes. Prostaglandins, Leukotrienes and Essential Fatty Acids 73: 51-58.

Meyer, H. H., and L. M. Rinke. 1991. The pharmacokinetics and residues of clenbuterol in veal calves. J Anim Sci 69: 4538-4544.

Michal, J. J., Z. W. Zhang, C. T. Gaskins, and Z. Jiang. 2006. The bovine fatty acid binding protein 4 gene is significantly associated with marbling and subcutaneous fat depth in Wagyu x Limousin F2 crosses. Anim Genet 37: 400-402.

Miller, C. W., D. A. Casimir, and J. M. Ntambi. 1996. The mechanism of inhibition of 3T3-l1 preadipocyte differentiation by prostaglandin F2alpha. Endocrinology 137: 5641-5650.

Miller, M. F., H. R. Cross, D. K. Lunt, and S. B. Smith. 1991. Lipogenesis in acute and 48-hour cultures of bovine intramuscular and subcutaneous adipose tissue explants. J. Anim Sci 69: 162-170.

Mills, S. E. 2002a. Biological basis of the ractopamine response. J Anim Sci 80: E28-32.

Mills, S. E. 2002b. Implications of feedback regulation of beta-adrenergic signaling. J Anim Sci 80 (E. Suppl. 1): E30-E35.

Mills, S. E., M. E. Spurlock, and D. J. Smith. 2003. Beta-adrenergic receptor subtypes that mediate ractopamine stimulation of lipolysis. J Anim Sci 81: 662-668.

Minge, C. E., R. L. Robker, and R. J. Norman. 2008. PPAR gamma: Coordinating metabolic and immune contributions to female fertility. PPAR Res 2008: 243791.

Miyazaki, M., S. M. Bruggink, and J. M. Ntambi. 2006. Identification of mouse palmitoyl-coenzyme a delta9-desaturase. J Lipid Res 47: 700-704.

Miyazaki, M., and J. M. Ntambi. 2003. Role of stearoyl-coenzyme a desaturase in lipid metabolism. Prostaglandins Leukot Essent Fatty Acids 68: 113-121.

Moldes, M., Y. Zuo, R. F. Morrison, D. Silva, B. H. Park, J. Liu, and S. R. Farmer. 2003. Peroxisome-proliferator-activated receptor gamma suppresses WNT/beta-catenin signaling during adipogenesis. Biochem J 376: 607-613.

Moloney, D. J., V. M. Panin, S. H. Johnston, J. Chen, L. Shao, R. Wilson, Y. Wang, P. Stanley, K. D. Irvine, R. S. Haltiwanger, and T. F. Vogt. 2000. Fringe is a glycosyltransferase that modifies notch. Nature 406: 369-375.

Montgomery, J. L., C. R. Krehbiel, J. J. Cranston, D. A. Yates, J. P. Hutcheson, W. T. Nichols, M. N. Streeter, D. T. Bechtol, E. Johnson, T. TerHune, and T. H. Montgomery. 2009a. Dietary zilpaterol hydrochloride. I. Feedlot performance and carcass traits of steers and heifers. J Anim Sci 87: 1374-1383.

Montgomery, J. L., C. R. Krehbiel, J. J. Cranston, D. A. Yates, J. P. Hutcheson, W. T. Nichols, M. N. Streeter, R. S. Swingle, and T. H. Montgomery. 2009b. Effects of dietary zilpaterol hydrochloride on feedlot performance and carcass characteristics of beef steers fed with and without monensin and tylosin. J Anim Sci 87: 1013-1023.

Moody, D., D. Hancock, and D. Anderson. 2000. Phenethanolamine repartitioning agents. In: J. D'Mello (ed.) Farm animal metabolism and nutrition. p 65-96. CABI Publishing, Wallinford, Oxon, UK.

Moody, W. B., and R. G. Cassens. 1968. A quantitative and morphological study of bovine Longissimus fat cells. Journal of Food Science 33: 47-55.

Moore, C. A., S. K. Milano, and J. L. Benovic. 2007. Regulation of receptor trafficking by GRKs and arrestins. Annu Rev Physiol 69: 451-482.

Moore, K. K., P. A. Ekeren, D. K. Lunt, and S. B. Smith. 1991. Relationship between fatty acid-binding protein activity and marbling scores in bovine Longissimus muscle. J Anim Sci 69: 1515-1521.

Morita, I. 2002. Distinct functions of COX-1 and COX-2. Prostaglandins Other Lipid Mediat 68-69: 165-175.

Morris, C. A., N. G. Cullen, B. C. Glass, D. L. Hyndman, T. R. Manley, S. M. Hickey, J. C. McEwan, W. S. Pitchford, C. D. Bottema, and M. A. Lee. 2007. Fatty acid synthase effects on bovine adipose fat and milk fat. Mamm Genome 18: 64-74.

Murphy, J. E., P. R. Tedbury, S. Homer-Vanniasinkam, J. H. Walker, and S. Ponnambalam. 2005. Biochemistry and cell biology of mammalian scavenger receptors. Atherosclerosis 182: 1-15.

Murray, R. K., D. K. Granner, P. A. Mayes, and V. W. Rodwell. 2003. Biosynthesis of fatty acids. In: J. Foltin, J. Ransom and J. M. Oransky (eds.) Harper's illustrated biochemistry 26th ed. p 173-179. McGraw-Hill, New York, Chicago, San Francisco.

Nakajima, I., T. Yamaguchi, K. Ozutsumi, and H. Aso. 1998. Adipose tissue extracellular matrix: Newly organized by adipocytes during differentiation. Differentiation 63: 193-200.

Nam, I. S., and P. C. Garnsworthy. 2007. Factors influencing biohydrogenation and conjugated linoleic acid production by mixed rumen fungi. J Microbiol 45: 199-204.

Négrel R., D. Gaillard and G. Ailhaud. 1989. Prostacyclin as a potent effector of adipose differentiation. Biochem J 257: 399-405.

Nekrasov, M. P., M. P. Ivshina, K. G. Chernov, E. A. Kovrigina, V. M. Evdokimova, A. A. Thomas, J. W. Hershey, and L. P. Ovchinnikov. 2003. The mRNA-binding protein yb-1 (p50) prevents association of the eukaryotic initiation factor eif4g with mRNA and inhibits protein synthesis at the initiation stage. J Biol Chem 278: 13936-13943.

Nettles, K. W. 2008. Insights into PPARγ from structures with endogenous and covalently bound ligands. Nat Struct Mol Biol 15: 893-895.

Neves, S. R., P. T. Ram, and R. Iyengar. 2002. G protein pathways. Science 296: 1636.

Nichols, A. M., Y. Pan, A. Herreman, B. K. Hadland, B. De Strooper, R. Kopan, and S. S. Huppert. 2004. Notch pathway is dispensable for adipocyte specification. Genesis 40: 40-44.

Nichols, J. T., A. Miyamoto, and G. Weinmaster. 2007. Notch signaling-constantly on the move. Traffic 8: 959-969.

Nicholson, A. C., M. Febbraio, J. Han, R. L. Silverstein, and D. P. Hajjar. 2000. CD36 in atherosclerosis. The role of a class B macrophage scavenger receptor. Ann N Y Acad Sci 902: 128-131.

Niranen, K. 2006. Consequences of spermine synthase of spermidine/spermine n^1-acetyltransferase deficiency in polyamine metabolism. Doctoral dissertation, University of Kuopio, Kuopio, Finland.

Noguchi, T., H. Inoue, and T. Tanaka. 1986. The M1- and M2-type isozymes of rat pyruvate kinase are produced from the same gene by alternative RNA splicing. J Biol Chem 261: 13807-13812.

Novakofski, J. 2004. Adipogenesis: Usefulness of *in vitro* and *in vivo* experimental models. J Anim Sci 82: 905-915.

Nygaard, V., and E. Hovig. 2006. Options available for profiling small samples: A review of sample amplification technology when combined with microarray profiling. Nucleic Acids Res 34: 996-1014.

Ohsaki, H., T. Sawa, S. Sasazaki, K. Kano, M. Taniguchi, F. Mukai, and H. Mannen. 2007. Stearoyl-CoA desaturase mRNA expression during bovine adipocyte differentiation in primary culture derived from Japanese Black and Holstein cattle. Comp Biochem Physiol A Mol Integr Physiol 148: 629-634.

Ory, D. S. 2004. The niemann-pick disease genes: Regulators of cellular cholesterol homeostasis. Trends in Cardiovascular Medicine 14: 66-72.

Otto, T., and M. Lane. 2005. Adipose development: From stem cell to adipocyte. Critical Reviews in Biochemistry and Molecular Biology 40: 229-242.

Page, K. A., D. L. Hartzell, C. Li, A. L. Westby, M. A. Della-Fera, M. J. Azain, T. D. Pringle, and C. A. Baile. 2004. β adrenergic receptor agonists increase apoptosis of adipose tissue in mice. Domestic Animal Endocrinology 26: 23-31.

Parker, M. T., and E. W. Gerner. 2002. Polyamine-mediated post-transcriptional regulation of COX-2. Biochimie 84: 815-819.

Parr, T., R. G. Bardsley, R. S. Gilmour, and P. J. Buttery. 1992. Changes in calpain and calpastatin mRNA induced by beta-adrenergic stimulation of bovine skeletal muscle. Eur J Biochem 208: 333-339.

Patil, P. N., C. Li, V. Kumari, and J. P. Hieble. 2008. Analysis of efficacy of chiral adrenergic agonists. Chirality 20: 529-543.

Paunesku, T., S. Mittal, M. ProtiÄ, J. Oryhon, S. V. Korolev, A. Joachimiak, and G. E. Woloschak. 2001. Proliferating cell nuclear antigen (PCNA): Ringmaster of the genome. International Journal of Radiation Biology 77: 1007-1021.

Peel, D. S. 2000. Stocker cattle: Shock absorber for the beef industry, Visions, 75: p 1-6. Oklahoma State University Agriculture Economics Department, Oklahoma State University, Stillwater, OK.

Peel, D. S. 2006. Economics of stocker production. Veterinary Clinics of North America: Food Animal Practice 22: 271-296.

Pegg, A. E. 2008. Spermidine/spermine-n1-acetyltransferase: A key metabolic regulator. AJP - Endocrinology and Metabolism 294: E995-1010.

Peters, A. R. 1989. Beta-agonists as repartitioning agents: A review. Vet Rec 124: 417-420.

Petersen, R. K., C. Jorgensen, A. C. Rustan, L. Froyland, K. Muller-Decker, G. Furstenberger, R. K. Berge, K. Kristiansen, and L. Madsen. 2003. Arachidonic acid-dependent inhibition of adipocyte differentiation requires PKA activity and is associated with sustained expression of cyclooxygenases. J Lipid Res 44: 2320-2330.

Pethick, D. W., G. S. Harper, and V. H. Oddy. 2004. Growth, development and nutritional manipulation of marbling in cattle: A review. Australian Journal of Experimental Agriculture 44: 705-715.

Pette, D., and R. Staron. 2000. Myosin isoforms, muscle fiber types, and transitions. Microscopy Research and Technique 50: 500-509.

Pierleoni, C., F. Verdenelli, M. Castellucci, and S. Cinti. 1998. Fibronectins and basal lamina molecules expression in human subcutaneous white adipose tissue. Eur J Histochem 42: 183-188.

Pietri-Rouxel, F., and A. D. Strosberg. 1995. Pharmacological characteristics and species-related variations of beta 3-adrenergic receptors. Fundam Clin Pharmacol 9: 211-218.

Plascencia, A., N. Torrentera, and R. A. Zinn. 1999. Influence of the beta-agonist, zilpaterol, on growth performance and carcass characteristics of feedlot steers. In: Western Section Proceedings, American Society of Animal Science, Brigham Young University, Provo, Utah. June 9 -11. p 331 - 334.

Pringle, T. D., C. R. Calkins, M. Koohmaraie, and S. J. Jones. 1993. Effects over time of feeding a beta-adrenergic agonist to wether lambs on animal performance, muscle growth, endogenous muscle proteinase activities, and meat tenderness. J Anim Sci 71: 636-644.

Prusty, D., B. H. Park, K. E. Davis, and S. R. Farmer. 2002. Activation of MEK/ERK signaling promotes adipogenesis by enhancing peroxisome proliferator-activated receptor gamma (PPARgamma) and C/EBP alpha gene expression during the differentiation of 3T3-l1 preadipocytes. J Biol Chem 277: 46226-46232.

Pyatt, N., and L. Berger. 2005. Review: Potential effects of vitamins A and D on marbling deposition in beef cattle. The Professional Animal Scientist 21: 174-181.

Qiao, L., C. Zou, P. Shao, J. Schaack, P. F. Johnson, and J. Shao. 2008. Transcriptional regulation of fatty acid translocase/cd36 expression by CCAAT/enhancer-binding protein alpha. J Biol Chem 283: 8788-8795.

Quinkler, M., I. J. Bujalska, J. W. Tomlinson, D. M. Smith, and P. M. Stewart. 2006. Depot-specific prostaglandin synthesis in human adipose tissue: A novel possible mechanism of adipogenesis. Gene 380: 137-143.

Rakheja, D., M. J. Bennett, and B. B. Rogers. 2002. Long-chain l-3-hydroxyacyl-coenzyme A dehydrogenase deficiency: A molecular and biochemical review. Lab Invest 82: 815-824.

Rathmann R.J., J.M. Mehaffey , T.J. Baxa , W.T. Nichols, D.A.Yates, J.P. Hutcheson, J.C. Brooks, B.J. Johnson, M.F. Miller. 2009. Effects of duration of zilpaterol hydrochloride and days on the finishing diet on carcass cutability, composition, tenderness and skeletal muscle gene expression in feedlot steers. J. Anim Sci.June 5. [Epub ahead of print]

Razani, B., T. P. Combs, X. B. Wang, P. G. Frank, D. S. Park, R. G. Russell, M. Li, B. Tang, L. A. Jelicks, P. E. Scherer, and M. P. Lisanti. 2002. Caveolin-1-deficient mice are lean, resistant to diet-induced obesity, and show hypertriglyceridemia with adipocyte abnormalities. J Biol Chem 277: 8635-8647.

Rechler, M. M., and D. R. Clemmons. 1998. Regulatory actions of insulin-like growth factor-binding proteins. Trends Endocrinol Metab 9: 176-183.

Reginato, M. J., S. L. Krakow, S. T. Bailey, and M. A. Lazar. 1998. Prostaglandins promote and block adipogenesis through opposing effects on peroxisome proliferator-activated receptor gamma. J Biol Chem 273: 1855-1858.

Rhee, S. Y., V. Wood, K. Dolinski, and S. Draghici. 2008. Use and misuse of the gene ontology annotations. Nat Rev Genet 9: 509-515.

Rhoades, R. D., J. E. Sawyer, K. Y. Chung, M. L. Schell, D. K. Lunt, and S. B. Smith. 2007. Effect of dietary energy source on *in vitro* substrate utilization and insulin sensitivity of muscle and adipose tissues of Angus and Wagyu steers. J. Anim Sci. 85: 1719-1726.

Ricks, C. A., R. H. Dalrymple, P. K. Baker, and D. L. Ingle. 1984. Use of a β-agonist to alter fat and muscle deposition in steers. J. Anim Sci. 59: 1247-1255.

Ring, A., S. Le Lay, J. Pohl, P. Verkade, and W. Stremmel. 2006. Caveolin-1 is required for fatty acid translocase (fat/CD36) localization and function at the plasma membrane of mouse embryonic fibroblasts. Biochim Biophys Acta 1761: 416-423.

Roman, R. J., and M. Alonso-Galicia. 1999. P-450 eicosanoids: A novel signaling pathway regulating renal function. News Physiol Sci 14: 238-242.

Rosen, E. D. 2002. The molecular control of adipogenesis, with special reference to lymphatic pathology. Ann N Y Acad Sci 979: 143-158; discussion 188-196.

Rosen, E. D. 2005. The transcriptional basis of adipocyte development. Prostaglandins, Leukotrienes and Essential Fatty Acids 73: 31-34.

Rosen, E. D., C. H. Hsu, X. Wang, S. Sakai, M. W. Freeman, F. J. Gonzalez, and B. M. Spiegelman. 2002. C/EBPα induces adipogenesis through PPARgamma: A unified pathway. Genes Dev 16: 22-26.

Rosen, E. D., and O. A. MacDougald. 2006. Adipocyte differentiation from the inside out. Nat Rev Mol Cell Biol 7: 885-896.

Rosen, E. D., and B. M. Spiegelman. 2000. Molecular regulation of adipogenesis Annual Review of Cell and Developmental Biology 16: 145-171.

Ross, D. A., S. Hannenhalli, J. W. Tobias, N. Cooch, R. Shiekhattar, and T. Kadesch. 2006. Functional analysis of hes-1 in preadipocytes. Mol Endocrinol 20: 698-705.

Ross, D. A., P. K. Rao, and T. Kadesch. 2004. Dual roles for the notch target gene hes-1 in the differentiation of 3T3-l1 preadipocytes. Mol Cell Biol 24: 3505-3513.

Ross, J. W., T. K. Smith, C. R. Krehbiel, J. R. Malayer, U. DeSilva, J. B. Morgan, F. J. White, M. J. Hersom, G. W. Horn, and R. D. Geisert. 2005. Effects of grazing program and subsequent finishing on gene expression in different adipose tissue depots in beef steers. J Anim Sci 83: 1914-1923.

Rouse, G. H., and D. E. Wilson. 2001. Managing fat – the future of the beef industry, Iowa State University, Ames, Iowa.

Roy, R., L. Ordovas, P. Zaragoza, A. Romero, C. Moreno, J. Altarriba, and C. Rodellar. 2006. Association of polymorphisms in the bovine FASN gene with milk-fat content. Anim Genet 37: 215-218.

Rozen, S., and H. Skaletsky. 2000. Primer3 on the www for general users and for biologist programmers. In: S. Misener and S. Krawetz (eds.) Bioinformatics: Methods and protocols: Methods in molecular biology. p pp 365-386. Humana Press Totowa, NJ.

Rubin, C. S., A. Hirsch, C. Fung, and O. M. Rosen. 1978. Development of hormone receptors and hormonal responsiveness in vitro. Insulin receptors and insulin sensitivity in the preadipocyte and adipocyte forms of 3T3-l1 cells. J Biol Chem 253: 7570-7578.

Rule, D. C., Thornton, J. H., McGilliard A.D., and Betz, C. D. 1992. Effect of adipose tissue site, animal size, and fasting on lipolysis in bovine adipose tissue *in vitro*. Int. J. Biochem. 24 (5): 789-793.

Sainz, R. D., and R. F. Vernazza Paganini. 2004. Effects of different grazing and feeding periods on performance and carcass traits of beef steers. J Anim Sci 82: 292-297.

Schaake, S. L., G. C. Skelley, E. Halpin, L. W. Grimes, R. B. Brown, D. L. Cross, and C. E. Thompson. 1993. Carcass and meat sensory traits of steers finished on fescue and clover, summer forage, or for different periods in drylot. J Anim Sci 71: 3199-3205.

Schiaffino, S., and C. Reggiani. 1994. Myosin isoforms in mammalian skeletal muscle. J Appl Physiol 77: 493-501.

Schoonmaker, J. P., F. L. Fluharty, and S. C. Loerch. 2004. Effect of source and amount of energy and rate of growth in the growing phase on adipocyte cellularity and lipogenic enzyme activity in the intramuscular and subcutaneous fat depots of Holstein steers. J Anim Sci 82: 137-148.

Schroeder, T. C., J. Mintert, and C. E. Ward. 2003. Fed-cattle grid-pricing valuation: Recommendations for improvement Kansas State Research and Extension No. MF2637. Kansas State University, Manhattan, KS.

Scott, R. E., D. L. Florine, J. J. Wille, Jr., and K. Yun. 1982a. Coupling of growth arrest and differentiation at a distinct state in the G1 phase of the cell cycle: GD. Proc Natl Acad Sci U.S.A. 79: 845-849.

Serrero, G., N. M. Lepak, and S. P. Goodrich. 1992. Paracrine regulation of adipose differentiation by arachidonate metabolites: Prostaglandin F2 alpha inhibits early and late markers of differentiation in the adipogenic cell line 1246. Endocrinology 131: 2545-2551.

Seydoux, J., P. Muzzin, M. Moinat, W. Pralong, L. Girardier, and J. P. Giacobino. 1996. Adrenoceptor heterogeneity in human white adipocytes differentiated in culture as assessed by cytosolic free calcium measurements. Cell Signal 8: 117-122.

Sfeir, Z., A. Ibrahimi, E. Amri, P. Grimaldi, and N. Abumrad. 1997. Regulation of fat/CD36 gene expression: Further evidence in support of a role of the protein in fatty acid binding/transport. Prostaglandins Leukot Essent Fatty Acids 57: 17-21.

Shelver, W. L., and D. J. Smith. 2006. Tissue residues and urinary excretion of zilpaterol in sheep treated for 10 days with dietary zilpaterol. J Agric Food Chem 54: 4155-4161.

Shen, W. J., K. Sridhar, D. A. Bernlohr, and F. B. Kraemer. 1999. Interaction of rat hormone-sensitive lipase with adipocyte lipid-binding protein. Proc Natl Acad Sci U.S.A. 96: 5528-5532.

Shook, J., D. VanOverbeke, L. K. Inman, C. Krehbiel, B. Holland, M. Streeter, D. Yates, and G. Hilton. 2009. Effects of zilpaterol hydrochloride and zilpaterol hydrochloride withdrawal time on beef carcass cutability, composition and tenderness. J Anim Sci. in press.

Shu, G., Q. Y. Jiang, X. T. Zhu, H. X. Zhang, P. Gao, Y. L. Zhang, and X. Q. Wang. 2008. Identification of porcine fatty acid translocase: High-level transcript in intramuscular fat. J Anim Physiol Anim Nutr (Berl) 92: 562-568.

Sillence, M. N. 2004. Technologies for the control of fat and lean deposition in livestock. The Veterinary Journal 167: 242-257.

Sillence, M. N., J. Hooper, G. H. Zhou, Q. Liu, and K. J. Munn. 2005. Characterization of porcine beta1- and beta2-adrenergic receptors in heart, skeletal muscle, and adipose tissue, and the identification of an atypical beta-adrenergic binding site. J Anim Sci 83: 2339-2348.

Sillence, M. N., and M. L. Matthews. 1994. Classical and atypical binding sites for beta-adrenoceptor ligands and activation of adenylyl cyclase in bovine skeletal muscle and adipose tissue membranes. Br J Pharmacol 111: 866-872.

Silverstein, F. E., G. Faich, J. L. Goldstein, L. S. Simon, T. Pincus, A. Whelton, R. Makuch, G. Eisen, N. M. Agrawal, W. F. Stenson, A. M. Burr, W. W. Zhao, J. D. Kent, J. B. Lefkowith, K. M. Verburg, and G. S. Geis. 2000. Gastrointestinal toxicity with celecoxib vs. nonsteroidal anti-inflammatory drugs for osteoarthritis and rheumatoid arthritis: The class study: A randomized controlled trial. Celecoxib long-term arthritis safety study. JAMA 284: 1247-1255.

Singh, N. K., H. S. Chae, I. H. Hwang, Y. M. Yoo, C. N. Ahn, S. H. Lee, H. J. Lee, H. J. Park, and H. Y. Chung. 2007. Transdifferentiation of porcine satellite cells to adipoblasts with ciglitizone. J. Anim Sci. 85: 1126-1135.

Sissom, E. K., C. D. Reinhardt, J. P. Hutcheson, W. T. Nichols, D. A. Yates, R. S. Swingle, and B. J. Johnson. 2007. Response to ractopamine-HCL in heifers is altered by implant strategy across days on feed. J Anim Sci 85: 2125-2132.

Smith, D. J. 1998. The pharmacokinetics, metabolism, and tissue residues of β-adrenergic agonists in livestock. J Anim Sci 76: 173-194.

Smith, E. R., and J. Storch. 1999. The adipocyte fatty acid-binding protein binds to membranes by electrostatic interactions. J Biol Chem 274: 35325-35330.

Smith, G. C., J. W. Savell, J. B. Morgan, and T. E. Lawrence. 2006a. Report of the June-September, 2005 national beef quality audit: A new benchmark for the U.S. beef industry. 38th Annual Beef Improvement Federation Meeting, Choctaw, Mississippi, April 18-21.

Smith, S. 1995. Substrate utilization in ruminant adipose tissue. In: S. Smith and D. Smith (eds.) The biology of fat in meat animals. pg 166-186. ASAS, Champaign IL.

Smith, S. 2006. Structural biology. Architectural options for a fatty acid synthase. Science 311: 1251-1252.

Smith, S., D. Lunt, K. Chung, C. Choi, R. Tume, and M. Zembayashi. 2006b. Adiposity, fatty acid composition, and delta-9 desaturase activity during growth in beef cattle. Animal Science Journal 77: 478-486.

Smith, S., A. Yang, T. Larsen, and R. Tume. 1998. Positional analysis of triacylglycerols from bovine adipose tissue lipids varying in degree of unsaturation. Lipids 33: 197-207.

Smith, S. B., and J. D. Crouse. 1984. Relative contributions of acetate, lactate and glucose to lipogenesis in bovine intramuscular and subcutaneous adipose tissue. J Nutr 114: 792-800.

Smith, S. B., H. Kawachi, C. B. Choi, C. W. Choi, G. Wu, and J. E. Sawyer. 2009. Cellular regulation of bovine intramuscular adipose tissue development and composition. J Anim Sci 87: E72-82.

Smith, S. B., and D. K. Lunt. 2007. Marbling: Management of cattle to maximize the deposition of intramuscular adipose tissue. In: Plains Nutrition Council, Publication No. AREC 07-20, Texas A&M University Agricultural Research and Extension Center, San Antonio TX, March 29-30

Smith, S. B., D. K. Lunt, and M. Zembayashi. 2000. Intramuscular fat deposition: The physiological process and the potential for its manipulation. In: 2000 Plains Nutrition Council Spring Conference, Texas A&M Research and Extension Center, Amarillo. p 1-12.

Soberman, R. J., and P. Christmas. 2003. The organization and consequences of eicosanoid signaling. J Clin Invest 111: 1107-1113.

Song-Yu Yang, X.Y. He. H. Schultz. 2005. 3-hydroxyacyl-coa dehydrogenase and short chain 3-hydroxyacyl-coa dehydrogenase in human health and disease. FEBS Journal 272: 4874-4883.

Spiegelman, B. M. 1998. PPAR-gamma: Adipogenic regulator and thiazolidinedione receptor. Diabetes 47: 507-514.

Spurlock, M. E., J. C. Cusumano, S. Q. Ji, D. B. Anderson, C. K. Smith, 2nd, D. L. Hancock, and S. E. Mills. 1994. The effect of ractopamine on beta-adrenoceptor density and affinity in porcine adipose and skeletal muscle tissue. J Anim Sci 72: 75-80.

Spurlock, M. E., J. C. Cusumano, and S. E. Mills. 1993. The affinity of ractopamine, clenbuterol, and l-644,969 for the beta-adrenergic receptor population in porcine adipose tissue and skeletal muscle membrane. J Anim Sci 71: 2061-2065.

Stachel, C. S., W. Radeck, and P. Gowik. 2003. Zilpaterol-a new focus of concern in residue analysis. Analytica Chimica Acta 493: 63-67.

Stoffel, B., and H. H. Meyer. 1993. Effects of the beta-adrenergic agonist clenbuterol in cows: Lipid metabolism, milk production, pharmacokinetics, and residues. J Anim Sci 71: 1875-1881.

Storch, J., and L. McDermott. 2008. Structural and functional analysis of fatty acid-binding proteins. J Lipid Res. S126-S131.

Storch, J., and A. E. Thumser. 2000. The fatty acid transport function of fatty acid-binding proteins. Biochim Biophys Acta 1486: 28-44.

Strosberg, A. D. 1993. Structure, function, and regulation of adrenergic receptors. Protein Sci 2: 1198-1209.

Su, X., and N. A. Abumrad. 2009. Cellular fatty acid uptake: A pathway under construction. Trends Endocrinol Metab 20: 72-77.

Sugimoto, Y., H. Tsuboi, Y. Okuno, S. Tamba, S. Tsuchiya, G. Tsujimoto, and A. Ichikawa. 2004. Microarray evaluation of EP4 receptor-mediated prostaglandin E2 suppression of 3T3-l1 adipocyte differentiation. Biochemical and Biophysical Research Communications 322: 911-917.

Sumner, J. M., and J. P. McNamara. 2007. Expression of lipolytic genes in the adipose tissue of pregnant and lactating Holstein dairy cows. J. Dairy Sci. 90: 5237-5246.

Swatland, H. J. 2009. Growth and structure of farm animals: Fat. Department of Animal and Poultry Science, University of Guelph, Canada, http://www.aps.uoguelph.ca/~swatland/ch2_0.htm, Accessed Feb. 1, 2009

Tan, N. S., N. S. Shaw, N. Vinckenbosch, P. Liu, R. Yasmin, B. Desvergne, W. Wahli, and N. Noy. 2002. Selective cooperation between fatty acid binding proteins and peroxisome proliferator-activated receptors in regulating transcription. Mol Cell Biol 22: 5114-5127.

Tanaka, T., N. Yoshida, T. Kishimoto, and S. Akira. 1997. Defective adipocyte differentiation in mice lacking the C/EBPβ and/or C/EBPδ gene. Embo J 16: 7432-7443.

Tang, Q. Q., T. C. Otto, and M. D. Lane. 2003a. Mitotic clonal expansion: A synchronous process required for adipogenesis. Proc Natl Acad Sci U.S.A. 100: 44-49.

Tang, Q. Q., T. C. Otto, and M. D. Lane. 2003b. CCAAT/enhancer-binding protein beta is required for mitotic clonal expansion during adipogenesis. Proc Natl Acad Sci U.S.A. 100: 850-855.

Taniguchi, M., H. Mannen, K. Oyama, Y. Shimakura, A. Oka, H. Watanabe, T. Kojima, M. Komatsu, G. S. Harper, and S. Tsuji. 2004. Differences in stearoyl-CoA desaturase mRNA levels between Japanese Black and Holstein cattle. Livestock Production Science 87: 215-220.

Tasken, K., and E. M. Aandahl. 2004. Localized effects of camp mediated by distinct routes of protein kinase A. Physiol Rev 84: 137-167.

Tchkonia, T., M. Lenburg, T. Thomou, N. Giorgadze, G. Frampton, T. Pirtskhalava, A. Cartwright, M. Cartwright, J. Flanagan, I. Karagiannides, N. Gerry, R. A. Forse, Y. Tchoukalova, M. D. Jensen, C. Pothoulakis, and J. L. Kirkland. 2007. Identification of depot-specific human fat cell progenitors through distinct expression profiles and developmental gene patterns. Am J Physiol Endocrinol Metab 292: E298-307.

Thomson, D. U., and B. J. White. 2006. Backgrounding beef cattle. Veterinary Clinics of North America: Food Animal Practice 22: 373-398.

Tilvis, R., P. Kovanen, and T. Miettinen. 1982. Metabolism of squalene in human fat cells. Demonstration of a two-pool system. J. Biol. Chem. 257: 10300-10305.

Tjabringa, G. S., B. Zandieh-Doulabi, M. N. Helder, M. Knippenberg, P. I. Wuisman, and J. Klein-Nulend. 2008. The polyamine spermine regulates osteogenic differentiation in adipose stem cells. J Cell Mol Med 12: 1710-1717.

Tong, L. 2005. Acetyl-coenzyme a carboxylase: Crucial metabolic enzyme and attractive target for drug discovery. Cellular and Molecular Life Sciences 62: 1784-1803.

Tontonoz, P., E. Hu, and B. M. Spiegelman. 1994. Stimulation of adipogenesis in fibroblasts by PPARγ 2, a lipid-activated transcription factor. Cell 79: 1147-1156.

Tontonoz, P., E. Hu, and B. M. Spiegelman. 1995. Regulation of adipocyte gene expression and differentiation by peroxisome proliferator activated receptor gamma. Curr Opin Genet Dev 5: 571-576.

Tontonoz, P., and B. M. Spiegelman. 2008. Fat and beyond: The diverse biology of PPARgamma. Annu Rev Biochem 77: 289-312.

Tsai, Y. S., and N. Maeda. 2005. PPARgamma: A critical determinant of body fat distribution in humans and mice. Trends Cardiovasc Med 15: 81-85.

USDA. 2001. United states standards for grades of carcass beef. No. 2005. United States Department of Agriculture. http://www.ams.usda.gov/AMSv1.0/getfile?dDocName=STELDEV3002979

USDA. 2007. Livestock slaughtered under federal inspection, United States Department of Agriculture (USDA), Washington, DC. http://usda.mannlib.cornell.edu/usda/nass/LiveSlauSu//2000s/2008/LiveSlauSu-03-07-2008_revision.pdf

Utrera, A. R., and L. D. Van Vleck. 2004. Heritability estimates for carcass traits of cattle: A review. Genet Mol Res 3: 380-394.

Van Liefde, I., A. Van Ermen, A. van Witzenburg, N. Fraeyman, and G. Vauquelin. 1994. Species and strain-related differences in the expression and functionality of beta-adrenoceptor subtypes in adipose tissue. Arch Int Pharmacodyn Ther 327: 69-86.

vanBeek, E., A. Bakker, P. Kruyt, M. Hofker, W. Saris, and J. Keijer. 2007. Intra- and inter-individual variation in gene expression in human adipose tissue Pflügers Archiv European Journal of Physiology 453 (6): 851-861.

Vasconcelos, J. T., R. J. Rathmann, R. R. Reuter, J. Leibovich, J. P. McMeniman, K. E. Hales, T. L. Covey, M. F. Miller, W. T. Nichols, and M. L. Galyean. 2008. Effects of duration of zilpaterol hydrochloride feeding and days on the finishing diet on feedlot cattle performance and carcass traits. J Anim Sci. 2133-2141.

Vassaux, G., D. Gaillard, C. Darimont, G. Ailhaud, and R. Negrel. 1992. Differential response of preadipocytes and adipocytes to prostacyclin and prostaglandin E2: Physiological implications. Endocrinology 131: 2393-2398.

Vázquez-Vela, M. E. F., N. Torres, and A. R. Tovar. 2008. White adipose tissue as endocrine organ and its role in obesity. Archives of Medical Research 39: 715-728.

Verhoeckx, K. C. M., R. P. Doornbos, J. Greef, R. F. Witkamp, and R. J. T. Rodenburg. 2005. Inhibitory effects of the beta-2-adrenergic receptor agonist zilpaterol on the LPS-induced production of TNF-alpha; *in vitro* and *in vivo*. Journal of Veterinary Pharmacology and Therapeutics 28: 531-537.

Vernon, R. (Editor), 1981. Lipid metabolism in the adipose tissue of ruminant animals. In. Christie W. W., (ed.) Lipid metabolism in ruminant animals. Pergamon Press (Oxford, New York): 279-362.

Vieselmeyer, B. A., R. J. Rasby, B. L. Gwartney, C. R. Calkins, R. A. Stock, and J. A. Gosey. 1996. Use of expected progeny differences for marbling in beef: I. Production traits. J Anim Sci 74: 1009-1013.

Villagra, A., N. Ulloa, X. Zhang, Z. Yuan, E. Sotomayor, and E. Seto. 2007. Histone deacetylase 3 down-regulates cholesterol synthesis through repression of lanosterol synthase gene expression. J Biol Chem 282: 35457-35470.

Voet, D., and J. G. Voet. 2004a. Glycolysis, In. D. Harris and P. Fitzgerald (eds.) Biochemistry 3rd ed. p 581-625. John Wiley and Sons, Inc. Hoboken, New Jersey.

Voet, D., and J. G. Voet. 2004b. Lipid metabolism In: D. Harris and P. Fitzgerald (eds.) Biochemistry 3rd ed. p 909-984. John Wiley and Sons, Inc., Hoboken, New Jersey.

Voet, D., and J. G. Voet. 2004c. Other pathways of carbohydrate metabolism. In. D. Harris and P. Fitzgerald (eds.) Biochemistry 3rd ed. p 843-870. John Wiley and Sons, Inc. Hoboken, New Jersey.

Voet, D., and J. G. Voet. 2004d. Signal transduction. In: D. Harris and P. Fitzgerald (eds.) Biochemsitry 3rd ed. p 657-725. John Wiley and Sons, Inc., Hoboken, New Jersey.

Walker, D. K., E. C. Titgemeyer, E. K. Sissom, K. R. Brown, J. J. Higgins, G. A. Andrews, and B. J. Johnson. 2007. Effects of steroidal implantation and ractopamine-HCL on nitrogen retention, blood metabolites and skeletal muscle gene expression in Holstein steers. Journal of Animal Physiology and Animal Nutrition 91: 439-447.

Wallace, H. M., A. V. Fraser, and A. Hughes. 2003. A perspective of polyamine metabolism. Biochem J 376: 1-14.

Wan, R., J. Du, L. Ren, and Q. Meng. 2009. Selective adipogenic effects of propionate on bovine intramuscular and subcutaneous preadipocytes. Meat Science 82 (3): 372-378.

Wang, M. D., R. S. Kiss, V. Franklin, H. M. McBride, S. C. Whitman, and Y. L. Marcel. 2007. Different cellular traffic of LDL-cholesterol and acetylated LDL-cholesterol leads to distinct reverse cholesterol transport pathways. J Lipid Res 48: 633-645.

Wang , P., E. Mariman, J. Renes, and J. Keijer. 2008. The secretory function of adipocytes in the physiology of white adipose tissue. J Cell Physiol 216: 3-13.

Wang, Y., A. Reverter, H. Mannen, M. Taniguchi, G. Harper, K. Oyama, K. Byrne, A. Oka, S. Tsuji, and S. Lehnert. 2005a. Transcriptional profiling of muscle tissue in growing Japanese Black cattle to identify genes involved with the development of intramuscular fat. Australian Journal of Experimental Agriculture 40 (8): 809-820

Wang, Y., A. Reverter, S. H. Tan, N. De Jager, R. Wang, S. M. McWilliam, L. M. Cafe, P. L. Greenwood, and S. A. Lehnert. 2008. Gene expression patterns during intramuscular fat development in cattle. J Anim Sci. 87(1):119-130.

Wang, Y. H., N. I. Bower, A. Reverter, S. H. Tan, N. De Jager, R. Wang, S. M. McWilliam, L. M. Cafe, P. L. Greenwood, and S. A. Lehnert. 2009. Gene expression patterns during intramuscular fat development in cattle. J Anim Sci 87: 119-130.

Wang, Y. H., K. A. Byrne, A. Reverter, G. S. Harper, M. Taniguchi, S. M. McWilliam, H. Mannen, K. Oyama, and S. A. Lehnert. 2005b. Transcriptional profiling of skeletal muscle tissue from two breeds of cattle. Mamm Genome 16: 201-210.

Warbrick, E. 2000. The puzzle of PCNA's many partners. Bioessays 22: 997-1006.

Weisiger, R. A. 2002. Cytosolic fatty acid binding proteins catalyze two distinct steps in intracellular transport of their ligands. Mol Cell Biochem 239: 35-43.

Weng, H., and P. Ayoubi. 2004. GPAP (genepix pro auto-processor) for online preprocessing, normalization and statistical analysis of primary microarray data. in preparation.

Wheeler, T. L., and M. Koohmaraie. 1992. Effects of the beta-adrenergic agonist l644,969 on muscle protein turnover, endogenous proteinase activities, and meat tenderness in steers. J Anim Sci 70: 3035-3043.

Whitehurst, G. B., D. C. Beitz, M. A. Pothoven, W. R. Ellison, and M. H. Crump. 1978. Lactate as a precursor of fatty acids in bovine adipose tissue. J Nutr 108: 1806-1811.

Whitehurst, G., D. Beitz, D. Cianzio and D. Topel. 1981. Fatty acid synthesis from lactate in growing cattle. J Nut 111: 1454-1461.

Williams, C. S., and R. N. DuBois. 1996. Prostaglandin endoperoxide synthase: Why two isoforms? Am J Physiol 270: G393-400.

Winterholler, S. J., G. L. Parsons, C. D. Reinhardt, J. P. Hutcheson, W. T. Nichols, D. A. Yates, R. S. Swingle, and B. J. Johnson. 2007. Response to ractopamine-hydrogen chloride is similar in yearling steers across days on feed. J Anim Sci 85: 413-419.

Winterholler S.J., G.L. Parsons , D.K. Walker , M.J. Quinn , J.S. Drouillard , B.J. Johnson. 2008 Effect of feedlot management system on response to ractopamine-HCl in yearling steers. J Anim Sci 86(9): 2401-2414.

Witkowski, A., A. Ghosal, A. K. Joshi, H. E. Witkowska, F. J. Asturias, and S. Smith. 2004. Head-to-head coiled arrangement of the subunits of the animal fatty acid synthase. Chemistry & Biology 11: 1667-1676.

Wolfe, L. 1982. Eicosanoids: Prostaglandins, thromboxanes, leukotrienes, and other derivatives of carbon-20 unsaturated fatty acids. Journal of Neurochemistry 38: 1-14.

Wood, J. D., M. Enser, A. V. Fisher, G. R. Nute, R. I. Richardson, and P. R. Sheard. 1999. Manipulating meat quality and composition. Proc Nutr Soc 58: 363-370.

Wooll, J. O., R. H. E. Friesen, M. A. White, S. J. Watowich, R. O. Fox, J. C. Lee, and E. W. Czerwinski. 2001. Structural and functional linkages between subunit interfaces in mammalian pyruvate kinase. Journal of Molecular Biology 312: 525-540.

Wu, Z., P. Puigserver, and B. M. Spiegelman. 1999a. Transcriptional activation of adipogenesis. Curr Opin Cell Biol 11: 689-694.

Wu, Z., E. D. Rosen, R. Brun, S. Hauser, G. Adelmant, A. E. Troy, C. McKeon, G. J. Darlington, and B. M. Spiegelman. 1999b. Cross-regulation of c/EBP alpha and PPAR gamma controls the transcriptional pathway of adipogenesis and insulin sensitivity. Mol Cell 3: 151-158.

Xu, S., B. Benoff, H. L. Liou, P. Lobel, and A. M. Stock. 2007. Structural basis of sterol binding by NPC2, a lysosomal protein deficient in niemann-pick type C2 disease. J Biol Chem 282: 23525-23531.

Yan, H., A. Kermouni, M. Abdel-Hafez, and D. C. Lau. 2003. Role of cyclooxygenases COX-1 and COX-2 in modulating adipogenesis in 3T3-l1 cells. J Lipid Res 44: 424-429.

Yancopoulos, G. D., S. Davis, N. W. Gale, J. S. Rudge, S. J. Wiegand, and J. Holash. 2000. Vascular-specific growth factors and blood vessel formation. Nature 407: 242-248.

Yang, X. J., E. Albrecht, K. Ender, R. Q. Zhao and J. Wegner. 2006. Computer image analysis of intramuscular adipocytes and marbling in the Longissimus muscle of cattle. J Anim Sci 84:3251-3258.

Yang, L. T., J. T. Nichols, C. Yao, J. O. Manilay, E. A. Robey, and G. Weinmaster. 2005. Fringe glycosyltransferases differentially modulate notch1 proteolysis induced by delta1 and jagged1. Mol Biol Cell 16: 927-942.

Yang, S. H., Tohru Matsui, Hiroyuki Kawachi, Tomoya Yamada, Naoto Nakanish and Hideo Yano. 2003. Fat depot-specific differences in leptin mRNA expression and its relation to adipocyte size in steers. Animal Science Journal 74: 17–21.

Yang, Y. H., S. Dudoit, P. Luu, D. M. Lin, V. Peng, J. Ngai, and T. P. Speed. 2002. Normalization for cDNA microarray data: A robust composite method addressing single and multiple slide systematic variation. Nucleic Acids Res 30 (4): e15.

Yang, Y. H., S. Dudoit, P. Luu, and T. P. Speed. 2001. Normalization for cDNA microarray data. In: SPIE BiOS; Society of Photographic Instrumentation Engineers, International Biomedical Optics Symposium San Jose, CA

Yang, A., T. W. Larsen, S. B. Smith, and R. K. Tume. 1999. Delta9 desaturase activity in bovine subcutaneous adipose tissue of different fatty acid composition. Lipids 34: 971-978.

Yang, Y. T., and M. A. McElligott. 1989. Multiple actions of beta-adrenergic agonists on skeletal muscle and adipose tissue. Biochem J 261: 1-10.

Yen, C. L., M. Monetti, B. J. Burri, and R. V. Farese, Jr. 2005. The triacylglycerol synthesis enzyme DGAT1 also catalyzes the synthesis of diacylglycerols, waxes, and retinyl esters. J Lipid Res 46: 1502-1511.

Yu, S. S., R. J. Lefkowitz, and W. P. Hausdorff. 1993. Beta-adrenergic receptor sequestration. A potential mechanism of receptor resensitization. J Biol Chem 268: 337-341.

Zhang, S., T. J. Knight, J. M. Reecy, and D. C. Beitz. 2008. DNA polymorphisms in bovine fatty acid synthase are associated with beef fatty acid composition. Anim Genet 39: 62-70.

Zhang, S., T. J. Knight, J. M. Reecy, A. H. Trenkle, and D. C. Beitz. 2007. DNA polymorphisms in the thioesterase domain of fatty acid synthase are associated with fatty acid composition of Longissimus dorsi muscle of Angus cattle. The FASEB Journal 21: A1120.

Zhang, X., Y. Ozawa, H. Lee, Y. D. Wen, T. H. Tan, B. E. Wadzinski, and E. Seto. 2005. Histone deacetylase 3 (HDAC3) activity is regulated by interaction with protein serine/threonine phosphatase 4. Genes Dev 19: 827-839.

Zheng, W., F. Sun, M. Bartlam, X. Li, R. Li, and Z. Rao. 2007. The crystal structure of human isopentenyl diphosphate isomerase at 1.7 å resolution reveals its catalytic mechanism in isoprenoid biosynthesis. Journal of Molecular Biology 366: 1447-1458.

Zimmerman, A. W., and J. H. Veerkamp. 2002. New insights into the structure and function of fatty acid-binding proteins. Cell Mol Life Sci 59: 1096-1116.

Zuk, P. A., M. Zhu, P. Ashjian, D. A. De Ugarte, J. I. Huang, H. Mizuno, Z. C. Alfonso, J. K. Fraser, P. Benhaim, and M. H. Hedrick. 2002. Human adipose tissue is a source of multipotent stem cells. Mol Biol Cell 13: 4279-4295.

APPENDICES

Appendices Table A1

Clone ID, Gene Symbol, Gene Name, Entrez Gene ID, dEST ID, GenBank Accession number, M-value, GO/KEGG ID, and GO term/KEGG pathway for the genes in Initial and each diet of the Growing Phase.

Clone ID	Gene Symbol	Gene Name	Entrez Gene ID	dbEST_Id	GenBank Accn	M-Value				(GO)/Kegg Path	Term/Pathway
						INT	WP	SF	PF		
Adipose Related											
a1d11	ACSM1	Acyl-CoA synthetase medium-chain family member 1 [Bos taurus]	282576	46400009	ES343884	-1.26	-1.19	-1.40	-1.37	00650	Butanoate metabolism
a1e11	ELOVL5	ELOVL family member 5, elongation of long chain fatty acids (FEN1/Elo2, SUR4/Elo3-like, yeast) [Bos taurus]	617293	46400023	ES343898	-0.56	-0.82	-1.33	-1.18	01040	Biosynthesis of unsaturated Fas
a1f09	CLU	Clusterin [Bos taurus]	280750	46400043	ES343918	-1.42	-0.94	-1.05	-0.67	(GO:0008219)	Cell Death
a2c10	DGAT2	Diacylglycerol O-acyltransferase homolog 2 (mouse) [Bos taurus]	404129	46400128	ES344003	-1.28	-2.74	-2.82	-1.95	00561 00830	Glycerolipid metabolism Retinol metabolism
a2f05	GPAM	Mitochondrial glycerol phosphate acyltransferase [Bos taurus]	497202	46400165	ES344040	-1.37	-1.08	-1.01	-1.48	00561 00564	Glycerolipid metabolism Glycerophospholipid metabolism
a2f07	CD36	CD36 molecule (thrombospondin receptor) [Bos taurus]	281052	46400170	ES344045	-1.30	-1.86	-2.07	-2.26	04920 03320 04512 04640	Adipocytokine signaling pathway PPAR signaling pathway ECM-receptor interaction Hematopoietic cell lineage
f5e12	FABP4	Fatty acid binding protein 4, adipocyte [Bos taurus]	281759	46400286	ES344161	-3.07	-2.34	-2.10	-3.02	03320	PPAR signaling pathway
f5f13	SAT1	Spermidine/spermine N1-acetyltransferase 1 [Bos taurus]	508861	46400314	ES344189	1.61	1.00	1.07	0.19	(GO:0008415)	Acyltransferase activity
f5k13	SCD	Stearoyl-CoA desaturase (delta-9-desaturase) [Bos taurus]	280924	46400413	ES344288	-2.49	-2.65	-2.51	-1.18	03320 01040	PPAR signaling pathway Biosynthesis of unsaturated FAs
f5l20	ADIPOQ	Adiponectin, C1Q and collagen domain containing [Bos taurus]	282865	46400433	ES344308	-2.91	-2.37	-1.87	-2.49	03320 04920	PPAR signaling pathway Adipocytokine signaling pathway
f5n20	NPC2	Niemann-Pick disease, type C2 [Bos taurus]	280815	46400479	ES344354	0.83	0.77	0.37	1.01	(GO:0042632)	Cholesterol homeostasis
f6k07	PLD1	Predicted: Phospholipase D1, phosphatidylcholine-specific [Homo sapiens]	5337	46400615	ES344490	-1.51	-1.2	-1.26	-1.5	00565 00564 04912	Ether lipid metabolism Glycerophospholipid metabolism GnRH signaling pathway
f7b22	CAV1	Caveolin 1, caveolae protein, 22kDa [Bos taurus]	281040	46400688	ES344563	-0.75	-0.91	-0.63	-0.65	04510	Focal adhesion
f8c02	PTGS2	Predicted: Prostaglandin-endoperoxide synthase 2 (prostaglandin G/H synthase & cyclooxygenase) [Bos taurus]	282023	46400821	ES344696	-1.49	-1.47	-1.13	-1.76	00590	Arachidonic acid metabolism
f8c05	TM7SF2	Transmembrane 7 superfamily member 2 [Bos taurus]	282384	46400823	ES344698	1.63	1.08	0.63	0.22	00100	Biosynthesis of steroids
f8g23	MSR1	Macrophage scavenger receptor 1 [Bos taurus]	281311	46400898	ES344773	-1.25	-1.29	-1.52	-0.14	(GO:0006817) (GO:0006898)	Phosphate transport Receptor-mediated endocytosis
g1g18	LPL	Lipoprotein lipase [Bos taurus]	280843	46401068	ES344943	-0.66	-0.69	-0.77	-1.24	00561 03320	Glycerolipid metabolism PPAR signaling pathway
g2j05	CXCL16	Chemokine (C-X-C motif) ligand 16 [Bos taurus]	511671	46401209	ES345084	-2.86	-2.52	-1.82	-2.79	04060	Cytokine-cytokine receptor interaction
g3e21	HADH	Hydroxyacyl-Coenzyme A dehydrogenase [Bos taurus]	613570	50172310	EX656787	-1.06	-0.82	-0.87	-1.35	(GO:0006631)	Fatty acid metabolism
g3g05	ACSL1	Acyl-CoA synthetase long-chain family member 1 [Bos taurus]	537161	50172312	EX656789	-0.06	-1.17	-0.74	-1.42	00071 03320 04920	Fatty acid metabolism PPAR signaling pathway Adipocytokine signaling pathway
g4g06	LYPLA1	Lysophospholipase I [Bos taurus]	539992	46401299	ES345174	1.17	0.92	0.31	0.05	(GO:0006631)	Fatty acid metabolic process
g4h03	APOE	Apolipoprotein E [Bos taurus]	281004	46401312	ES345187	-1.28	-0.78	-0.87	-1.28	01510	Neurodegenerative Diseases
g4j10	IDI1	Isopentenyl-diphosphate delta isomerase 1 [Bos taurus]	514293	46401348	ES345223	-0.14	1.08	0.28	0.64	00100 00900	Biosynthesis of steroids Terpenoid biosynthesis
Apoptosis/Cell Death											
f5o23	GCLC	Glutamate-cysteine ligase, catalytic subunit [Bos taurus] (Anti-apoptosis, Cell Redox Homeostasis)	512468	46400499	ES344374	-1.55	-1.13	-1.20	-1.97	(GO:0006916)	Aniti-apoptosis
f7l20	CLPTM1L	CLPTM1-like [Bos taurus]	506200	46400761	ES344636	0.93	1.10	0.71	1.53	(GO:0006915)	Apoptosis
g1m22	DNASE1	Deoxyribonuclease I [Bos taurus]	282217	46401119	ES344994	0.61	0.47	0.16	1.02	(GO:0006915)	Apoptosis
g4h07	PEA15	Phosphoprotein enriched in astrocytes 15 [Bos taurus]	510586	46401315	ES345190	1.20	1.09	0.94	0.41	(GO:0042981)	Regulation of apoptosis
Binding											
a2b04	CFL2	Cofilin 2 (muscle) [Bos taurus]	539332	46400102	ES343977	0.86	1.03	0.69	0.99	04360 04810	Axon guidance Regulation of actin cytoskeleton
a2d01	EGFL7	EGF-like-domain, multiple 7 [Bos taurus]	613671	46400129	ES344004	-0.41	-0.36	-0.77	-1.50	(GO:0005509)	Ca binding
a2d02	CKB	Creatine kinase, brain [Bos taurus]	516210	46400130	ES344005	2.59	2.64	1.63	0.76	00330	Arginine and proline metabolism
f5b11	BCAM	Basal cell adhesion molecule (Lutheran blood group) [Bos taurus]	282862	46400224	ES344099	0.64	0.99	0.65	1.00	(GO:0005515)	Protein binding
f5c12	SPTAN1	Predicted: similar to spectrin, alpha, non-erythrocytic 1 (alpha-fodrin) [Bos taurus]	540108	46400244	ES344119	0.49	0.96	0.79	0.97	(GO:0005509)	Ca binding
f5h18	ZMYM4	Zinc finger, MYM-type 4 [Bos taurus]	529962	46400361	ES344236	0.85	0.99	0.50	1.13	(GO:0008270) (GO:0005179)	Zn binding Hormone activity
f5i10	RNH1	Ribonuclease/angiogenin inhibitor 1 [Bos taurus]	517087	46400377	ES344252	0.65	0.66	0.49	1.17	(GO:0005515)	Protein binding
f5k15	CCDC75	Coiled-coil domain containing 75 [Bos taurus]	512655	46400414	ES344289	-1.53	-1.35	-1.08	-1.73	(GO:0003676)	binding nucleic acids
f6f08	ZDHHC3	Zinc finger, DHHC-type containing 3 [Bos taurus]	506728	46400572	ES344447	0.87	1.19	0.65	1.09	(GO:0008270)	Zn binding
f6f23	ZCCHC7	Zinc finger, CCHC domain containing 7 [Bos taurus]	511821	46400576	ES344451	-1.35	-1.08	-0.92	-1.56	(GO:0003676)	binding nucleic acids
f6k04	PDK4	Pyruvate dehydrogenase kinase, isozyme 4 [Bos taurus]	507367	46400613	ES344488	0.94	0.50	0.76	0.24	(GO:0005524)	ATP binding
f6k21	GSN	Gelsolin (amyloidosis, Finnish type) [Bos tauru]	535077	46400620	ES344495	-1.05	-1.01	-0.72	-0.80	04810	Regulation of actin cytoskeleton

Clone ID	Gene Symbol	Gene Name	Entrez Gene ID	dbEST_Id	GenBank Accn	M-Value				(GO)/Kegg Path	Term/Pathway
						INT	WP	SF	PF		
f6p17	ATP11B	ATPase, class VI, type 11B [Homo sapiens]	23200	46400673	ES344548	-1.43	-1.35	-1.22	-1.99	(GO:0005524) (GO:0004012)	ATP binding Phospholipid-translocating ATPase activity
f8b05	ABCG2	ATP-binding cassette, sub-family G (WHITE), member 2 [Bos taurus]	536203	46400813	ES344688	-1.68	-1.34	-1.08	-1.63	02010	
f8c15	SPARC	Secreted protein, acidic, cysteine-rich (osteonectin) [Bos taurus]	282077	46400831	ES344706	-1.70	-2.49	-1.02	-0.37	(GO:0005509) (GO:0005507)	Ca binding Cu binding
f8f21	DACH1	Similar to dachshund homolog 1 (Drosophila) [Bos taurus]	537184	46400882	ES344757	-1.53	-1.28	-1.10	-1.72	(GO:0000166)	binding nucleotides
f8h20	ILF2	Interleukin enhancer binding factor 2, 45kDa [Bos taurus]	539760	46400911	ES344786	-1.23	-0.80	-0.82	-1.08	(GO:0005524) (GO:0003723)	ATP binding RNA binding
f8i24	EHD2	EH-domain containing 2 [Bos taurus]	538348	46400926	ES344801	-1.01	-0.98	-0.37	-1.09	(GO:0005509) (GO:0005525)	Ca binding GTP binding
f8o12	MRLC2	Fast skeletal myosin light chain 2 [Bos taurus]	531505	46400996	ES344871	2.85	2.25	2.60	1.49	04510 04530 04670 04810	Focal adhesion Tight junction Leukocyte transendothelial migration Regulation of actin cytoskeleton
f8p11	CHRAC1	Chromatin accessibility complex 1 [Bos taurus]	510942	46401008	ES344883	2.18	1.34	2.06	0.85	(GO:0043565)	Sequence Specific DNA binding
g1m24	C7H19orf22	Chromosome 19 open reading frame 22 ortholog [Bos taurus]	614948	46401120	ES344995	0.97	0.79	0.69	1.01	(GO:0003676)	Nucleic Acid binding
g2a22	RNASET2	Ribonuclease T2 [Bos taurus]	508245	46401152	ES345027	-0.95	-0.68	-0.05	-1.31	(GO:0003723)	RNA binding
g2c09	S100G	S100 calcium binding protein G [Bos taurus]	281658	46401165	ES345040	-0.63	-1.02	-1.15	-1.04	(GO:0005509) (GO:0005499)	Ca binding Vit.D binding
g2c20	SQSTM1	Sequestosome 1 [Bos taurus]	338045	46401167	ES345042	0.72	0.96	0.66	0.37	(GO:0008270)	Zn binding
g2i01	HSPA5	Heat shock 70kDa protein 5 (glucose-regulated protein, 78kDa) [Bos taurus]	415113	46401200	ES345075	1.04	0.80	0.75	1.27	01510 05060	Neurodegenerative Diseases Prion disease
g3c21	MYL6	Myosin, light chain 6, alkali, smooth muscle and non-muscle [Bos taurus]	281341	50172305	EX656782	0.79	0.51	1.14	1.20	(GO:0005509)	Ca binding
g3e11	SPARCL1	SPARC-like 1 (mast9, hevin) [Bos taurus]	507537	50172306	EX656783	-0.28	0.59	1.54	0.03	(GO:0005509)	Ca binding
g3i11	TPT1	Tumor protein, translationally-controlled 1 [Bos taurus]	326599	50172315	EX656792	1.46	1.05	1.24	0.45	(GO:0005509)	Ca binding
g3m23	VPS4A	Vacuolar protein sorting 4 homolog A (S. cerevisiae) [Bos taurus]	618168	50172325	EX656802	0.70	0.31	1.00	0.69	(GO:0005524) (GO:0000166)	ATP binding Nucleotide bindiing
g4a20	PDCD6	Programmed cell death 6 [Bos taurus]	100125927	46401231	ES345106	0.76	0.62	0.70	1.17	(GO:0005509)	Ca binding
g4b22	JUB	Predicted: Jub, ajuba homolog (Xenopus laevis) [Bos taurus]	519937	46401244	ES345119	1.56	1.08	0.75	0.66	(GO:0008270)	Zn binding
g4d13	DCN	Decorin [Bos taurus]	280760	46401261	ES345136	-1.42	-1.39	-0.76	-0.23	04350	TGF-beta signaling pathway
g4i08	HEG1	Predicted: HEG homolog 1 (zebrafish) [Homo sapiens]	57493	46401330	ES345205	1.372	1.214	0.902	1.112	(GO:0005509)	Ca binding
g4i21	ZDHHC5	Zinc finger, DHHC-type containing 5 [Bos taurus]	533250	46401339	ES345214	0.91	1.33	0.90	1.24	(GO:0008270)	Zn binding
g4i23	RNF139	Ring finger protein 139 [Bos taurus]	788471	46401340	ES345215	1.00	1.12	0.52	0.95	(GO:0008270) (GO:0005515)	Zn binding Protein binding
g4i24	CALM1	Calmodulin 1 (phosphorylase kinase, delta) [Bos taurus]	617095	46401341	ES345216	1.28	0.84	-0.07	0.66	04020 04070 04720 04740 04910 04912	Calcium signaling pathway Phosphatidylinositol signaling system Long-term potentiation Olfactory transduction Insulin signaling pathway GnRH signaling pathway
g4k02	GNL3	Guanine nucleotide binding protein-like 3 (nucleolar) [Bos taurus]	506152	46401362	ES345237	-1.57	-1.03	-0.74	-1.67	(GO:0005525)	GTP binding
g4m13	SH3PXD2A	Homo sapiens SH3 and PX domains 2A, mRNA	9644	46401408	ES345283	1.06	0.89	0.23	0.76	(GO:0005488)	Binding
g4m20	FHL1	Four and a half LIM domains 1 [Bos taurus]	509056	46401413	ES345288	2.13	2.16	2.36	1.24	(GO:0008270) (GO:0046872)	Zn binding Metal ion binding
g4o07	TLN1	Talin 1 [Bos taurus]	783470	46401435	ES345310	-1.17	-1.05	-0.69	-1.34	(GO:0005488)	Binding
g4p23	LIMS2	LIM and senescent cell antigen-like domains 2 [Bos taurus]	515401	46401460	ES345335	0.89	0.77	0.61	1.10	(GO:0008270) (GO:0046872)	Zn binding Metal ion binding
Carbohydrate Metabolism											
a2g06	GAPDH	Glyceraldehyde-3-phosphate dehydrogenase [Bos taurus]	786101	46400184	ES344059	3.23	3.01	2.92	2.24		
f7b08	PKM2	Predicted: similar to Pyruvate kinase,muscle [Bos taurus]	512571	46400685	ES344560	3.05	2.95	2.14	1.80	(GO:0006096)	Glycolysis
f8a13	ALG11	Asparagine-linked glycosylation 11 homolog (S. cerevisiae, alpha-1,2-mannosyltransferase) [Bos taurus]	540845	46400809	ES344684	-0.86	-1.03	-1.00	-1.65	01030 00510	N-Glycan biosynthesis Glycan structures - biosynthesis 1
f8d01	LDHB	Lactate dehydrogenase B [Bos taurus]	281275	46400838	ES344713	-1.64	-1.62	-0.73	-0.72	00272 00010 00640 00620	Cysteine metabolism Glycolysis / Gluconeogenesis Propanoate metabolism Pyruvate metabolism
f8e13	UGP2	UDP-glucose pyrophosphorylase 2 [Bos taurus]	281565	46400864	ES344739	0.87	1.03	0.70	0.87	00500 00040 00052 00520	Starch and sucrose metabolism Pentose/glucuronate interconversions Galactose metabolism Nucleotide sugars metabolism

Clone ID	Gene Symbol	Gene Name	Entrez Gene ID	dbEST_Id	GenBank Accn	M-Value				(GO)/Kegg Path	Term/Pathway
						INT	WP	SF	PF		
g4i09	MDH2	Malate dehydrogenase 2, NAD (mitochondrial) [Bos taurus]	281306	46401331	ES345206	1.11	0.84	0.74	1.35	00710 00020 00630 00620 00720	Carbon fixation Citrate cycle (TCA cycle) Glyoxylate and dicarboxylate metab. Pyruvate metabolism Reductive carboxylate cycle
g4p13	GPI	Glucose phosphate isomerase [Bos taurus]	280808	46401454	ES345329	1.05	1.23	0.76	1.05	00010 00030 00500	Glycolysis / Gluconeogenesis Pentose phosphate pathway Starch and sucrose metabolism
Cell Growth/Differentiation											
f5h11	NBN	Nibrin [Bos taurus]	522943	46400351	ES344226	-1.30	-0.71	-0.98	-1.41	(GO:0031575)	G1/S transition checkpoint
f5n03	EMP	Epithelial membrane protein 3 [Bos taurus]	535273	46400459	ES344334	0.04	-0.28	-0.24	-0.98	(GO:0016049)	Cell Growth
f7e10	TIPIN	TIMELESS interacting protein [Bos taurus]	506176	46400705	ES344580	-0.81	-0.94	-0.95	-1.66	(GO:0007049)	Cell-division cycle
f8k17	MGP	Matrix Gla protein [Bos taurus]	282660	46400949	ES344824	-0.98	-1.27	-0.50	0.05	(GO:0030154)	Cell differentiation
g1c17	IGFBP5	Predicted: Insulin-like growth factor binding protein 5 [Homo sapiens]	3488	46401038	ES344913	0.51	0.40	0.01	0.95	(GO:0001558)	Regulation of cell growth
g1p15	SEPT4	Septin 4 [Bos taurus]	538801	46401139	ES345014	-1.41	-1.16	-1.47	-1.25	(GO:0007049)	Cell-division cycle
g4j21	IGFBP6	Insulin-like growth factor binding protein 6 [Bos taurus]	404186	46401357	ES345232	0.55	1.33	0.72	1.27	(GO:0001558)	Regulation of cell growth
g4n15	CDKN1C	Predicted: Cyclin-dependent kinase inhibitor 1C (p57, Kip2) [Bos taurus]	510972	46401425	ES345300	-0.30	-1.06	-0.46	-1.90	04110	Cell cycle
Cell Cytoskeletal/Adhesion/Extracellular Matrix Related											
a1g04	FN1	Fibronectin 1 [Bos taurus]	280794	46400056	ES343931	-1.37	-0.98	-0.27	0.03	01430 04510 04810	Cell communication Focal adhesion Regulation of actin cytoskeleton
a1h01	ACTB	Actin, beta [Bos taurus]	280979	46400070	ES343945	3.15	1.99	2.63	1.44	01430 04510 04670 04530 04520 04810	Cell communication Focal adhesion Leukocyte transendothelial migration Tight junction Adherens junction Regulation of actin cytoskeleton
a1h04	COL4A1	Collagen, type IV, alpha 1 [Bos taurus]	282191	46400074	ES343949	-0.92	-1.20	-0.81	-0.72	01430 04510 04512	Cell communication Focal adhesion ECM-receptor interaction
a2a12	COL1A1	Collagen, type I, alpha 1 [Bos taurus]	282187	46400097	ES343972	-0.53	-1.17	-0.04	0.17	01430 04510 04512	Cell communication Focal adhesion ECM-receptor interaction
f5g12	COL6A2	Collagen, type VI, alpha 2 [Bos taurus]	282194	46400332	ES344207	-1.03	-1.13	-0.74	-0.93	(GO:0007155)	Cell adhesion
f5m18	COL3A1	Collagen, type III, alpha 1 [Bos taurus]	510833	46400452	ES344327	-1.60	-1.41	-1.09	-0.36	(GO:0005201)	ECM glycoprotein
f6c20	COL1A2	Collagen, type I, alpha 2 [Bos taurus]	282188	46400538	ES344413	-0.64	-1.49	-0.19	0.45	01430 04510 04512	Cell communication Focal adhesion ECM-receptor interaction
f8o03	SPP1	Secreted phosphoprotein 1 [Bos taurus]	281499	46400992	ES344867	0.94	0.92	0.82	0.96	01430 04512 04510 04620	Cell communication ECM-receptor interaction Focal adhesion Toll-like receptor signaling pathway
g3i19	TMSB10	Thymosin beta 10 [Bos taurus]	282385	50172317	EX656794	0.10	-1.39	-0.37	-2.06	(GO:0007010)	Cytoskeleton organization/biogenesis
g4m22	LOC788312	LOC788312 similar to Formin-like protein 2 (Formin homology 2 domain-containing protein 2) [Bos taurus]	788312	46401414	ES345289	0.80	1.00	1.15	1.26	(GO:0030036)	Actin cytoskeleton organization
Hydrolase/Transferase/Catalytic/Activity											
a1c02	NMT1	N-myristoyltransferase 1 [Bos taurus]	281351	46399979	ES343854	1.22	1.01	0.73	1.45	(GO:0042158)	Lipoprotein biosynthesis
a2b12	CA5B	Carbonic anhydrase VB, mitochondrial [Bos taurus]	514494	46400113	ES343988	-0.95	-1.12	-1.65	-0.43	(GO:0004089)	Carbonate dehydratase activity
a2h09	NMT2	N-myristoyltransferase 2 [Bos taurus]	282049	46400202	ES344077	-1.61	-1.39	-2.93	-3.53	(GO:0042158)	Lipoprotein biosynthesis
f5p04	ACP5	Acid phosphatase 5, tartrate resistant [Bos taurus]	517002	46400504	ES344379	-0.91	-0.83	-1.12	-1.34	(GO:0003993)	Acid phosphatase activity
f6e04	PTP4A2	Protein tyrosine phosphatase type IVA, member 2 [Bos taurus]	614435	46400555	ES344430	1.02	0.61	0.74	0.45	GO:0004725	Protein tyrosine phosphatase activity
f8a23	PPAPDC1B	Phosphatidic acid phosphatase type 2 domain containing 1B [Bos taurus]	616337	46400811	ES344686	0.91	1.19	0.92	1.39	(GO:0003824)	Catalytic activity
f8g21	LOC789894	LOC789894 Similar to PAP-associated domain-containing protein 5 (TRF4-2) [Bos taurus]	789894	46400896	ES344771	-1.07	-0.60	-0.80	-0.84	(GO:0016779)	Nucleotidyltransferase activity
g1c14	PPP1CA	Protein phosphatase 1, catalytic subunit, alpha isoform [Bos taurus]	516175	46401036	ES344911	0.44	0.96	0.62	0.38	04510 04720 04910	Focal adhesion Long-term potentiation Insulin signaling pathway
g2c06	PTP4A2	Protein tyrosine phosphatase type IVA, member 2 [Bos taurus]	614435	46401163	ES345038	-2.67	-2.79	-2.27	-3.06	(GO:0004725)	Protein tyrosine phosphatase activity
g2k01	LOC100137872	LOC100137872 similar to RAC-gamma serine/threonine-protein kinase (RAC-PK-gamma) (Protein kinase Akt-3) (Protein kinase B, gamma) (PKB gamma) (STK-2) [Bos taurus]	100137872	46401211	ES345086	-0.77	-0.70	-0.50	-1.32	(GO:0004674)	Protein serine/threonine kinase activity
g4k06	LYZ	Lysozyme (renal amyloidosis) [Bos taurus]	781349	46401366	ES345241	-1.22	-1.12	-1.00	-1.62	(GO:0016798)	Hydrolase activity on glycosyl bonds

Clone ID	Gene Symbol	Gene Name	Entrez Gene ID	dbEST_Id	GenBank Accn	M-Value				(GO)/Kegg Path	Term/Pathway
						INT	WP	SF	PF		
g4l16	ACK1	Activated p21cdc42Hs kinase [Bos taurus]	280710	46401393	ES345268	0.61	1.19	0.78	1.11	(GO:0016740) (GO:0004713)	Transferase activity Protein-tyrosine kinase activity
Nucleic Acid Metabolism											
f8f24	NP	Nucleoside phosphorylase [Bos taurus]	493724	46400885	ES344760	-1.32	-1.21	-0.86	-1.46	00230 00760 00240	Purine metabolism Nicotinate/nicotinamide metabolism Pyrimidine metabolism
f6k24	DPYD	Dihydropyrimidine dehydrogenase [Bos taurus]	281124	46400622	ES344497	-1.31	-1.10	-0.97	-1.84	00770 00240 00410	Pantothenate and CoA biosynthesis Pyrimidine metabolism beta-Alanine metabolism
Oxidative Phosphorylation											
a1e03	COX1	Cytochrome c oxidase subunit I [Bos taurus]	3283879	46400013	ES343888	0.47	0.40	0.50	1.20	00190	Oxidative phosphorylation
a2a06	UQCRC1	UQCRC1 protein [Bos taurus]	282393	46400092	ES343967	1.14	1.11	1.10	0.88	00190	Oxidative Phosphorylation
f5f02	NDUFV1	NADH dehydrogenase (ubiquinone) flavoprotein 1, 51kDa [Bos taurus]	287014	46400298	ES344173	0.66	0.86	0.63	1.22	00190	Oxidative Phosphorylation
g2a07	NDUFS4	NADH dehydrogenase (ubiquinone) Fe-S protein 4, 18kDa (NADH-coenzyme Q reductase) [Bos taurus]	327680	46401147	ES345022	0.83	0.89	0.75	1.01	00190	Oxidative Phosphorylation
g3a15	ND1	NADH dehydrogenase subunit 1 [Bos taurus]	3283877	..	EX656781	0.51	0.57	0.49	1.54	00190	Oxidative phosphorylation
g3e01	ND4L	NADH dehydrogenase subunit 4L [Bos taurus]	3283885	..	EE956799	1.12	1.26	0.85	0.85	00190 00130	Oxidative Phosphorylation Ubiquinone biosynthesis
g3g19	COX3	Cytochrome c oxidase subunit III [Bos taurus]	3283883	..	FE014434	0.22	0.10	0.47	1.04	00190	Oxidative Phosphorylation
g3k23	ATP6V1H	ATPase, H+ transporting, lysosomal 50/57kDa, V1 subunit H [Bos taurus]	282657	50172321	EX656798	0.22	1.12	-0.22	0.37	00190	Oxidative Phosphorylation
g4m07	NDUFS5	NADH dehydrogenase (ubiquinone) Fe-S protein 5, 15kDa (NADH-coenzyme Q reductase) [Bos taurus]	338057	46401405	ES345280	0.75	0.57	1.10	0.56	00190	Oxidative Phosphorylation
Oxidoreductase Activity											
f5l19	PRDX2	Peroxiredoxin 2 [Bos taurus]	286793	46400431	ES344306	0.97	1.06	0.73	1.08	(GO:0016491)	Oxidoreductase Activity
f5j13	PRDX6	Peroxiredoxin 6 [Bos taurus]	282438	46400402	ES344277	-0.80	-0.40	-0.67	-1.13	00650 00680 00960	Butanoate metabolism Methane metabolism Alkaloid biosynthesis II
f6b09	CRYZ	Crystallin, zeta (quinone reductase) [Bos taurus]	281093	46400523	ES344398	-1.48	-1.27	-1.14	-1.84	(GO:0016491)	Oxidoreductase Activity
f6k09	MGST1	Microsomal glutathione S-transferase 1 [Bos taurus]	493719	46400617	ES344492	-1.95	-2.15	-1.95	-1.01	00480	Glutathione metabolism
f7m02	CYBB	Cytochrome b-245, beta polypeptide [Bos taurus]	281112	46400763	ES344638	0.98	1.31	0.78	1.60	04670	Leukocyte transendothelial migration
f8b22	CYBASC3	Cytochrome b, ascorbate dependent 3 [Bos taurus]	615893	46400820	ES344695	1.21	1.28	1.05	1.32	(GO:0016491)	Oxidoreductase Activity
f8m04	ALDH1A1	Aldehyde dehydrogenase 1 family, member A1 [Bos taurus]	281615	46400968	ES344843	-0.78	-0.62	-1.09	-0.35	00830	Retinol metabolism
f8m08	C1orf27	Predicted: Chromosome 1 open reading frame 27 [Homo sapiens]	54953	46400970	ES344845	-0.20	-0.96	-0.09	-0.35	(GO:0016491)	Oxidoreductase Activity
g4a10	PLEKHM2	Pleckstrin homology domain containing, family M (with RUN domain) member 2 [Bos taurus]	515552	46401226	ES345101	1.03	1.06	0.56	0.56	(GO:0016491)	Oxidoreductase Activity
g4g07	PAOX	Polyamine oxidase (exo-N4-amino) [Bos taurus]	282639	46401300	ES345175	-0.43	-0.35	-0.17	-1.13	(GO:0016491)	Oxidoreductase Activity
g4l15	CYP2D6	Cytochrome P450, family 2, subfamily D, polypeptide 6 [Bos taurus]	282211	46401392	ES345267	0.42	0.98	0.85	0.95	(GO:0016491)	Oxidoreductase Activity
Protein Synthesis:Turn Over/Proteolysis/Amino Acid Metabolism											
f5n06	CFB	Complement factor B [Bos taurus]	514076	46400462	ES344337	-1.94	-1.81	-1.82	-2.53	04610	Complement/coagulation cascades
f5n08	GOT2	Glutamic-oxaloacetic transaminase 2, mitochondrial (aspartate aminotransferase 2) [Bos taurus]	286886	46400465	ES344340	1.28	1.26	1.53	0.92	00252 00950 00330 00710 00272 00251 00360 00350 00400	Alanine and aspartate metabolism Alkaloid biosynthesis I Arginine and proline metabolism Carbon fixation Cysteine metabolism Glutamate metabolism Phenylalanine metabolism Tyrosine metabolism Phenylalanine/tyrosine/tryptophan biosynthesis
f5n10	ADAMTS16	Predicted: similar to ADAM metallopeptidase with thrombospondin type 1 motif, 16 [Bos taurus]	520133	46400468	ES344343	1.03	0.46	0.45	1.18	(GO:0006508)	Proteolysis
f6b22	PMPCA	Peptidase (mitochondrial processing) alpha [Bos taurus]	767847	46400525	ES344400	0.71	0.85	0.42	0.95	(GO:0006508)	Proteolysis
f8d03	UBL7	Ubiquitin-like 7 (bone marrow stromal cell-derived) [Bos taurus]	511289	46400840	ES344715	1.16	1.36	0.70	0.98	(GO:0006464)	Protein modification process
f8d19	BCAT2	Branched chain aminotransferase 2, mitochondrial [Bos taurus]	281643	46400850	ES344725	-0.77	-1.29	-0.56	0.21	00770 00290 00280	Pantothenate & CoA biosynthesis Valine/leucine/isoleucine biosynthesis
f8e02	DPP8	Dipeptidyl-peptidase 8 [Bos taurus]	536604	46400855	ES344730	-0.02	-0.99	-1.48	-0.42	(GO:0006508)	Proteolysis
f8f15	STXBP4	Syntaxin binding protein 4 [Bos taurus]	537963	46400879	ES344754	1.07	1.37	0.98	1.33	(GO:0005515)	Protein binding
f8k22	LAP3	Leucine aminopeptidase 3 [Bos taurus]	781648	46400952	ES344827	-1.47	-0.86	-1.05	-1.18	00330	Arginine and proline metabolism
g4d21	PCSK7	Predicted: similar to Proprotein convertase subtilisin/kexin type 7 [Bos taurus]	515398	46401265	ES345140	1.77	0.87	1.12	0.98	(GO:0006508)	Proteolysis
g4h01	PLAT	Plasminogen activator, tissue [Bos taurus]	281407	46401311	ES345186	0.97	1.01	0.51	0.77	04610	Complement/coagulation cascades
g4h21	CAPN10	Predicted: similar to CAPN10 calpain 10 [Bos taurus]	789674	46401322	ES345197	0.58	0.43	0.50	1.49	(GO:0006508)	Proteolysis

Clone ID	Gene Symbol	Gene Name	Entrez Gene ID	dbEST_Id	GenBank Accn	M-Value				(GO)/Kegg Path	Term/Pathway
						INT	WP	SF	PF		
g4j14	OAT	Ornithine aminotransferase (gyrate atrophy) [Bos taurus]	505323	46401352	ES345227	-1.41	-1.81	-1.66	-2.02	(GO:0004587)	Ornithine-oxo-acid transaminase
g4j17	SERPINE1	Serpin peptidase inhibitor, clade E (nexin, plasminogen activator inhibitor type 1), member 1 [Bos taurus]	281375	46401354	ES345229	0.12	-0.93	-0.30	-0.23	04115 04610	p53 signaling pathway Complement/coagulation cascades
Response to Stress/Stimuli											
f8d20	HSPA8	Heat shock 70kDa protein 8 [Bos taurus]	281831	46400851	ES344726	0.59	0.37	1.19	0.87	04010 04612	MAPK signaling pathway Antigen processing and presentation
f8k01	LOC616903	LOC616903 similar to cutA divalent cation tolerance homolog [Bos taurus]	616903	46400939	ES344814	-1.16	-1.04	-0.88	-1.60	(GO:0010038)	Response to metal
g4o19	HSPCA	Heat shock 90kD protein 1, alpha [Bos taurus]	281832	46401443	ES345318	1.18	1.29	0.97	1.61	(GO:0006950)	Response to stress
Signal Transduction											
a1g08	MYD88	Myeloid differentiation primary response gene (88) [Bos taurus]	444881	46400063	ES343938	-1.27	-0.94	-0.06	-2.25	04210 04620	Apoptosis Toll-like receptor signaling pathway
a2a08	TLR2	Toll-like receptor 2 [Bos taurus]	281534	46400093	ES343968	-1.02	-1.59	-0.31	-0.12	04620	Toll-like Receptor Pathway
a2b11	T2R65A	Bitter taste receptor Bota-T2R65A [Bos taurus]	664647	46400111	ES343986	-0.71	-1.03	-0.18	-0.58	(GO:0007186)	G-protein coupled receptor protein
f5d09	CSNK1A1	Predicted: Casein kinase 1, alpha 1 [Canis lupus familiaris]	479331	46400260	ES344135	-1.40	-1.15	-1.00	-1.71	04310 04340	Wnt & Hedgehog Pathway Hedgehog signaling pathway
f6b10	GHRH	Growth hormone releasing hormone [Bos taurus]	281191	46400524	ES344399	-1.03	-1.30	-0.93	-1.80	04080	Neuroactive ligand-receptor interaction
f8e19	MFNG	MFNG O-fucosylpeptide 3-beta-N-acetylglucosaminyltransferase [Bos taurus]	505267	46400869	ES344744	0.48	0.67	0.39	1.20	04330	Notch Pathway
f8g08	AGTR1	Angiotensin II receptor, type 1 [Bos taurus]	281607	46400890	ES344765	-1.31	-1.00	-0.99	-1.71	04020 04080 04614	Calcium signaling pathway Neuroactive ligand-recept. interaction Renin-angiotensin system
f8k18	NCSTN	Predicted: Nicastrin [Pan troglodytes]	457435	46400950	ES344825	-1.17	0.89	-0.06	-0.52	04330	Notch Pathway
g1e23	RAP1A	RAP1A, member of RAS oncogene family [Bos taurus]	282031	46401057	ES344932	-0.93	-0.49	-0.69	-1.06	04010 04510 04670 04720	Focal adhesion MAPK signaling pathway Leukocyte transendothelial migration Long-term potentiation
g1k22	CHD8	Chromodomain helicase DNA binding protein 8 [Bos taurus]	507111	46401102	ES344977	1.30	0.68	0.23	1.04	04310	Wnt Pathway
g1p07	PPM1A	Protein phosphatase 1A (formerly 2C), magnesium-dependent, alpha isoform [Bos taurus]	281994	46401138	ES345013	1.04	1.08	0.86	0.81	04010	MAPK Pathway
g1p19	TAOK1	TAO kinase 1 [Pan troglodytes]	454548	46401142	ES345017	0.87	0.73	0.45	1.15	04010	MAPK signaling pathway
g4e08	RFNG	RFNG O-fucosylpeptide 3-beta-N-acetylglucosaminyltransferase [Bos taurus]	532242	46401272	ES345147	-0.81	1.32	0.80	0.64	04330	Notch Pathway
g4e11	PTPRC	Protein tyrosine phosphatase, receptor type, C [Bos tauru]	407152	46401273	ES345148	0.96	1.17	0.48	0.55	04514 04660 05340	Cell adhesion molecules (CAMs) T cell receptor signaling pathway Primary immunodeficiency
g4f11	LFNG	LFNG O-fucosylpeptide 3-beta-N-acetylglucosaminyltransferase [Bos taurus]	516209	46401288	ES345163	0.76	0.78	0.44	1.17	04330	Notch Pathway
g4g20	RIT1	Ras-like without CAAX 1 [Bos taurus]	533646	46401307	ES345182	-0.81	-1.07	-0.53	0.48	(GO:0007264)	GTPase Mediated Signaling
g4p15	ADRBK2	Adrenergic, beta, receptor kinase 2 [Bos taurus]	282136	46401456	ES345331	-1.62	-1.41	-1.16	-1.88	04740	Olfactory transduction
Transcription/Translation											
a1h07	EIF4G	Eukaryotic translation initiation factor 4 gamma, 2 [Bos taurus]	286870	46400078	ES343953	0.78	0.52	0.92	0.26	(GO:0006417)	Regulation of translation
f5c16	LOC507271	Similar to ribosomal protein L4 [Bos taurus]	507271	..	AV592480	-1.37	-1.12	-1.04	-1.53	(GO:0006412)	Translation
f5f05	PCNA	Similar to proliferating cell nuclear antigen [Bos taurus]	515499	46400301	ES344176	2.50	1.31	1.06	1.14	03030 03410 03420 03430 04110	DNA replication Base excision repair Nucleotide excision repair Mismatch repair Cell cycle
f5f19	SAP18	Sin3A-associated protein, 18kDa [Bos taurus]	615692	46400323	ES344198	0.91	0.86	0.54	0.91	(GO:0006355)	Regulation of transcription-DNA dependent
f5i13	EXOSC9	Predicted: Exosome component 9 [Bos taurus]	508005	..	EV607261	-0.63	-0.32	-0.46	-1.06	(GO:0006364)	rRNA processing
f5p15	RPS26	Ribosomal protein S26 [Bos taurus]	509426	46400511	ES344386	0.09	-0.47	-1.03	-0.34	03010	Ribosome
f6m04	RPL13A	RPL13A ribosomal protein L13a [Bos taurus]	767925	46400639	ES344514	0.45	0.75	0.71	1.00	03010	Ribosome
f6o23	FUS	Fusion (involved in t(12;16) in malignant liposarcoma) [Bos taurus]	280796	46400665	ES344540	0.13	-0.20	-0.03	0.97	(GO:0045944)	Positive regulation of transcription from RNA polymerase II promoter
f7f23	ZNF618	Predicted: Zinc finger protein 618 [Homo sapiens]	114991	46400718	ES344593	-0.59	-0.88	-1.50	-0.23	(GO:0006355)	Regulation of transcription-DNA dependent
f7k04	NACA	Nascent polypeptide-associated complex alpha subunit [Bos taurus]	513312	46400751	ES344626	0.72	0.49	1.03	0.83	(GO:0006350)	Transcription
f7n23	PRNP	Prion protein (p27-30) [Bos taurus]	281427	46400780	ES344655	-1.40	-1.25	-0.93	-1.77	01510 05060	Neurodegenerative Diseases Prion disease
f8b15	YBX1	Y box binding protein 1 [Bos taurus]	287023	46400815	ES344690	1.26	1.26	0.98	1.45	(GO:0006397) (GO:0008380) (GO:0006355)	mRNA processing RNA splicing Regulation of transcription, DNA-dependent RNA splicing

Clone ID	Gene Symbol	Gene Name	Entrez Gene ID	dbEST_Id	GenBank Accn	M-Value				(GO)/Kegg Path	Term/Pathway
						INT	WP	SF	PF		
f8b20	CHD2	Chromodomain helicase DNA binding protein 2 [Bos taurus]	535026	46400818	ES344693	1.04	1.21	0.75	1.02	(GO:0006417) (GO:0006333)	Regulation of translation Chromatin assembly or disassembly
f8b21	WDR36	WD repeat domain 36 [Bos taurus]	514267	46400819	ES344694	1.01	1.35	1.01	1.09	(GO:0006364)	rRNA processing
f8l16	RPL10	Ribosomal protein L10 [Bos taurus]	286790	46400959	ES344834	0.95	1.17	0.81	1.48	03010	Ribosome
f8m23	EIF1	Eukaryotic translation initiation factor 1 [Bos taurus]	509764	46400974	ES344849	1.00	0.53	0.55	0.16	(GO:0006413)	Translational initiation
g1c20	RBMS1	RNA binding motif, single stranded interacting protein 1 [Bos taurus]	526135	46401040	ES344915	1.00	0.86	0.15	1.03	(GO:0006260)	DNA replication
g1i17	PRNP	Prion protein (p27-30) (Creutzfeldt-Jakob disease, Gerstmann-Strausler-Scheinker syndrome, fatal familial insomnia) [Bos taurus]	281427	46401085	ES344960	-1.25	-1.18	-0.91	-1.55	(GO:0006355)	Regulation of transcription, DNA-dependent
g1l16	S100B	S100 calcium binding protein B [Bos taurus]	525716	46401108	ES344983	0.864	0.951	0.375	1.014	(GO:0006417)	Regulation of translation
g2d17	ZNF280C	Zinc finger protein 280C [Homo sapiens]	55609	46401174	ES345049	0.928	0.616	0.325	0.892	(GO:0006355)	Regulation of transcription-DNA dependent
g2h03	JTV1	JTV1 gene [Bos taurus]	520979	46401196	ES345071	0.86	1.17	0.73	1.44	(GO:0006412)	Translation
g4a06	LOC537712	LOC537712 similar to early B-cell factor [Bos taurus]	537712	46401224	ES345099	-0.34	-0.96	-0.95	-1.73	(GO:0006355)	Regulation of transcription, DNA-dependent
g4a16	AARS	Alanyl-tRNA synthetase [Bos taurus]	510933	46401230	ES345105	1.05	0.33	0.62	-0.17	00252 00970	Alanine and aspartate metabolism Aminoacyl-tRNA biosynthesis
g4b11	RPL18	Ribosomal protein L18 [Bos taurus]	509163	46401239	ES345114	1.43	0.85	0.73	1.47	(GO:0006412)	Translation
g4d03	LOC524507	Predicted: Similar to S19 ribosomal protein [Bos taurus]	524507	46401256	ES345131	0.31	0.88	0.67	1.31	(GO:0006412)	Translation
g4f21	H1F0	Histone family, member 0 [Bos taurus]	617975	46401293	ES345168	-0.73	-0.78	-0.54	-1.12	(GO:0006334)	Nucleosome assembly
g4g08	PRPF38A	PRP38 pre-mRNA processing factor 38 (yeast) domain containing A [Bos taurus]	507240	46401301	ES345176	1.20	1.14	0.71	0.38	(GO:0006397) (GO:0008380)	mRNA processing RNA splicing
g4j03	HNRNPF	Heterogeneous nuclear ribonucleoprotein F [Bos taurus]	506917	46401343	ES345218	-1.74	-1.37	-1.54	-2.27	(GO:0006397) (GO:0008380)	mRNA processing RNA splicing
g4j18	LOC788943	Similar to XBP1 [Bos taurus]	788943	46401355	ES345230	-1.32	-1.33	-0.76	0.95	(GO:0006355)	Regulation of transcription-DNA dependent
g4m10	LOC790411	Endonuclease reverse transcriptase [Bos taurus]	790411	46402948	ES346823	-1.94	-1.61	-1.50	-2.31	(GO:0006278)	RNA -dependent DNA replication
g4m15	HDAC3	Histone deacetylase 3 [Bos taurus]	404125	46401409	ES345284	1.16	0.92	0.50	1.43	(GO:0016575)	Histone deacetylation
g4o23	CNBP	CCHC-type zinc finger, nucleic acid binding protein [Bos taurus]	504831	46401445	ES345320	0.65	0.74	0.66	1.14	(GO:0045944)	Positive regulation of transcription from RNA polymerase II promoter
Transporters											
a1d10	SLC25A4	Solute carrier family 25 (mitochondrial carrier; adenine nucleotide translocator), member 4 [Bos taurus]	282478	46400007	ES343882	1.08	1.21	1.00	1.00	04020	Calcium signaling pathway
a1f08	USE1	Unconventional SNARE in the ER 1 homolog (S. cerevisiae) [Bos taurus]	512890	46400041	ES343916	-0.45	-0.26	-0.80	-0.97	04130	SNARE interactions vesicular transport
a2a10	SLC7A7	Solute carrier family 7 (cationic amino acid transporter, y+ system), member 7 [Bos taurus]	504220	46400094	ES343969	-1.07	-0.89	-0.42	-1.57	(GO:0006865)	Amino acid transport
f5d18	CYB5	CYB5 protein [Bos taurus]	281110	46400269	ES344144	-0.76	-1.00	-1.24	1.47	(GO:0006810)	Transport
f5d23	AQP4	Aquaporin 4 [Bos taurus]	281008	46400277	ES344152	-1.05	-0.92	-0.23	-1.22	(GO:0006810)	Transport
f5g20	SHKBP1	SH3KBP1 binding protein 1 [Bos taurus]	512402	46400339	ES344214	-1.03	-0.03	-0.88	-0.36	(GO:0006813)	Potassium ion transport
f5i12	CLIC1	Chloride intracellular channel 1 [Bos taurus]	515646	46400379	ES344254	-0.56	-0.64	-0.88	-1.48	(GO:0006821)	Chloride transport
f7h10	SLC15A4	Solute carrier family 15, member 4 [Bos taurus]	510499	46400732	ES344607	-1.26	-0.71	-1.10	-1.67	(GO:0006857)	Oligopeptide transport
f8l23	ANKH	Ankylosis, progressive homolog (mouse) [Bos taurus]	511800	46400964	ES344839	1.04	0.57	0.34	0.90	(GO:0006817)	Phosphate tranasport
g2m01	ARL6IP5	ADP-ribosylation-like factor 6 interacting protein 5 [Bos taurus]	509977	46401218	ES345093	0.82	1.29	0.60	0.99	(GO:0015813)	Glutamate transport
g2m04	LAPTM5	Similar to Lysosomal associated multispanning membrane protein 5 [Bos taurus]	512361	46401219	ES345094	0.99	0.97	0.80	0.98	(GO:0006810)	Transport
g4g16	COPG	Coatomer protein complex, subunit gamma [Bos taurus]	338055	46401305	ES345180	1.04	0.98	0.28	0.96	(GO:0016192) (GO:0006886)	Vesicle mediated transport Intracellular protein transport
g4l13	BET1L	Blocked early in transport 1 homolog (S. cerevisiae)-like [Bos taurus]	509758	46401390	ES345265	-1.85	-1.10	-0.83	-1.45	04130	SNARE interactions vesicular transport
g4o01	TMED9	Transmembrane emp24 protein transport domain containing 9 [Bos taurus]	618580	46401432	ES345307	0.37	0.51	0.44	1.07	(GO:0006810)	Transport
Clone ID	**Gene Symbol**	**Gene Name**	**Entrez Gene ID**	**dbEST_Id**	**GenBank Accn**	**M-Value**					
						INT	**WP**	**SF**	**PF**		
Other											
a1c03	EDEM2	EDEM2 ER degradation enhancer, mannosidase alpha-like 2 [Bos taurus]	513253	46399981	ES343856	1.16	1.15	0.80	1.17		
a1d05	LAMA2	Predicted: Laminin, alpha 2 (merosin, congenital muscular dystrophy) [Equus caballus]	100073067	46400000	ES343875	0.78	0.94	0.43	0.85		
a1c06	LOC100154500	LOC100154500 similar to SAM domain and HD domain-containing protein 1 (Dendritic cell-derived IFNG-induced protein) (Monocyte protein 5) [Sus scrofa]	100154500	46399986	ES343861	0.741	0.695	0.643	1.002		
a1d12	YIPF6	Yip1 domain family, member 6 [Bos taurus]	540347	46400010	ES343885	-0.39	-0.34	-0.55	-1.04		
a1e02	THRSP	Thyroid hormone responsive (SPOT14 homolog, rat) [Bos taurus]	515940	46400011	ES343886	-1.25	-0.74	-0.21	0.19		
a1e08	CD99	CD99 molecule [Bos taurus]	509230	46400018	ES343893	-0.69	-0.71	-0.54	-1.07		
a1g02	LOC783504	Predicted: Similar to ribosomal protein S23 [Bos taurus]	783504	46400051	ES343926	-1.34	-1.20	-1.32	-2.00		
a2b02	LOC695413	LOC695413 hypothetical protein LOC695413 [Macaca mulatta]	695413	46400100	ES343975	0.82	0.93	0.47	1.27		
a2c05	PTP4A2	Predicted: Protein tyrosine phosphatase type IVA, member 2 [Canis lupus familiaris]	609835	46400124	ES343999	1.13	1.09	1.16	0.36		
a2e07	LOC518495	Predicted: Hypothetical LOC518495 [Bos taurus]	518495	46400152	ES344027	0.02	-0.62	-0.43	-1.90		
a2h06	BAP1	BRCA1 associated protein-1 [Bos taurus]	100124510	46400199	ES344074	1.72	1.45	1.72	0.92		

Clone ID	Gene Symbol	Gene Name	Entrez Gene ID	dbEST_Id	GenBank Accn	M-Value			
						INT	WP	SF	PF
f5b22	C28H10ORF116	Chromosome 10 open reading frame 116 ortholog [Bos taurus]	613941	46400234	ES344109	0.28	0.52	0.54	1.04
f5c10	LOC619156	Predicted: Similar to ribosomal protein L17 [Bos taurus]	619156	46400242	ES344117	-1.16	-0.91	-0.68	-1.36
f5c22	LOC100051338	Predicted: LOC100051338 similar to arginine and glutamate rich 1 [Equus caballus]	100051338	46400253	ES344128	0.68	0.609	0.635	1.081
f5d04	PTRF	Polymerase I and transcript release factor [Bos taurus]	538457	46400255	ES344130	0.64	0.47	0.52	1.06
f5d14	SLC24A6	Predicted: Solute carrier family 24 (sodium/potassium/calcium exchanger), member 6 [Bos taurus]	508887	46400264	ES344139	-1.32	-0.91	-0.68	-1.54
f5d21	LEMD2	LEM domain containing 2 [Bos taurus]	518023	46400274	ES344149	0.47	0.45	0.46	1.06
f5e04	KIAA1715	KIAA1715 [Bos taurus]	533298	46400280	ES344155	0.56	0.82	0.63	1.16
f5e15	TMEM66	Transmembrane protein 66 [Bos taurus]	515461	..	EW681864	0.81	0.89	1.06	0.33
f5e23	LOC511553	LOC511553 similar to clone 22 [Bos taurus]	511553	46400295	ES344170	0.73	0.91	0.83	0.79
f5g03	MGC139109	MGC139109 hypothetical LOC533333 [Bos taurus]	533333	..	EH180189	0.25	0.60	0.58	1.06
f5g22	LOC100054421	LOC100054421 similar to procollagen alpha 2(V) [Equus caballus]	100054421	46400341	ES344216	-1.45	-1.49	-0.70	0.20
f5g23	PLAA	Phospholipase A2-activating protein [Bos taurus]	506073	..	CK954151	0.56	0.97	0.62	1.01
f5h04	APCDD1	Adenomatosis polyposis coli down-regulated 1 [Bos taurus]	509040	46400346	ES344221	0.66	0.91	0.62	1.03
f5h19	ZNFN1A1	Predicted: Zinc finger protein, subfamily 1A, 1 (Ikaros) [Macaca mulatta]	693936	46400362	ES344237	0.89	1.08	0.53	1.22
f5h20	SYAP1	Synapse associated protein 1, SAP47 homolog (Drosophila) [Bos taurus]	509355	46400364	ES344239	0.988	0.752	0.590	0.823
f5i04	RIPK3	Receptor-interacting serine-threonine kinase 3 [Bos taurus]	507427	..	CO260804	0.92	0.99	0.67	0.86
f5i11	MTMR14	Myotubularin related protein 14 [Bos taurus]	514596	46400378	ES344253	-1.12	-0.13	-0.79	-0.71
f5i23	CCNL2	Cyclin L2 [Bos taurus]	538796	46400383	ES344258	-2.80	-2.13	-2.19	-2.43
f5j12	LRRC55	Leucine rich repeat containing 55 [Pan troglodytes]	466584	46400401	ES344276	-1.32	-0.98	-1.16	-1.81
f5k16	LOC100151946	Predicted: LOC100151946 similar to hect domain and RLD 4 [Sus scrofa]	100151946	46400415	ES344290	-1.09	-0.78	-1	-1.48
f5l13	LOC100139815	PREDICTED: Bos taurus hypothetical protein LOC100139815	100139815	46400426	ES344301	-1.74	-1.19	-1.09	-1.62
f5m10	LOC100138783	LOC100138783 similar to Uncharacterized protein C9orf114 [Bos taurus]	100138783	46400447	ES344322	0.74	1.38	0.62	1.08
f5m15	gabP	GABA permease [Pseudomonas fluorescens Pf-5]	3480936	46400450	ES344325	0.68	0.89	0.54	1.06
f5n19	SEH1L	SEH1-like (S. cerevisiae) [Bos taurus]	506509	46400477	ES344352	1.08	0.89	0.35	0.86
f5o05	LOC789925	Predicted: LOC789925 similar to Mid-1-related chloride channel 1 [Bos taurus]	789925	..	EE961626	-2.08	-1.57	-1.57	-2.27
f5o07	LOC783366	LOC783366 similar to Ankyrin repeat domain-containing protein 26 [Bos taurus]	783366	46400488	ES344363	-1.61	-1.14	-1.01	-1.69
f5p05	GRN	Granulin [Bos taurus]	767942	46400505	ES344380	-0.98	-0.67	-1.48	-0.96
f6a22	SMPD4	Sphingomyelin phosphodiesterase 4, neutral membrane (neutral sphingomyelinase-3) [Bos taurus]	507207	46400521	ES344396	0.28	0.44	0.43	1.19
f6c09	BRP44L	Brain protein 44-like [Bos taurus]	767977	46400529	ES344404	-1.35	-1.13	-0.93	-1.43
f6d04	LOC100152073	Predicted: LOC100152073 similar to Stress 70 protein chaperone, microsome-associated, 60kD [Sus scrofa]	100152073	46400543	ES344418	-1.3	-1.22	-0.8	-1.6
f6d23	LOC100055747	LOC100055747 similar to Rab10 [Equus caballus]	100055747	46400553	ES344428	-0.31	-0.32	0.26	-1.22
f6l17	SUSD5	Predicted: SUSD5 sushi domain containing 5 [Pan troglodytes]	470782	46400633	ES344508	-1.51	-1.62	-1.18	-1.55
f6m23	WDR68	WD repeat domain 68 [Bos taurus]	516678	46400643	ES344518	-0.97	-0.67	-0.78	-1.57
f6o15	LOC786819	Muscleblind-like (Drosophila) [Bos taurus]	781653	46400661	ES344536	1.30	0.21	1.71	0.50
f6p11	CPM	Carboxypeptidase M [Bos taurus]	513281	46400671	ES344546	-0.95	-1.02	-1.07	-1.50
f7a12	C16H1ORF21	Chromosome 1 open reading frame 21 ortholog [Bos taurus]	781721	46400680	ES344555	1.22	1.04	1.06	0.97
f7b07	LOC788567	Hypothetical protein LOC788567 [Bos taurus]	788567	46400684	ES344559	0.74	0.95	0.02	0.60
f7e16	LOC533350	Predicted: LOC533350 similar to KIAA1451 protein [Bos taurus]	533350	46400709	ES344584	-1.72	-0.94	-0.39	0.44
f7f04	LOC523451	LOC523451 similar to tetratricopeptide repeat domain 9 [Bos taurus]	523541	46400715	ES344590	0.62	0.95	-0.65	-0.74
f7g21	MANBAL	Mannosidase, beta A, lysosomal-like [Bos taurus]	787482	46400727	ES344602	-1.06	-0.67	-0.80	-0.96
f7l07	EFEMP1	Similar to EGF-containing fibulin-like extracellular matrix protein 1 [Bos taurus]	511566	46400758	ES344633	1.12	0.58	0.92	0.55
f7m07	ANLN	Anillin, actin binding protein [Bos taurus]	518274	46400764	ES344639	-0.70	-0.63	-0.10	-1.18
f7p08	LOC781116	Hypothetical protein LOC781116 [Bos taurus]	781116	46400796	ES344671	-0.93	-0.93	-0.55	-1.24
f7p13	LOC100059158	Predicted: LOC100059158 similar to Chain A, Crystal Structure Of Human Translationally Controlled Tumor Associated Protein [Equus caballus]	100059158	46400800	ES344675	1.315	0.865	1.077	0.538
f8a08	LOC100137838	LOC100137838 similar to tripartite motif protein TRIM4 [Bos taurus]	100137838	46400806	ES344681	-1.27	-1.03	-0.52	-1.55
f8c16	NAIF1	Nuclear apoptosis inducing factor 1 [Bos tauru]	510689	46400832	ES344707	-1.04	-1.05	-0.97	0.13
f8d09	RASEF	Predicted: RAS and EF-hand domain containing [Bos taurus]	513223	46400842	ES344717	-1.14	-0.73	-0.36	-1.01
f8d16	TRUB2	TruB pseudouridine (psi) synthase homolog 2 (E. coli) [Bos taurus]	511988	46400847	ES344722	1.17	0.93	0.73	1.02
f8f14	C28H10ORF35	Predicted: similar to C28H10ORF35 chromosome 10 open reading frame 35 ortholog [Bos taurus]	510161	46400878	ES344753	0.86	1.06	0.82	1.26
f8g07	SYNPO2	Predicted: Synaptopodin 2 [Pan troglodytes]	461456	46400889	ES344764	1.25	0.56	0.32	0.63
f8g22	LOC613996	LOC613996 similar to FLJ10769 protein [Bos taurus]	613996	46400897	ES344772	-0.77	-0.53	-0.79	-1.34
f8k06	SEC63	SEC63 homolog (S. cerevisiae) [Bos taurus]	541040	46400943	ES344818	-0.18	-1.00	-0.53	-1.19
f8l21	MAGED2	Melanoma antigen family D, 2 [Bos taurus]	514372	46400963	ES344838	-0.93	-0.49	-0.64	-0.80
f8m14	LOC782097	Hypothetical protein LOC782097 [Bos taurus]	782097	46400972	ES344847	-1.14	-1.28	-1.09	-1.72
f8o07	GBAS	Glioblastoma amplified sequence [Bos taurus]	767938	46400993	ES344868	0.67	0.98	0.54	0.97
g1a20	TGFBRAP1	Transforming growth factor, beta receptor associated protein 1 [Bos taurus]	514660	46401020	ES344895	-2.66	-1.83	-1.04	-1.03

Clone ID	Gene Symbol	Gene Name	Entrez Gene ID	dbEST_Id	GenBank Accn	M-Value			
						INT	WP	SF	PF
g1c02	PCYOX1	Prenylcysteine oxidase 1 [Bos taurus]	100125835	46401033	ES344908	0.33	0.19	-0.21	0.92
g1c10	LOC788499	LOC788499 similar to Metastasis suppressor protein 1 (Metastasis suppressor YGL-1) [Bos taurus]	788499	46401034	ES344909	0.62	0.95	0.32	0.98
g1e21	LOC783910	LOC783910 similar to brain creatine kinase [Bos taurus]	783910	46401055	ES344930	0.77	0.93	0.46	0.67
g1f04	LOC523451	LOC523451 similar to tetratricopeptide repeat domain 9 [Bos taurus]	523451	46401059	ES344934	2.04	1.49	0.65	0.85
g1f13	CIDEA	Cell death-inducing DFFA-like effector a [Bos taurus]	527051	46401062	ES344937	-0.28	-0.98	-0.82	-0.46
g1g04	LOC516875	LOC516875 similar to phosphoinositide-binding proteins [Bos taurus]	516875	46401064	ES344939	0.33	0.26	0.32	1.07
g1g22	CADM1	Predicted: Cell adhesion molecule 1 [Macaca mulatta]	695983	46401069	ES344944	0.88	1.27	0.62	1.12
g1h03	LIPA	Lipase A, lysosomal acid, cholesterol esterase [Bos taurus]	100125267	46401072	ES344947	-0.95	-0.48	-0.77	-0.14
g1h23	UBAC2	UBA domain containing 2 [Bos taurus]	100125312	46401079	ES344954	-1.17	-1.51	-1.28	-0.14
g1i15	GPBP1L1	GC-rich promoter binding protein 1-like 1 [Bos taurus]	505780	46401084	ES344959	-1.28	-1.01	-0.75	-1.40
g1j01	CCDC80	Predicted: similar to Coiled-coil domain containing 80 [Bos taurus]	515235	46401089	ES344964	0.40	0.86	0.58	1.08
g1j13	LOC783015	Hypothetical protein LOC783015 [Bos taurus]	783015	46401093	ES344968	-0.86	-1.21	-0.71	-0.45
g1k14	LOC504909	LOC504909 similar to ATP-binding cassette sub-family A member 10 [Bos taurus]	504909	46401100	ES344975	-0.26	-0.84	-0.94	-1.61
g1k20	LIX1L	Lix1 homolog (mouse)-like [Bos taurus]	788858	46401101	ES344976	0.73	0.93	0.56	0.91
g1l14	LSM14A	LSM14A, SCD6 homolog A (S. cerevisiae) [Bos taurus]	538838	46401107	ES344982	-1.85	-2.49	-1.29	-0.94
g1l24	NDFIP1	Predicted: Nedd4 family interacting protein 1 [Canis lupus familiaris]	478044	46401112	ES344987	-0.49	-0.94	-1.12	0.198
g1n05	TRAF3IP1	TNF receptor-associated factor 3 interacting protein 1 [Bos taurus]	504984	46401121	ES344996	-1.00	-1.54	-1.02	-0.97
g1o09	POLR1D	Polymerase (RNA) I polypeptide D [Bos taurus]	616972	46401130	ES345005	-1.08	-1.44	-0.37	-1.61
g1o20	MGC148679	Hypothetical LOC505853 [Bos taurus]	505853	46401134	ES345009	0.77	0.83	0.33	1.09
g1o22	LYRM5	LYR motif containing 5 [Bos taurus]	783110	46401135	ES345010	0.94	1.04	0.49	1.17
g2a08	FBXO36	F-box protein 36 [Bos taurus]	617339	46401148	ES345023	-0.41	-0.31	-1.08	-0.97
g2b03	LOC707050	Predicted: LOC707050 similar to caldesmon 1 isoform 4 [Macaca mulatta]	707050	46401155	ES345030	0.914	0.132	1.103	0.643
g2c22	LOC532244	LOC532244 similar to microtubule associated monoxygenase, calponin and LIM domain containing 3 [Bos taurus]	532244	46401168	ES345043	-2.13	-1.83	-1.85	-0.78
g2e23	VEZT	Vezatin, adherens junctions transmembrane protein [Bos taurus]	535351	46401185	ES345060	-0.31	-0.64	-0.52	-1.25
g2l22	LOC786726	LOC786726 similar to Heterogeneous nuclear ribonucleoprotein K [Bos taurus]	786726	46401205	ES345080	0.848	0.814	0.749	1.004
g2j06	LOC511121	LOC511121 similar to Ubiquitin carboxyl-terminal hydrolase 47 [Bos taurus]	511121	46401210	ES345085	0.76	1.01	0.84	1.04
g2p24	ZNF367	Predicted: similar to Zinc finger protein 367 [Bos taurus]	540823	46401223	ES345098	0.74	0.85	0.64	1.09
g3c15	VSTM1	V-set and transmembrane domain containing 1 [Bos taurus]	618514	50172304	EX656781	-1.54	-1.45	-1.21	-2.08
g3g07	IFI35	Interferon-induced protein 35 [Bos taurus]	510697	50172313	EX656790	0.88	0.91	0.70	0.83
g3i05	LOC528398	LOC528398 similar to Abelson helper integration site 1 [Bos taurus]	528398	..	..	1.50	0.92	1.30	0.44
g4b07	NLRX1	NLR family member X1 [Bos taurus]	539974	46401235	ES345110	-0.81	-0.65	-0.68	-1.70
g4b10	ZNF192	Zinc finger protein 192 [Bos taurus]	511794	46401238	ES345113	0.88	0.91	0.63	1.22
g4b19	LOC509457	Predicted: LOC509457 WD repeat domain 73-like Bos taurus]	509457	46401243	ES345118	0.40	0.49	0.82	1.10
g4c24	ABCA9	ATP-binding cassette, sub-family A (ABC1), member 9 [Bos taurus]	504278	46401255	ES345130	-0.59	-0.66	-0.78	-1.18
g4f14	LOC787439	Hypothetical protein LOC787439 [Bos taurus]	787439	46401290	ES345165	-0.68	-0.32	-0.59	-1.25
g4h15	A2M	Alpha-2-macroglobulin [Bos taurus]	513856	46401318	ES345193	1.14	0.92	0.17	0.63
g4i12	FOXP1	Predicted: Forkhead box P1 [Pan troglodytes]	736525	46401333	ES345208	1.10	0.87	0.52	0.86
g4i14	LOC703367	Predicted: LOC703367 similar to autophagy-related cysteine endopeptidase 2 isoform b [Macaca mulatta]	703367	46401334	ES345209	1.07	1.09	0.48	0.76
g4j15	KIAA1704	Similar to KIAA1704 [Homo sapiens]	55425	46401353	ES345228	1.08	0.96	0.80	0.67
g4j19	NID2	Nidogen 2 (osteonidogen) [Bos taurus]	521854	46401356	ES345231	-1.07	-1.46	-0.73	-0.65
g4j22	RASAL2	Predicted:RAS protein activator like 2 [Pan troglodytes]	457547	46401358	ES345233	0.94	1.20	0.68	1.21
g4k15	LOC100050227	LOC100050227 similar to Phosphatidylinositol 3-kinase regulatory subunit alpha [Equus caballus]	100050227	46401374	ES345249	0.79	1.23	0.88	1.44
g4l21	THUMPD3	Predicted: THUMP domain containing 3 [Pan troglodytes]	460147	46401397	ES345272	-1.05	-0.84	-0.79	-1.55
g4m11	FAM32A	Family with sequence similarity 32, member A [Bos taurus]	508634	46401407	ES345282	-0.68	-0.50	-0.58	-1.16
g4n02	PTRF	Polymerase I and transcript release factor [Bos taurus]	538457	46401416	ES345291	-1.11	-1.11	-0.65	-1.40
g4n13	SETMAR	SET domain and mariner transposase fusion gene [Bos taurus]	534913	46401423	ES345298	-0.83	-0.74	-0.75	-0.90
g4n21	TMEM128	Transmembrane protein 128 [Bos taurus]	513824	46401430	ES345305	0.97	0.81	0.76	1.44
g4o14	TWSG1	Twisted gastrulation homolog 1 (Drosophila) [Bos taurus]	537290	46401441	ES345316	0.89	1.24	0.66	1.34
g4p10	RSRC1	Arginine/serine-rich coiled-coil 1 [Bos taurus]	509437	46401451	ES345326	-0.59	-0.92	-0.84	0.22

No Biological Data Available

Clone ID	Gene Symbol	Gene Name	Entrez Gene ID	dbEST_Id	GenBank Accn	M-Value			
						INT	WP	SF	PF
f5c15	..	Pan troglodytes RBP4 gene for retinol binding protein4	AB124586	46400247	ES344122	-1.53	-1.32	-0.97	-1.84
f5n09	..	Sus scrofa toll-like receptor 4 (TLR4) gene,	AY753179	46400467	ES344342	0.98	1.18	1.21	0.73
a1h03	..	cattle subcutaneous adipose tissue cDNA library Bos taurus cDNA clone a1h03ca 5-, mRNA sequence	ES343948.1	46400073	ES343948	0.64	1.04	1.06	0.70
f5a18	..	cattle subcutaneous adipose tissue cDNA library Bos taurus cDNA clone f5a18ca 3-, mRNA sequence	ES344086.1	46400211	ES344086	-1.59	-1.11	-1.70	-1.57
f5c24	..	1268336 MARC 7BOV Bos taurus cDNA 3-, mRNA sequence	DN524662.1	..	DN524662	-0.26	-1.04	-0.19	-1.37
f5j14	..	cattle subcutaneous adipose tissue cDNA library Bos taurus cDNA clone f5j14ca 5', mRNA sequence.	ES344278.1	46400403	ES344278	-1.70	-1.42	-1.11	-1.99
f5l22	..	cattle subcutaneous adipose tissue cDNA library Bos taurus cDNA clone f5l22ca 3-, mRNA sequence	ES344310.1	46400435	ES344310	-0.96	-1.01	-1.01	-1.70
f5m11	..	cattle subcutaneous adipose tissue cDNA library Bos taurus cDNA clone f5m11ca 3-, mRNA sequence	ES344323.1	46400448	ES344323	0.57	0.91	0.63	0.24
f5p07	..	cattle subcutaneous adipose tissue cDNA library Bos taurus cDNA clone f5p07ca 3-, mRNA sequence	ES344381.1	46400506	ES344381	-1.61	-1.31	-1.09	-1.83
f5p21	..	cattle subcutaneous adipose tissue cDNA library Bos taurus cDNA clone f5p21ca 5-, mRNA sequence	ES344392.1	46400517	ES344392	-1.22	-1.66	-1.66	-0.93
f6e15	..	cattle subcutaneous adipose tissue cDNA library Bos taurus cDNA clone f6e15ca 3-, mRNA sequence	ES344439.1	46400564	ES344439	-1.35	-1.00	-0.89	-1.42
f6l01	..	cattle subcutaneous adipose tissue cDNA library Bos taurus cDNA clone f6l01ca 3-, mRNA sequence	ES344498.1	46400623	ES344498	-1.17	-1.27	-0.95	-1.75
f6o01	..	cattle subcutaneous adipose tissue cDNA library Bos taurus cDNA clone f6o01ca 3-, mRNA sequence	ES344529.1	46400654	ES344529	-0.39	-0.32	-0.30	-1.15
f6o18	..	cattle subcutaneous adipose tissue cDNA library Bos taurus cDNA clone f6o18ca 3-, mRNA sequence	ES344538.1	46400663	ES344538	-1.05	-0.99	-0.74	-1.33
f7g24	..	cattle subcutaneous adipose tissue cDNA library Bos taurus cDNA clone f7g24ca 3-, mRNA sequence	ES344605.1	46400730	ES344605	-1.09	-0.57	-1.83	-0.22
f7m19	..	cattle subcutaneous adipose tissue cDNA library Bos taurus cDNA clone f7m19ca 3-, mRNA sequence	ES344643.1	46400768	ES344643	-1.40	-1.16	-0.99	-1.36
f8d06	..	cattle subcutaneous adipose tissue cDNA library Bos taurus cDNA clone f8d06ca 3-, mRNA sequence	ES344716.1	46400841	ES344716	-0.89	-0.94	-0.76	-0.69
f8j04	..	cattle subcutaneous adipose tissue cDNA library Bos taurus cDNA clone f8j04ca 3-, mRNA sequence	ES344804.1	46400929	ES344804	-1.50	-1.41	-1.11	-1.94
f8k08	..	cattle subcutaneous adipose tissue cDNA library Bos taurus cDNA clone f8k08ca 3-, mRNA sequence	ES344819.1	46400944	ES344819	-1.52	-1.05	-0.85	-1.45
f8l04	..	cattle subcutaneous adipose tissue cDNA library Bos taurus cDNA clone f8l04ca 3-, mRNA sequence	ES344829.1	46400954	ES344829	-1.15	-0.98	-0.56	-1.31
f8m02	..	cattle subcutaneous adipose tissue cDNA library Bos taurus cDNA clone f8m02ca 3-, mRNA sequence	ES344842.1	46400967	ES344842	-1.43	-1.29	-1.01	-1.63
g1b14	..	cattle subcutaneous adipose tissue cDNA library Bos taurus cDNA clone g1b14ca 3-, mRNA sequence	ES344901.1	46401026	ES344901	1.40	0.84	1.04	0.52
g1c01	..	cattle subcutaneous adipose tissue cDNA library Bos taurus cDNA clone g1c01ca 3-, mRNA sequence	ES344907.1	46401032	ES344907	0.87	0.94	0.63	1.36
g1f07	..	cattle subcutaneous adipose tissue cDNA library Bos taurus cDNA clone g1f07ca 3-, mRNA sequence	ES344935.1	46401060	ES344935	-0.37	-0.65	-0.61	-0.97
g1h04	..	cattle subcutaneous adipose tissue cDNA library Bos taurus cDNA clone g1h04ca 3-, mRNA sequence	ES344948.1	46401073	ES344948	-0.47	-1.23	-0.90	-0.50
g1n20	..	cattle subcutaneous adipose tissue cDNA library Bos taurus cDNA clone g1n20ca 3-, mRNA sequence	ES345001.1	46401126	ES345001	-0.54	-0.47	-1.03	-0.90
g2b09	..	cattle subcutaneous adipose tissue cDNA library Bos taurus cDNA clone g2b09ca 3-, mRNA sequence	ES345032.1	46401157	ES345032	0.73	0.74	0.83	0.92
g2h22	..	cattle subcutaneous adipose tissue cDNA library Bos taurus cDNA clone g2h22ca 3-, mRNA sequence	ES345073.1	46401198	ES345073	1.41	1.08	1.16	0.46
g3e17	..	cattle adipose tissue cDNA library Bos taurus cDNA clone g3e17ca 5-, mRNA sequence	EX656785.1	50172308	EX656785	-1.08	-0.99	-0.98	-1.40
g4a24	..	cattle subcutaneous adipose tissue cDNA library Bos taurus cDNA clone g4a24ca 3-, mRNA sequence	ES345107.1	46401232	ES345107	0.43	0.99	0.59	0.82
g4b04	..	cattle subcutaneous adipose tissue cDNA library Bos taurus cDNA clone g4b04ca 3-, mRNA sequence	ES345108.1	46401233	ES345108	1.23	1.03	0.73	1.32
g4b18	..	cattle subcutaneous adipose tissue cDNA library Bos taurus cDNA clone g4b18ca 3-, mRNA sequence	ES345117.1	46401242	ES345117	0.59	0.99	0.82	1.34
g4d08	..	cattle subcutaneous adipose tissue cDNA library Bos taurus cDNA clone g4d08ca 3-, mRNA sequence	ES345133.1	46401258	ES345133	-1.62	-1.26	-0.94	-1.71
g4j08	..	cattle subcutaneous adipose tissue cDNA library Bos taurus cDNA clone g4j08ca 3-, mRNA sequence	ES345222.1	46401347	ES345222	1.06	1.33	0.57	0.87
g4j23	..	cattle subcutaneous adipose tissue cDNA library Bos taurus cDNA clone g4j23ca 3-, mRNA sequence	ES345234.1	46401359	ES345234	1.08	1.22	0.91	1.40
g4l20	..	cattle subcutaneous adipose tissue cDNA library Bos taurus cDNA clone g4l20ca 3-, mRNA sequence	ES345271.1	46401396	ES345271	-1.14	-1.33	-0.94	-0.68
g4n20	..	cattle subcutaneous adipose tissue cDNA library Bos taurus cDNA clone g4n20ca 3-, mRNA sequence	ES345304.1	46401429	ES345304	0.74	0.61	0.64	1.19
f6b03	..	cattle subcutaneous adipose tissue cDNA library Bos taurus cDNA clone f6b03ca 3-, mRNA sequence	ES344397.1	46400522	ES344397	0.85	0.94	0.92	0.80
f5d22	..	cattle subcutaneous adipose tissue cDNA library Bos taurus cDNA clone f5d22ca 5-, mRNA sequence	ES344151.1	46400276	ES344151	1.01	0.61	0.75	1.26
f5i14	..	cattle subcutaneous adipose tissue cDNA library Bos taurus cDNA clone f5i14ca 5-, mRNA sequence	ES344255.1	46400380	ES344255	-0.76	-0.51	-0.48	-0.96
f5k10	..	cattle subcutaneous adipose tissue cDNA library Bos taurus cDNA clone f5k10ca 3-, mRNA sequence	ES344287.1	46400412	ES344287	-0.67	-0.97	-0.73	-0.88
f6o17	..	cattle subcutaneous adipose tissue cDNA library Bos taurus cDNA clone f6o17ca 3-, mRNA sequence	ES344537.1	46400662	ES344537	-0.60	-0.49	-0.66	-0.93
g1m11	..	cattle subcutaneous adipose tissue cDNA library Bos taurus cDNA clone g1m11ca 3-, mRNA sequence	ES344992.1	46401117	ES344992	-1.64	-1.12	-1.38	-1.28
g3k13	..	cattle adipose tissue cDNA library Bos taurus cDNA clone g3k13ca 5-, mRNA sequence	EX656796.1	50172319	EX656796	0.67	0.75	1.25	0.48
g4l18	..	cattle subcutaneous adipose tissue cDNA library Bos taurus cDNA clone g4l18ca 3-, mRNA sequence	ES345269.1	46401394	ES345269	-1.28	-1.35	-1.24	-0.64

Appendices Table A2

Clone ID, Gene Symbol, Gene Name, Entrez Gene ID, dEST ID, GenBank Accession number, M-value, GO/KEGG ID, and GO term/KEGG pathway for the genes in each diet of the Finishing Phase.

Clone ID	Gene Symbol	Gene Name	Entrez Gene ID	dbEST_ID	GenBank Accn	M-Value WP	SF	PF	CF	(GO)/KEGG	Term/Pathway
Adipose Related											
a1d11	ACSM1	Acyl-CoA synthetase medium-chain family member 1 [Bos taurus]	282576	46400009	ES343884	-0.55	-0.71	-0.37	-1.13	00650	Butanoate metabolism
a1e11	ELOVL5	ELOVL family member 5, elongation of long chain fatty acids (FEN1/Elo2, SUR4/Elo3-like, yeast) [Bos taurus]	617293	46400023	ES343898	-1.09	-1.25	-1.51	-1.37	01040	Biosynthesis of unsaturated FAs
a1f09	CLU	Clusterin [Bos taurus]	280750	46400043	ES343918	-0.87	-1.01	-0.81	-1.22	(GO:0008219)	Cell Death
a2c10	DGAT2	Diacylglycerol O-acyltransferase homolog 2 (mouse) [Bos taurus]	404129	46400128	ES344003	-1.55	-1.69	-1.67	-2.76	00561 00830	Glycerolipid metabolism Retinol metabolism
a2f05	GPAM	Mitochondrial glycerol phosphate acyltransferase [Bos taurus]	497202	46400165	ES344040	1.31	-0.67	-0.91	-0.43	00561 00564	Glycerolipid metabolism Glycerophospholipid metabolism
a2f07	CD36	CD36 molecule (thrombospondin receptor) [Bos taurus]	281052	46400170	ES344045	-2.14	-1.00	-1.50	-1.89	04920 03320 04512 04640	Adipocytokine signaling pathway PPAR signaling pathway ECM-receptor interaction Hematopoietic cell lineage
f5e12	FABP4	Fatty acid binding protein 4, adipocyte [Bos taurus]	281759	46400286	ES344161	-1.63	-1.28	-1.96	-1.72	03320	PPAR signaling pathway
f5h15	PSAP	Prosaposin (variant Gaucher disease and variant metachromatic leukodystrophy) [Bos taurus]	281433	46400357	ES344232	-0.97	-0.08	-0.20	-0.19	(GO:0006629)	Lipid metabolism
f5k13	SCD	Stearoyl-CoA desaturase (delta-9-desaturase) [Bos taurus]	280924	46400413	ES344288	-1.27	-1.89	-2.36	-2.68	03320 01040	PPAR signaling pathway Biosynthesis of unsaturated FAs
f5l20	ADIPOQ	Adiponectin, C1Q and collagen domain containing [Bos taurus]	282865	46400433	ES344308	-1.07	-1.25	-1.46	-1.80	03320 04920	PPAR signaling pathway Adipocytokine signaling pathway
f6k07	PLD1	Predicted: Phospholipase D1, phosphatidylcholine-specific [Homo sapiens]	5337	46400615	ES344490	1.18	-0.62	-0.29	-0.49	00565 00564 04912	Ether lipid metabolism Glycerophospholipid metabolism GnRH signaling pathway
f8c02	PTGS2	Predicted: Prostaglandin-endoperoxide synthase 2 (prostaglandin G/H synthase & cyclooxygenase) [Bos taurus]	282023	46400821	ES344696	1.08	-0.67	-0.34	-0.66	00590	Arachidonic acid metabolism
f8c05	TM7SF2	Transmembrane 7 superfamily member 2 [Bos taurus]	282384	46400823	ES344698	1.14	0.66	0.83	1.38	00100	Biosynthesis of steroids
f8g23	MSR1	Macrophage scavenger receptor 1 [Bos taurus]	281311	46400898	ES344773	-1.13	-1.61	-1.57	-1.65	(GO:0006817) (GO:0006898)	Phosphate transport Receptor-mediated endocytosis
g2j05	CXCL16	Chemokine (C-X-C motif) ligand 16 [Bos taurus]	511671	46401209	ES345084	-1.71	-1.32	-1.92	-1.63	04060	Cytokine-cytokine receptor interaction
g3e21	HADH	Hydroxyacyl-Coenzyme A dehydrogenase [Bos taurus]	613570	50172310	EX656787	1.47	-0.51	-0.13	-0.12	(GO:0006631)	Fatty acid metabolism
g4h03	APOE	Apolipoprotein E [Bos taurus]	281004	46401312	ES345187	-0.55	-0.56	-0.81	-0.93	01510	Neurodegenerative Diseases
g4l23	ACSS2	Predicted: Acyl-CoA synthetase short-chain family member 2 [Bos taurus]	506459	46401399	ES345274	-0.96	-1.46	-1.37	-1.25	(GO:0003824)	Catalytic activity
Apoptosis/Cell Death											
a2d07	CYCS	Predicted: Cytochrome c, somatic [Bos taurus]	510767	46400140	ES344015	1.30	-0.04	-0.09	-0.05	04115 04210	p53 signaling pathway Apoptosis
f5o23	GCLC	Glutamate-cysteine ligase, catalytic subunit [Bos taurus] (Anti-apoptosis)	512468	46400499	ES344374	1.28	-0.59	-0.22	-0.52	(GO:0006916)	Aniti-apoptosis
f6h07	RTN3	Reticulon 3 [Bos taurus]	359721	46400586	ES344461	-1.13	0.17	-0.48	-0.78	(GO:0006915)	Apoptosis
g1m22	DNASE1	Deoxyribonuclease I [Bos taurus]	282217	46401119	ES344994	-1.10	0.20	-0.22	-0.25	(GO:0006915)	Apoptosis
g4h07	PEA15	Phosphoprotein enriched in astrocytes 15 [Bos taurus]	510586	46401315	ES345190	0.35	0.76	0.94	1.00	(GO:0042981)	Regulation of apoptosis
Binding											
a2d02	CKB	Creatine kinase, brain [Bos taurus]	516210	46400130	ES344005	0.46	0.83	1.32	2.24	00330	Arginine and proline metabolism
f5d07	BSG	Basigin [Bos taurus]	508716	46400258	ES344133	-1.04	-0.51	-0.80	-0.21	(GO:0005524)	ATP binding
f5f18	YY1	YY1 transcription factor [Bos taurus]	534353	46400322	ES344197	-0.93	0.30	0.30	-0.29	(GO:0003676) (GO:0008270)	Nucleic acid binding Zn binding
f5h18	ZMYM4	Zinc finger, MYM-type 4 [Bos taurus]	529962	46400361	ES344236	-1.17	0.33	0.08	-0.10	(GO:0008270) (GO:0005179)	Zn binding Hormone activity
f5j11	ANXA5	Annexin A5 [Bos taurus]	281626	46400399	ES344274	0.92	-0.49	-0.45	-0.45	(GO:0005515) (GO:0005509) (GO:0005544)	Protein binding Ca binding Phospholipid binding
f5j12	LRRC55	Predicted: Leucine rich repeat containing 55 [Pan troglodytes]	**466584**	46400401	ES344276	1.46	-0.58	-0.31	-0.45		
f6k04	PDK4	Pyruvate dehydrogenase kinase, isozyme 4 [Bos taurus]	507367	46400613	ES344488	-0.03	0.67	1.47	0.61	(GO:0005524)	ATP binding
f5k15	CCDC75	Coiled-coil domain containing 75 [Bos taurus]	512655	46400414	ES344289	1.05	-0.56	-0.32	-0.66	(GO:0003676)	binding nucleic acids
f6f23	ZCCHC7	Zinc finger, CCHC domain containing 7 [Bos taurus]	511821	46400576	ES344451	1.09	-0.60	-0.22	-0.38	(GO:0003676)	binding nucleic acids
f6p17	ATP11B	ATPase, class VI, type 11B [Homo sapiens]	23200	46400673	ES344548	1.131	-0.63	-0.32	-0.45	(GO:0005524) (GO:0004012)	ATP binding Phospholipid-translocating ATPase activity
f8b05	ABCG2	ATP-binding cassette, sub-family G (WHITE), member 2 [Bos taurus]	536203	46400813	ES344688	1.30	-0.66	-0.32	-0.56	02010	ABC transporters - General
f8c15	SPARC	Secreted protein, acidic, cysteine-rich (osteonectin) [Bos taurus]	282077	46400831	ES344706	-0.67	-1.03	-1.49	-1.47	(GO:0005509) (GO:0005507)	Ca binding Cu binding
f8f21	**DACH1**	Similar to dachshund homolog 1 (Drosophila) [Bos taurus]	537184	46400882	ES344757	1.10	-0.65	-0.32	-0.48	(GO:0000166)	binding nucleotides
f8g05	MGC152084	Predicted: Hypothetical protein LOC522276 [Bos taurus]	522276	46400888	ES344763	-1.20	0.13	-0.26	-0.70	(GO:0005509)	Ca binding
f8h02	LRG1	Leucine-rich alpha-2-glycoprotein 1 [Bos taurus]	514663	46400900	ES344775	0.95	-0.34	-0.16	-0.42	(GO:0005515)	Protein binding

Clone ID	Gene Symbol	Gene Name	Entrez Gene ID	dbEST_ID	GenBank Accn	M-Value WP	SF	PF	CF	(GO)/KEGG	Term/Pathway
f8h20	ILF2	Interleukin enhancer binding factor 2, 45kDa [Bos taurus]	539760	46400911	ES344786	1.02	-0.43	-0.22	-0.41	(GO:0005524) (GO:0003723)	ATP binding RNA binding
f8i24	EHD2	EH-domain containing 2 [Bos taurus]	538348	46400926	ES344801	-0.71	-1.18	-0.97	-0.62	(GO:0005509) (GO:0005525)	Ca binding GTP binding
f8o12	MRLC2	Fast skeletal myosin light chain 2 [Bos taurus]	531505	46400996	ES344871	1.05	2.13	1.75	1.73	04510 04530 04670 04810	Focal adhesion Tight junction Leukocyte transendothelial migration Regulation of actin cytoskeleton
f8p11	CHRAC1	Chromatin accessibility complex 1 [Bos taurus]	510942	46401008	ES344883	1.51	1.59	1.75	1.19	(GO:0043565)	Sequence Specific DNA binding
g2c09	S100G	S100 calcium binding protein G [Bos taurus]	281658	46401165	ES345040	-0.69	-0.91	-0.12	-0.27	(GO:0005509) (GO:0005499)	Ca binding Vit.D binding
g3c21	MYL6	Myosin, light chain 6, alkali, smooth muscle and non-muscle [Bos taurus]	281341	50172305	EX656782	0.99	1.42	1.11	1.04	(GO:0005509)	Ca binding
g3e11	SPARCL1	SPARC-like 1 (mast9, hevin) [Bos taurus]	507537	50172306	EX656783	1.54	0.86	1.66	1.16	(GO:0005509)	Ca binding
g3i11	TPT1	Tumor protein, translationally-controlled 1 [Bos taurus]	326599	50172315	EX656792	-0.09	0.98	0.84	1.38	(GO:0005509)	Ca binding
g4d13	DCN	Decorin [Bos taurus]	280760	46401261	ES345136	-0.23	-1.32	-0.86	-0.91	04350	TGF-beta signaling pathway
g4k02	GNL3	Guanine nucleotide binding protein-like 3 (nucleolar) [Bos taurus]	506152	46401362	ES345237	1.15	-0.61	-0.23	-0.07	(GO:0005525)	GTP binding
g4l06	LCP1	Lymphocyte cytosolic protein 1 (L-plastin) [Bos taurus]	540990	46401383	ES345258	1.08	-0.38	0.09	-0.08	(GO:0005509) (GO:0003779)	Ca binding Actin binding
g4m13	SH3PXD2A	Homo sapiens SH3 and PX domains 2A, mRNA	9644	46401408	ES345283	0.30	0.42	0.66	0.91	(GO:0005488)	Binding
g4m20	FHL1	Four and a half LIM domains 1 [Bos taurus]	509056	46401413	ES345288	0.63	1.71	1.56	2.55	(GO:0008270) (GO:0046872)	Zn binding Metal ion binding
g4o07	TLN1	Talin 1 [Bos taurus]	783470	46401435	ES345310	1.07	-0.25	0.09	-0.13	(GO:0005488)	Binding
Carbohydrate Metabolism											
a2g06	GAPDH	Glyceraldehyde-3-phosphate dehydrogenase [Bos taurus]	786101	46400184	ES344059	2.49	2.13	2.61	3.62		
f6a03	PCK2	Phosphoenolpyruvate carboxykinase 2 (mitochondrial) [Bos taurus]	282856	46400519	ES344394	-0.95	-0.28	0.00	-0.17	04920 00020 04910 03320 00620	Adipocytokine signaling pathway Citrate cycle (TCA cycle) Insulin signaling pathway PPAR signaling pathway Pyruvate metabolism
f7b08	PKM2	Predicted: similar to Pyruvate kinase, muscle [Bos taurus]	512571	46400685	ES344560	0.99	1.79	2.02	2.70	(GO:0006096)	Glycolysis
f8a13	ALG11	Asparagine-linked glycosylation 11 homolog (S. cerevisiae, alpha-1,2-mannosyltransferase) [Bos taurus]	540845	46400809	ES344684	1.25	-0.34	-0.27	-0.29	01030 00510	N-Glycan biosynthesis Glycan structures - biosynthesis
f8d01	LDHB	Lactate dehydrogenase B [Bos taurus]	281275	46400838	ES344713	0.28	-0.12	-0.38	-1.10	00272 00010 00640 00620	Cysteine metabolism Glycolysis / Gluconeogenesis Propanoate metabolism Pyruvate metabolism
g4i20	PFKL	Phosphofructokinase, liver [Bos taurus]	508683	46401338	ES345213	0.23	0.20	0.99	0.36	(GO:0006096)	Glycolysis
g4p13	GPI	Glucose phosphate isomerase [Bos taurus]	280808	46401454	ES345329	0.25	0.57	0.74	1.08	00010 00030 00500	Glycolysis / Gluconeogenesis Pentose phosphate pathway Starch and sucrose metabolism
Cell Growth/Differentiation											
f5b15	MAPRE1	Microtubule-associated protein, RP/EB family, member 1 [Bos taurus]	507845	46400229	ES344104	0.93	-0.18	-0.06	-0.20	(GO:0007049)	Cell-division cycle
f5h11	NBN	Nibrin [Bos taurus]	522943	46400351	ES344226	1.07	-0.53	-0.18	-0.11	(GO:0031575)	G1/S transition checkpoint
f7e10	TIPIN	TIMELESS interacting protein [Bos taurus]	506176	46400705	ES344580	1.16	-0.68	-0.34	-0.50	(GO:0007049)	Cell-division cycle
g1c17	IGFBP5	Predicted: Insulin-like growth factor binding protein 5 [Homo sapiens]	3488	46401038	ES344913	-1.38	0.09	-0.40	-0.61	(GO:0001558)	Regulation of cell growth
g1p15	SEPT4	Septin 4 [Bos taurus]	538801	46401139	ES345014	1.11	0.02	-0.48	-0.64	(GO:0007049)	Cell-division cycle
g2e02	SBDS	Shwachman-Bodian-Diamond syndrome [Bos taurus]	513237	46401177	ES345052	-1.34	-0.65	-1.06	-0.76	(GO:0042254) (GO:0008283)	Ribosome biogenesis/assembly Cell proliferation
Cell Cytoskeletal/Adhesion/Extracellular Matrix Related											
a1g04	FN1	Fibronectin 1 [Bos taurus]	280794	46400056	ES343931	-0.52	-0.85	-1.36	-0.70	01430 04510 04810	Cell communication Focal adhesion Regulation of actin cytoskeleton
a1h01	ACTB	Actin, beta [Bos taurus]	280979	46400070	ES343945	1.93	2.02	1.75	2.19	01430 04510 04670 04530 04520 04810	Cell communication Focal adhesion Leukocyte transendothelial migration Tight junction Adherens junction Regulation of actin cytoskeleton
f5g12	COL6A2	Collagen, type VI, alpha 2 [Bos taurus]	282194	46400332	ES344207	-0.46	-0.72	-0.68	-1.02	(GO:0007155)	Cell adhesion
f5m18	COL3A1	Collagen, type III, alpha 1 [Bos taurus]	510833	46400452	ES344327	-0.72	-1.21	-0.75	-0.81	(GO:0005201)	ECM glycoprotein

Clone ID	Gene Symbol	Gene Name	Entrez Gene ID	dbEST_ID	GenBank Accn	M-Value				(GO)/KEGG	Term/Pathway
						WP	SF	PF	CF		
f6l17	SUSD5	Sushi domain containing 5 [Homo sapiens]	26032	46400633	ES344508	0.63	-0.72	-0.92	-1.42	(GO:0007155)	Cell adhesion
f7d14	DPT	Dermatopontin [Bos taurus]	504963	46400699	ES344574	-1.25	0.37	-0.37	-1.03	(GO:0007155)	Cell adhesion
f7e19	TMSB4X	Thymosin beta 4, X-linked [Bos taurus]	282386	46400710	ES344585	-0.92	-0.98	-0.67	-1.20	04810	Regulation of actin cytoskeleton
f8o03	SPP1	Secreted phosphoprotein 1 (osteopontin, bone sialoprotein I, early T-lymphocyte activation 1) [Bos taurus]	281499	46400649	ES344524	1.31	-0.61	-0.26	-0.36	01430 04512 04510 04620	Cell communication ECM-receptor interaction Focal adhesion Toll-like receptor signaling pathway
Hydrolase/Transferase/Catalytic/Activity											
a2h09	NMT2	N-myristoyltransferase 2 [Bos taurus]	282049	46400202	ES344077	-1.60	-1.70	-2.00	-2.25	(GO:0042158)	Lipoprotein biosynthesis
f8g21	LOC789894	LOC789894 similar to PAP-associated domain-containing protein 5 (TRF4-2) [Bos taurus]	789894	46400896	ES344771	1.25	-0.33	-0.07	0.14	(GO:0016779)	Nucleotidyltransferase activity
g4k06	LYZ	Lysozyme (renal amyloidosis) [Bos taurus]	781349	46401366	ES345241	1.08	-0.47	-0.34	-0.55	(GO:0016798)	Hydrolase activity on glycosyl bonds
Nucleic Acid Metabolism											
f6k24	DPYD	Dihydropyrimidine dehydrogenase [Bos taurus]	281124	46400622	ES344497	1.33	-0.62	-0.30	-0.68	00770 00240 00410	Pantothenate and CoA biosynthesis Pyrimidine metabolism beta-Alanine metabolism
f8f24	NP	Nucleoside phosphorylase [Bos taurus]	493724	46400885	ES344760	0.98	-0.56	-0.28	-0.63	00230 00760 00240	Purine metabolism Nicotinate/nicotinamide metabolism Pyrimidine metabolism
f8j18	HPRT1	Hypoxanthine phosphoribosyltransferase 1 (Lesch-Nyhan syndrome) [Bos taurus]	281229	46400938	ES344813	-0.64	-0.46	-0.88	-1.30	00230	Purine metabolism
Oxidative Phosphorylation											
a2a06	UQCRC1	UQCRC1 protein [Bos taurus]	282393	46400092	ES343967	0.26	0.93	0.86	0.87	00190	Oxidative Phosphorylation
g4m07	NDUFS5	NADH dehydrogenase (ubiquinone) Fe-S protein 5, 15kDa (NADH-coenzyme Q reductase) [Bos taurus]	338057	46401405	ES345280	0.16	0.44	0.73	1.19	00190	Oxidative Phosphorylation
g4p08	ATP5O	ATP synthase, H+ transporting, mitochondrial F1 complex, O subunit [Bos taurus]	281640	46401450	ES345325	1.15	0.06	-0.28	0.10	00190	Oxidative Phosphorylation
Oxidoreductase Activity											
f6b09	CRYZ	Crystallin, zeta (quinone reductase) [Bos taurus]	281093	46400523	ES344398	1.01	-0.66	-0.49	-0.45	(GO:0016491)	Oxidoreductase Activity
f6k09	MGST1	Microsomal glutathione S-transferase 1 [Bos taurus]	493719	46400617	ES344492	-1.89	-1.43	-1.99	-2.00	00480	Glutathione metabolism
g1a05	GPX3	Glutathione peroxidase 3 (plasma) [Bos taurus]	281210	46401015	ES344890	-1.07	0.14	-0.37	-0.93	00590 00480	Arachidonic acid metabolism Glutathione metabolism
g4g07	PAOX	Polyamine oxidase (exo-N4-amino) [Bos taurus]	282639	46401300	ES345175	0.98	-0.25	-0.08	0.51	(GO:0016491)	Oxidoreductase Activity
g4h09	PCYOX1	Prenylcysteine oxidase 1 [Homo sapiens]	51449	46401317	ES345192	-0.51	0.17	0.82	0.93	(GO:0016491)	Oxidoreductase Activity
g4l15	CYP2D6	Cytochrome P450, family 2, subfamily D, polypeptide 6 [Bos taurus]	282211	46401392	ES345267	0.07	0.34	0.80	0.91	(GO:0016491)	Oxidoreductase Activity
g4o09	CYP2B	Cytochrome P450 subfamily 2B [Bos taurus]	504769	46401437	ES345312	1.04	-0.39	-0.18	-0.17	00590 00830	Arachidonic acid metabolism Retinol metabolism
Protein Synthesis:Turn Over/Proteolysis/Amino Acid Metabolism											
f5i05	SCPEP1	Serine carboxypeptidase 1 [Bos taurus]	505054	46400371	ES344246	0.75	0.39	0.44	0.90	(GO:0006508)	Proteolysis
f5n06	CFB	Complement factor B [Bos taurus]	514076	46400462	ES344337	-1.06	-1.13	-1.66	-1.33	04610	Complement/coagulation cascades
f5n08	GOT2	Glutamic-oxaloacetic transaminase 2, mitochondrial (aspartate aminotransferase 2) [Bos taurus]	286886	46400465	ES344340	0.56	0.83	1.04	1.68	00252 00950 00330 00710 00272 00251 00360 00400 00350	Alanine and aspartate metabolism Alkaloid biosynthesis I Arginine and proline metabolism Carbon fixation Cysteine metabolism Glutamate metabolism Phenylalanine metabolism Phenylala/tyrosine/tryptophan biosyn Tyrosine metabolism
f8a09	FKBP3	FK506 binding protein 3, 25kDa [Bos taurus]	515069	46400807	46400807	1.08	-0.24	0.19	0.17	(GO:0006457)	Protein folding
f8e02	DPP8	Dipeptidyl-peptidase 8 [Bos taurus]	536604	46400855	ES344730	-0.35	-0.58	-1.07	-1.23	(GO:0006508)	Proteolysis
f8k22	LAP3	Leucine aminopeptidase 3 [Bos taurus]	781648	46400952	ES344827	1.05	-0.57	-0.26	-0.49	00330	Arginine and proline metabolism
g2e20	PLAU	Plasminogen activator, urokinase [Bos taurus]	281408	46401183	ES345058	-1.15	0.02	-0.24	-0.52	04610	Complement /coagulation cascades
g2g22	CSTB	Cystatin B (stefin B) [Bos taurus]	512805	46401193	46401193	-0.93	0.19	-0.13	-0.06	(GO:0004869)	Thiol protease inhibitor
g4d21	PCSK7	Predicted: similar to Proprotein convertase subtilisin/kexin type 7 [Bos taurus]	515398	46401265	ES345140	0.80	0.92	0.78	1.48	(GO:0006508)	Proteolysis
g4j14	OAT	Ornithine aminotransferase (gyrate atrophy) [Bos taurus]	505323	46401352	ES345227	-1.62	-1.86	-2.23	-1.44	(GO:0004587)	Ornithine-oxo-acid transaminase
g4l09	AHCYL1	S-adenosylhomocysteine hydrolase-like 1 [Bos taurus]	505511	46401386	ES345261	-0.86	-0.16	-0.88	-1.00	00271 00451	Methionine metabolism Selenoamino acid metabolism

Clone ID	Gene Symbol	Gene Name	Entrez Gene ID	dbEST_ID	GenBank Accn	M-Value WP	SF	PF	CF	(GO)/KEGG	Term/Pathway
Response to Stress/Stimuli											
f8d20	HSPA8	Heat shock 70kDa protein 8 [Bos taurus]	281831	46400851	ES344726	0.43	0.57	0.64	1.04	04010 04612	MAPK signaling pathway Antigen processing and presentation
f8k01	LOC616903	LOC616903 similar to cutA divalent cation tolerance homolog [Bos taurus]	616903	46400939	ES344814	1.35	-0.58	-0.16	-0.04	(GO:0010038)	Response to metal
Signal Transduction											
a2c08	MYLK	Myosin light chain kinase [Bos taurus]	338037	46400126	ES344001	0.94	0.75	1.02	1.15	04020 04510 04810	Calcium signaling pathway Focal adhesion Regulation of actin cytoskeleton
f5d09	CSNK1A1	Predicted: Casein kinase 1, alpha 1 [Canis lupus familiaris]	479331	46400260	ES344135	0.96	-0.65	-0.42	-0.47	04340 04310	Hedgehog signaling pathway Wnt signaling pathway
f5e16	STARD13	StAR-related lipid transfer (START) domain containing 13 [Bos taurus]	538697	46400290	ES344165	0.77	0.48	0.59	1.16	(GO:0007165)	Signal cascade
f6b10	GHRH	Growth hormone releasing hormone [Bos taurus]	281191	46400524	ES344399	1.21	-0.56	-0.44	-0.28	04080	Neuroactive ligand-recept interaction
f7i11	TBC1D2B	Predicted: TBC1 domain family, member 2B [Bos taurus]	535927	46400737	ES344612	0.98	-0.37	-0.23	-0.45	(GO:0032313)	Regulates RAB GTPase
f8g08	AGTR1	Angiotensin II receptor, type 1 [Bos taurus]	281607	46400890	ES344765	1.06	-0.53	-0.35	-0.59	04020 04080 04614	Calcium signaling pathway Neuroactive ligand-recept interaction Renin-angiotensin system
f8k18	NCSTN	Predicted: Nicastrin [Pan troglodytes]	457435	46400950	ES344825	-0.41	-0.54	-1.31	-1.06	04330	Notch Pathway
g1e23	RAP1A	RAP1A, member of RAS oncogene family [Bos taurus]	282031	46401057	ES344932	1.27	-0.23	-0.22	-0.29	04510 04670 04720 04010	Focal adhesion Leukocyte transendothelial migration Long-term potentiation MAPK signaling pathway
g1g17	CDH13	Cadherin 13, H-cadherin (heart) [Bos taurus]	512302	46401067	ES344942	-0.73	-0.25	-0.98	-0.64	(GO:0016601) (GO:0007266) (GO:0055096) (GO:0050850)	Rac protein signaling Rho protein signaling Lipoprotein med.signaling + regulation of Ca mediated signaling
g1k22	CHD8	Chromodomain helicase DNA binding protein 8 [Bos taurus]	507111	46401102	ES344977	-1.30	0.21	-0.08	-0.04	04310	Wnt signaling pathway
g1p19	TAOK1	Similar to TAO kinase 1 [Pan troglodytes]	454548	46401142	ES345017	-1.24	0.163	-0.01	-0.2	04010	MAPK signaling pathway
g2c06	PTP4A2	Protein tyrosine phosphatase type IVA, member 2 [Bos taurus]	614435	46401163	ES345038	-1.28	-1.13	-1.83	-1.93	(GO:0004725)	Protein-tyrosine-phosphatase activity
g3e13	SRPR	Signal recognition particle receptor ('docking protein') [Bos taurus]	281504	50172307	50172307	0.14	0.56	1.43	0.35	(GO:0005047)	Signal recognition particle receptor
g4c09	STAT1	Signal transducer and activator of transcription 1, 91kDa [Bos taurus]	510814	46401248	ES345123	1.47	0.25	0.53	0.59	04630	Jak-STAT signaling pathway
g4p15	ADRBK2	Adrenergic, beta, receptor kinase 2 [Bos taurus]	282136	46401456	ES345331	1.22	-0.71	-0.23	-0.39	04740	Olfactory transduction
Transcription/Translation											
a2d06	ZNF547	Zinc finger protein 547 [Bos taurus]	512684	46400137	ES344012	0.33	0.27	0.77	1.08	(GO:0006355)	Regulation of transcription-DNA dependent
f5c16	LOC507271	LOC507271 Similar to ribosomal protein L4 [Bos taurus]	507271	N/A	AV592480	1.17	-0.50	-0.21	-0.48	(GO:0006412)	Translation
f5d16	EIF1	Eukaryotic translation initiation factor 1 [Bos taurus]	509764	46400267	ES344142	0.91	0.18	0.26	0.34	(GO:0006413)	Translational initiation
f5f05	PCNA	Similar to proliferating cell nuclear antigen [Bos taurus]	515499	46400301	ES344176	-0.12	0.72	0.59	0.97	03410 04110 03030 03430 03420	Base excision repair Cell cycle DNA replication Mismatch repair Nucleotide excision repair
f5f21	FHL2	Four and a half LIM domains 2 [Bos taurus]	510008	46400324	ES344199	-0.38	0.51	1.13	0.37	(GO:0006357)	Regulation of transcription from RNA-Polymerase II
f7f23	ZNF618	Predicted: Zinc finger protein 618 [Homo sapiens]	114991	46400718	ES344593	-1.08	-1.14	-1.19	-1.74	(GO:0006355)	Regulation of transcription-DNA dependent
f7n23	PRNP	Prion protein (p27-30) [Bos taurus]	281427	46400780	ES344655	1.19	-0.57	-0.27	-0.39	01510 05060	Neurodegenerative Diseases Prion disease
f7p02	EIF3B	Predicted: Eukaryotic translation initiation factor 3, subunit B [Bos taurus]	789999	46400794	ES344669	-1.18	-0.03	-0.41	-0.55	(GO:0006413)	Translational initiation
g1c20	RBMS1	RNA binding motif, single stranded interacting protein 1 [Bos taurus]	526135	46401040	ES344915	1.03	0.90	0.87	0.80	(GO:0006260)	DNA replication
g1i17	PRNP	Prion protein (p27-30) (Creutzfeldt-Jakob disease, Gerstmann-Strausler-Scheinker syndrome, fatal familial insomnia) [Bos taurus]	281427	46401085	ES344960	1.04	-0.60	-0.25	-0.49	(GO:0006355)	Regulation of transcription, DNA-dependent
g1k09	NFKB1	Nuclear factor of kappa light polypeptide gene enhancer in B-cells 1 (p105) [Bos taurus]	616115	46401099	46401099	-0.82	0.25	-0.28	-1.01	04920 04660 04210 04662 04010 04620	Adipocytokine signaling pathway T cell receptor signaling pathway Apoptosis B cell receptor signaling pathway MAPK signaling pathway Toll-like receptor signaling pathway
g2d17	ZNF280C	Zinc finger protein 280C [Homo sapiens]	55609	46401174	ES345049	-1.38	0.16	-0.17	-0.54	(GO:0006355)	Regulation of transcription-DNA dependent
g4a06	LOC537712	LOC537712 similar to early B-cell factor [Bos taurus]	537712	46401224	ES345099	1.08	-0.49	-0.25	-0.40	(GO:0006355)	Regulation of transcription, DNA-dependent

Clone ID	Gene Symbol	Gene Name	Entrez Gene ID	dbEST_ID	GenBank Accn	M-Value				(GO)/KEGG	Term/Pathway
						WP	SF	PF	CF		
g4g08	PRPF38A	PRP38 pre-mRNA processing factor 38 (yeast) domain containing A [Bos taurus]	507240	46401301	ES345176	0.17	0.51	0.73	1.18	(GO:0006397) (GO:0008380)	mRNA processing RNA splicing
g4j03	HNRNPF	Heterogeneous nuclear ribonucleoprotein F [Bos taurus]	506917	46401343	ES345218	-1.29	-0.80	-1.42	-1.23	(GO:0006397) (GO:0008380)	mRNA processing RNA splicing
g4l05	PFN1	Predicted: Profilin 1 [Bos tauru]	513895	46401382	ES345257	1.03	0.21	-0.03	0.67	04810	Regulation of actin cytoskeleton
g4m10	LOC790411	LOC790411 endonuclease reverse transcriptase [Bos taurus]	790411	46402948	ES346823	1.46	-0.47	-0.13	-0.63	(GO:0006278)	RNA -dependent DNA replication
Transporters											
a1d10	SLC25A4	Solute carrier family 25 (mitochondrial carrier; adenine nucleotide translocator), member 4 [Bos taurus]	282478	46400007	ES343882	-0.08	0.74	0.42	1.00	04020	Calcium signaling pathway
f5d18	CYB5	CYB5 protein [Bos taurus]	281110	46400269	ES344144	-1.11	-0.93	-1.33	-1.38	(GO:0006810)	Transport
f5d23	AQP4	Aquaporin 4 [Bos taurus]	281008	46400277	ES344152	0.91	-0.37	0.01	-0.22	(GO:0006810)	Transport
f7h10	SLC15A4	Solute carrier family 15, member 4 [Bos taurus]	510499	46400732	ES344607	1.21	-0.48	-0.24	-0.53	(GO:0006857)	Oligopeptide transport
g1l22	NUP107	Nucleoporin 107kDa [Bos taurus]	504823	46401111	ES344986	-0.97	-0.18	0.12	0.23	(GO:0006810)	Transport
g4l13	BET1L	Blocked early in transport 1 homolog (S. cerevisiae)-like [Bos taurus]	509758	46401390	ES345265	1.17	-0.51	-0.22	-0.30	04130	SNARE interaction in vesicle transport
Clone ID	**Gene Symbol**	**Gene Name**	**Entrez Gene ID**	**dbEST_ID**	**GenBank Accn**	**M-Value**					
						WP	**SF**	**PF**	**CF**		
Other											
a1e02	THRSP	Thyroid hormone responsive (SPOT14 homolog, rat) [Bos taurus]	515940	46400011	ES343886	-1.23	-0.97	-0.92	-1.34		
a1f06	NOD1	Nucleotide-binding oligomerization domain containing 1 [Bos taurus]	520275	46400037	ES343912	1.10	-0.34	-0.57	-0.04		
a1f11	PEX11G	Peroxisomal biogenesis factor 11 gamma [Bos taurus]	506518	46400046	ES343921	0.01	0.25	0.99	0.72		
a1g02	LOC783504	Predicted: LOC783504 similar to ribosomal protein S23 [Bos taurus]	783504	46400051	ES343926	1.29	-0.64	-0.34	-0.53		
a2c05	PTP4A2	Predicted: Protein tyrosine phosphatase type IVA, member 2 [Canis lupus familiaris]	609835	46400124	ES343999	0.73	0.78	0.81	1.06		
a2h06	BAP1	BRCA1 associated protein-1 [Bos taurus]	100124510	46400199	ES344074	0.88	0.76	1.07	1.49		
f5b22	C28H10ORF116	Chromosome 10 open reading frame 116 ortholog [Bos taurus]	613941	46400234	ES344109	-0.94	0.25	0.13	0.04		
f5c10	LOC619156	Predicted: LOC619156 similar to ribosomal protein L17 [Bos taurus]	619156	46400242	ES344117	1.00	-0.42	-0.07	-0.16		
f5d14	SLC24A6	Predicted: Solute carrier family 24 (sodium/potassium/calcium exchanger), member 6 [Bos taurus]	508887	46400264	ES344139	1.14	-0.49	-0.29	-0.26		
f5d15	LOC533444	LOC533444 similar to WD repeat protein Gemin5 [Bos taurus]	533444	46400266	ES344141	0.96	0.49	0.58	0.88		
f5e15	TMEM66	Transmembrane protein 66 [Bos taurus]	515461	N/A	EW681864	0.77	0.69	0.90	0.93		
f5g03	MGC139109	MGC139109 hypothetical LOC533333 [Bos taurus]	533333	N/A	EH180189	-0.91	-0.15	-0.32	-0.17		
f5g22	LOC100054421	LOC100054421 similar to procollagen alpha 2(V) [Equus caballus]	100054421	46400341	ES344216	-1.04	-0.81	-0.86	-0.58		
f5h19	ZNFN1A1	Predicted: Zinc finger protein, subfamily 1A, 1 (Ikaros) [Macaca mulatta]	693936	46400362	ES344237	-1.16	0.34	0.10	0.04		
f5i23	CCNL2	Cyclin L2 [Bos taurus]	538796	46400383	ES344258	-1.72	-1.27	-1.91	-1.81		
f5j06	LOC782311	LOC782311 similar to Tyrosylprotein sulfotransferase 1 [Bos taurus]	782311	46400393	ES344268	0.81	0.61	0.52	0.99		
f5o05	LOC789925	Predicted: LOC789925 similar to Mid-1-related chloride channel 1 [Bos taurus]	789925	N/A	EE961626	-1.20	-1.12	-1.52	-1.40		
f5o07	LOC783366	LOC783366 similar to Ankyrin repeat domain-containing protein 26 [Bos taurus]	783366	46400488	ES344363	1.07	-0.61	-0.41	-0.58		
f5p16	GRN	Granulin [Bos taurus]	767942	46400512	ES344387	-0.18	0.27	-0.43	-0.95		
f6d04	LOC100152073	Predicted: LOC100152073 similar to Stress 70 protein chaperone, microsome-associated, 60kD [Sus scrofa]	100152073	46400543	ES344418	1.11	-0.58	-0.24	-0.34		
f6d07	LOC509875	Predicted: Hypothetical protein LOC509875 [Bos taurus]	509875	46400545	ES344420	-0.94	-0.08	-0.48	-0.69		
f6e07	LOC505415	Hypothetical protein LOC505415 [Bos taurus]	505415	46400558	46400558	-0.95	0.17	-0.16	-0.42		
f6f04	DHX16	Predicted: DEAH (Asp-Glu-Ala-His) box polypeptide 16 [Bos taurus]	506405	46400570	ES344445	-1.05	-0.05	-0.59	-1.07		
f6i07	LOC506707	Predicted: LOC506707 similar to C4BP alpha chain [Bos taurus]	506707	46400598	ES344473	1.65	0.07	-0.50	-0.23		
f6l15	SCAMP2	Secretory carrier membrane protein 2 [Bos taurus]	534312	46400631	46400631	0.94	-0.14	0.01	0.16		
f6m23	WDR68	WD repeat domain 68 [Bos taurus]	516678	46400643	ES344518	-0.67	-0.82	-0.94	-0.81		
f6p11	CPM	Carboxypeptidase M [Bos taurus]	513281	46400671	ES344546	2.04	-0.33	-0.07	-0.61		
f7a12	C16H1ORF21	Chromosome 1 open reading frame 21 ortholog [Bos taurus]	781721	46400680	ES344555	0.00	0.50	0.78	0.99		
f7a14	MRAS	Muscle RAS oncogene homolog [Bos taurus]	540803	46400681	ES344556	-1.31	0.32	-0.35	-0.94		
f7b07	LOC788567	Hypothetical protein LOC788567 [Bos taurus]	788567	46400684	ES344559	0.10	0.36	0.50	1.09		
f7c11	LOC509995	LOC509995 similar to Leucine-rich PPR motif-containing protein, mitochondrial precursor (130 kDa leucine-rich protein) (LRP 130) (GP130) [Bos taurus]	509995	46400691	ES344566	1.36	-0.22	0.00	-0.72		
f7e16	LOC533350	Predicted: LOC533350 similar to KIAA1451 protein [Bos taurus]	533350	46400709	ES344584	-1.19	-1.16	-0.86	-1.17		
f7g21	MANBAL	Mannosidase, beta A, lysosomal-like [Bos taurus]	787482	46400727	ES344602	1.31	-0.42	-0.02	-0.18		
f7k10	ITM2B	Predicted: Integral membrane protein 2B [Canis lupus familiaris]	476916	46400755	ES344630	-0.94	0.01	-0.37	-0.47		
f7m07	ANLN	Anillin, actin binding protein [Bos taurus]	518274	46400764	ES344639	1.20	-0.30	-0.42	0.05		
f7o22	GOLGA7	Golgi autoantigen, golgin subfamily a, 7 [Bos taurus]	616809	46400793	ES344668	-0.84	-0.99	-1.06	-0.94		
f7p13	LOC100059158	Predicted: LOC100059158 similar to Chain A, Crystal Structure Of Human Translationally Controlled Tumor Associated Protein [Equus caballus]	100059158	46400800	ES344675	0.13	0.98	0.70	1.25		
f8a08	LOC100137838	LOC100137838 similar to tripartite motif protein TRIM4 [Bos taurus]	100137838	46400806	ES344681	1.49	-0.38	-0.16	-0.70		

Clone ID	Gene Symbol	Gene Name	Entrez Gene ID	dbEST_ID	GenBank Accn	M-Value			
						WP	SF	PF	CF
f8c13	SNF8	SNF8, ESCRT-II complex subunit, homolog (S. cerevisiae) [Bos taurus]	505628	46400829	ES344704	-1.08	0.26	-0.02	-0.16
f8d09	RASEF	Predicted: RAS and EF-hand domain containing [Bos taurus]	513223	46400842	ES344717	1.02	-0.47	-0.13	-0.10
f8g22	LOC613996	LOC613996 Similar to FLJ10769 protein [Bos taurus]	613996	46400897	ES344772	1.37	-0.37	-0.10	0.04
f8l21	MAGED2	Melanoma antigen family D, 2 [Bos taurus]	514372	46400963	ES344838	1.06	-0.36	-0.10	-0.28
f8m14	LOC782097	Hypothetical protein LOC782097 [Bos taurus]	782097	46400972	ES344847	1.17	-0.58	-0.27	-0.43
f8n02	DMRT2	Doublesex and mab-3 related transcription factor 2 [Bos taurus]	514435	46400977	ES344852	1.25	0.50	0.62	-0.18
f8o18	BLOC1S2	Biogenesis of lysosome-related organelles complex-1, subunit 2 [Bos taurus]	519172	46401000	ES344875	-0.61	-0.67	-0.86	-0.96
g1a20	TGFBRAP1	Transforming growth factor, beta receptor associated protein 1 [Bos taurus]	514660	46401020	ES344895	-0.77	-1.06	-0.91	-1.25
g1b19	EHBP1	Predicted: EH domain binding protein 1 [Bos taurus]	533149	46401030	46401030	1.00	-0.04	0.22	-0.44
g1c02	PCYOX1	Prenylcysteine oxidase 1 [Bos taurus]	100125835	46401033	ES344908	-1.21	0.32	-0.38	-0.87
g1f04	LOC523451	LOC523451 similar to tetratricopeptide repeat domain 9 [Bos taurus]	523451	46401059	ES344934	-0.06	0.76	0.81	1.19
g1f13	CIDEA	Cell death-inducing DFFA-like effector a [Bos taurus]	527051	46401062	ES344937	-0.62	-0.80	-1.05	-0.98
g1h03	LIPA	Lipase A, lysosomal acid, cholesterol esterase [Bos taurus]	100125267	46401072	ES344947	-1.14	-0.85	-1.09	-1.01
g1h23	UBAC2	UBA domain containing 2 [Bos taurus]	100125312	46401079	ES344954	-1.30	-1.15	-1.36	-1.42
g1k14	LOC504909	LOC504909 Similar to ATP-binding cassette sub-family A member 10 [Bos taurus]	504909	46401100	ES344975	1.29	-0.59	-0.23	-0.24
g1l14	LSM14A	LSM14A, SCD6 homolog A (S. cerevisiae) [Bos taurus]	538838	46401107	ES344982	-0.72	-1.32	-1.72	-1.35
g1l24	NDFIP1	Predicted: Nedd4 family interacting protein 1 [Canis lupus familiaris]	478044	46401112	ES344987	-1.32	-0.49	-0.64	-1.47
g1n05	TRAF3IP1	TNF receptor-associated factor 3 interacting protein 1 [Bos taurus]	504984	46401121	ES344996	-1.40	-0.07	-0.76	-1.94
g1n21	LOC521099	Predicted: Hypothetical proetin LOC521099 [Bos taurus]	521099	46401127	ES345002	-1.32	0.14	-0.39	-0.48
g1o09	POLR1D	Polymerase (RNA) I polypeptide D [Bos taurus]	616972	46401130	ES345005	-0.65	-0.75	-1.20	-0.70
g1o20	MGC148679	Hypothetical LOC505853 [Bos taurus]	505853	46401134	ES345009	-1.60	0.13	-0.29	-0.52
g2a08	FBXO36	F-box protein 36 [Bos taurus]	617339	46401148	ES345023	1.45	-0.18	0.16	0.40
g2c21	STRN3	Striatin, calmodulin binding protein 3 [Bos taurus]	516375	N/A	DV895764	-1.41	-0.78	-1.08	-1.57
g2c22	LOC532244	LOC532244 similar to microtubule associated monoxygenase, calponin and LIM domain containing 3[Bos taurus]	532244	46401168	ES345043	-1.93	-0.33	-1.22	-2.58
g2e17	LOC100158124	LOC100158124 similar to MID1 interacting G12-like protein [Sus scrofa]	100158124	46401181	ES345056	-1.06	-0.23	-0.59	-0.88
g2e23	VEZT	Vezatin, adherens junctions transmembrane protein [Bos taurus]	535351	46401185	ES345060	1.03	-0.52	-0.31	-0.27
g2k24	MGC127989	Hypothetical protein MGC127989 [Bos taurus]	767921	46401215	ES345090	-1.10	0.22	0.29	0.08
g3c15	VSTM1	V-set and transmembrane domain containing 1 [Bos taurus]	618514	50172304	EX656781	1.19	-0.65	-0.34	-0.32
g3i05	LOC528398	LOC528398 similar to Abelson helper integration site 1 [Bos taurus]	528398	N/A	N/A	0.474	0.993	0.579	1.535
g4b07	NLRX1	NLR family member X1 [Bos taurus]	539974	46401235	ES345110	1.30	-0.59	-0.08	0.13
g4c24	ABCA9	ATP-binding cassette, sub-family A (ABC1), member 9 [Bos taurus]	504278	46401255	ES345130	1.38	-0.29	-0.13	0.22
g4e15	CDC42BPA	CDC42-binding protein kinase alpha [Pan troglodytes]	738981	46401276	ES345151	0.79	0.33	0.96	0.75
g4f14	LOC787439	Hypothetical protein LOC787439 [Bos taurus]	787439	46401290	ES345165	0.98	-0.22	0.06	-0.04
g4i06	SETD3	Predicted: SET domain containing 3 [Bos taurus]	512324	46401328	ES345203	-0.92	-0.44	-0.73	-0.62
g4j12	ROR2	Predicted: Receptor tyrosine kinase-like orphan receptor 2 [Bos taurus]	785924	46401350	ES345225	1.41	0.05	-0.33	-0.46
g4l21	THUMPD3	Predicted: THUMP domain containing 3 [Pan troglodytes]	460147	46401397	ES345272	0.98	-0.49	-0.17	-0.31
g4m11	FAM32A	Family with sequence similarity 32, member A [Bos taurus]	508634	46401407	ES345282	1.19	-0.26	0.22	-0.19
g4n13	SETMAR	SET domain and mariner transposase fusion gene [Bos taurus]	534913	46401423	ES345298	1.11	-0.38	-0.16	-0.30
g4o12	SASH3	Predicted: SAM and SH3 domain containing 3 [Bos taurus]	534137	46401439	46401439	1.50	-0.05	-0.16	0.68
g4o16	TXNIP	Thioredoxin interacting protein [Bos taurus]	506790	46401442	ES345317	-0.97	-0.13	0.03	-0.16
g4p10	RSRC1	Arginine/serine-rich coiled-coil 1 [Bos taurus]	509437	46401451	ES345326	-1.15	-0.81	-1.12	-0.99

No Biological Data Available									
f5c15	..	Pan troglodytes RBP4 gene for retinol binding protein4	AB124586	46400247	ES344122	1.00	-0.56	-0.36	-0.65
f5n09	..	Sus scrofa toll-like receptor 4 (TLR4) gene, complete cds	AY753179	46400467	ES344342	0.33	0.48	0.85	0.95
g2a15	..	Bos taurus X-inactivation center region, Jpx and Xist genes	AJ421481	46401151	ES345026	1.16	-0.18	0.38	0.38
g2h22	..	Csf1R gene, smf gene, tigd14 gene, slc26a2 gene [Equus caballus]	AJ698944	46401198	ES345073	-0.20	0.97	1.06	1.27
f5a18	..	cattle subcutaneous adipose tissue cDNA library Bos taurus cDNA clone f5a18ca 3-, mRNA sequence	ES344086.1	46400211	ES344086	0.29	-0.83	-0.50	-1.66
f5j14	..	cattle subcutaneous adipose tissue cDNA library Bos taurus cDNA clone f5j14ca 5', mRNA sequence.	ES344278.1	46400403	ES344278	1.20	-0.72	-0.43	-0.68
f5l22	..	cattle subcutaneous adipose tissue cDNA library Bos taurus cDNA clone f5l22ca 3-, mRNA sequence	ES344310.1	46400435	ES344310	1.08	-0.48	-0.16	-0.49
f5p07	..	cattle subcutaneous adipose tissue cDNA library Bos taurus cDNA clone f5p07ca 3-, mRNA sequence	ES344381.1	46400506	ES344381	1.11	-0.69	-0.42	-0.72
f5p21	..	cattle subcutaneous adipose tissue cDNA library Bos taurus cDNA clone f5p21ca 5-, mRNA sequence	ES344392.1	46400517	ES344392	-1.32	-1.31	-1.43	-1.95
f6e15	..	cattle subcutaneous adipose tissue cDNA library Bos taurus cDNA clone f6e15ca 3-, mRNA sequence	ES344439.1	46400564	ES344439	1.12	-0.56	-0.21	-0.34
f6l01	..	cattle subcutaneous adipose tissue cDNA library Bos taurus cDNA clone f6l01ca 3-, mRNA sequence	ES344498.1	46400623	ES344498	1.11	-0.60	-0.40	-0.41
f6o01	..	cattle subcutaneous adipose tissue cDNA library Bos taurus cDNA clone f6o01ca 3-, mRNA sequence	ES344529.1	46400654	ES344529	1.01	-0.21	0.01	0.17
f6o18	..	cattle subcutaneous adipose tissue cDNA library Bos taurus cDNA clone f6o18ca 3-, mRNA sequence	ES344538.1	46400663	ES344538	1.45	-0.43	-0.51	-0.74
f7g24	..	cattle subcutaneous adipose tissue cDNA library Bos taurus cDNA clone f7g24ca 3-, mRNA sequence	ES344605.1	46400730	ES344605	-1.18	-1.11	-1.30	-1.07
f7m19	..	cattle subcutaneous adipose tissue cDNA library Bos taurus cDNA clone f7m19ca 3-, mRNA sequence	ES344643.1	46400768	ES344643	0.99	-0.47	-0.43	-0.56
f8f01	..	cattle subcutaneous adipose tissue cDNA library Bos taurus cDNA clone f8f01ca 3-, mRNA sequence	ES344747.1	46400872	ES344747	-1.11	-0.76	-1.30	-0.89
f8j04	..	cattle subcutaneous adipose tissue cDNA library Bos taurus cDNA clone f8j04ca 3-, mRNA sequence	ES344804.1	..	46400929	1.11	-0.66	-0.46	-0.59
f8j07	..	cattle subcutaneous adipose tissue cDNA library Bos taurus cDNA clone f8j07ca 3-, mRNA sequence	ES344807.1	46400932	ES344807	0.96	-0.13	0.53	-0.10
f8k08	..	cattle subcutaneous adipose tissue cDNA library Bos taurus cDNA clone f8k08ca 3-, mRNA sequence	ES344819.1	46400944	ES344819	1.22	-0.58	-0.24	-0.25
f8l04	..	cattle subcutaneous adipose tissue cDNA library Bos taurus cDNA clone f8l04ca 3-, mRNA sequence	ES344829.1	46401104	ES344979	0.92	-0.45	-0.17	-0.28
f8m02	..	cattle subcutaneous adipose tissue cDNA library Bos taurus cDNA clone f8m02ca 3-, mRNA sequence	ES344842.1	46400967	ES344842	0.99	-0.47	-0.29	-0.60
g1b14	..	cattle subcutaneous adipose tissue cDNA library Bos taurus cDNA clone g1b14ca 3-, mRNA sequence	ES344901.1	46401026	ES344901	0.03	0.83	1.03	0.80
g1h04	..	cattle subcutaneous adipose tissue cDNA library Bos taurus cDNA clone g1h04ca 3-, mRNA sequence	ES344948.1	46401073	ES344948	-0.74	-0.28	-1.23	-1.25
g1l10	..	cattle subcutaneous adipose tissue cDNA library Bos taurus cDNA clone g1l10ca 3-, mRNA sequence	ES344979.1	46401104	46401104	-1.36	0.40	-0.31	-0.91
g1m12	..	4095050 BARC 10BOV Bos taurus cDNA clone 10BOV34_B01 3-, mRNA sequence	CK955313.1	..	AM30074	0.97	0.48	0.26	0.59
g3e17	..	cattle adipose tissue cDNA library Bos taurus cDNA clone g3e17ca 5-, mRNA sequence	EX656785.1	50172308	EX656785	1.41	-0.64	-0.14	-0.37
g3k13	..	cattle adipose tissue cDNA library Bos taurus cDNA clone g3k13ca 5-, mRNA sequence	EX656796.1	50172319	EX656796	0.76	0.94	0.71	1.34
g4d08	..	cattle subcutaneous adipose tissue cDNA library Bos taurus cDNA clone g4d08ca 3-, mRNA sequence	ES345133.1	46401258	ES345133	1.26	-0.58	-0.23	-0.45
f6b03	..	cattle subcutaneous adipose tissue cDNA library Bos taurus cDNA clone f6b03ca 3-, mRNA sequence	ES344397.1	46400522	ES344397	0.30	0.48	1.12	0.84

VITA

Daniel Ray Stein

Candidate for the Degree of Doctor of Philosophy

Dissertation: EFFECTS OF GROWING PROGRAMS AND β- ADRENERGIC AGONISTS ON GENE EXPRESSION IN ADIPOSE TISSUE DEPOTS IN FINISHING BEEF STEERS

Major Field: Animal Breeding and Reproduction

Biographical:

Personal Data: Born in Cherokee OK, the son of Leroy C. and Rosevelyn Stein

Education: Graduated from Cherokee High School, Cherokee, OK in May 1974. Received Bachelor of Science in Agriculture Ecology from Northwestern Oklahoma State University, Alva, OK in May 1974. Received Master of Science in Animal Science at Oklahoma State University, Stillwater, OK in December 2005. Completed the requirements for the Doctor of Philosophy in Animal Breeding and Reproduction at Oklahoma State University, Stillwater, OK in July 2009.

Experience:

January 2005 to Present

Graduate Assistant, Oklahoma State University Animal Science

Lead instructor for Animal Reproduction, ANSI 3443; fall 2006 and 2007

August 2002 – December 2004

Graduate Assistant, Oklahoma State University Animal Science

Awards:

Outstanding Animal Science Ph.D. Graduate Student Award, 2007

Outstanding Animal Science M.S. Graduate Student Award, 2005

Professional Memberships:

Society for the Study of Reproduction, American Society of Animal Science American Dairy Science Association, Sigma Xi Research Society, NACTA – Gamma Sigma Delta, American Embryo Transfer Association

Name: Daniel Ray Stein Date of Degree: July, 2009

Institution: Oklahoma State University Location: Stillwater, OK

Title of Study: EFFECTS OF GROWING PROGRAMS AND β-ADRENERGIC AGONISTS ON GENE EXPRESSION IN ADIPOSE TISSUE DEPOTS IN FINISHING BEEF STEERS

Pages in Study: 275 Candidate for the Degree of Doctor of Philosophy

Major Field: Animal Breeding and Reproduction

Scope and Method of Study:

As adipose tissue accretion in the bovine is controlled by a balance of adipocyte proliferation and differentiation; it is essential to evaluate how diet or the administration of exogenous compounds, such as β-agonists, affects and/or regulates adipocyte proliferation in order to improve the quality of the beef produced. Knowledge and understanding of the relationships between mechanisms regulating metabolic and signaling pathways and other contributing factors which orchestrate adipose tissue deposition within and between adipose tissue depots could possibly be integrated into management practices in a value-based marketing system to produce a consistent and desirable product that would ultimately enhance consumer beef consumption, increase efficiency of production, and increase profitability for the beef industry.

Findings and Conclusions:

Three hundred sixty-eight array elements were observed to be differentially expressed between s.c. and i.m. adipose tissue depots in the Initial and/or one of the diets of the Growing Phase. Two hundred forty-eight array elements were found to be differentially expressed between s.c. and i.m. adipose tissue depots in at least one of the four treatment diets during the Finishing Phase. The data indicates the metabolic machinery for adipose tissue accretion was down-regulated in the i.m. adipose tissue depot compared to s.c. adipose tissue depot and the main effect of previous diet could possibly influence adipose tissue deposition at the end of both the growing and finishing production phases in beef cattle. Microarray analysis showed no array elements to be differentially expressed in the i.m., s.c., or visceral adipose tissue depots or *Longissimus* muscle tissue between the control steers and steers supplemented with Zilpaterol hydrochloride for 20 d with a 3-d withdrawal. Of the genes selected for validation using RT-PCR in respective tissues, only cytochrome C-1 and β_2-AR in i.m. adipose tissue and β_1-AR in s.c. adipose tissue did not support the results of the microarray analysis. RT-PCR revealed cytochrome C-1, β_1-AR, and β_2-AR mRNA expression to be up-regulated threefold, fourfold and fourfold in Zilpaterol hydrochloride supplemented steers vs. control steers, respectively.

ADVISER'S APPROVAL: Dr. Clint R. Krehbiel

ADVISER'S APPROVAL: Dr. Clint R. Krehbiel